# NEW BICYCLIC NITROGENOUS COMPOUNDS FOR ENZYMOLOGY AND PHARMACOLOGY

By

FEDRA MARINA LEONIK

A DISSERTATION PRESENTED TO THE GRADUATE SCHOOL
OF THE UNIVERSITY OF FLORIDA IN PARTIAL FULFILLMENT
OF THE REQUIREMENTS FOR THE DEGREE OF
DOCTOR OF PHILOSOPHY

UNIVERSITY OF FLORIDA

2008

© 2008 Fedra Marina Leonik

To the most important people in my life, my husband Daniel, my brother Yuri and my parents Susana and Jorge.

ACKNOWLEDGMENTS

My study would not have been accomplished without the support and help of many people. To begin with, I would like to specially thank my advisor Dr. Nicole Horenstein for all her scientific guidance and support during the course of my studies. I also express my gratitude to my doctoral committee members, Dr Ronald Castellano, Dr. Tom Lyons, Dr. Linda Bloom and Dr. Roger Papke, for their advice and support. I would like to acknowledge Dr. Ion Ghiviriga for helping with the characterization of the compounds by 2D NMR spectroscopy.

I am very grateful to the past and present Dr. Horenstein's group members, specially, Jen, Erin, Jeremiah and Jingyi for their friendship and support that made, the day to day in the lab, a better bearable experience. I extend my thanks to my colleagues of the Biochemistry division, in particular, Alonso, Mike, Cory, Kevin, Nancy and Jessica for lending equipment, instructive scientific conversations and sharing success and frustration.

My special acknowledgments go to the financial support from NIH, NSF, Ruegamer Fellowship, College of Liberal Arts and Science Russell Dissertation Fellowship and University of Florida Chemistry Department.

I would also like to thank my friends for making my stay in Florida an unforgettable experience. Specially, my gratitude goes to Jorge, Sarah, Ozge, Giorgos, Fabricio and Andrea. We have been, side to side, supporting each other from the very first day. Additionally, I also thank Ece, Giovanni, Laurel, Sophie and Julio.

My particular thanks go to the Argentinean professors, Valeria Kleiman and Adrian Roitberg, for their constant support and guidance on both academic and personal. I have mainly enjoyed our "mate and chat" afternoons, "asados" and "burako" tournament.

My friends from home have also been a valuable support with ceaseless telephone conversations and visits to Gainesville, in particular, Ale, Pablo Mafia, Tamara, Ele, Pablo Engle, Gustavo and Maria Ana.

I could not possibly have completed my doctoral studies without my husband Daniel. He has been the foundation of my life and career through his encouragement, patience and love.

Special thanks go to my family in law, Laura, Yuji, Fernanda and Marcelo for their unconditional support.

Finally, I would like to express my eternal gratitude to my brother Yuri and my parents Jorge Leonik and Susana Sarabia. Although we are far away from each other, they have always encouraged me to continue this difficult journey, by simple believing in me.

TABLE OF CONTENTS

LIST OF TABLES

LIST OF FIGURES

ABREVIATIONS

| | |
|---|---|
| p-ABSA | p-acetamidobenzenesulfonyl azide |
| ACh | acetylcholine |
| AChBP | acetylcholine binding protein |
| $Ac_2O$ | acetic anhydride |
| HOAc | acetic acid |
| AD | Alzheimer's |
| BA | benzilidene anabaseine |
| Boc | t-butyloxycarbonyl |
| BSA | bovine serum albumin |
| Bn | benzyl |
| CI | chemical ionization |
| CMP | cytidine 5'-monophosphate |
| CDP | cytidine 5'-diphosphate |
| CTP | cytidine 5'-triphosphate |
| $Cu(acac)_2$ | copper (II) acetylacetonate |
| CuOTf | copper triflate |
| DBU | 1,8-diazabicyclo[5.4.0]undec-7-ene |
| DCC | N,N'-dicyclohexylcarbodiimine |
| DCU | dicyclohexylurea |
| DMAP | dimethylaminopyridine |
| DME | 1,2-dimethoyethane |
| DMF | N,N-dimethyl formamide |
| DMSO | dimethyl sulfoxide |
| DMTCl | 4,4′-Dimethoxytrityl chloride |
| DNA | deoxyribonucleic acid |
| DPPA | diphenylphosphoryl azide |
| EI | electron Ionization |
| ESI | electrospray ionization |
| EtOAc | ethyl acetate |
| EtOH | ethanol |
| FAB | fast atom bombardment |
| FMoc | 9-fluorenylmethyloxycarbonyl |
| GABA | γ-aminobutyric acid |
| GDP | guanosine 5'-diphosphate |
| GMP | guanosine 5'-monophosphate |
| HA | hemagglutinin |
| HIV | human immunodeficiency virus |
| HPLC | high performance liquid chromatography |
| KIE | kinetic isotope effect |
| $KMnO_4$ | potassium permanganate |
| LacNAc | N-acetyl lactosamine |
| LG | leaving group |
| LSC | liquid scintillation counting |
| MeOH | methanol |
| MES | 4-morpholineethanesulfonic acid |

| | |
|---|---|
| MS | mass spectrometry |
| MsCl | methyl sulfonyl chloride |
| MSNT | 1-(2-Mesitylenesulfonyl)-3-nitro-1H-1,2,4-triazole |
| nAChR | nicotinic acetylcholine receptor |
| NaOEt | sodium ethoxide |
| NBS | N-bromosuccinimide |
| NeuAc or Neu5Ac | N-acetyl neuraminic acid |
| NMO | N-methylmorpholine |
| NMR | nuclear magnetic resonance |
| NOESY | nuclear overhauser enhancement spectroscopy |
| NS | nucleotide sugar |
| ONPG | o-nitrophenyl β-D-galactopyranoside |
| PCC | pyridinium chlorochromate |
| Pi | inorganic phosphate |
| PIDA | iodobenzene diacetate |
| PIFA | bis(trifluoroacetoxy)iodobenzene |
| PNP | p-nitro phenyl |
| $Rh_2OAc_4$ | rhodium acetate |
| RNA | ribonucleic acid |
| $SLe^X$ | sialyl lewis |
| ST | sialyltransferase |
| tBuOH | *tert*-butanol |
| TBAF | tetra-n-butylammonium fluoride |
| TBDMSCl | *tert*-butyldimethylsilyl chloride |
| TBDPSCl | *tert*-butyldiphenylsilyl chloride |
| TFA | trifluoro acetic acid |
| TMSI | trimethylsilyl iodide |
| THF | tetrahydrofuran |
| TLC | thin layer chromatography |
| TPAP | tetra-n-propylammonium perruthenate |
| TsCl | toluensulfonyl chloride |
| TS | transition state |
| UDP | uracil 5'-diphosphate |
| UMP | uracil 5'-monophosphate |
| UTP | uracil 5'-triphosphate |
| UV | ultraviolet |

Abstract of Dissertation Presented to the Graduate School
of the University of Florida in Partial Fulfillment of the
Requirements for the Degree of Doctor of Philosophy

NEW BICYCLIC NITROGENOUS COMPOUNDS FOR ENZYMOLOGY AND PHARMACOLOGY

By

Fedra Marina Leonik

August 2008

Chair: Nicole A. Horenstein
Major: Chemistry

Glycosyltransferases and glycosidases catalyze the transfer of the glycon unit to the acceptor hydroxyl group of carbohydrates and water, respectively. Because glycoconjugates are involved in a variety of metabolic roles, these enzymes play a key role in biological processes such as tumor metastasis, cell-cell development and immune responses. Sialyltransferases (ST's) are enzymes that transfer sialic acid from the donor cytidine monophosphate-N-acetylneuraminate (CMP-NeuAc) to the acceptor sugar. STs utilize an $S_N1$-like mechanism in which the leaving group (nucleotide) is mostly dissociated before attack of the incoming nucleophile (oligosaccharide) has started. Previous studies strongly supported a mechanism that involves a transition state (TS) where positive charge is accumulated between the anomeric carbon and oxygen atom of the neuraminate glycon. This study reports the synthesis of diazabicyclic transition state analogs for ST. In the design, a bicyclic system is used to hold the leaving group above the anomeric center mimic, and the amidine functionality will imitate the planarity and positive charge at the transition state. This molecular framework mimics the hypervalent bonding that occurs during a glycosyl transfer reaction. Inhibition experiments were completed with seven-membered ring amidines on different glycosidases and the inhibition constants ($K_i$) were determined for the most potent inhibitors. The TS analogs tested displayed

$K_i$ between 0.15 to 2 mM range. In addition, preliminary inhibition studies were performed on human recombinant α(2→6)-sialyltranferase and the $K_i$ of CMP-amidine was estimated to be 50 μM.

A second project involved the design and synthesis of agonists to probe the basis for selective activation of neuronal α7-type nicotinic acetylcholine receptors (nAChRs). This receptor is a transmembrane ligand gated ion channel, whose three-dimensional structure is not yet known to high resolution. In order to determine the features of the α7 nAChR that function as selectivity filters for α7 agonist activity, differentially functionalized compounds sharing a common ammonium pharmacophore were synthesized. Among them, derivatives of quinuclidine and quinuclidinone were synthesized which have shown mixed agonist activity.

# CHAPTER 1
# INTRODUCTION

## Glycoconjugates

Oligosaccharides are one of the most important biological polymers in part due to their ability to function in metabolic energy storage (glycogen and starch) and their use in structure (cellulose and chitin).[1] They constitute a large portion of the carbon composition in the biosphere, perhaps due to their elevated stability. The glycosidic bond is less susceptible to spontaneous hydrolysis (half life of around 5 million years) than the linkage of amino acids in polypeptides (half life of 460 years) and even DNA nucleotides (half life of 140 thousand years).[1] Although they represent the most abundant biopolymeric structure, there is still lack of information about their biological roles. Proposing a single common hypothesis about an oligosaccharide function is fruitless task, not only because of its extremely complex and varied structure but also because of its diverse biological contex.[2] Among their different biological roles, they can a) participate in cell-cell interactions; b) modulate protein folding and stability; c) act as target or masking for certain microorganisms, toxins or binding events; and d) they could serve as structural elements.[2]

As a consequence of the broad variety of polysaccharides, there is a wide assortment of enzymes that are in charge of hydrolyzing and forming these glycosidic bonds. In addition, carbohydrate-processing enzymes are considered among the most catalytically efficient due to their ability to cleave such a stable bond.[1]

## Carbohydrate-Processing Enzymes

The enzymes that are responsible for the glycosidic bond cleavage are divided into two clans, glycosidases, which catalyze the hydrolysis of the glycosidic bond by using only water as the nucleophile and glycosyltransferases, which transfer a sugar unit to another nucleophilic

acceptor.[3,4] Moreover, glycosyltransferases can be divided into two other groups, the transferases that use an oligosaccharide as the donor substrate and those that utilize a nucleotide sugar as donor (NS glycosyltransferases).[3] Our research only focused on glycosidases and NS glycosyltransferases.

As previously mentioned, glycosidases and glycosyltransferases play a key role in biological processes. One example of their metabolic roles is in protein glycosylation. Depending on the structural features of the attached oligosaccharides, the protein will be trafficked to different intracellular compartments.[5] Oligosaccharides could be linked to the protein in two different manners: a) by β-N glycosidic bond to an asparagine or b) by a α-O-glycosidic bond to serine or threonine.[6] Starting at the endoplasmic reticulum, the synthesis of the core oligosaccharide requires the sequential addition of monosaccharide units. This task is performed by specific glycosyltransferases. For example, in the first step of the oligosaccharide building process, a unit of N-acetylglucosamine is added by the enzyme N-acteylglucosaminyltransferase.[6,7] Then, several mannose and glucose units are inserted, but each addition requires the action of unique mannosyl and glucosyltransferases. After the core oligosaccharide is transferred to the protein, three units of glucose are trimmed by glucosidases (Figure 1-1).[6,7] The glycoprotein processing continues in the Golgi apparatus, where more sugar units are trimmed by glycosidases and more monosaccharide units are added by glycosyltransferases. The final oligosaccharide composition will depend on the conformation and sequence of the protein that is being processed and the glycosyltransferase composition of the particular Golgi apparatus.[6,7] Among other species, different viruses utilize this same pathway to form their viral and cellular surface coats, making the elucidation and complete understanding of the glycosylation process a very attractive topic for the pharmaceutical industry. In addition,

bacterial wall biosynthesis proceeds through a similar glycosyl transfer mechanism. Two compounds that block this oligosaccharide synthesis are tunicamycin and bacitracin.[6,7] In particular, bacitracin is actually used as an antibiotic because it can not cross mammalian cell membranes.

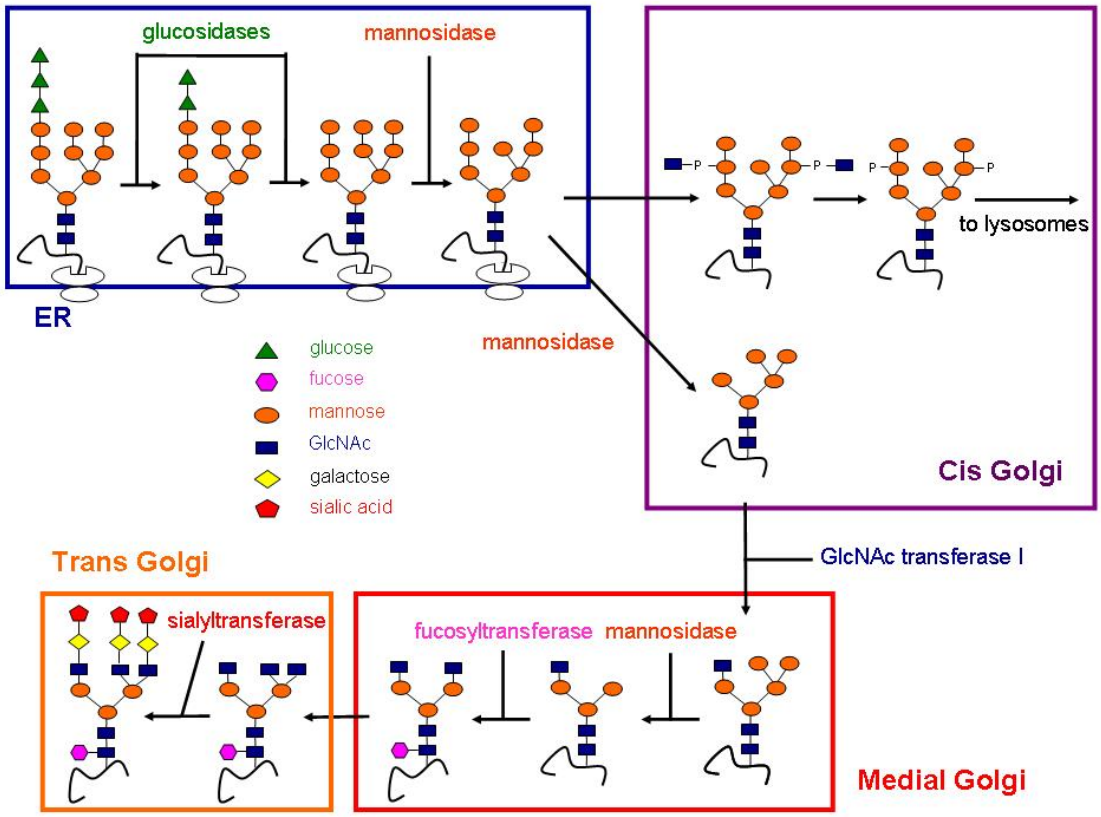


Figure 1-1. Schematic pathway of protein glycosylation adapted from Stryer, L., Biochemistry, 4th ed.[8]

It has been shown that carbohydrate-processing enzymes are also implicated in the development of several types of tumors.[9] High levels of glycosidases in blood are observed in patients with different cancerous pathologies. Moreover, many tumor cells showed distorted expression of glycosyltranferases, which is ultimately reflected in an abnormal glycosylation pattern.[9]

**Basic Mechanism**

In general, enzymatic glycoside bond hydrolysis is a nucleophilic substitution at the anomeric carbon of a sugar, which can occur through either retention or inversion (Figure 1-2).[4]

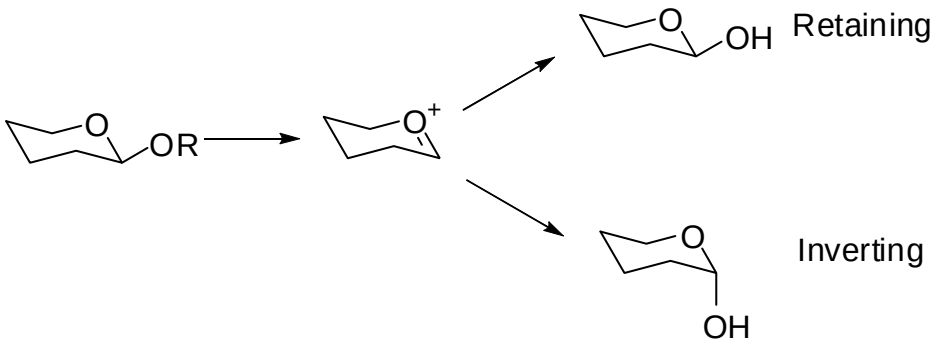


Figure 1-2. Possible configurations in glycosidic bond cleavage

Consequently, retaining and inverting enzymes will proceed through two different mechanisms, and it should be pointed out that due to typically rapid mutarotation rates, the product configuration at the anomeric carbon will be rapidly scrambled. The inverting enzymes possess a general acid residue at their active site, which assists by protonating the departing aglycon oxygen of the glycosidic bond, and a basic amino acid that deprotonates the attacking hydroxyl of the acceptor. This process is consistent with a single-displacement mechanism involving an oxocarbenium ion-like transition state (TS).[3,4,10-14] On the other hand, the retaining carbohydrate-processing enzymes are suggested to proceed through a double-displacement mechanism. In this case, one of the active site residues acts as a nucleophile, forming a labile glycosyl-enzyme intermediate, which is immediately attacked by the incoming sugar acceptor. The glycosidic oxygen (first step) and the sugar acceptor (second step) are previously activated by another active site residue that operates as an acid/base catalyst. Both steps are considered to proceed through a TS with extensive oxocarbenium ion character.[3,4,10-14] X-ray crystallography of proteins covalently labeled with fluorosugar substrate analogs and kinetic characterization of

wild-type and mutant enzymes have been utilized to study these two possible mechanisms.[3,13] For example, kinetic isotope effects have served not only to explore the formation of the covalent glycosyl-enzyme intermediate (secondary deuterium isotope effect greater than 1 for deglycosylation step) but also to determine the oxocarbenium ion character of the TS (inverse isotope effect due to $sp^2$ hybridization of the anomeric carbon).[3] In addition, trapping and crystallography experiments with deoxyfluoroglycosides were also highly valuable for the characterization of the covalent intermediate.[3,13] Finally, site directed mutagenesis has been used to identify the residues that may participate as general acid/base catalysts. Changing the critical amino acid required for catalysis will have a strong effect not only on the kinetic parameters but also on the pH profile of the enzyme.[3,13] In most cases, asparagine, glutamine and alanine are the substitute residues for glutamic and aspartic acid. They conserve approximately the size of the amino acids that are replacing but lack the possibility to function as acid or base catalysts.[3,13]

Non-enzymatic studies of the glycosyl bond hydrolysis have shown that the reaction involved the departure of the aglycon, which is assisted by the oxygen lone pair electrons, followed by the formation of an extremely short lived glycosyl cation.[4,15] The stability of this oxocarbenium ion will depend on the solvent and nucleophile used in the reaction.[4,15] Based on these studies and other evidence obtained in enzymatic systems, it was proposed that the enzymatic glycosyl hydrolysis occurs as well via an oxocarbenium ion TS. One example of this correlation was presented by Bruner and Horenstein with their mechanistic studies on $\alpha(2\rightarrow6)$-sialyltransferases.[16] Measurement of beta secondary dideuterium isotope effects showed that this enzyme TS involves considerable glycosyl cation formation. Comparison of this result with the one obtained for the acid-catalyzed solvolysis of CMP-N-acetyl neuraminate had established that the sialyltranferase transition state has oxocarbenium ion character quite similar to the one for

solvent hydrolysis. In addition, the solvolysis results were complemented with an ab-initio computational analysis of the predicted kinetic isotope effects. Both approaches were in agreement with the oxocarbenium ion TS structure.[17] Another example on the oxocarbenium ion TS characterization was obtained by Withers and co workers research on *Agrobacterium* β-glucosidase.[14,18] This enzyme is a retaining glycosidase and accordingly, it proceeds through a two step mechanism. Another valuable tool used to explore details of glycosyl-transferring enzyme mechanisms are TS analogs. Properly designed inhibitors could provide useful information about enzyme-substrate contacts, and a good transition state analog would be expected to be a potent inhibitor of the enzyme. Hence, studies aimed at the synthesis of such compounds are of considerable interest. This aspect of the enzyme mechanism field will be further discussed in the course of this chapter.

**Glycosidase Families**

Glycosidases (EC 3.2.1.x) catalyze the hydrolysis of the glycosidic bond that connects a sugar anomeric carbon with a glycan (Figure 1-3).

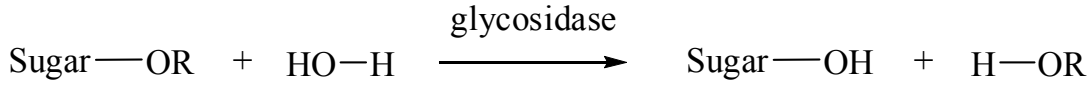


Figure 1-3. Glycosidase catalyzed reaction

Based on the recently updated internet database (www.expasy.ch/cgi-bin/lists?glycosid.txt), glycosidases constitute a clan of around 100 families of more than 1000 enzymes, which are classified by Henrisatt on the basis of sequence similarities.[19,20] Around 150 of these enzymes still remained unclassified and for more than 60 families the three-dimensional structures are known.[20]

**Structure**

Based on crystallographic characterizations, the general amino acid arrangement on the catalytic domain of many glycosidases is $(\alpha/\beta)_8$ or a TIM barrel.[10,21] This barrel structure was first found in triose-phosphate isomerase (TIM) but is frequently present is several protein folds.[22] The TIM barrel is constituted by eight α helices and eight parallel β strands. This protein fold has the shape of a toroid in which the β strands are located inside the doughnut, with the α helices forming the outer surface. In the TIM barrel, the secondary structures are connected by loop regions that could differ in length depending on the enzyme family. Among the glycosidases that present the $(\alpha/\beta)_8$ motif are for example, α and β-amylases, glucanotransferases, xylanase/glucanase from *C. fimi* and the widely studied β-galactosidase from *E. coli*. Some other families that have a distorted TIM barrel are endoglucanase E2 and β-glucanases.[10] Due to the diversity of glycosidase substrates, there are other folds that could be observed such as α/α barrel, β-barrel or β-sandwich.[10] Usually, glycosidases have one or more catalytic subdomains, one of them utilized for catalysis and the other one for substrate binding.[10,23] Active site topologies could be divided in three categories: 1) pocket or crater, found in exoglycosidases such as β-galactosidases, β-glucosidases, sialidases and neuramidases, which hydrolyze sugar units from the non reducing end of glycoconjugates; 2) cleft or groove, found in endoglycosidases such as lysozyme, endocellulases, chitinases and glucanases, which cleave the internal glycosidic bond within oligosaccharides; and 3) tunnel, observed in cellobiohydrolases when the cleft is covered by some of the protein loops.[23]

**Inverting and Retaining Mechanisms**

Regarding glycosidase active sites, it was already mentioned that glycosidic bond hydrolysis could be accomplished with either retention or inversion of the anomeric carbon

configuration. In most glycosidases, the typical active site has an arrangement of two carboxylic amino acids situated on opposite faces of the catalytic pocket.[4,10-14] For the inverting glycosidases, they are located around 10.5 Å apart from each other, leaving enough space to hold the substrate and a molecule of water.[4,10-14] In particular, while one carboxylic acid acts as a general base, helping water attack at the anomeric center, the other one proceeds as a general acid facilitating the glycosidic bond hydrolysis (Figure 1-4).

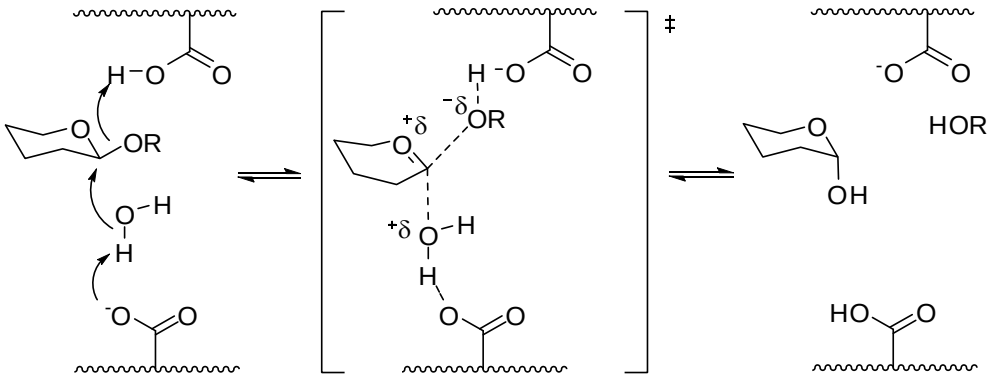

Figure 1-4. Proposed mechanism for inverting glycosidases adapted from the article published by Zechel, D. L. and Withers, S. G.[14]

The enzymatic reaction takes place with a single-displacement mechanism having a TS with oxocarbenium ion character. On the other hand, for retaining glycosidases, these carboxylic residues are closer to each other (approximately 4.8-5.5 Å), which is consistent with a double-displacement pathway (Figure 1-5).[4,10-14]

In the glycosylation (first) step, one carboxylic acid acts as a nucleophile forming the enzyme-glycosyl bond, while the other assists the reaction by protonating the glycosyl oxygen. In the deglycosylating (second) step, the general acid catalytic residue proceeds now as the general base deprotonating a molecule of water that will cleave the covalent enzyme-substrate intermediate.[4,10-14] Both steps are known to involve a TS with oxocarbenium ion character. Typically, in retaining glycosidases, these two carboxylic acids are identified as glutamate or

aspartate. These amino acids were originally identified in lysozymes, which are the first glycosidases characterized by X-ray christallography[4,23]. Nevertheless, with the constant discovering and characterization of new glycosidases families, it was observed that other amino acid such as tyrosine or tryptophan could be critical for enzymatic hydrolysis.[10,14]

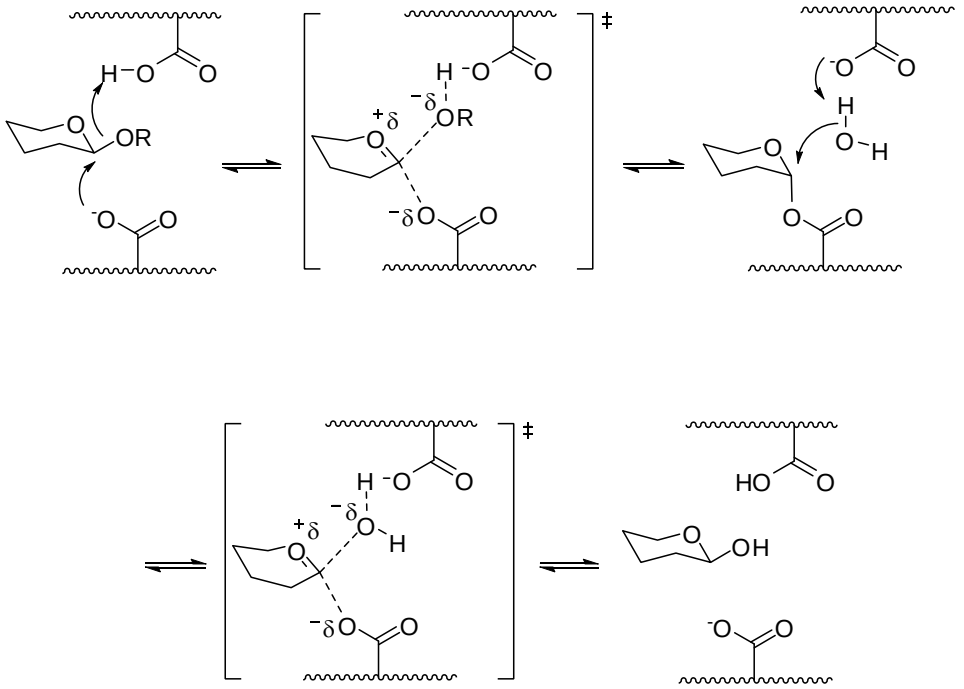

Figure 1-5. Proposed mechanism for retaining glycosidases adapted from the article published by Zechel, D. L. and Withers, S. G.[14]

Examples of enzymes that escape from the two types of mechanisms discussed above can also be found. Member of families 18 and 20, N-acetyl-β-hexosaminidases catalyzed hydrolysis by neighboring group assistance of their substrate N-acetyl group (Figure 1-6). In this case, the acetyl group acts as the nucleophile, forming an oxazoline, with the enzymic carboxylate residue proposed to stabilized the intermediate (or its formation).[11] Another particular class of α-glycosidases utilize an elimination reaction for glycosidic bond hydrolysis, liberating 1,5-anhydro-D-fructose instead of glucose (Figure 1-7).[11]

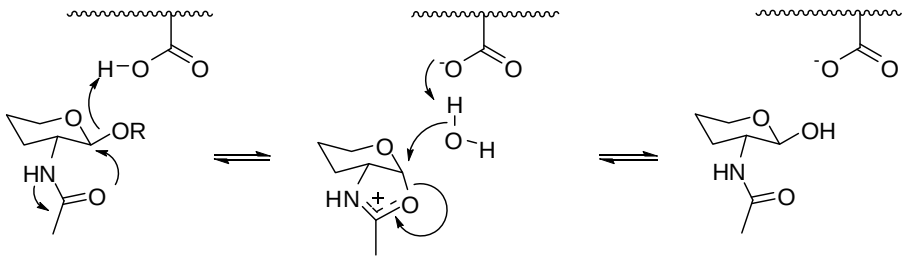

Figure 1-6. N-acteylhexaminidase catalyzed hydrolysis adapted from the article published by Rye, C. S. and Withers, S. G.[11]

**Mutagenesis and Labeling Investigations**

β-galactosidase from *E. coli*, a member of family 2 of glycosyl hydrolases, is one of the most studied retaining glycosidases. Based on its three-dimensional structure, the enzyme is a 1023 amino-acid polypeptide formed by four tetramers (465 kDa each).[24] Five separate domains and an extended N-terminus constitute the β-galactoside monomer. The catalytic domain displays an unconventional TIM barrel where the fifth α-helix is missing and the sixth β-strand is deformed.[24]

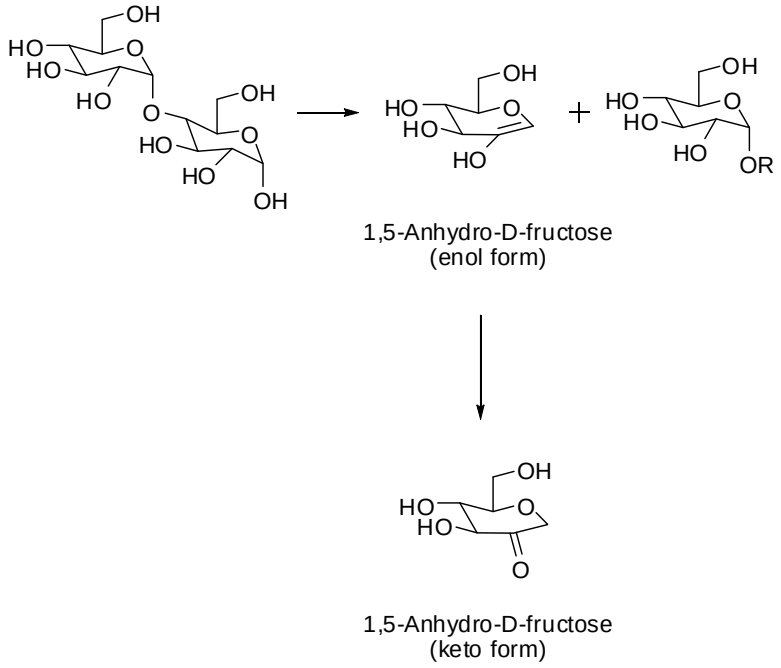


Figure 1-7. 1,5-anhydro-D-fructose generation from glycosidic bond hydrolysis. Adapted from the article published by Rye, C. S. and Withers, S. G.[11]

Affinity labeling experiments with conduritol C epoxide (Figure 1-8) initially identified Glu461 as the amino acid responsible of the glycosyl-enzyme intermediate.[25] Nevertheless, studies with different β-galactosidase mutants of Glu461 displayed a considerable remnant activity, which was a highly suspicious result for a critical catalytic residue.

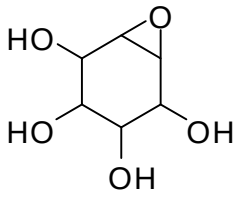


Figure 1-8. Conduritol C epoxide[25]

After trapping studies with 2-deoxy-2-fluoro-β-galactopyranoside and the three dimension structure resolution on this enzyme, Glu537 was assigned as the nucleophilic amino acid instead of Glu461.[3,10,24,26] Mutagenic experiments, in which Glu461 was replaced by Gly, Gln and Asp in conjunction with the crystal structure, revealed that this residue was also important for glycosidic bond cleavage due to its role as a general acid/base catalyst. In addition, it was observed that the essential $Mg^{2+}$ , required for the β-galactosidase reaction, acts as a $pK_a$ modulator for this residue.[3,10] Another example where site directed mutagenesis and crystallography have helped identify the amino acid responsible for catalysis is found in the case of *B. circulans* xylanase (Bcx). In this case, Glu172 was found to be the acid/base catalyst while Glu78 operates as the nucleophile (Figure 1-9).[3] Interestingly, Tyr69 is located close (~2.95 Å) to the enzyme-glycosidic intermediate. Consequently, it was proposed that this residue has a dual electrostatic interaction with the sugar oxygen and the oxygen of Glu78 which forms the bond with the substrate.[13,14] Withers and coworkers suggested that Tyr69 plays a critical role stabilizing at the same time, the positive charge developed on the monosaccharide ring oxygen by electrostatic interaction with the Tyr oxygen lone pair electrons, and the negative charge on

Glu78 by hydrogen bonding during the deglycosylation step.[13,14] This hypothesis was supported by observing a total loss of activity on the Tyr69Phe mutant.[27] Moreover, in the Bcx active site cleft, there is another tyrosine assisting Glu172 identified as Tyr80.[27] In conjunction with Tyr80, Glu172 activates the water molecule for the nucleophilic attack.

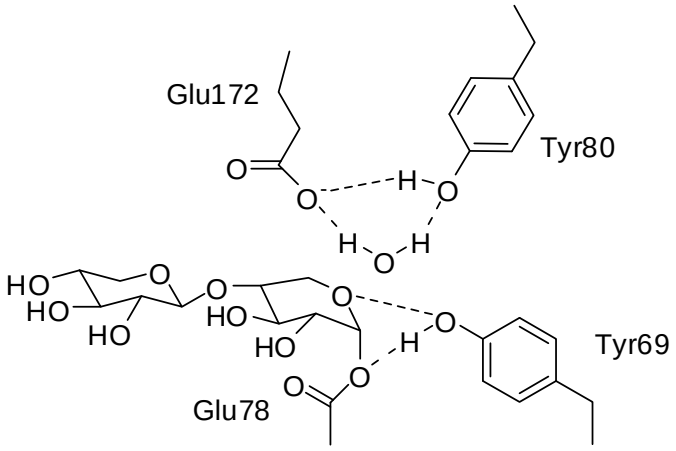


Figure 1-9. Active site structure of *Bacillus circulans* xylanase adapted from the article published by Zechel, D. L. and Withers, S. G.[13,14]

A surprising approach accomplished by mutagenesis is the possibility to switch the stereochemical outcome of a glycosidase.[13] Due to the close similarities of the hydrolases TS, an inverting glycosidase could, in principle, be converted into retaining and vice versa.[13] For retaining glycosidases, the most extensively utilized method is revoking the activity of the enzyme by exchanging the nucleophilic residue for a non-nucleophilic one.[3,13,14] An example in support of this hypothesis was observed when the nucleophilic Glu358 of β-glucosidase from *Agrobacterium sp.* (Abg) was replaced by an alanine.[18] This enzyme was chosen because of its extended substrate specificity. In principle, the Glu358Ala mutant was inactive to perform hydrolysis but, when placed in a medium that contained good nucleophiles such as azide, formate or acetate, the β-glucosidase activity was restored.[3,13,14] Thus, the product of this enzymatic reaction was obtained with inversion stereochemistry. Moreover, Glu358Ala Abg was

able to synthesize a β-disaccharide from α-glucosyl fluoride without any addition of an external nucleophile. In this way, a glycosidase could be turn into a mutant glycosynthase capable of building polysaccharides.[3,13,14] In a parallel manner, inverting glycosidases can be transformed into retaining ones by incorporating a nucleophilic amino acid (Glu or His).[3,14] The residue needs to be situated in the space typically occupied by the water molecule. This experiment was successfully carried out by Kuroki *et al.* on bacteriophage T4 lysozyme.[28] This enzyme was also found to be capable of transglycosylation.[28]

**Design and Synthesis of Glycosidase Inhibitors**

Considerable effort has been dedicated to the design and synthesis of inhibitors of carbohydrate processing enzymes, not only to elucidate the role of sugar residues in biological systems but also to provide information on enzyme-substrate binding contacts through investigation of structure-activity relationships. In addition, some glycosidase inhibitors have already been tested as possible therapeutic agents, for instance, against diabetes[29] and HIV viral replication.[30] Although glycosidases have been the subject of intense research, and considerable information is already available on their active site structures, inhibitor design remains a complicated task. It is not yet possible to reliably design a potent inhibitor by merely inspecting a crystal structure.

The work described in this dissertation takes a mechanism based approach to inhibitor design, in which our knowledge of the shape and charge of a transition state serves as the template for the design of synthetic targets. A key requirement for an efficient inhibitor includes high stability and high binding affinity for the enzyme active site. The latter is usually provided by TS analogs.[31] Aldolactones and gluconolactones were among the first discovered competitive

glycosidase TS analog inhibitors; D-glucono-1,5-lactone (Figure 1-10) was among the most potent.[32,33]

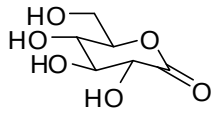


D-glucono-1,5-lactone

Figure 1-10. D-glucono-1,5-lactone structure[32,33]

The inhibitory potency of these compounds against numerous glycosidases in part comes from their resemblance to the pyranosyl and furanosyl part of the substrate sugars. In addition, it was believed that the source of the lactones' inhibiting activity was due to their ability to adopt a half chair conformation similar to the glucopyranosyl cation.[33] In other words, the flattened lactone ring is a geometric analog of a glycosyl transfer transition state. Subsequently, a lot of potent ($K_i$ in the μM range) nitrogen-containing glycosidase inhibitors have been identified, including a) polyhydroxylated piperidines and pyrrolidines; b) indolizidine alkaloids[34]; c) amino sugars[35,36]; d) amidines, amidrazones and amidoximes[37-40]; and e) imidazoles, tetrazoles and triazole.[41-43] These differ from the lactone inhibitors in that the basic ring nitrogen can be protonated, providing a mimic of the oxocarbenium ion transition state's charge.

**Polyhydroxylated piperidines and pyrrolidines**

The first nitrogenous glycosidase inhibitor known was the polyhydroxylated piperidine nojirimycin (Figure 1-11).

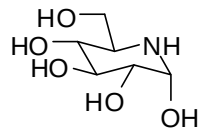


Nojirimycin

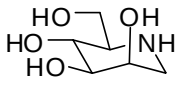


1-deoxymannojirimycin (DMJ)

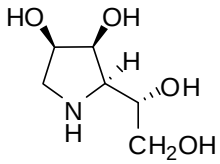


1,4-dideoxy-1,4-imino-D-mannitol

Figure 1-11. Polyhydroxylated piperidines and pyrrolidines analogs[9,44,45]

Being a D-glucose analog where the oxygen has been replaced by NH[33,45], this compound resulted in a potent α and β-glucosidase inhibitor. Another piperidine based inhibitor is 1-deoxymannonojirimycin (DMJ) (Figure 1-11). This compound is obtained from nojirimycin B (mannojirimycin) by biosynthetic reduction of the anomeric hydroxyl group.[46] DMJ blocks the production of high-mannose oligosaccharides to more complex glycans by inhibiting the Golgi α-mannosidase ($K_i$ of 750 μM).[9] Hydroxylated pyrrolidines, which mimic the furanosyl moiety, also display inhibition of the corresponding glycosidase. An example of this family of compounds is 1,4-dideoxy-1,4-imino-D-mannitol, which turned out to be a good inhibitor for jack bean and human lysosomal α-D-mannosidase with $K_i$s of 0.8 μM and 13 μM, respectively (Figure 1-11).[9]

**Indolizidine alkaloids**

This kind of glycosidase inhibitor has a fused piperidine and pyrrolidine as a core structure (Figure 1-12).

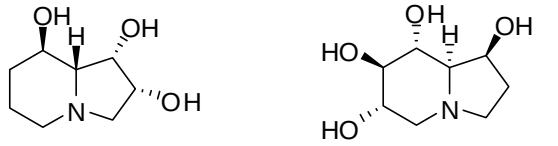


Swainsonine Castanospermine

Figure 1-12. Indolizidine alkaloids[9,34]

In general, target glycosidases are inhibited by these alkaloids because either the piperidine mimics the pyranosyl, or the pyrrolidine mimics the furanosyl moiety of their substrate.[9] The interest on indolizidine alkaloids arose from the study of swainsoma toxicosis (an animal neurological disease caused by a plant). The toxin, identified as the alkaloid swainsonine (Figure 1-12), is a very potent lysosomal α-mannosidase and Golgi α-mannosidase II inhibitor.[9] Another common alkaloid is castanospermine (Figure 1-12). In this case, the piperidine portion of the

molecule mimics the structure of glucose. Consequently, this indolizidine acts on lysosomal α and β-glucosidases ($K_i$ of 0.1 μM and $K_i$ of 7 μM respectively)[9] and endoplasmic reticulum α-glucosidases I and II.[9,34] Both castanospermine and swainsonine were found to be useful in preventing metastasis dissemination in mice. These compounds block the formation of complex oligosaccharides implicated in metastasis, implying their potential used in cancer treatment.[9] Due to its ability to inhibit carbohydrate-processing glycosidases, castanospermine can influence the infectivity of certain viruses like HIV.[9] However, when influenza virus was generated in the presence of this indolizidine, its infective strength remained intact.[34]

**Amino sugars**

Falling in the category of amino-pentose, nectrisine (Figure 1-13) was a very potent α-glucosidase and α-mannosidase inhibitor with an $IC_{50}$ of 0.05 μM and 6.5 μM respectively.[35] This inhibitor was first isolated from the fungus *Nectria lucida* which was found to act as the own fungus inmunomodulator.[35] Full synthesis of nectrisine has been reported by Kayakiri *et al.* from D-glucose[35] and by Chen *et al.* from D-arabinose.[47]

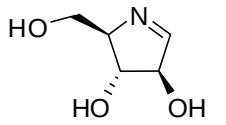

Nectrisine

Figure 1-13. Nectrisine structure[35]

**Amidines, amidrazones and amidoximes**

The importance of this class of compounds arises from their capability of simulating, at the same time, the charge and the planarity of glycosidase's oxocarbenium ion-like TS.[48] The diaza functional group can be easily protonated, allowing equal distribution of charge within the trigonal planar system. Based on different literature reports,[39,43,48] not only the charge

distribution, but also the spatial configuration are important issues to take in account in order to produce potential inhibitors that duplicate the hypervalent transition state geometry.

A broad range of amidine-containing compounds had been synthesized by different research groups.[37,48,49] Among the amidines family, D-glucoamidine **1** (Figure 1-14) exhibited a potent inhibitory activity on sweet almond β-glucosidases ($K_i$ of 10 μM) and jack bean α-mannosidase ($K_i$ of 9 μM).[48]

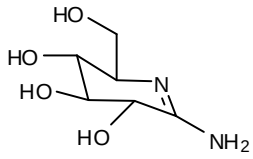


D-glucoamidine 1

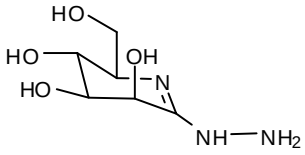


D-mannoamidrazone 2

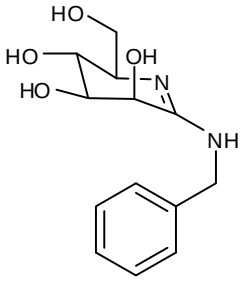


3

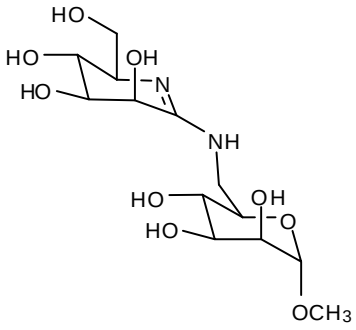


4

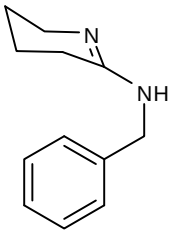


5

Figure 1-14. Amidines and amidrazones glycosidases TS analogs[37,48,49]

Using a group of amidines with a different number of hydroxyl substituents, Bleriot *et al.* showed the importance of mimicking the backbone of glycosidases sugar substrate. From these studies, the fully hydroxylated amidines **3** and **4** (Figure 1-14) displayed the strongest competitive potency against jack bean α-mannosidase and sweet almond β-glucosidases, with a $K_i$ of 0.55 μM and 5 μM, respectively. On the contrary, the non hydroxylated analog **5** (Figure 1-14) showed a $K_i$ of only 14 mM for the α-mannosidase and 3.7 mM for the β-glucosidases.[37]

With respect to the amidrazones series, Ganem and coworkers's D-mannoamidrazone[38,39] **2** (Figure 1-14) proved to be one of the most potent inhibitors for α-mannosidases, with a $K_i$ of 170 nM. Furthermore, this compound turned out to be a broad spectrum inhibitor because it had also shown activity against β-glucosidases, as well as β-galactosidases and other mannosidases.[38,39] It was suggested that the conformational structure of D-mannoamidrazone is one of the features responsible for its extensive inhibitory activity. When it is compared with the exocyclic carbonyl of aldo and gluconolactones, the amidrazone endocyclic tautomer seems a better mimic of the half chair conformation adopted by the substrate at the TS.[38]

**Imidazoles, tetrazoles and triazole**

Tetrazole and triazoles derivatives[43] are aldolactones analogs which have a half chair conformation as a consequence of the fused aromatic ring (Figure 1-15). The similar conformation adopted by aldolactones and the azole derivatives was actually confirmed by three dimension crystallography.[43]

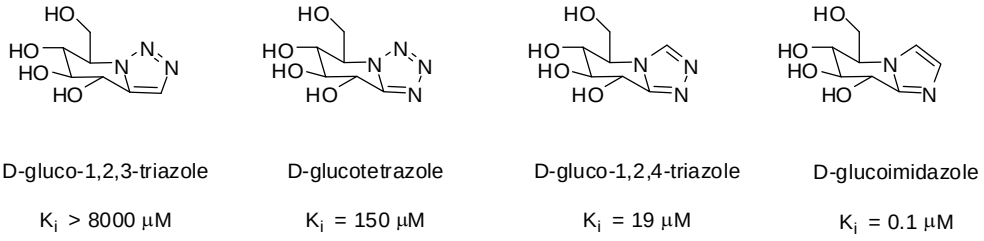


Figure 1-15. $K_i$ comparison of D-glucoazole TS analogs[43]

Tetrazole inhibitory potency was found to be comparable with D-glucono-1,5-lactone. Moreover, based on kinetic and mutagenic studies on different glycosidases,[43] tetrazole monosaccharides could be considered a good representation of a TS analog.[43] On the other hand, 1,2,3-triazole analogs showed a drastic decrease in activity when compared with the related tetrazoles ($K_i$ > than 8000 μM for triazole and 200 μM for tetrazole when tested on almond β-glucosidase).[43]

The importance of substrate protonation during glycosidase enzymatic reaction was addressed with non annulated imidazole derivatives.[42,50] In this case, it was suggested that the proton transfer proceeds from one carboxylic acid to the neighbor through the heterocyclic ring. These kinds of analogs showed modest inhibitory potency, in particular for β-glucosidases.[42,50] Having these results in mind, several authors reported the synthesis and corresponding kinetic analysis on annulated imidazoles derivatives (Figure 1-15).[43] Being part of this category of imidazole analogs, tetrahydropyridoinidazole **6** (Figure 1-16) is one of the most potent glycosidases inhibitors known so far,[41] with a $K_i$ of 1.2 nM and 0.11 nM for β-glucosidase from almonds and *Caldocellum s.* respectively.

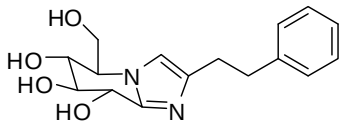


5-hydroxymethyl-2-(2-phenylethyl)-
5,6,7,8-tetrahydroxyimidazole

6

Figure 1-16. Tetrahydroxyimidazole derivative[41]

This class of compounds was also a valuable tool for a better characterization and understanding of glycosidases proton transfer. To complete the analysis of enzyme-azole derivatives interaction, 1,2,4-triazoles were synthesized.[43] A comparison of $K_i$ among the series of annulated azole TS analogs on β-glucosidase from almonds is shown in Figure 1-15. From the difference between tetrazole and 1,2,3-triazole behavior, and the assumption that proton transfer from the enzyme to the substrate is important for inhibition, it was proposed that, instead of the generally presumed "above-the-anomeric-plane" protonation, an "in-plane" or lateral proton transfer might be occurring (Figure 1-17).[43] This theory is also consistent with glycosyl bond hydrolysis because the glycosidic oxygen lone pair electrons are oriented, one perpendicular to

the other one. Consequently, "above-the-plane" and "in-plane protonation" are both perfectly possible. Another result that supported the lateral proton transfer is the correlation of the inhibitory potency and the basicity of the analogs. The more basic the heterocycle, the stronger should be its potency, which is observed on the corresponding $K_i$ sequence where tetrazole > 1,2,4-triazole > imidazole.[41,43] Additional evidence of lateral protonation was found in docking experiments using tetrazole analogs on β-galactosidase from *E. coli*, white clover β-glucosidase, *Cellulomonas fimi* cellulose and 6-phosphogalactosidase from *L.lactis*.[43] For this last enzyme, an X-ray structure in the presence of its substrate also suggested the in-plane proton transfer mechanism was operative.[43] Additionally, if the catalytic carboxylic acid is situated on the same plane of the sugar ring, there is more room for the pseudoaxial departure of the glycon, which facilitates the hydrolysis.

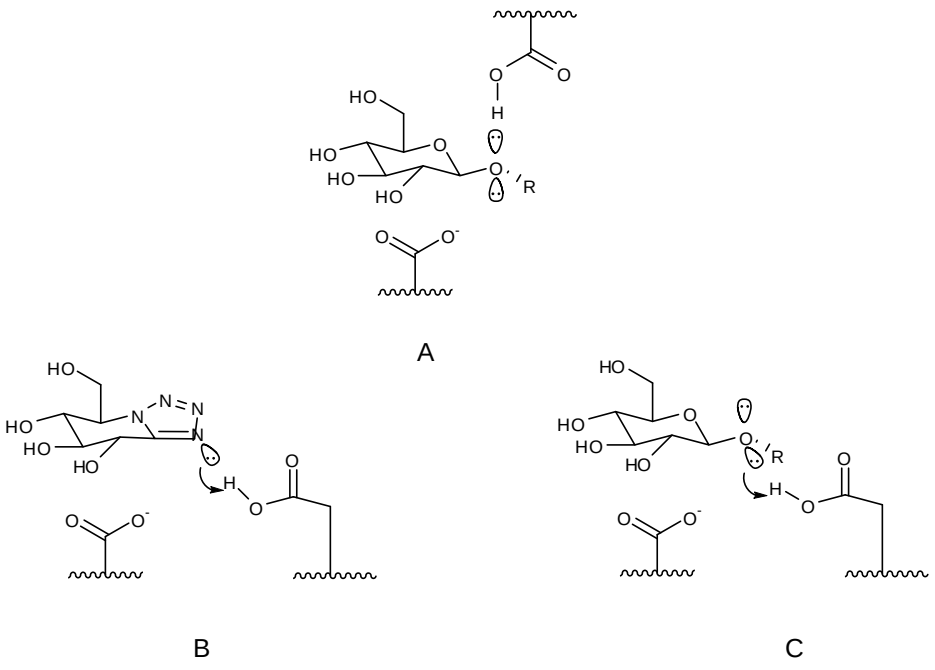


Figure 1-17. Proposed glycosidases in-plane or lateral protonation. A) above the plane glucoside protonation. B) and C) tetrazole and glucoside protonation in the plane of the pyranose ring. The figure was adapted from the article published by Heightman, T. D. and Vasella, A. T.[43]

## Glycosyltransferases

Compared with glycosidases, there is much less information about NS glycosyltransferases (EC 2.4.x.y). In this case, 78 families have been arranged by sequence homology from which only 20 families have been characterized by X-ray.[20,51] Glycosyltransferases catalyze the transfer of a single monosaccharide unit from an activated nucleotide donor to the hydroxyl group of an acceptor saccharide (Figure 1-18).[52,53]

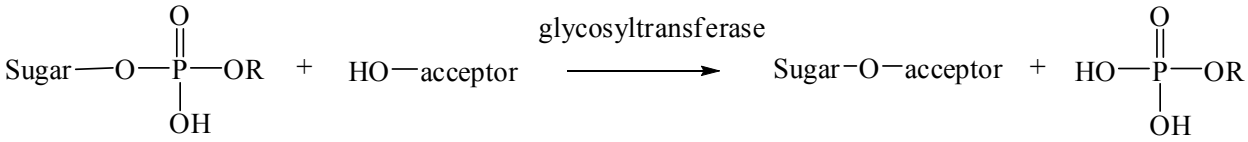


Figure 1-18. Glycosyltransferases catalyzed reaction[52]

The most common nucleotide sugars are: UDP-glucose (glucosyltransferase), UDP-galactose (galactosyltransferase), UDP-N-acetylglucosamine (N-acetylglucosaminyltransferase), UDP-N-acetyl-galactosamine (N-acetylgalactosaminyl transferase), GDP-mannose (mannosyltransferase), CMP-N-acetylneuramic acid (sialyltransferase), and GDP-fucose (fucosyltransferase).[52,53]

### Structure

Typically, glycosyltransferases are transmembrane glycoproteins localized in the Golgi apparatus.[53] Surprisingly, they do not share sequence homology within the family, but they all have the same overall domain structure. In general, glycosyltransferases are characterized by a short N-terminal cytoplasmic tail, a 16-20 amino acid signal-anchor sequence, an extended stem section and a large lumenal C-terminal catalytic domain (Figure 1-19).[53] The signal-anchor fragment has the function of not only fixing the enzyme to the membrane, but also giving the catalytic domain a certain direction inside the Golgi.[53] The stem domain (35 to 62 residues) may

provide the flexibility needed for the glycosylation of soluble and membrane proteins during their processing.[53]

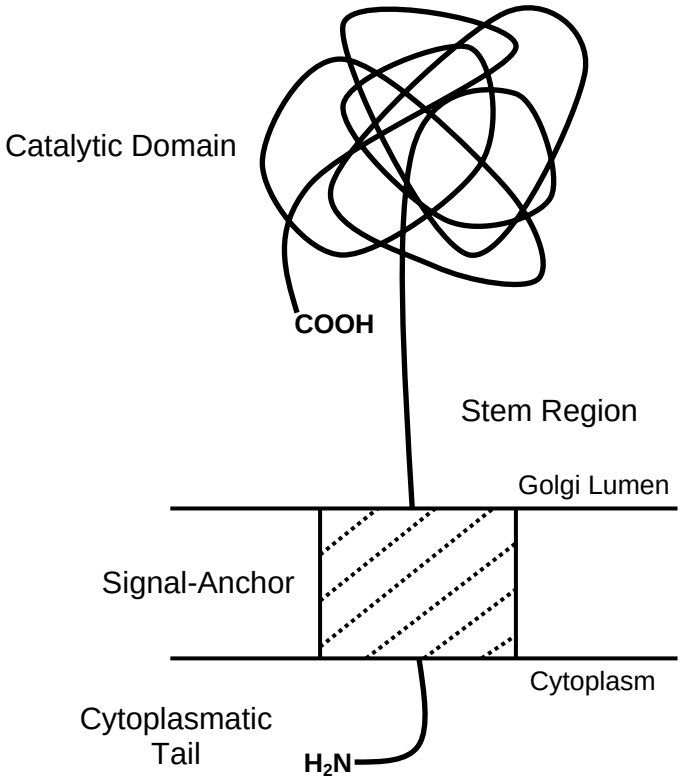


Figure 1-19. Glycosyltransferases topological structure adapted from the article published for Paulson, J. C. and Colley, K. J.[53]

From the X-ray structures solved to date, it was observed that glycosyltransferases adopt two folds. One of them is the so-called GT-A fold, which was initially discovered in the transferase *Bacillus subtilis* SpsA, and the other one is the GT-B fold found in phage T4 β-glucosyltranferase.[54-56] The GT-A fold is constituted by two β/α/β domains that appeared to form a continuous sheet of eight β-strands. On the other hand, the GT-B fold exhibits two Rossmann β/α/β domains separated by a large cleft, frequently observed in nucleotide binding proteins.[54] It was shown for both GT-A and GT-B members that while one domain is involved in nucleotide binding, the second is engaged in acceptor binding.[54] Interestingly, the GT-A members share the

common feature of containing an $M^{2+}$ ion (M = metal) which is coordinated by side residues and the nucleotide phosphates. This arrangement, usually called DXD motif, is commonly constituted by carboxylic amino acids.[54,55] Metal ions are not normally found in the crystal structure of GT-B enzymes, which is consistent with the absence of DXD motif within their catalytic active site.[54]

**Inverting and Retaining Mechanisms**

As for glycosidases, glycosyltranferases could be divided into retaining and inverting enzymes, based on the stereochemical outcome of their products. In this case, the inverting transferases have been well characterized but, on the contrary, retaining glycosyltransferase mechanisms are still under debate.[54,56] In both cases, it was found that the mechanism involves an oxocarbenium ion TS. For the inverting enzymes, it is typically proposed that the reaction proceeds through a concerted displacement in which the metal cation is used as the general acid catalyst.[56] For the retaining glycosyltransferases, no glycosyl-enzyme intermediated has been found. Consequently, the double-displacement mechanism, suggested for glycosidases, seems inconsistent with the experimental results obtained for glycosyltransferases. From site directed mutagenesis and 3D structure of *Neisseria meningitides* α-galactosyltranferase LgtC, Withers *et al.* proposed that the enzymatic reaction occurs by a "front side $SN_2$-like attack" or $S_Ni$-like mechanism, where the acceptor nucleophilic attack and the leaving group departure proceed on the same phase (Figure 1-20).[57] Based on this proposed mechanism, the departing aglycon is protonated by the incoming acceptor. Nevertheless, the feasibility of this reaction is inconsistent with the low acidity of the acceptor hydroxylic hydrogen. More experimental results will be required for a clearer understanding of the retaining glycosyltransferases mechanism.

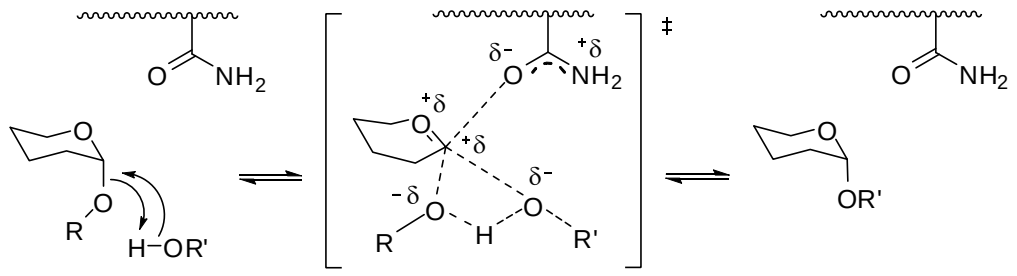

Figure 1-20. Proposed $S_Ni$-like mechanism for *Neisseria meningitides* α-galactosyltransferase LgtC adapted from the article published by Lairson, L. L. and Withers, S. G.[56]

**Sialyltransferases**

Sialyltransferases (ST) catalyze the transfer of sialic acid from an activated nucleotide donor cytidine monophosphate-N-acetylneuraminate (CMP-NeuAc) to the hydroxyl group of an acceptor saccharide (Figure 1-21).[52] The enzymatic reaction occurs through a nucleophilic attack with inversion of configuration at the anomeric carbon of sialic acid. The ST family shares the common feature of identifying only β-linked CMP-NeuAc as the sialyl moiety donor, but they diverge in their specificity on glycan acceptor and the class of glycosidic bond they form.[58,59] As mentioned before, ST are localized in the Golgi apparatus of both microorganism and mammals cell, but they can also be found as the free soluble enzyme in the colostrum of different animals.[59]

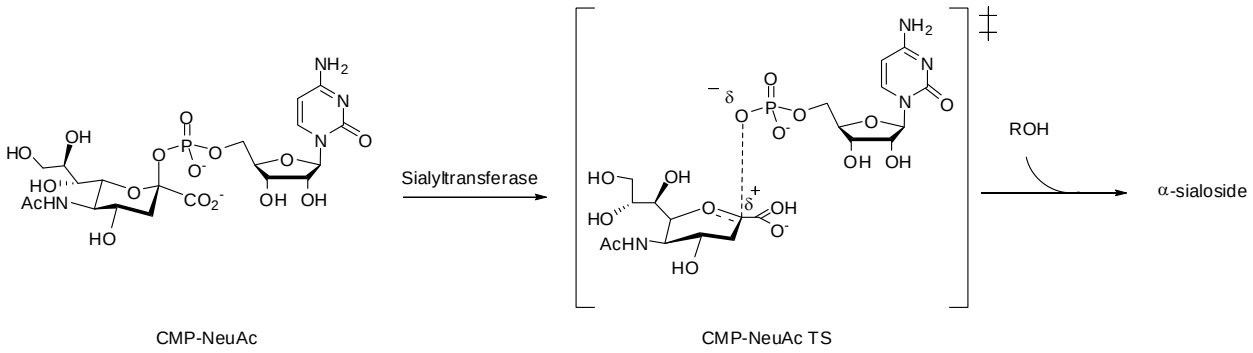


Figure 1-21. Sialyltransferase catalyzed reaction[60]

**Sialic acid**

Sialic acids are a family of related nine-carbon carboxylated sugars derived from neuramic acid (Figure 1-22).

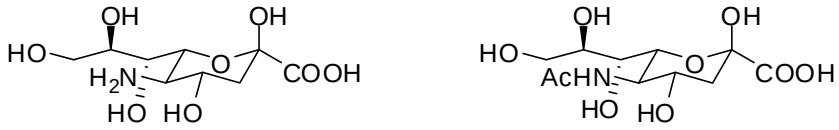


Sialic acid
(Neuramic acid)

N-acetylneuramic acid
(Neu5Ac)

Figure 1-22. Sialic acid and N-acetylneuraminic acid structures

They could be found at the non-reducing terminal position of sugar chains localized at the surface of microorganism and higher animals cells.[61] Differing in the position and characteristic of O- or N-linked substituents, 50 different sialic acid derivatives have been observed so far in nature. However, the most abundant are *N*-acetylneuraminic acid (Neu5Ac), *N*-glycolylneuraminic acid (Neu5Gc) and *N*-acetyl-9-*O*-acetylneuraminic acid (Neu5,9$Ac_2$).[61,62] The distribution of sialic acid derivatives in different organisms is related to the species and the cell function. For example, in humans, the most frequently found sialic acids are Neu5Ac and the O-acetylated and O-lactylated derivatives.[61] The main sialic acid linkages found in glycoproteins, glycolipids or oligosaccharides are: a) α(2→3) or α(2→6) to a galactose, such us Neu5Acα(2→3)Gal or Neu5Acα(2→6)Gal; b) α(2→6) to N-acetylgalactosamine or N-acetylglucosamine, such as Neu5Acα(2→6)GalNAc and Neu5Acα(2→6)GlcNAc; or c) α(2→8) or α(2→9) to a second sialic acid in Neu5Acα(2→8)Neu5Ac and Neu5Acα(2→9)Neu5Ac.[58,62]

Due to the charge character of sialic acids, they can modulate the electrostatic interaction between cells, act as anti-proteolytic agents on glycoproteins, and transport and bind positively charged molecules. Furthermore, the sialic acid chemical properties can be transformed by the inclusion of hydrophobic substituent such us O-acetyl and O-methyl.[61]

Having a strategic terminal position on glycoconjugates, sialic acids are involved in a variety of cell-cell recognition processes including cell development and differentiation. Moreover, they have also been implicated in oncogenic transformations, and they could serve as receptors for influenza virus.[58,61,62] The influenza virus interacts with the oligosaccharides situated in the outer side of their host cell surfaces. After its attachment to the cell, the virus utilizes a viral lectin (protein that binds oligosaccharides), known as Hemagglutinin (HA), and a viral sialidase to enter and infect the host. While the HA acts as an anchor to the plasma membrane, the sialidase removes the terminal sialic acid of the host oligosaccharide. This mechanism promotes the spreadability of the influenza virus because, without the terminal sialic acid, the cell tissue can no longer interact with other cells and mucus that protect the respiratory tract.[61,63] Other viruses that recognize the host, or use their own sialylated carbohydrates, are HIV and herpes.

Sialic acid can also be found as part of the structure of Sialyl Lewis ($SLe^x$) oligosaccharides. $SLe^x$ are ligands for the selectin proteins family which are involved in cell-cell adhesion processes. [58,61,64] The selectins are displayed on the endothelium (P- and E-selectin), platelets (P-selectin) and leukocytes (L-selectin). P-selectins assist, for example, the movement of T lymphocytes to infection or inflammation sites. Then, in order to start the immune response, the selectin attaches the lymphocytes to the infected tissue, using the lymphocytes $SLe^x$ oligosaccharide. These $SLe^x$ structures are also found in tumor cells, where the expression of sialyltransferases is usually deregulated.[58,65] Hypersialylated cell surfaces might camouflage the core oligosaccharide structure and keep the cancerous cell away from the immune response. In addition, selectins are generally implicated in metastases because they recognize these $SLe^x$ oligosaccharides. Consequently, in order to avoid the expansion of the tumor, the patient could

be treated with selectin antibodies, $SLe^x$ analogs or inhibitors like KI-8110 which prevents the transport of CMP-NeuAc into the Golgi vesicles (Figure 1-23).[58,61,66]

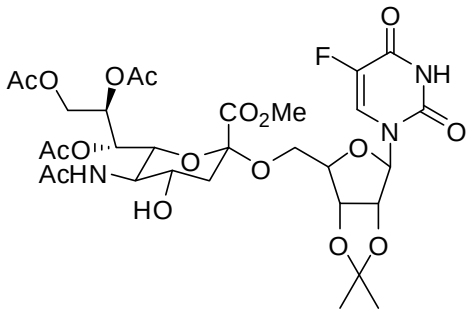


KI-8110

Figure 1-23. Inhibitor KI-8110[66]

Finally, some bacteria like *E. coli*, *Streptococci* and *Helicobacter pylori*, exhibit sialylated carbohydrates receptors on their surface. Therefore, they can adhere to the human digestive system and generate gastric inflammation and occasionally cancer. Bacteria adhesion can be revoked by the presence of soluble sialyl containing oligosaccharides, which can be found in human and animal milk.[61]

**Structure**

Although ST shares the common structural features of other glycosyltransferases, there is a reduced sequence homology (only 10 to 12% on their catalytic domain) within the family. This small conserved portion of the C-terminus catalytic domain is usually divided into three sialylmotifs. One of them is the large L-sialylmotif, which consists of a sequence of 48 to 49 amino acids. Site directed mutagenesis using alanine mutants has suggested that this motif is involved in the donor substrate binding. On the other hand, the short S-sialylmotif contains 23 residues, and it is proposed to bind both acceptor and donor substrate.[62,67,68] Both motifs contain a conserved cysteine amino acid and share donor binding participation. Thus, it was proposed that the L- and S-sialylmotif are linked by a disulfide bond which contributes to the catalytic

activity of the enzyme. [62,67] There is a third, very short, SV-sialylmotif which is suggested to operate in the stereochemical control of the ST reaction.[62]

The catalytic role of L-, S- and SV-sialylmotifs was also confirmed by deletion experiments on ST. It was shown that the enzyme conserves its activity, even after trimming 71 amino acids from the N-terminus. However, C-terminal truncation only delivers inactive enzyme.[67] Despite these ST sequence analyses and characterizations, the first crystal structure of a ST was obtained by Wither's group in 2004.[69] In this case, the enzyme was crystallized in the presence of free CMP and the substrate analog CMP-3-fluoro-N-acetyl neuramic acid. The soluble ST CstII was acquired from the human mucosal pathogen *Campylobacter jejuni* by truncating a section of the C-terminus region that fixes the enzyme to the membrane without disturbing the catalytic activity. CstII presents a tetramer architecture in which each monomer is conformed by 259 amino acids distributed into two domains. The secondary structure of one of these domains is organized in a α/β fold which has four α helices and a seven-stranded twisted β-sheet.[69] While the nucleotide binding region is arranged in a Rossman fold, the pocket for the nucleotide sugar is on the border of the β-sheet. Compared with this first domain (1-154 and 189-259 residues), the second domain is much smaller, composed only by 33 amino acids. In this case, the ensemble of α and β structures form a cap that rests over the active site.[69] Based on the classification of glycosyltransferases, CstII should be considered a member of the GT-A family due to its single Rossman fold. However, this enzyme lacks the DXD and metal cofactor that are generally found on the GT-A transferases.[69]

The crystal structure also helped to identify some of the key amino acids that participate in catalysis. Some examples are Tyr156 and Tyr162, which stabilized the nucleotide phosphate departure by hydrogen bond and His188, which might have the role of the general base

catalyst.[69] Mutation of all these residues resulted in a complete inactive CstII.[69] Unfortunately, CstII sialyltransferase and the mammalian enzymes do not share any significant sequence homology. As a result, any assumptions on mammals ST mechanism or structure, based on CstII 3D analysis, will be pure hypothesis, and await new crystallographic data.

**Mechanism**

Based on steady-state kinetics and kinetic isotope effect (KIE) experiments, the ST-catalyzed reaction is suggested to proceed through an $S_N1$-like mechanism with inversion of configuration, in which the leaving group CMP is almost completely dissociated before the incoming nucleophile attacks (sugar-acceptor) (Figure 1-21).[16,70] These studies were performed by Horenstein's group on α(2→6)ST from rat liver, which is one of the best characterized ST. KIE studies on this enzyme, using CMP-NeuAc and UMP-NeuAc, strongly supported an oxocarbenium ion-like transition state where positive charge is accumulated at C-1' and O-1', and the carboxylate group approaches coplanarity with the oxocarbenium ion plane.[16,70] It was also proposed that the reaction occurs without significant nucleophilic participation from the acceptor substrate side. Using UMP-NeuAc as the substrate, a bell-shape pH-rate profile of this enzyme was obtained. From this experiment, two ionizable groups, with pKa of 6.2 and 8.9, were observed.[70] The pH-rate profile in conjunction with theoretical calculations suggested that the nonbridging oxygen of CMP phosphate group was the target of protonation by the ST general-acid catalyst. Finally, KIE and steady state kinetic studies are consistent with a α-(2→6)ST random sequential mechanism.[16] It should also be noted that there is no evidence for a role for divalent metal cations in sialyltransferase catalysts which differentiate them from glycosyltransferases that use sugar nucleotide diphosphates as donor substrates.

**Sialyltransferase inhibitor design**

The search for ST inhibitors has been difficult due to intrinsic features of the enzymes such as a complex four-partner transition state, weak binding with their natural substrates, and limited structural data.

Based on inhibitory experiments performed on ST nucleotide analogs, the cytidine portion of the donor substrate seemed to be essential for ST recognition. This hypothesis was demonstrated by the fact that free sialic acid did not show any inhibition on a human serum α(2→6)ST catalytic reaction. On the other hand, early inhibition studies with different nucleotides placed CMP, CDP and CTP as the best ST competitive inhibitors with $K_i$ of 50 μM, 19 μM and 16 μM, respectively.[59,71] Other uridine- or adenosine-based nucleotides presented a non-competitive type of inhibition with $K_i$ in the range of 0.2 to 7 mM.[71] In addition, it was noticed that the number of phosphates present in the nucleotide affected the inhibitory potency in a sequential manner with CTP > CDP > CMP > cytidine or UTP > UDP > UMP. Comparative studies on cytidine, deoxycytidine and cytosine (with cytosine being the worst inhibitor) exhibited that, in some way, the ribose moiety provides favorable enzyme-substrate contacts (Figure 1-24).[71]

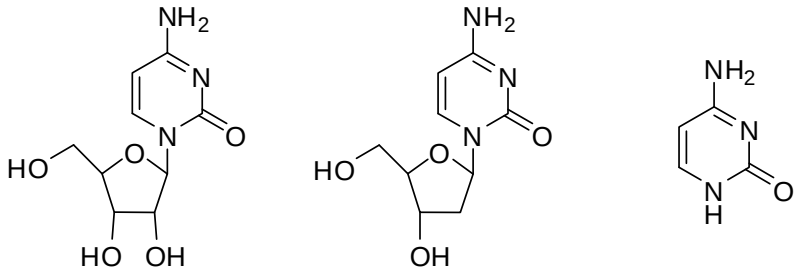


Figure 1-24. Cytidine, deoxycytidine and cytosine structures

Using these early results, several groups have designed ST transition state analogs that contained the cytidine moiety. For example, Schmidt and co-workers synthesized a series of CMP-quinic-acid-based ST analogs which displayed a ST inhibitory potency in the μM range (Figure 1-25).[72,73]

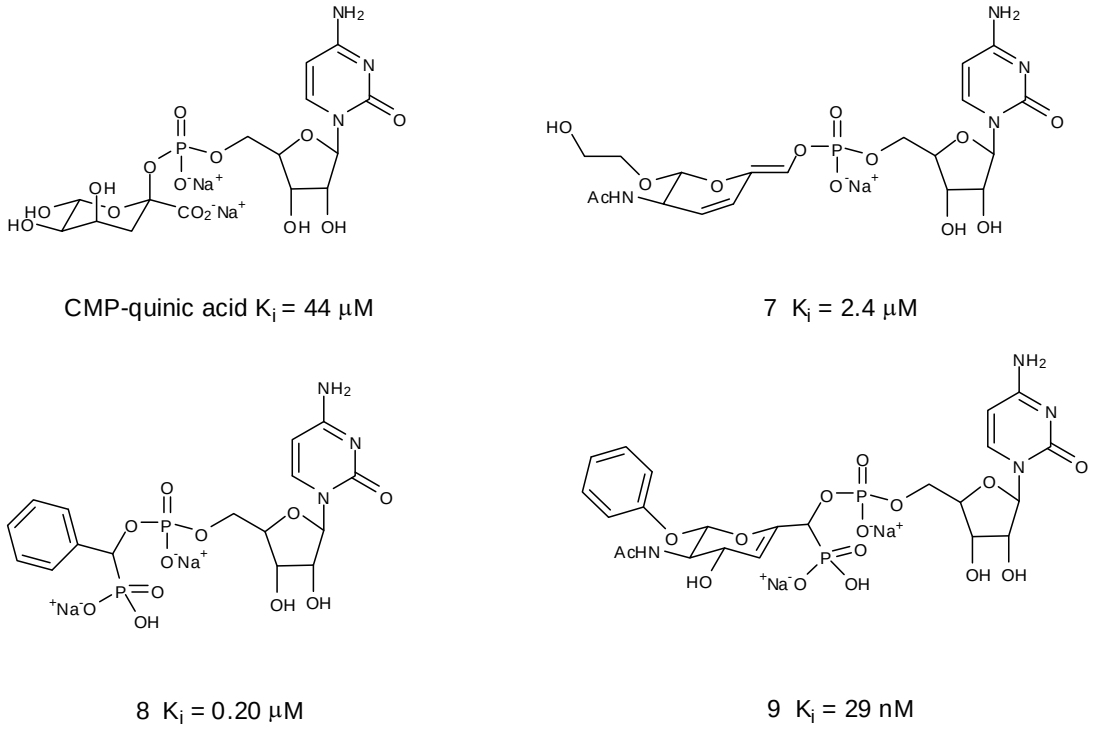


Figure 1-25. Schimdt's ST inhibitors[60,72-74]

Other series of compounds (see **7** in Figure 1-25) had planarity at the anomeric center mimicry, which incorporated a new TS feature in ST analogs design.[60,73,74] This element gives a better representation of the sugar conformation during the TS. Moreover, these compounds' activity was improved by not only increasing the distance between the anomeric center and the nucleotide but also including an extra negative charge into the glycosyl bond mimic (see compounds **8** and **9** in Figure 1-25).[60,73,74] From studies on these series of molecules, it was also observed that replacement of the sialic acid portion for an aromatic or alkyl group does not affect the inhibitory activity of the analog (compound **8** in Figure 1-25).[60,62] The enzyme might have a

hydrophobic pocket, closed to the catalytic site, that could help on the enzyme-substrate binding. In accordance with all these studies, the most potent inhibitor for ST (compound **9**) was found to be the molecule that possessed all of the structural elements discussed so far (Figure 1-25).[74,75]

Previously, our group has proposed and studied a new class of sialyltransferase inhibitors in which a bicyclic system, was used to mimic the TS conformation of these enzyme reactions.[76] The shape of these molecules loosely resembled a scorpion, hence the use of "scorpio" to denote members of this family. In these inhibitors, the CMP group attached to the bicyclic system was strategically held at a distance to simulate a late transition state for bond cleavage.[76] The first generation of scorpio inhibitors consisted of an unsaturated bicyclic structure conjugated with a carboxylated group (Figure 1-26).

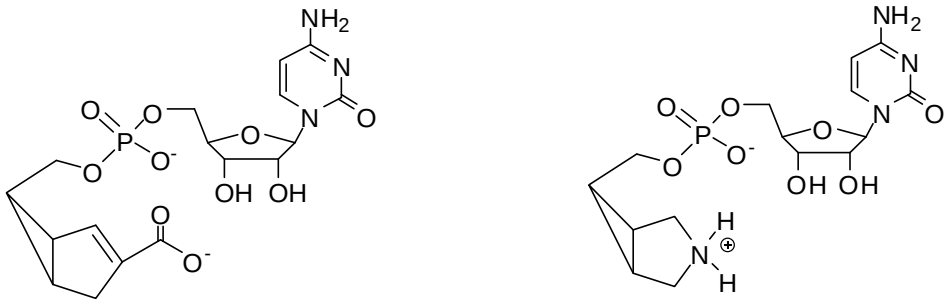

First Scorpio Generation

$K_i$ = 10 μM for α(2,3)ST
$K_i$ = 20 μM for α(2,6)ST

Second Scorpio Generation

$K_i$ = 5 μM for α(2,3)ST

Figure 1-26. ST transition state analogs synthesized by Horenstein's group[76,77]

Although these TS analogs presented a good inhibitory activity towards both α(2→3)ST and α(2→6)ST, with a $K_i$ of 10 μM and 20 μM respectively, they lacked positive charge at the anomeric center mimicry that could simulate the oxocarbenium ion TS. A second generation of scorpio molecules synthesized in our group mimicked the oxocarbenium TS positive charge with an amine functional group. This compound displayed a good potency on α(2→3)ST with a $K_i$ of 5 μM[77] (Figure 1-26). Following this structural mimetics approach and trying to improve the

inhibitory potency of the donor derivative, diazabicyclic transition state analogs were synthesized for ST inhibition studies (Figure 1-27).


Target Molecules

Figure 1-27. Proposed diazabicyclic TS analogs

Compounds possessing diaza functionality will mimic the development of positive charge on the anomeric center, allowing equal distribution of charge within the trigonal planar system. With the diazabicyclic compounds we will be incorporating certain key structural elements for sialyltransferase recognition: a) geometric requirements, i.e., trigonal planar center, b) CMP functionality, c) positive charge to mimic oxocarbenium character, and d) proper mimicry of bond distance between the departing phosphate and the position analogous to the anomeric carbon. Due to the close similarity between sialyltransferase and glycosidase catalytic mechanisms, the diazabicyclic TS analogs will be also suitable for the study and characterization of carbohydrate hydrolyzing enzymes (Chapter 4).

**Cyclopropane Derivatives**

Historically, cyclopropane derivatives have caught the attention of different chemistry-related scientific fields. The compounds importance arises not only from their unusual C-C single bonding that resembles a double bond but also from their great angular ring strain (27.5 kcal/mol).[78,79] In particular, cyclopropane derivatives have served as unique building blocks for the synthesis of biological related molecules. Either as a natural product or as a synthetic derivative, the cyclopropane ring has been part of molecules that have shown a variety of

biological functions like antiviral, antitumor or antibiotic agents, enzymes inhibitors, insecticides and agonists or antagonists for neural receptors. Consequently, cyclopropanoid molecules are useful in the design of novel therapeutic agents and characterization of biological mechanisms.

**Cyclopropanes Biological Implications**

An example of a bioactive cyclopropane derivative is 1-hydroxycyclopropanecarboxylic acid phosphate HPC (Figure 1-28). This compound acts as a competitive inhibitor for the enzymes that utilize phosphoenolpyruvate (PEP) (Figure 1-28) like PEP carboxylase, enolase and pyruvate kinase. It was proposed that HPC potency is related to its geometric and electronic structure similarity to PEP.[78]

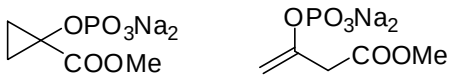


HPC PEP

Figure 1-28. HPC and PEP structures[78]

2,3-dihydroxy acids are used by microorganisms and higher organisms like plants and animals to synthesize amino acids. This synthesis is regulated by dihydroxy acid hydrolases through enzyme bound enol intermediates (see compound **10** in Figure 1-29). TS analogs for these enzymes could serve as herbicides or antibiotic agents. Via their electronic similarity with C-C double bond, cyclopropanoid compounds like **11a-d** are known to be good TS analogs for the hydrolases dehydration reaction.[78]


10 a $R_1$,$R_2$ = H
b $R_1$,$R_2$ = Me
c $R_1$ = Et, $R_2$ = Me
d $R_1$ = Me, $R_2$ = Et

11 a-d

Figure 1-29. Dihydroxy acid hydrolases enol intermediates and TS analogs[78]

In the mammalian central nervous system, L-glutamic acid works as an excitatory neurotransmitter. In order to investigate the mechanism and function of the glutamate receptors (GluR), different carboxycyclopropyl glycine (CCG) isomers have been prepared (Figure 1-30). In several cases the biological activity of a molecule is associated with its specific conformation and constraint. These two properties can be achieved by cyclopropane rings, which is demonstrated by the fact that only CCG **12** displayed a selective and potent agonist activity towards GluR.[78]

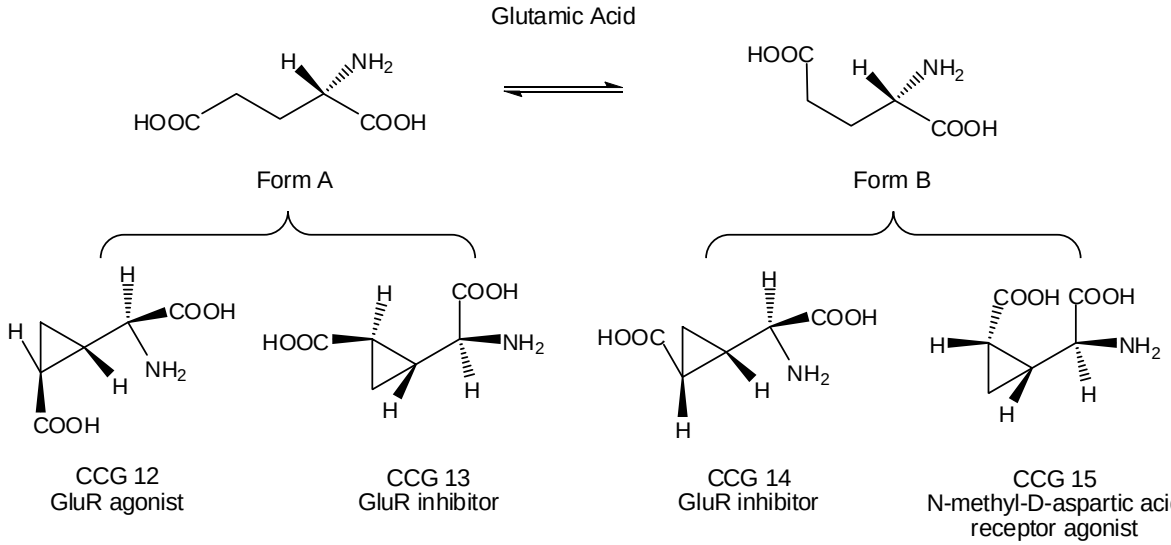


Figure 1-30. Glutamate receptor (GluR) agonists and inhibitors adapted from the article published by Salaun, J.[78]

As a final example, it was reported that dichloro *cis* diphenylcyclopropanes possess antiestrogenic activity (Figure 1-31). Antiestrogens not only regulate and correct diverse endocrine disorders but also they obstruct the growth of estrogen-dependent mammary tumors. Tamoxifen (TAM) is a clinically used antiestrogen drug that operates by competitive inhibition of the estrogen receptor (Figure 1-31). This compound is useful for either treating hormone-dependent tumors or preventing their appearance in premenopausal women. Stilbene-derived

cyclopropyl compounds showed better responses in estrogen-dependent and independent breast cancers than the parent TAM.[78]

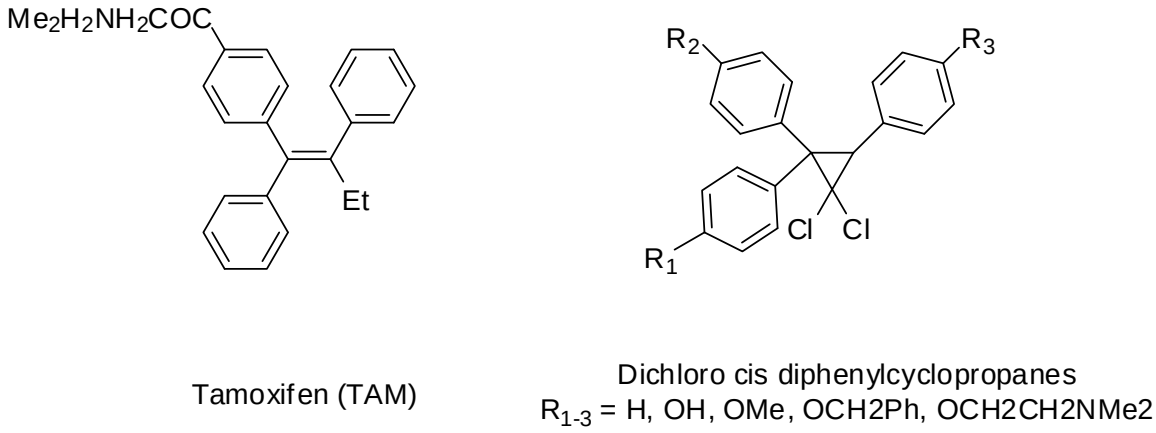


Figure 1-31. TAM and stilbene-derived compounds[78]

**Cyclopropane Preparation**

The work described in this dissertation is focused on the synthesis of diazabicyclic TS analogs for ST and glycosidases. Based on the inhibitors design and shape, an all *cis* trisubstituted cyclopropane was required as the starting core structure. Three membered carbocycles can be synthesized by several different methods. Some of the most relevant reactions that can form the cyclopropyl ring were reviewed by Tsuji and Nishida in 1987.[80] The review included: a) 1,3 bond formations; b) rearrangement reactions; c) transformation of cyclopropyl derivatives; and d) combination of two building blocks. Among these cyclopropane ring preparation techniques, the combination of two carbon units is the most commonly utilized. Examples of each procedure will be given bellow.

**1,3 cyclopropane bond formation**

The 1,3 bond formation can be achieved by a simple intramolecular nucleophilic displacement. Because the reaction proceeds through an $S_N2$ mechanism, inversion of configuration is observed at the carbon that holds the leaving group. The reaction of a conjugate

enone to give a β-cyclopropyl-α,β-unsaturated carbonyl compound is one example (Figure 1-32).[81]

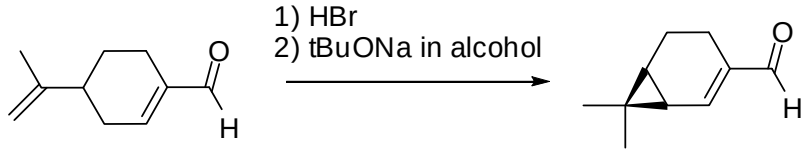


Figure 1-32. Cyclopropanation of α,β-unsaturated carbonyl compound[81]

Cyclopropyl rings have also been obtained from the nucleophilic substitution of Michael acceptors.[82,83] A common intermediate in this reaction is a carbanion with a good leaving group, usually a halogen, situated at a three carbon distance. In addition, the carbanion is frequently stabilized by an adjacent electron-withdrawing group (Figure 1-33).

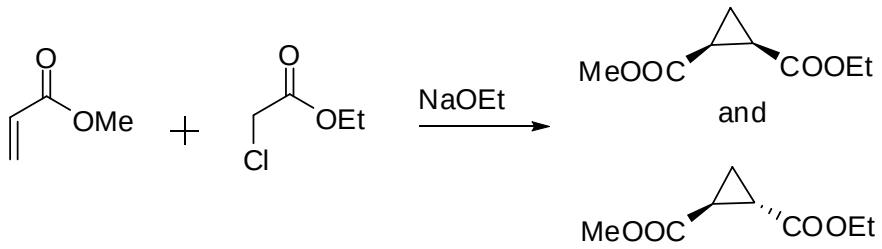


Figure 1-33. Cyclopropanation by nucleophilic substitution of a Michael acceptor[82]

Finally, a reaction that also falls in this category of cyclopropanation is the electrophilic addition to the terminal position of 3-butenyl organometallic compounds. Robbins *et al.* reported the use of 3-butenylstannanes as an example of this reaction (Figure 1-34).[84]

**Rearrangement reactions**

Substituted cyclopropanes can be prepared from cyclobutanes by ring contraction. If the cyclobutane is substituted by an electron-donating group and a leaving group, the ring contraction is easily accomplished. Usually, this reaction occurs with inversion of configuration at the carbon containing the leaving group.[80] Cyclobutanes that normally undergo this transformation include 2-substituted cyclobutanols and α-substituted cyclobutanones. An

example of this method utilized boron trifluoride butyl etherate acidic condition on 2-hydroxycyclobutanone (Figure 1-35).[85]

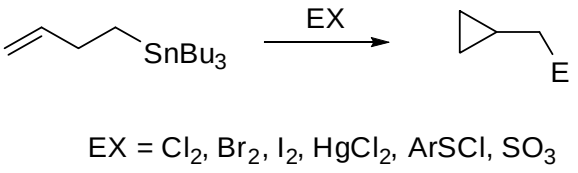


Figure 1-34. Cyclopropanation of 3-butenylstannanes[84]

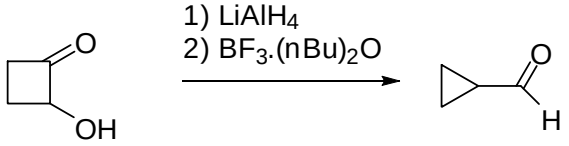


Figure 1-35. Ring contraction of 2-hydroxycyclobutanone[85]

**Transformation of cyclopropyl derivatives**

Substitution transformations on three membered carbocycles are commonly performed via organometallic intermediates. Organometallic cyclopropyl complexes are in general stable and can react avoiding ring opening. This concept was used in the synthesis of cyclopropyltrimethylsilanes from the 1-bromocyclopropyltrimethylsilane precursors (Figure 1-36).[86]

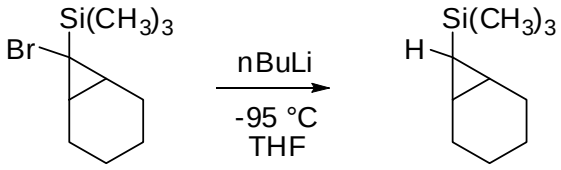


Figure 1-36. Synthesis of cyclopropyltrimethylsilanes[86]

Interestingly, cyclopropyl halides can be easily converted into cyclopropyllithiums or Grignard reagents, which could be further utilized in other organic transformations (Figure 1-37).[87]

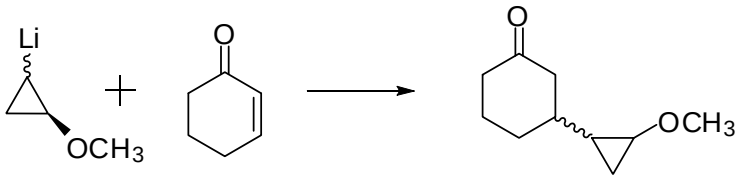


Figure 1-37. Reaction of cyclopropyllithium reagent[87]

**Combination of $C_2$ and $C_1$ building blocks**

One example of this kind of cyclopropanation is the coupling reaction between ylides and compounds that are vulnerable to Michael additions. The reaction of the N-Boc pyrrolinone glutamic acid derivative with diphenylsulfonium isopropyl ylide successfully delivered the 3-azabicyclo[3.1.0]hexan-2-one in a 79% yield (Figure 1-38).[88]

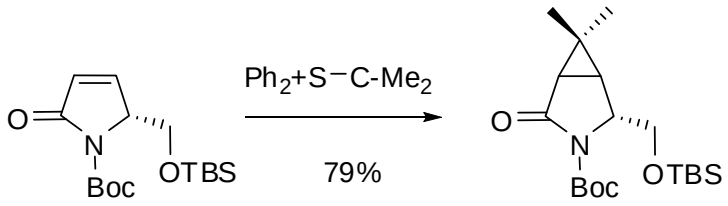


Figure 1-38. Reaction of N-Boc pyrrolinone and diphenylsulfonium isopropyl ylide[88]

The preparation of cyclopropanes via carbene intermediates is among the most studied cyclization reaction, not only for pure organic synthetic rationale but also for the better understanding of carbene chemistry. An effective transfer of a methylene unit to an alkene is done using the Simmons-Smith reagent.[89] A combination of methylene iodide and Zn/Cu couple gives the active iodomethyl zinc iodide alkylating agent. This is a very clean reaction that does not promote alkene isomerization or insertion side products frequently generated in carbene additions. The stereochemistry of the Simmons-Smith reaction is controlled by steric effects and the coordination of the zinc atom with other heteroatoms and functional groups such as oxygen, nitrogen and -OH.[80] A modification of this reaction utilizes diethylzinc and diodomethane as the carbene source.[90] Examples of the Simmons-Smith reaction are shown in Figure 1-39.[90,91]

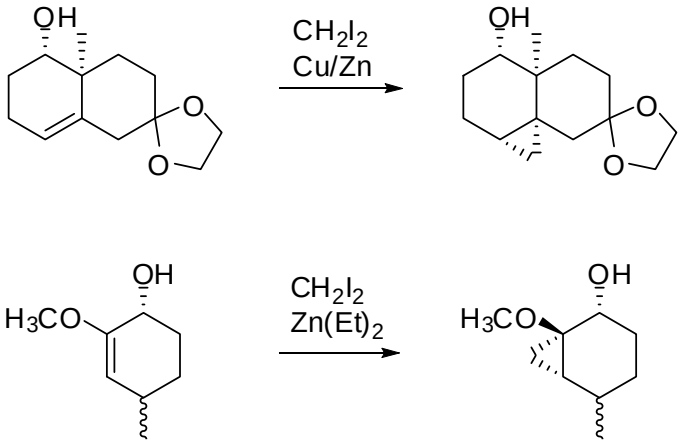


Figure 1-39. Simmons-Smith cyclopropanation reactions[90,91]

For the preparation of acyl- and alkoxylcyclopropanes, carbenes are generated by thermal or photochemical decomposition of diazo compounds. Normally, the cyclopropanation is performed under dilute conditions. This procedure is utilized to avoid normal side reactions such as, dimerization of the carbenoid, C-H insertions, hydrogen abstraction, 1,3 dipolar additions and Wolff rearrangement.[80] Copper, rhodium and palladium salts or complexes with organic ligands are among the most successful catalysts. Among them, Rh(II) carboxylates, having only one coordination site per metal, form stable complexes with basic ligand but not with alkenes.[92] They are very tolerant to steric factors, which allow them to participate in cyclizations of disubstituted olefins. On the other hand, Pd derivatives are very suitable for olefin coordination, but they are only effective in monosubstitued double bond cyclopropanations. With respect to copper catalysts, copper triflates (CuOTf) can be complexed with other ligands due to the triflate anion's lack of coordination ability. They generally exhibit intermediate efficiency on the cyclopropanation of alkenes when compared with Rh and Pd derivatives.[92]

In general, the active species in cyclizations is defined as a metallocarbene intermediate which transfers the carbene unit to the desired molecule. The metallocarbene intermediate can be

considered an electrophile in which the carbocation is stabilized by the metal (Figure 1-40). A summarized representation of the cyclopropanation reaction is shown in Figure 1-41.[93]

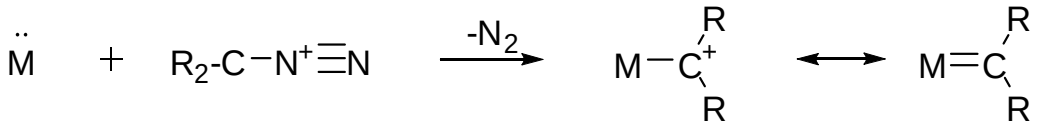


Figure 1-40. Metallocarbene intermediate adapted from Carey, F. A., *Advanced organic chemistry*; 4th ed.[93]

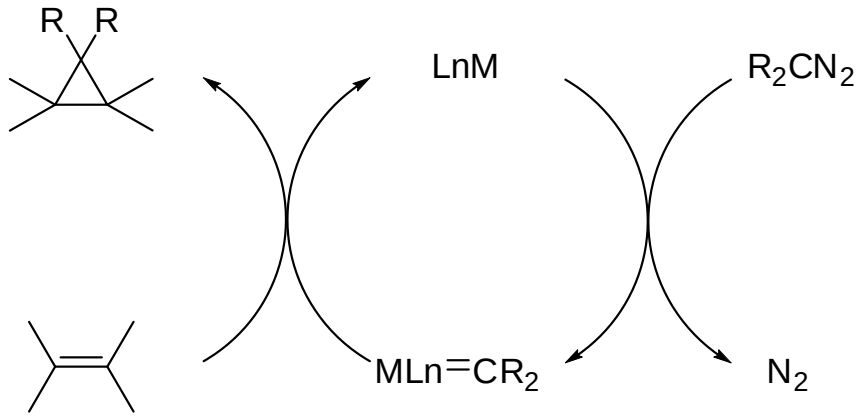


Figure 1-41. Cyclopropanation general reaction adapted from Carey, F. A., *Advanced organic chemistry*; 4th ed.[93]

In the transition state model proposed by Casey[94], there is an initial electrostatic interaction between the metallocarbene center and one end of the alkene ($C_A$) (Figure 1-42). Then, the positive charge generated on the other alkene carbon ($C_B$) removes the metal with a simultaneous carbene-$C_B$ bond formation which gives rise to the cis cyclopropane.[95] If the size of the alkene substituent groups increase, a metal four-member ring intermediate might form, delivering the *trans* cyclopropane isomer.[94,95] This model explained the product stereoselectivity obtained with alkylcarbene-metal complexes, but it did not explained the trans favored selectivity when diazo carbonyl compounds were used.

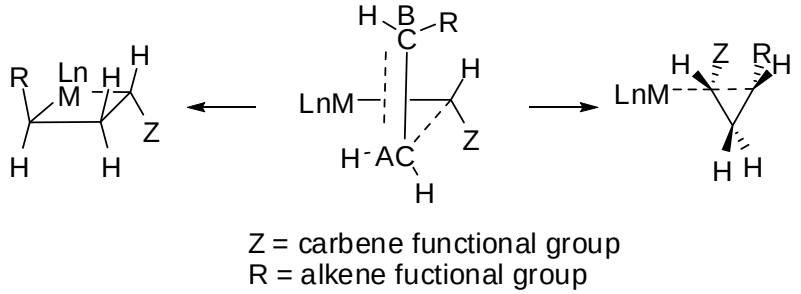


Figure 1-42. Cyclopropanation TS proposed by Casey adapted from the article published by Doyle, M. P.[94,95]

A second model was presented by Doyle *et al.* in which they proposed that the initial interaction between the metal-carbene complex and the alkene π system is in equilibrium with the free olefin (Figure 1-43).

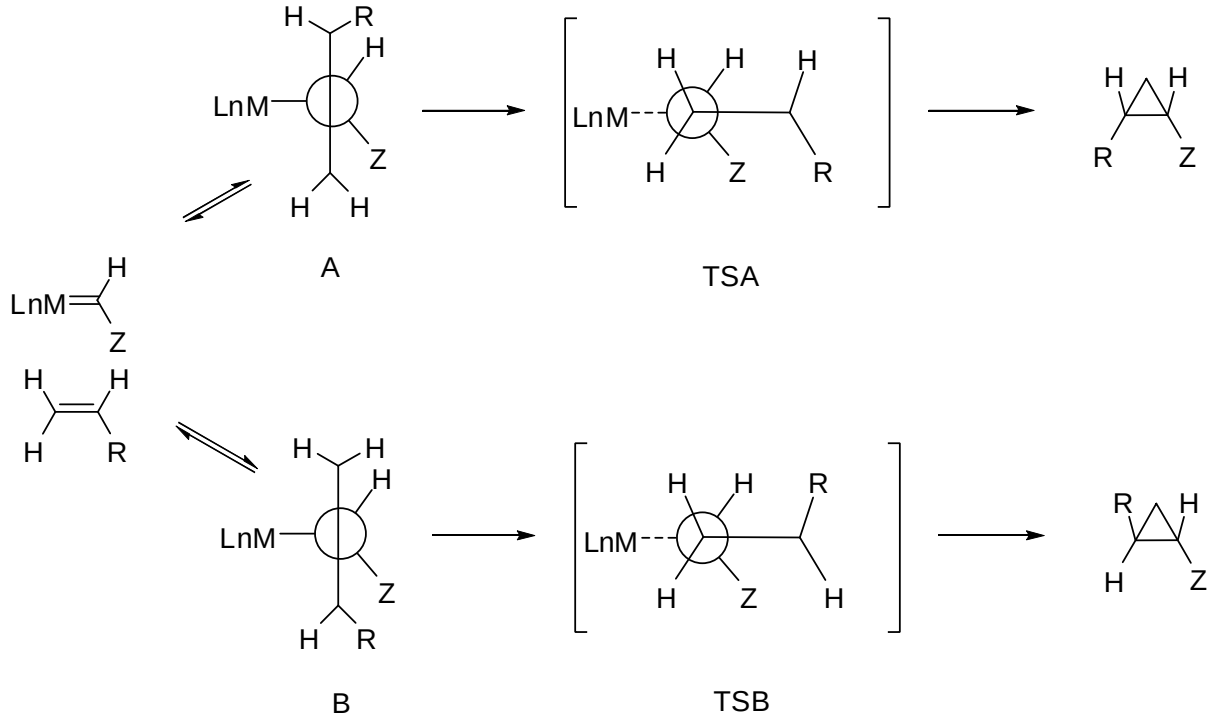


Figure 1-43. Cyclopropanation TS adapted from the article published by Doyle, M. P. [95]

Then, the parallel position of the double bond relative to the carbene center is established by the electro-donating group R stabilization towards the electrophilic center. Consequently, there are two possible TS's (no metallocyclobutane intermediate) that can account for the two

stereoisomers formed. The TS is then regulated by the initial π-metal-carbene steric and electronic interactions. Finally, the ring closure occurs through backside displacement of the metal-ligand complex.[95] With Doyle's model, it is possible to explain why the trans cyclopropanes are favored with diazo carbonyl carbenes. In this case, the carbonyl group can stabilize the forming electrophilic center with its oxygen lone pair electrons, forcing the olefin position to the one that will give the *trans* configuration (Figure 1-44).[95]

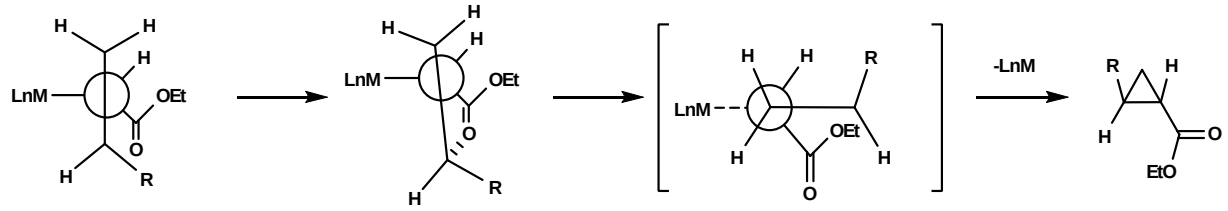


Figure 1-44. Cyclopropanation TS proposed by Doyle's for carbonyl carbenes adapted from the article published by Doyle, M. P.[95]

There are two types of diazo cyclopropanations, either intermolecular or intramolecular. Usually, the intermolecular cyclization delivers the *anti* isomer as the favored one due to steric or electronic factors. However, the enantioselectivity of the reaction, in some cases, might be led by a metal catalyst possessing chiral ligands.[80,96] Fortunately, intramolecular carbenoid reactions can be the solution to this problem. Based on Doyles reports, intramolecular cyclizations only deliver one of the possible three member rings due to geometric constrains.[97] The restriction of this kind of reaction is that the double bond of the substrate has to be in close proximity to the diazo center. Thus, only bicyclo[3.1.0]hexanes and bicyclo[4.1.0]heptanes were successfully obtained. From studies performed on Rh catalyzed cyclizations, the stereoselectivity of the reaction will be dictated by the ligands configuration around the metal, the course of the olefin approach and its orientation towards the face of the catalyst. From theoretical calculation on the complex $Rh_2$(5S-MEPY)$_4$, the lower energy TS geometry was found to have the spatial orientation shown in Figure 1-45.

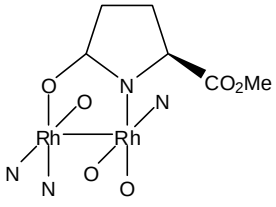


$Rh_2(5S\text{-}MEPY)_4$

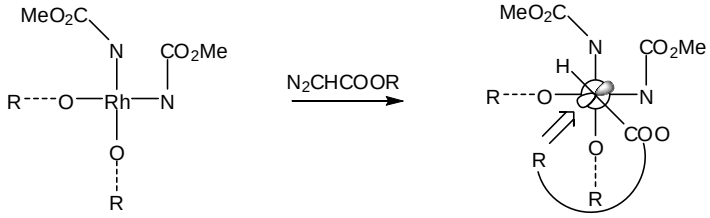


Figure 1-45. $Rh_2(5S\text{-}MEPY)_4$ TS geometry adapted from the article published by Doyle, M. P.[95]

It was observed that the carbene C-H bond falls between the Rh two ligands and the olefin approaches the carbenoid center from its less sterically hindered face (Figure 1-46).[97] This alkene orientation leads to two possible enantiomers. An example of the two enantiomeric adducts is presented in Figure 1-46.[97]

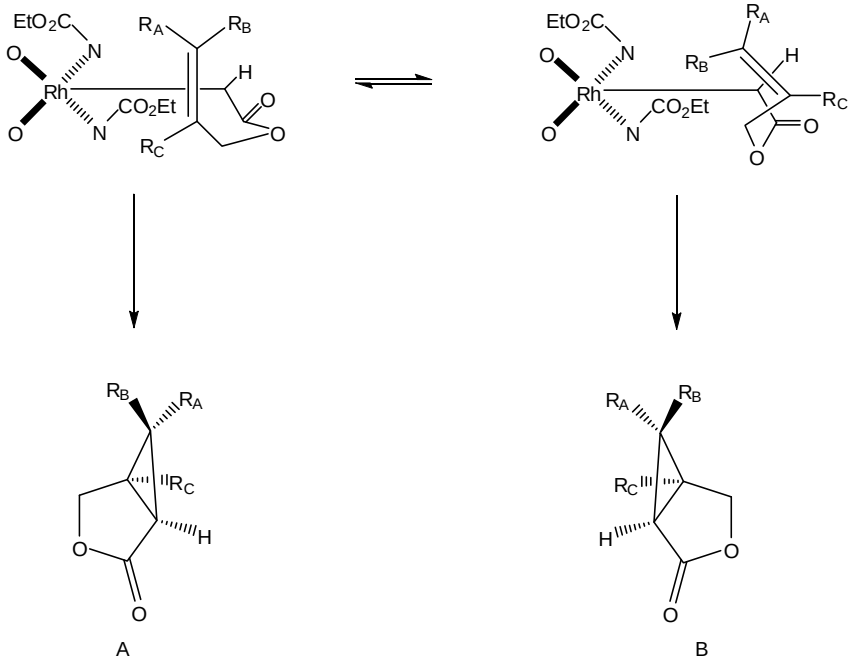


Figure 1-46. The two possible products from the alkene intramolecular cyclopropanation adapted from the article published by Doyle, M. P.[95]

CHAPTER 2
SYNTHESIS OF GLYCOSIDASES AND GLYCOSYLTRANFERASES TRANSITION STATE ANALOGS CORE STRUCTURE

## Introduction

As already mentioned in chapter 1, our group has developed a new class of sialyltransferases inhibitors. These compounds' [3.1.0] bicyclic systems were used to mimic the apical orientation of a leaving group relative to the oxocarbenium ion plane in the transition state conformation of these enzyme reactions. Following this structural mimetics approach, a family of diazabicyclic compounds will be synthesized trying to improve the inhibitory properties of the compounds known at the moment, and further refine our understanding of what constitutes an effective set of features for a good inhibitor. Based on the close similarity between glycosidases and ST mechanisms and TS, diazabicyclic analogs will be suitable to study both enzymes catalytic reaction. Because the departing leaving group (LG) mimicry will be achieved by holding the aglycon moiety above the amidine group, one of the synthetic challenges rests in producing the differentially functionalized all *cis* 1,2,3 cyclopropanes that could serve as the starting core structure. A simplified retrosynthetic route utilized in the design of TS analogs is shown in Figure 2-1.

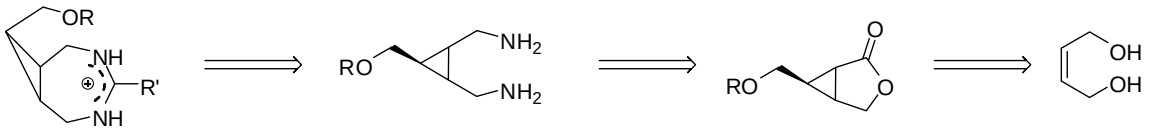


Figure 2-1. Retrosynthetic route for seven-membered diazabicyclic TS analogs

## Results and Discussion

To have a sense of how to synthesize the requisite amidine moiety, model compound 2-carboxy-4,5-dihydro imidazole **4** was prepared using ethylenediamine and ethyl glycoloimidate **2** as starting materials (Figure 2-2). This method was utilized by Hamilton *et al.* in the preparation of 2-carboxy-4,5,6,7-tetrahydro-1,3-diazepine.[98]

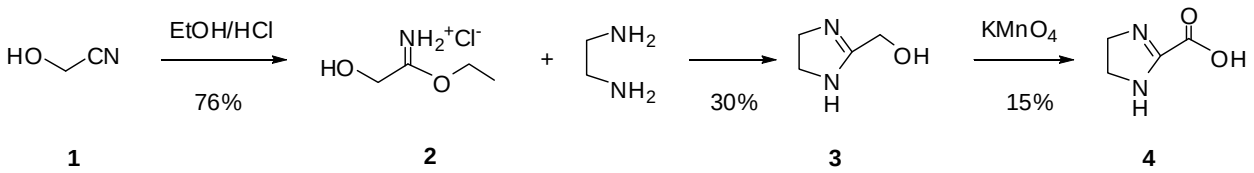


1 2 3 4

Figure 2-2. Synthesis of 2-carboxy-4,5-dihydro imidazole

Firstly, ethyl glycoloimidate hydrochloride **2** was prepared from the reaction of glycolonitrile **1** with ethanol in acidic media. After that, reaction of the imidate with ethylenediamine afforded **3** as colorless crystals in 30% yield without further purification. Finally, oxidation of hydroxymethyl imidazole was accomplished with potassium permanganate at pH = 11. Centrifugation and decantation of the aqueous solution removed the brown manganese dioxide precipitate. The final product was purified by Dowex 50 resin in the acid form to give 2-carboxy-4,5-dihydroimidazole **4** as a white solid. It was found that this amidine was stable for 3 days in water at pH = 4 which demonstrated the stability of the carboxyamidine functional group. As already described in Chapter 1, the sialyltransferase donor substrate CMP-NeuAc bears a carboxylic acid moiety at the anomeric carbon. Thus, the relative stability of the carboxyamidine is an important piece of evidence that the group might be able to be incorporated into TS analog inhibitors.

The reaction between a Michael acceptor and an active methylene compound was used as the preliminary attempt to synthesize a *cis* cyclopropane dicarboxylic acid (Figure 2-3). Then, methyl acrylate and ethyl chloroacetate were treated with NaOEt at room temperature. The crude reaction mixture resulted in a very complex combination of unreacted starting materials, diastereoisomers and side products. Any efforts to purify the mixture by fractional distillation or column chromatography resulted in a group of impure fractions from which it was difficult to determine the presence of the desired products.

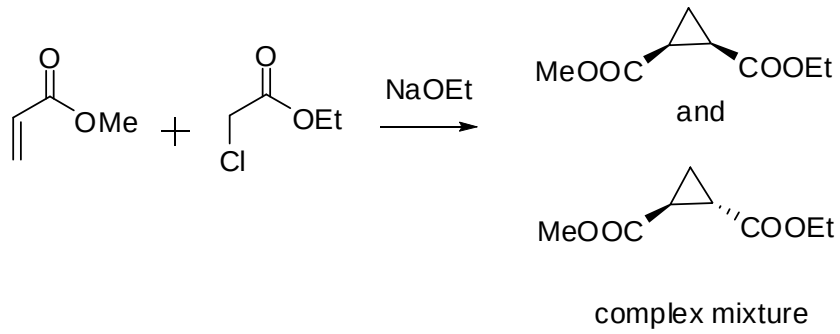


Figure 2-3. Cyclopropanation using a Michael acceptor

Intermolecular cyclopropanation conditions were then utilized as the second approach toward the stereoselective synthesis of trisubstituted *cis* cyclopropanes. Consequently, the efficacy of metal-catalyzed cyclizations of *Z*-2-butene-1,4-diol with ethyl diazoacetate were explored. This approach was chosen with foreknowledge that although a preference for exo addition (leading to a trans cyclopropane) might predominate, the poor stereoselectivity of the reaction might yield sufficient endo addition product to allow rapid exploration of downstream synthetic steps. Since allylic alcohol derivatives are known to react with carbenoids to form ylids that undergo [2,3]-sigmatropic rearrangements, the allylic diol was protected to sterically obviate such processes. The requisite *Z*-2-butene-1,4-diol **5** was transformed to the corresponding acetal form by protecting with 2,2-dimethoxypropane in presence of catalytic amounts of p-toluenesulfonic acid (Figure 2-4).[99,100] Fractional distillation at low pressure gave 2,2-dimethyl-1,3-dioxole **6** in a 63% overall yield.

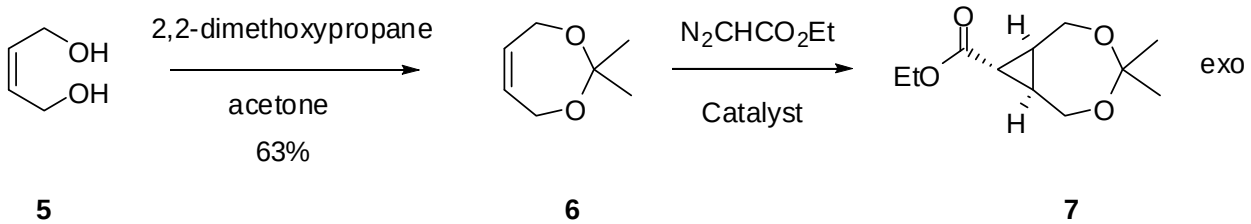


Figure 2-4. Intermolecular cyclopropanation of Z-2-butene-1,4-diol[99,100]

Toward the goal to achieve the desired endo-trisubstituted isomer on the cyclopropanation step, the catalyzed reaction of *cis*-protected diol **6** by rhodium (II) acetate in dichloromethane was first investigated. After tedious purification of the cycloaddition reaction mixture between ethyl diazoacetate and **6**, only the *exo*-substituted isomer (8:1 *exo*:*endo*) was isolated in a 24% yield. This preferential stereochemistry of the product was fully confirmed by $H^1$ NMR and 2D-NOESY experiments. The NOESY spectrum of **7** exhibited crosspeaks between Hd-Hb, Ha-Hc and Ha-$CH_3$a (Figure 2-5). Following the idea that the favored *exo* over *endo* stereochemistry could have been taking place due to a possible coordination between rhodium catalyst and the two oxygens of the allylic protected alcohol, other solvents as THF and benzene were utilized for the cycloaddition. Once again, the results showed that only *exo* isomer was present in the mixture. Furthermore, despite other attempts using catalyst like CuOTf and $Cu(acac)_2$ , it was not possible to force the stereochemical outcome of the cycloaddition reaction to yield more endo product.

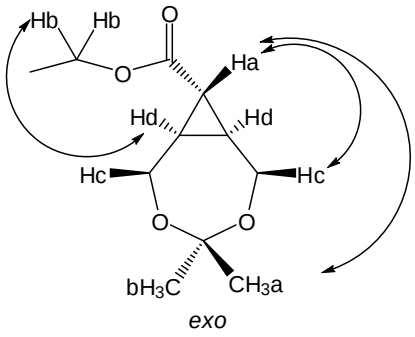


Figure 2-5. Characterization of dioxabicyclo[5.1.0]octane by 2D-NOESY

Since bimolecular cyclopropanations were not useful for the problem at hand, the intramolecular cycloaddition of allyl diazoacetic esters was utilized as the synthetic solution. Based on previous studies,[95,97] intramolecular cyclizations necessarily deliver cyclopropanes with all three substituents in the *cis* conformation. Because the requisite cyclopropane might also have all three substituents chemoselectively differentiated from each other, the

bicyclo[3.1.0]lactone **9** (Figure 2-6) was chosen to be the key core intermediate in the TS analog synthetic route. Consequently, corresponding diazoacetic ester **8** was prepared (Figure 2-6).

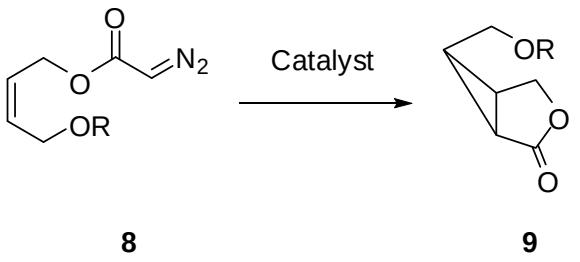


**8** **9**

Figure 2-6. Metal-catalyzed diazoester intramolecular cycloprapanation[97]

The first step on the ester synthesis involved mono-protection of *Z*-2-butene-1,4-diol with *tert* butyldimethysilyl chloride (TBDMSCl). Subsequent reaction of the free hydroxyl group in compound **10** with Boc-protected glycine resulted in the bi functionalized alcohol **11** in 80% yield (Figure 2-7). Treatment of the Boc-protected ester with a solution of trifluoroacetic acid (TFA) in dichloromethane or trimethylsilyl iodide (TMSI) did not result in the desired free amine. Instead, either compound **10** or silyl cleavage of **11** were observed as side products by $^{1}H$ NMR and TLC.

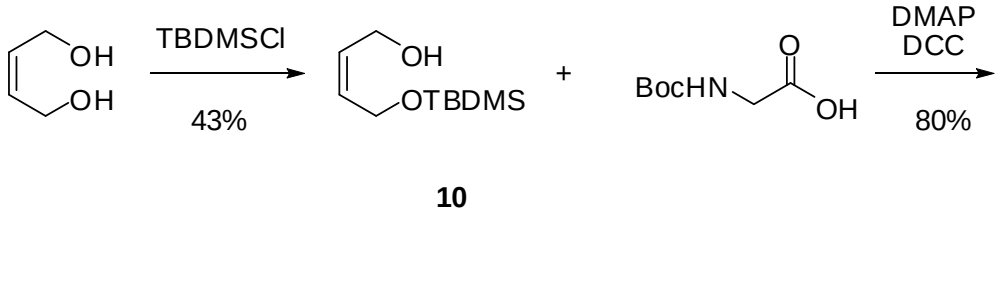


**10**

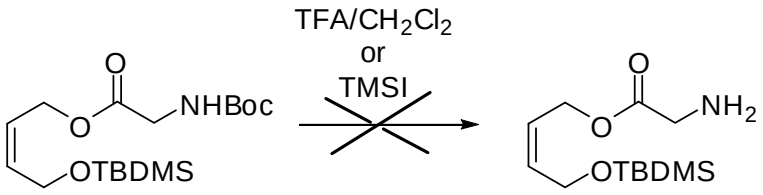


**11**

Figure 2-7. Synthesis of the *Z*-bifunctionalized ester **11**

Therefore, the allylic alcohol Z-butene-1,4-diol was converted into the less labile monoprotected benzyl alcohol **12** using standard methods (Figure 2-8).[101]

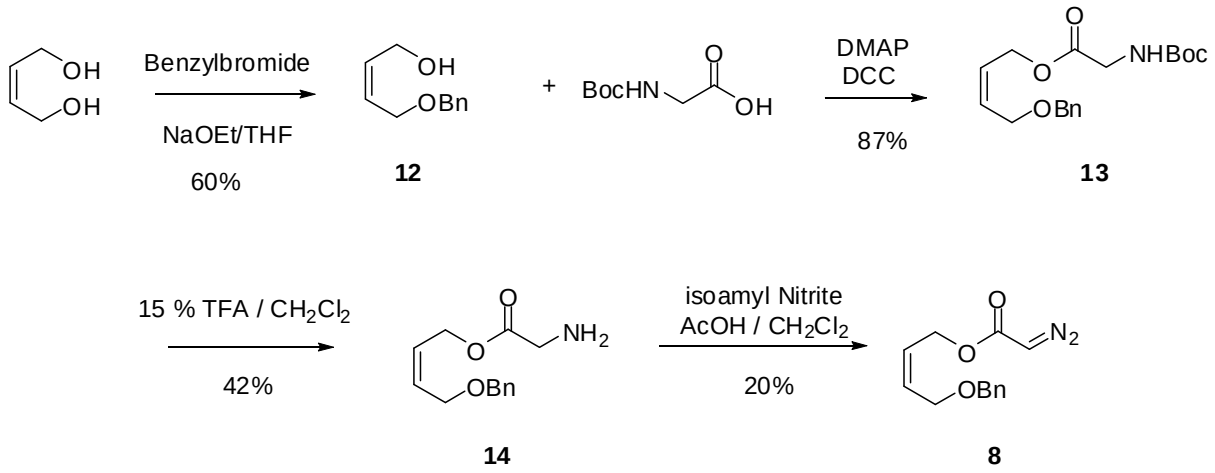


Figure 2-8. Synthesis of diazo ester **8**

Subsequent reaction of 4-benzyloxy diol **12** with Boc-glycine gave the *cis* alkene **13** in an 87% yield. When the Boc-protected ester was treated with 15% TFA in dichloromethane, the reaction delivered the desired glycinate **14** in a 42% yield.[102] The benzyl amino alkene **14** was converted to the *cis* diazoacetic ester **8** by a conventional nitration reaction using isoamyl nitrite in a 20% yield (Figure 2-8).[103] Unfortunately, this synthetic route produced the *cis* diazo ester in a very low yield.

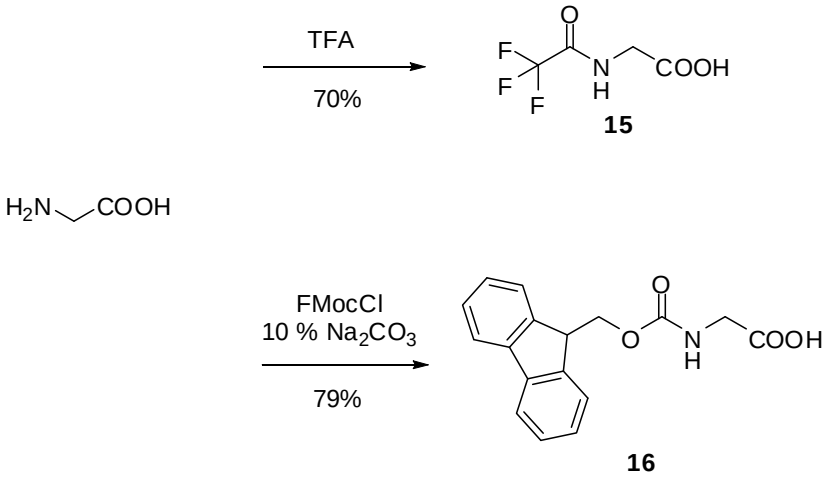


Figure 2-9. Synthesis of N-trifluoro and FMoc protected glycine

At this stage, because the diazo ester was the starting material for all the different multistep synthetic pathways, the yield obtained in each reaction was particularly important. It was observed that the deprotection of compound **13** with TFA not only was generating the free amine but also was causing the hydrolysis of the ester linkage. The reactivity of other amine protecting groups was tested in order to obtain **14** under reaction conditions that might not affect the ester bond. Then, different N-trifluoro and 9-fluorenylmethyloxycarbonylglycine (FMoc-glycine) moieties were synthesized by literature methods.[104,105] These two amino protecting groups are usually used in peptide synthesis and can be removed in mild basic conditions (Figure 2-9).

The *cis* protected diol **12** was coupled to N-trifluoro and FMoc-glycine by the same method utilized for compound **13**. The esters N-trifluoro **17** and FMocacetate **18** were obtained in 74% and 38% yield respectively (Figure 2-10).

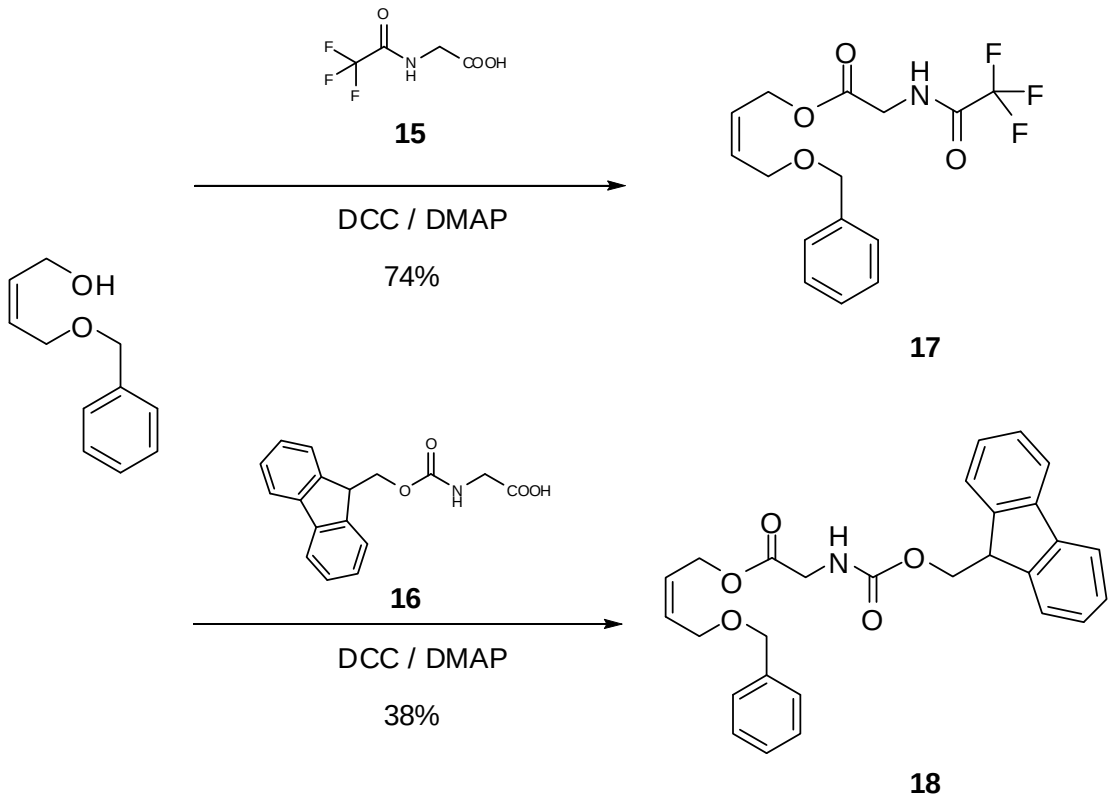


Figure 2-10. Synthesis of N-trifluoro and FMoc esters

Unfortunately, attempts to deblock the trifluoro amide protecting group with $K_2CO_3$ in MeOH resulted, once more, in the hydrolysis of the ester connectivity giving back diol **12**. Based on a Carpino *et al.* report, the FMoc group can be removed by nonhydrolytic conditions for example, when the protected derivative is treated with liquid ammonia for several hours.[104] The hydrogen at the β position from the carbamate unit of the FMoc conjugated system becomes greatly acidic and can be easily abstracted by weak bases. This hydrogen acidity is driven by the fact that the conjugated system becomes aromatic after the abstraction of the proton. The same result can be obtained when secondary amines like morpholine or piperidine are utilized as the deprotecting agents. In both cases, dibenzofulvene is formed as a by-product which could be isolated without difficulty from the reaction mixture. Following Carpino's methodology, cis ester **18** was treated with a piperidine at room temperature. After the reaction was stirred for 30 minutes, analysis of the crude mixture by TLC showed total conversion of **18** again into the starting material **12**. This result was also confirmed by $H^1$ NMR. From all these unsuccessful efforts to obtain compound **14**, it is believed that the weakness of the ester bond might be related to its proximity to the alkene group. Consequently, a different method to synthesize the cis diazo ester **8** had to be pursued. In 2004, Collado *et al.* presented a new methodology for the synthesis of these kind of diazo compounds in which they are generated from an acetoacetate ester intermediate.[106]

This synthesis utilized benzyl *cis* butene-1,4-diol **12** as the starting material. The reaction of its free hydroxyl group with the extremely reactive diketene gave compound **18** in an 61% yield (Figure 2-11). Then, treatment of the acetoacetate ester with p-ABSA (p-acetamido benzenesulfonyl azide) in $Et_3N$ resulted in the desired *cis* diazoacetic ester. This reaction starts

with a diazo transfer from the sulfonyl azide. Then, compound **8** is generated by base-induced deacylation of the α-diazo acetoacetic ester intermediate.

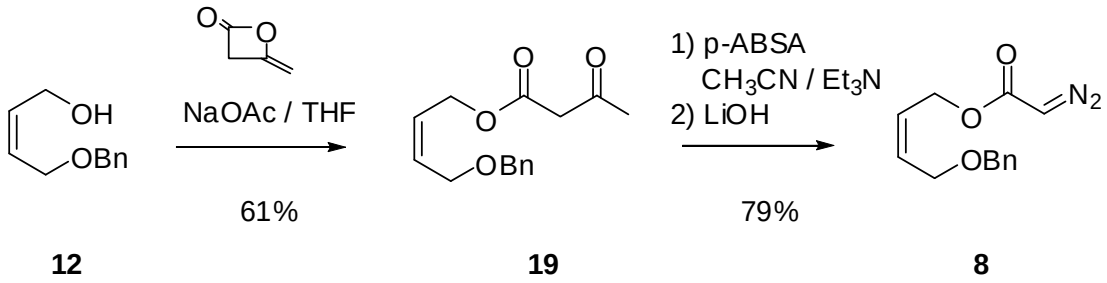


**12** **19** **8**

Figure 2-11. Improved synthesis of diazoester **8**[106]

A key step in the synthetic design was the intramolecular cyclopropanation of **8** to give the all *cis* trisubstituted cyclic system. Hence, starting from the *cis* alkene **8**, the resulting fused cyclopropyl lactone **9** will have all its substituents in the *cis* configuration. The first cyclization reaction was performed utilizing the commercially available $Rh_2OAc_4$ as the catalyst. The reaction was executed under dilute conditions, adding the diazo compound via a syringe pump over 18 h. In this case, the lactone **9** was obtained in a 32% yield. Due to the poor yield obtained in this reaction, the catalytic efficiency of $CuSO_4$ in benzene was then tested. After refluxing the reaction for 12 h, the cyclic lactone was isolated in 48% yield. The last metal catalyst investigated was Cu(I)TfO. This catalyst was utilized in presence of the Evan's ligand.

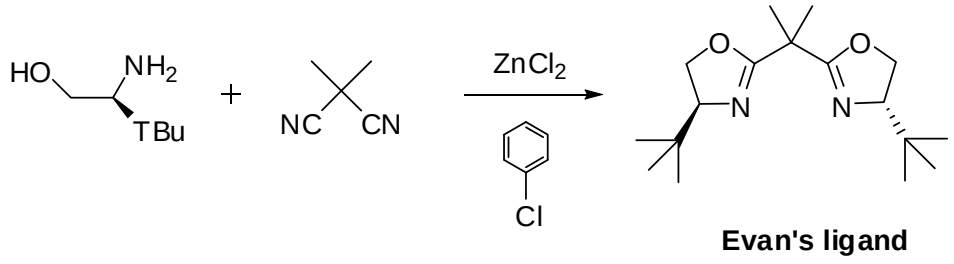


**Evan's ligand**

Figure 2-12. Synthesis of Evan's ligand[107]

The Evan's bis oxazoline ligand was synthesized by a literature procedure using L-tert-leucinol as starting material (Figure 2-12).[107] This reaction conditions were finally chosen for the

cyclization reaction because they afforded the best product yield. A summary of the yields obtained in the intramolecular cyclizations is presented in Table 2-1.

Table 2-1. Comparison of the intramolecular cyclopropanation yield obtained with different catalyst

| Catalyst | Yield |
|---|---|
| $Rh_2OAc_4$ | 32% |
| $CuSO_4$ | 48% |
| CuTfO / Evan's ligand | 60% |

In order to confirm that lactone **9** had the all cis configuration, the molecule was characterized by 2D-NMR spectroscopy.

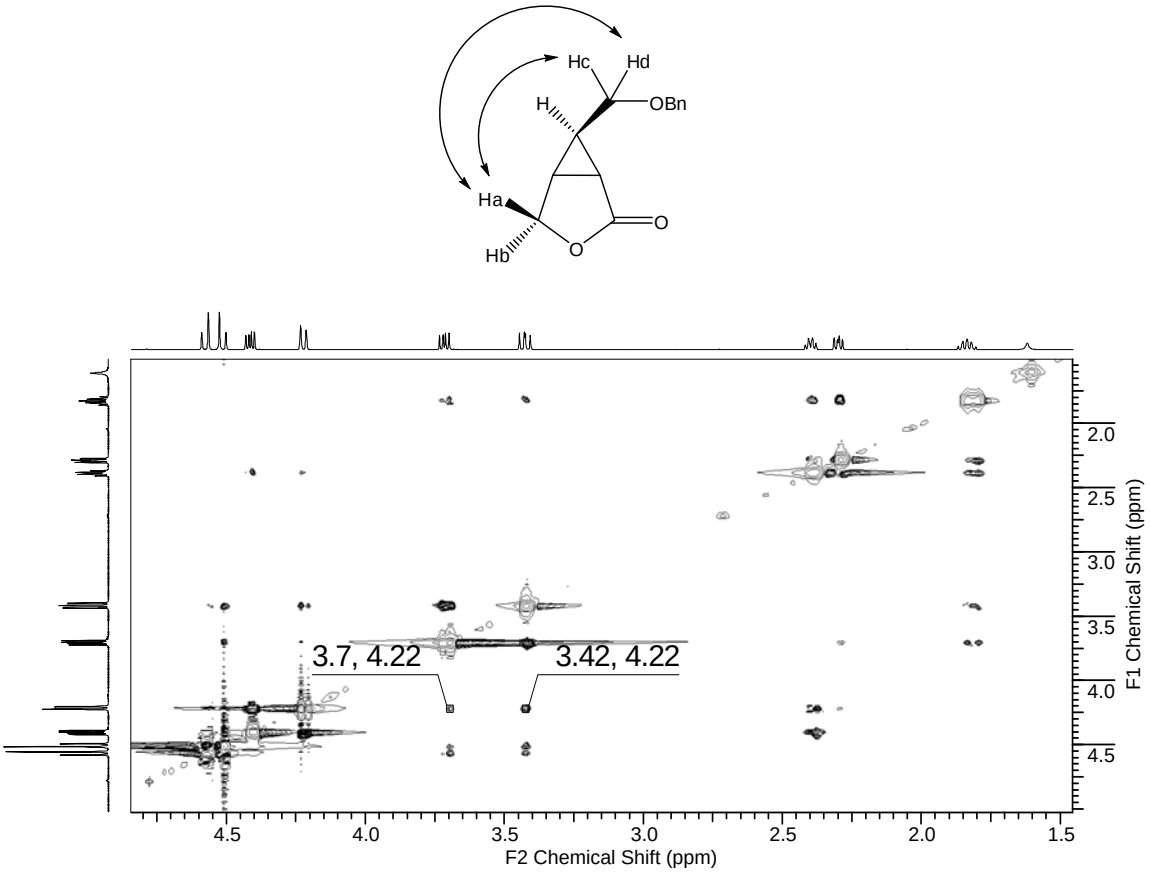


Figure 2-13. Lactone **9** 2D-NOESY characterization

Crosspeaks between Ha-Hc ($\delta_{Ha}$ = 4.22 and $\delta_{Hc}$ = 3.42 respectively) and Ha-Hd ($\delta_{Hd}$ = 3.71) were observed in the NOESY spectrum of **9**. This set of hydrogen atoms has a spatial interaction due to the *endo* configuration of the ring. The NOESY spectrum obtained is shown in Figure 2-13.

## Experimental Section

**General methods.** Solvents and reagents were purchased from Aldrich Chemical Company and Acros Organics. The organic solvents were dried overnight over $CaH_2$ or 4 Å molecular sieves and freshly distilled before use. NMR spectra were obtained using VXR 300, Gemini 300 and 500, or Mercury 300 and 500 MHz spectrometers in appropriate deuterated solvents. Mass spectra were obtained on a Finnegan MAT 95Q spectrometer operated in FAB, CI, ESI or EI modes. Infrared (IR) spectra were obtained by deposition of $CHCl_3$ solutions on NaCl plates followed by evaporation of the solvent.

**Ethyl 2-hydroxyacetimidate hydrochloride 2.** To a solution of acetylchloride (390 μL, 5.51 mmol) in ether (5.00 mL), ethanol (640 μL) was added with stirring at room temperature, to generate HCl in situ. The mixture was stirred for 3 h and then glycolonitrile **1** (0.50 ml, 5.51 mmol of a 55 wt% solution in $H_2O$) was added at -10 °C. The mixture was stirred for 4 h. Then, ether was added and the reaction was kept for 24 h at -20 °C. After this time, crystals formed which were collected by filtration, washed with ether and then dried under vacuum. Compound **2** was obtained as white crystals in 76% yield (0.43 g). $^1$H NMR ($D_2O$) δ ppm 1.28 (t, 3H), 4.22 (s, 2H), 4.23 (q, 2H), $^{13}$CNMR ($D_2O$) δ ppm 174.6, 62.2, 59.8, 13.4.

**(4,5-Dihydro-1H-imidazol-2-yl)-methanol 3.** To a solution of ethylenediamine (67 μl, 1.1 mmol) at 0 °C in absolute ethanol (740 μL), ethyl glycoloimidate **2** (130 mg, 1.32 mmol) was added with stirring. The mixture was kept at 0 °C for 1 h and then heated up to reflux within 0.5

h. Reflux was maintained until no more ammonia gas evolution was observed (approximately 1.5 h).The hot solution was mixed with alcoholic HCl and then filtered while still hot. After leaving the filtrate overnight at -20 °C, colorless crystals were collected in 30% yield (0.03 g). $^{1}$H NMR ($D_2O$) δ ppm 3.93 (s, 4H), 4.51 (s, 2H),$^{13}$C NMR ($D_2O$) δ ppm 171.7, 55.2, 44.6.

**2-Carboxy-4,5-dihydro imidazole 4.** After dissolving **3** (35 mg, 0.4 mmol) in water (0.6 mL), adjusting the pH to 11 with 6 N KOH and cooling the solution to 0 °C, small portions of $KMnO_4$ (86 mg, 0.4 mmol) were added with continuous stirring over a 3 h period. The reaction solution was then centrifuged for 15 min at 12000 rpm, the aqueous solution decanted and the brown precipitate $MnO_2$ washed with water (2 x 1 mL). After combining the aqueous solutions, the reaction mixture was concentrated under reduced pressure, and 5 mL of ethanol were added. The white inorganic solid was removed by filtration. The solvent was removed by reduced pressure and the product was purified by ion exchange chromatography. The residue was dissolved in water (1 mL) and applied to Dowex 50 ($H^+$) resin. Product was eluted with 0.5 M aqueous $NH_4OH$ to give the carboxy amidine in 15% yield (6.8 mg). $^{1}$H NMR ($D_2O$) δ ppm 3.42 (s, 2H), 3.55 (s, 2H). EI LRMS Calcd for $C_4H_7N_2O_2$ $(M + H)^+$: 115, found: 115.

**2,2-Dimethyl-1,3-dioxocyclohept-5-ene 6.** A mixture of Z-2-butene-1,4-diol **5** (4.8 mL, 58 mmol), 2,2-dimethoxypropane (7.1 mL, 58 mmol), acetone (4.2 mL) and benzene (11 mL) with catalytic amount of p-toluenesulfonic acid (29 mg) were heated near 65 °C for about 1 h. During this time, some methanol, benzene and acetone were distilled off. Dry benzene was added periodically to the reaction flask. The mixture was purified by fractional distillation at 20 mm Hg. Pure product **6** (4.7 g, 63%) was collected from the fraction that distilled in a range of 53-54 °C. $^{1}$H NMR ($C_6D_6$) δ ppm 1.34 (s, 6H), 4.06 (d, 4H), 5.38 (t, 2H), $^{13}$C NMR ($C_6D_6$) δ ppm 129.7, 101.8, 61.2, 24.0. The NMR spectrum was consistent with the literature.[100]

**4,4-Dimethy-8-ethylformyl-3,5-dioxa-bicyclo[5.1.0]octane 7.** To a solution of **6** (1 g, 8 mmol) in $CH_2Cl_2$ (8 mL), $Rh_2(OAc)_4$ catalyst (34 mg, 78 μmol) was added with stirring. After this mixture has been stirred for 1 h, a homogeneous green solution was obtained. Ethyl diazoacetate (0.7 mL, 6.3 mmol) in $CH_2Cl_2$ (6.3 mL) was added to the solution using a syringe pump at a rate of 8 μL/h over 24 h. The reaction was monitored by TLC (10:1 toluene/EtOAc) and stirred for an additional 2 days. After this period solution was filtered through a Celite bed. The filtrate was concentrated under reduced pressure. The mixture was purified by flash chromatography (silica, 100:1 toluene/EtOAc). The *exo* product was isolated in 25% yield (0.4 g). The same reaction was performed using CuOTf/Evan's ligand in $CH_2Cl_2$, $Rh_2(OAc)_4$ in THF and $Rh_2(OAc)_4$ in benzene. The *exo* product was isolated in 23% (0.4 g), 24% (0.4 g) and 30% yield (0.5 g) respectively. $^1$H NMR ($C_6D_6$) δ ppm 0.95 (t, 3H), 1.04 (s, 3H), 1.11 (s, 3H), 1.66 (m, 2H), 2.07 (t, 1H), 3.48 (dd, 2H), 3.74 (dd, 2H), 3.96 (q, 2H). ESI HRMS Calcd for $C_{11}H_{18}O_4Na$ $(M + Na)^+$ : 237.1097, found: 237.1112.

**4-tert-Butyl-dimethyl-silanyloxy)-but-2-en-1-ol 10.** To a stirred solution of cis diol **5** (4.2 g, 48 mmol) in DMF (25 mL) were added imidazole (0.7 g, 10 mmol) and TBDMS chloride (1.6 g, 10 mmol) at -10 °C. Then, the mixture was stirred at room temperature for 1 h and water was added at 0 °C. The reaction mixture was extracted with ether, washed with brine and dried over $Na_2SO_4$. The product was purified by flash chromatography (silica, 8:1 petroleum ether/EtOAc). Compound **10** was obtained as a colorless oil in 43% yield (3.9 g). $^1$H NMR ($CDCl_3$) δ ppm 0.05 (s, 6H), 0.9 (s, 9H), 2.22 (bs, 1H), 4.21 (dd, 4H), 5.65 (m, 2H). The NMR spectrum was consistent with the literature.[101]

**4(Z)-4-Benzyloxy-but-2-en-1-ol 12.** The title compound was synthesized using the literature procedure.[101] Cis diol **5** (56.7 mL, 690 mmol) was added to a stirred suspension of

NaH (60% dispersion in mineral oil, 5.50 g, 138 mmol) in THF (460 mL) which was previously cooled to 0°C. Stirring was continued at room temperature for 30 minutes. After this, benzyl bromide (14 mL, 118 mmol) was added. The reaction mixture was left overnight at room temperature until benzyl bromide starting material was not observed by TLC. Next, the solvent was evaporated and the residue was dissolved in ether (400 mL). The organic layer was washed with water (3 x 150 mL) and dried with $MgSO_4$. Fractional distillation of the crude product at 5 mm Hg (bp 156-159 °C) gave the desired mono protected diol in 60% yield (73.7 g). $^1$H NMR ($CDCl_3$) δ ppm 2.02 (bs, 2H), 4.06 (d, 2H), 4.13 (d, 2H), 4.50 (s, 2H), 5.75 (m, 2H), 7.32 (m, 5H). The NMR spectrum was consistent with the literature.

**N-Trifluoroacetylglycine 15.**[105] Glycine (1.0 g, 13 mmol) in a dry round bottom flask was cooled to 0 °C. Freshly distilled triflouroacetic anhydride (TFA) (3.0 ml, 21 mmol) was added slowly, and the reaction was allowed to warm to room temperature. When no more glycine starting material was observed by TLC, TFA was evaporated under reduced pressure. The residue was dissolved in 20 mL of boiling benzene and filtered while still hot. The trifluoroglycine crystallized as a white solid in a 70% yield (1.6 g) (m.p. 114-116 °C). The NMR spectra and m.p were consistent with the literature.

**9-fluorenylmethyloxycarbonylglyicine 16.** This compound was prepared following the literature procedure.[104] A solution of glycine (0.3 g, 4.0 mmol) in 10 mL of 10% aqueous $Na_2CO_3$ was cooled on an ice bath. Then, a solution of FMocCl (1.1 g, 3.9 mmol) in dioxane was added with stirring. The ice bath was removed and the mixture was stirred for 2 h at room temperature. The reaction was quenched with 200 mL of water and extracted with ether. The aqueous phase was acidified with concentrated HCl until a precipitate was observed. This solid was extracted with EtOAc. The product FMoc protected glycine was obtained in 79% yield (0.9

g) as a white solid with a m.p. of 174-175 °C. The NMR spectrum and m.p. were consistent with the literature.

**General procedure for the preparation of (Z)-4-protected but-2-enyl esters 11, 13, 17 and 18.** (Z)-4-protected-but-2-en-1-ol **10** or **12** (10 mmol), dicyclohexylcarbodiimide (DCC) (10.5 mmol) and dimethylaminopyridine (DMAP) (0.5 mmol) were dissolved in EtOAc (7 mL). The reaction mixture was cooled to 0 °C. Afterwards, N-protected glycine (10 mmol) dissolved in EtOAc (7 mL) was added dropwise to the cold mixture (half way through the addition, the solution became cloudy white). After stirring reaction for 5 min at 0 °C, the ice bath was removed and the mixture was left at room temperature for 3 h more. EtOAc was added to dilute the reaction mixture which was then filtered to eliminate dicyclohexylurea DCU. The organic filtrate was washed with 1 N HCl (1 x 40 mL), 10% aqueous $NaHCO_3$ (1 x 50 mL), saturated NaCl (1 x 40 mL) and dried over $MgSO_4$.

**tert-Butoxycarbonylamino-acetic acid 4-(tert-butyl-dimethyl-silanyloxy)-but-2-enyl ester 11.** This compound was prepared from N-Boc glycine and compound **10**. Purification of the product by column chromatography (silica, 50:1 $CHCl_3$/EtOAc) gave **11** in an 80% yield as a colorless oil. $^1$H NMR ($CDCl_3$) δ ppm 0.08 (s, 6H), 0.9 (s, 9H), 1.44 (s, 9H), 3.92 (d, 2H), 4.30 (d, 2H), 4.74 (d, 2H), 5.02 (bs, 1H), 5.56 (m, 2H), 5.76 (m, 2H),$^{13}$C NMR ($CDCl_3$) δ (ppm) 170.4, 155.9, 134.7, 123.7, 80.2, 61.4, 59.7, 42.6, 28.5, 26.1,18.5, -5.0. ESI HRMS Calcd for $C_{17}H_{33}NO_5SiNa$ $(M + Na)^+$ : 382.2020, found: 382.2033.

**tert-Butoxycarbonylamino-acetic acid 4-benzyloxy-but-2-enyl ester 13.** This compound was prepared from N-Boc glycine and alcohol **12**. The product was purified by flash column chromatography (silica, 6:1 hexane/EtOAc). The desired ester **13** was obtained in a 87% yield as colorless oil. $^1$H NMR ($CDCl_3$) δ ppm 1.43 (s, 9H), 3.89 (d, 2H), 4.12 (d, 2H), 4.50 (s, 2H), 4.68

(d, 2H), 5.03 (bs, 1H), 5.69 (m, 1H), 5.81 (m, 1H), 7.32 (m, 5H),$^{13}$C NMR ($CDCl_3$) δ (ppm) 170.6, 156.1, 138.3, 131.8, 128.9, 128.3, 126.5, 80.5, 72.9, 66.1, 61.5, 42.8, 28.8. ESI HRMS Calcd for $C_{18}H_{25}NO_5Na$ $(M + Na)^+$ : 358.1625, found: 358.1652.

**(Z)-4-(benzyloxy)but-2-enyl 2-(2,2,2-trifluoroacetamido)acetate 17.** This compound was prepared from N-trifluoroglycine and alcohol **12**. The product was purified by flash column chromatography (silica, 6:1 hexane/EtOAc). The product was obtained as a white solid in a 74% yield. $^1$H NMR ($CDCl_3$) δ ppm 4.11 (d, 2H), 4.14 (d, 2H), 4.53 (s, 2H), 4.77 (d, 2H), 5.72 (m, 1H), 5.86 (m, 1H), 7.34 (m, 5H),$^{13}$C NMR ($CDCl_3$) δ (ppm) 168.4, 157.3, 138.4, 128.9, 128.2, 125.8, 73.1, 66.1, 62.3, 41.8. ESI HRMS Calcd for $C_{15}H_{16}F_3NO_4Na$ $(M + Na)^+$ : 354.0924, found: 354.0947.

**(Z)-4-(benzyloxy)but-2-enyl 2-(((9H-fluoren-9-yl)methoxy)carbonylamino)acetate 18.** This compound was prepared from FMoc-glycine and alcohol **12**. The product was purified by flash column chromatography (silica, 6:1 hexane/EtOAc). The product was obtained as a white solid in a 38% yield. $^1$H NMR ($CDCl_3$) δ ppm 3.96 (d, 2H), 4.10 (d, 2H), 4.21 (t, 1H), 4.37 (d, 2H), 4.49 (s, 2H), 4.69 (d, 2H), 5.24 (bs, 1H), 5.68 (m, 1H), 5.84 (m, 1H), 7.37 (m, 9H), 7.58 (d, 2H), 7.74 (d, 2H). ESI HRMS Calcd for $C_{28}H_{27}NO_5Na$ $(M + Na)^+$ : 480.1781, found: 480.1819.

**Amino-acetic acid 4-benzyloxy-but-2-enyl ester 14.** Compound **13** (2.0 g, 5.9 mmol) was dissolved in $CH_2Cl_2$ (47 mL) at 0 °C followed by slow addition of TFA (7.1 mL). The mixture was stirred at room temperature for 1 h. After this time, the solvent was evaporated under reduced pressure. The residue was dissolved in 100 mL of $CH_2Cl_2$ and washed with a saturated solution of $NaHCO_3$ (4 x 50 mL) and saturated solution of NaCl (2 x 50 mL). The organic phase was dried with $MgSO_4$ and evaporated under vacuum. The product was obtained as yellowish oil in a 76% yield (1.1 g) and used in the following reaction without purification. $^1$H NMR ($CDCl_3$)

δ ppm 1.57 (bs, 2H), 3.41 (s, 2H), 4.12 (m, 2H), 4.51 (s, 2H), 4.69 (d, 2H), 5.71 (m, 1H), 5.81 (m, 1H), 7.33 (m, 5H),$^{13}$C NMR ($CDCl_3$) δ (ppm) 174.5, 138.3, 131.6, 128.9, 128.2, 126.7, 73.0, 66.1, 61.1, 44.4.

**Diazo-acetic acid 4-benzyloxy-but-2-enyl ester 8. Method A.** Glycinate **13** (2.2 g, 9.3 mmol), acetic acid (0.2 mL, 0.3 mmol) and isoamyl nitrite (1.7 mL, 13 mmol) were dissolved in $CH_2Cl_2$ (19 mL) and heated under reflux for 3.5 h. Afterwards, the mixture was diluted with $CH_2Cl_2$ (100 mL) and washed with 1M HCl (2 x 50 mL), deionized water (1 x 50 mL), saturated aqueous $NaHCO_3$ ( 2 x 50 mL), and deionized water (1 x 50 mL). The product was purified by flash chromatography (silica, 10:1 hexane/EtOAc) giving 0.5 g of an intense yellow oil in 20% yield. $^1$H NMR ($CDCl_3$) δ ppm 4.10 (d, 2H), 4.49 (s, 2H), 4.70 (d, 2H), 4.71 (bs, 1H), 5.70 (m, 1H), 5.78 (m, 1H), 7.31 (m, 5H),$^{13}$C NMR ($CDCl_3$) δ (ppm) 167.0, 138.4, 131.4, 128.9, 128.3, 127.0, 72.9, 66.1, 61.0, 46.7. IR: 2116s, 1690.s. EI HRMS Calcd for $C_{13}H_{14}N_2O_3Na$ $(M + Na)^+$: 269.0897, found: 269.0901.

**Diazo-acetic acid 4-benzyloxy-but-2-enyl ester 8. Method B.** The title compound was synthesized using literature procedure.[106] A solution of acetoacetate **19** (1.7 g, 6.6 mmol) and $Et_3N$ (1.2 mL, 8.5 mmol) in anhydrous acetonitrile (18 mL) were stirred at room temperature. Then, a solution of p-ABSA (2.1 g, 8.5 mmol) in acetonitrile (18 mL) was added dropwise over a 30 minute period. The reaction mixture was let stir for 3 h and an aqueous solution of 3N LiOH was added. The mixture was left for 27 h. After this time, the mixture was extracted with a mixture of ether/EtOAc 2:1 (3 x 50 mL). The organic layers were combined and extracted with brine (100 mL), dried over $MgSO_4$ and evaporated under vacuum. The crude product was purified by flash chromatography (silica, 10:1 petroleum Ether/EtOAc) to give 1.4 g of **8** as a

yellow oil in a 86% yield. Spectroscopy data were consistent with Method A results and literature information.

**(Z)-4-(benzyloxy)but-2-enyl 3-oxobutanoate 19.** The title compound was synthesized using the literature procedure.[106] Cis mono protected diol **12** (2.0 g, 11 mmol) was dissolved in 8 mL of anhydrous THF and NaOAc (56 mg, 0.7 mmol) was added with stirring. A solution of diketene (1.0 mL, 13 mmol) in 4 mL of THF was added dropwise over 1 h to the refluxing mixture. Then, the mixture was refluxed for 1 h more until total consumption of the mono protected diol starting material had occured. The reaction mixture was dissolved in ether (40 mL) and washed with brine (60 mL). The organic phase was dried over $MgSO_4$ and evaporated under vacuum. The crude oil was purified by flash chromatography (silica, 6:1 petroleum ether/EtOAc) to give **19** in a 60% yield (1.7 g). $^1$H NMR ($CDCl_3$) δ ppm 2.25 (s, 3H), 3.44 (s, 2H), 4.12 (d, 2H), 4.51 (s, 2H), 4.68 (d, 2H), 5.71 (m, 1H), 5.82 (m, 1H), 7.33 (m, 5H), $^{13}$C NMR ($CDCl_3$) δ (ppm) 200.7, 167.3, 138.4, 131.9, 128.9, 128.2, 126.4, 73.0, 66.1, 61.6, 50.4, 30.6. Spectroscopy data were consistent with literature information.

**6-Benzyloxymethyl-3-oxa-bicyclo[3.1.0]hexan-2-one 9.** Diazoester **8** (3.0 g, 12 mmol) was dissolved in dry $CH_2Cl_2$ (131 mL) to make a 0.09 M solution of the ester starting material. This solution was added from an addition funnel to a refluxing suspension of CuOTf (61 mg, 0.3 mmol) and Evan's ligand (80 mg, 0.3 mmol) in 400 mL of $CH_2Cl_2$ over a period of 18 h. When the addition was finished, the solvent was evaporated under vacuum and the residue was purified by flash chromatography (silica, 5:1 hexane/EtOAc). The bicyclic product was obtained as a colorless oil in 60% yield. The same reaction was performed using $Rh_2(OAc)_4$ in $CH_2Cl_2$ and $CuSO_4$ in benzene. The products were isolated in 32% and 48% yield respectively. $^1$H NMR ($CDCl_3$) δ ppm 1.83 (m, 1H), 2.32 (dd, 1H), 2.39 (q, 1H), 3.42 (dd, 1H), 3.71 (dd, 1H), 4.22 (d,

1H), 4.41 (dd, 1H), 4.54 (q, 2H), 7.35 (m, 5H), $^{13}$C NMR ($CDCl_3$) δ (ppm) 174.7, 138.2, 128.9, 128.3, 73.8, 66.8, 65.1, 22.9, 21.8. EI HRMS Calcd for $C_{13}H_{14}O_3$ $(M)^+$: 218.0943, found: 218.0944

CHAPTER 3
SYNTHESIS OF DIAZABICYCLIC TRANSITION STATE ANALOGS

## Introduction

After the synthesis of the core all *cis* trisubstituted cyclopropane ring, the diaza moiety of the TS analogs needed to be constructed. While the three membered ring gives the desired shape and conformation of the proposed inhibitors, the heterocyclic portion of the compound plays the role of mimicking the anomeric center of the enzymes sugar-based substrates. In the course of the multistep synthesis, some features of these molecules design were modified in order to generate other potential inhibitors. Accordingly, the resulting expanded set of analogs might provide a greater understanding of glycosidase and glycosyltransferase catalytic reactions and the requirements for inhibition of the enzymes. One of the variables was the size of the diaza ring. Consequently, synthetic pathways that lead to seven-, six- and five-membered rings containing the amidine functionality were designed (Figure 3-1). The size of the heterocyclic ring modifies the position of the LG with respect of the trigonal planar center, and varies the flexibility of the ring; factors which might have an effect on enzyme-TS analog interaction.

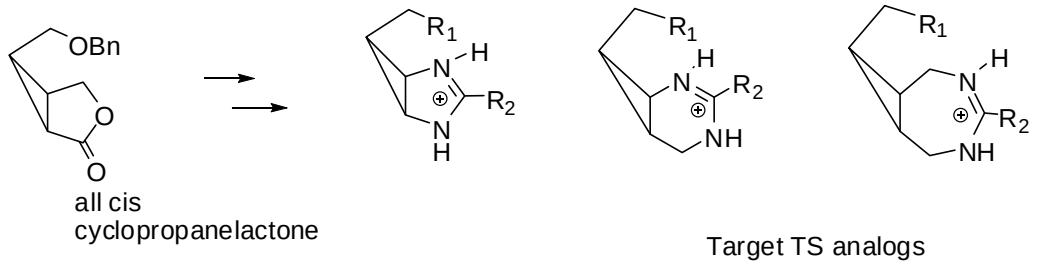


Figure 3-1. Proposed TS analogs with different ring sizes

In addition, replacing the ring nitrogen atom (aza) by an oxygen (oxa) will alter the electronic delocalization around the anomeric center mimic, which could be useful for the study of charge-charge interactions between the inhibitor and the catalytic residues. Finally, preliminary results on the synthesis of diazabicyclic molecules with functionalized side chains

were also obtained. Different side chains attached to the bicyclic core will help to better simulate the substrates' structure and provide additional binding energy.

## Results and Discussions

As already mentioned in the introduction of this chapter, different synthetic routes will be followed for the preparation of the inhibitors. They all started with the cyclopropane lactone **9,** whose synthesis was described in Chapter 2.

### Synthesis of Seven-Membered Ring Amidines

In this case, the lactone moiety was opened by $LiAlH_4$ reduction to give the diol **20** in 79% yield. This reaction is shown in Figure 3-2.

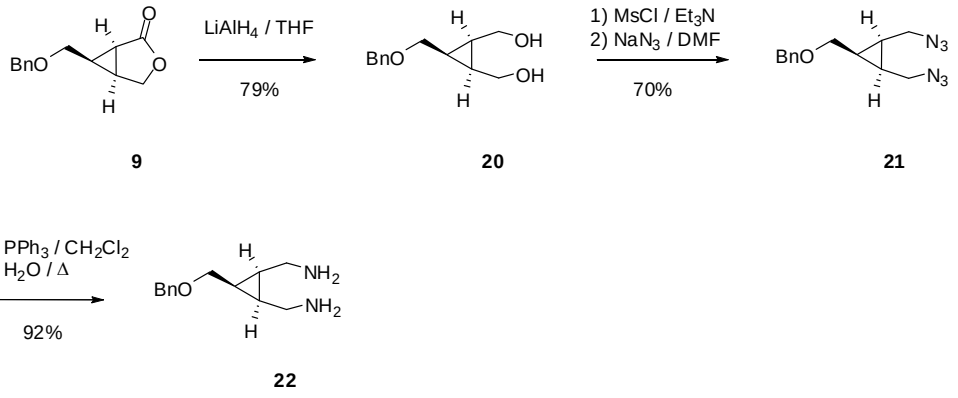


Figure 3-2. Synthesis of diamine **22**

Activation of compound **20**'s two primary hydroxyl groups with methanesulfonyl chloride (MsCl) and subsequent nucleophilic displacement with $NaN_3$ in DMF, resulted in the diazide **21**. The diamine **22** was obtained in 95% yield from the diazide **21** using mild and selective Staudinger reaction conditions.[108] The reduction of the azide functionality proceeds via an iminophosphorane intermediate. Subsequent hydrolysis with water generates the diamine which was found to be an extremely polar compound. Purification of **22** was performed by flash chromatography on silica gel using $CH_2Cl_2$:MeOH:$NH_4OH$ 1:1:0.01 as the eluent solvent system. Following the Hamilton *et al.* Methodology (described also in Chapter 2),[98] the reaction

of ethyl glycoloimidate and diamine **22** in EtOH, allowed the second ring closure to afford the amidine functional group (Figure 3-3).

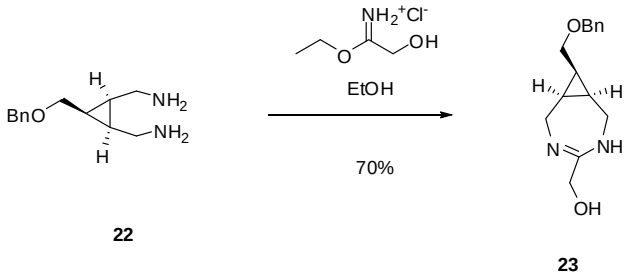


Figure 3-3. Synthesis of hydromethylamidine **23**

The hydroxymethyl amidine **23** was obtained as a white solid in 70% yield. This hydroxylmethyl amidine was envisioned as the precursor to the α-carboxy amidine via an oxidation reaction, as precedented in Hamiltons work.[98] The carboxy amidine would provide functionality analogous to the carboxylate group that would be found in the oxocarbenium ion derived from N-acetylneuraminic acid (sialic acid). Compound **23** was submitted to different oxidative reaction conditions. The first attempt involved $KMnO_4$ as the oxidating agent, which was successfully utilized previously to prepare 2-carboxy imidazole **4** (Chapter 2).

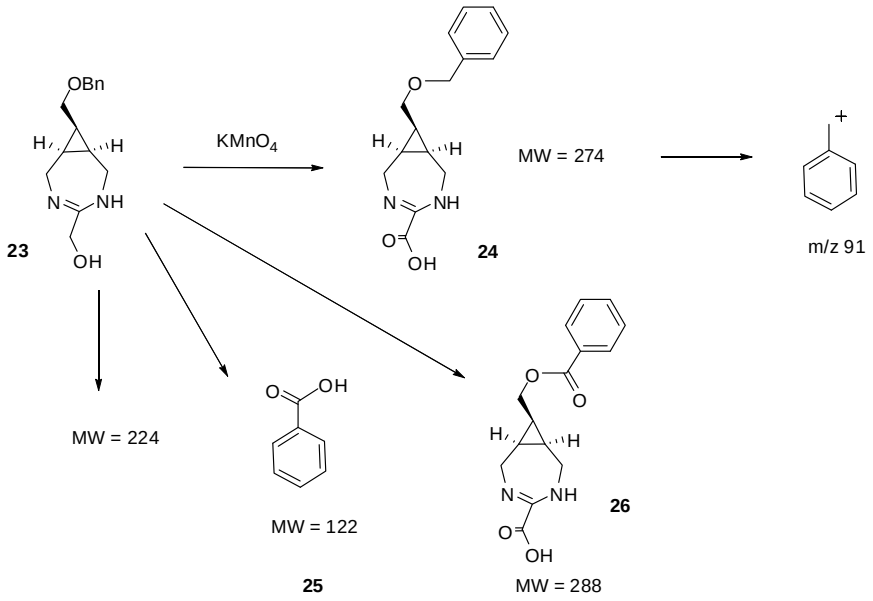


Figure 3-4. Oxidation of hydromethy amidine **23**

After purifying the reaction mixture by preparative thin layer chromatography (TLC), the samples were analyzed by $^1$H NMR and HPLC/MS spectroscopy. Several products were detected by these techniques. Although present as a minor component, one of these compounds was identified as the desired carboxy amidine which has a MW of 274 (Figure 3-4). The fragmentation pattern of this peak yielded the m/z 91 ion which corresponds to the benzyl moiety. Unfortunately, the major impurities present in the sample were benzoic acid with a MW of 122, compound **26** and a non UV-absorbing molecule with MW of 224 which could not be identified. The same alcohol oxidation was tried but utilizing ruthenium oxide under the Sharpless conditions.[109] In this reaction $RuCl_3$ is oxidized *in situ* by sodium periodate and then coordinated by acetonitrile. This creates a rapid and mild oxidizing agent. However, when compound **23** was treated with this reagent, the loss of the benzyl protecting group was again observed. The reaction mixture displayed a very similar $^1$H NMR spectrum to that observed for the $KMnO_4$ reaction. Consequently, the oxidation of the hydroxymethyl group to the aldehyde, instead of the carboxylic acid, was investigated. Several reagents were employed such as pyridinium chlorochromate (PCC) in $CH_2Cl_2$, DMSO and oxalyl chloride under Swern oxidation conditions and Dess-Martin periodinate. In most cases, degradation of the substrate was observed. It was noted though, that the poor solubility of **23** in organic solvents may have reduced the efficiency of the oxidation reaction.

Numerous authors had reported the conversion of the trichloromethyl functionality into the corresponding ester.[110-114] This reaction was performed by either basic hydrolysis with NaOH or by treatment with $AgNO_3$ in MeOH. Therefore, the trichloromethyl amidine was synthesized. The corresponding imidate was prepared by adding trichloroacetonitrile in a solution containing $K_2CO_3$.[115] The reaction of trichloroimidate **27** with diamine **22** afforded compound **28** in 40%

yield (Figure 3-5). Any attempts to convert amidine **28** into the carboxyamidine using the two methods previously described resulted in unreacted starting material. After these unsuccessful efforts to obtain the carboxyamidine from compound **23**, the synthesis of another amidine substituent synthon was explored.

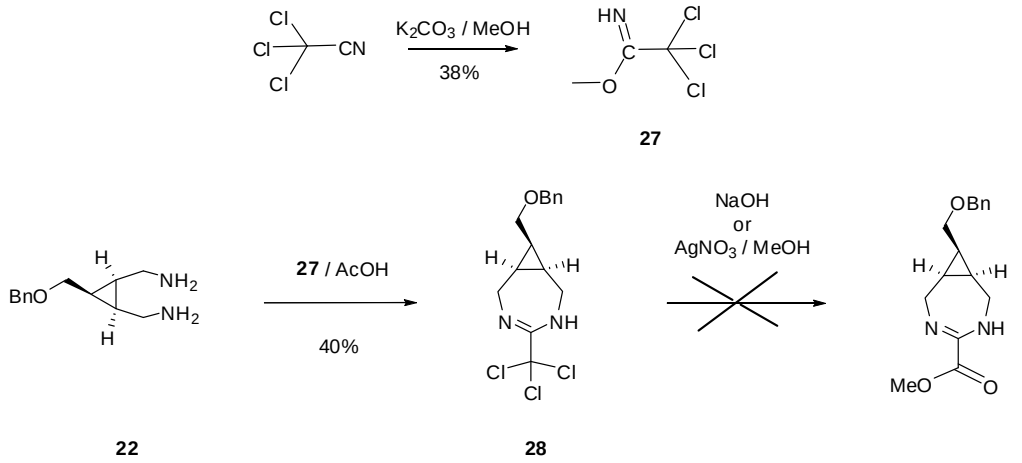


Figure 3-5. Synthesis of trichloroamidine **28**

The methyl phosphonate functionality might be a suitable substitution for the carboxyl acid. Based on Schmidt's TS analogs studies on sialyltransferases,[60,72-74] the carboxylic residue can be replaced by related functional groups. The incorporation of a second charge through a phosphonate group on Schmidt's anlogs exhibited an increased inhibitor-enzyme binding affinity (see analog 8 and 9 in Figure 1-25). Following these observations, the phosphonate amidine **30** was pursued (Figure 3-6).

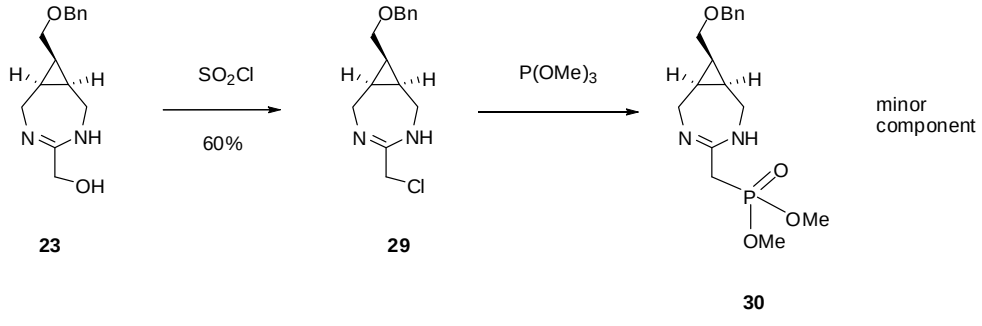


Figure 3-6. Synthesis of chloroamidine **29**

In order to synthesize **30**, chloromethyl amidine **29** was prepared first. This synthesis was carried out by treating the hydroxymethyl derivative with thionyl chloride under reflux conditions.[116] The α-chlorinated amidine **29** was obtained in 60% yield as a yellow solid after flash chromatography purification (Figure 3-6).

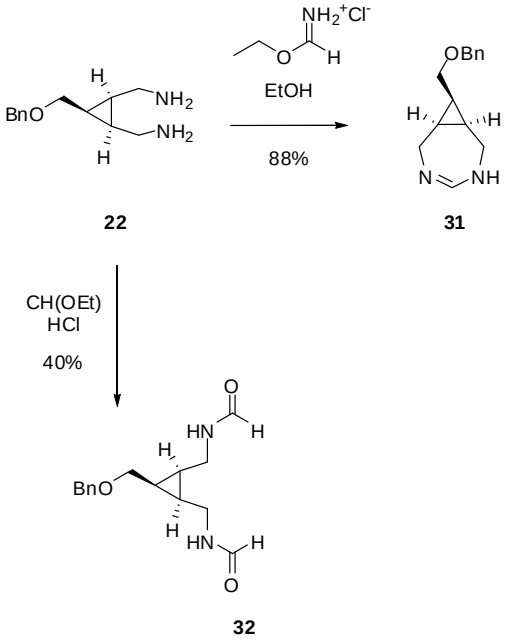


Figure 3-7. Synthesis of amidine **31** and diacylated amine **32**

The reaction of an alkyl halide with a phosphite ester is known as the Michaelis-Arbuzov reaction which proceeds through an unstable trialkoxyphosphonium intermediate. This ion has a great reactivity towards nucleophilic attack which causes the rupture of the C-O bond and the formation of the phosphoryl P=O bond. Thus, a mixture of compound **29** and trimethyl phosphite was stirred under reflux until no more chloro amidine starting material was observed by TLC. The reaction was purified by silica gel flash chromatography using $CH_2Cl_2$:MeOH 4:1 as the eluent solvent. Analysis of a promising fraction by MS spectrometry showed the presence of the desired molecule (MW of 352) and several non identified by-products. Attemps to improve the yield of phosphonate derivative by the modified Arbuzov reaction, which utilize KI and

trimethyl phosphite in an acetone-acetonitrile solvent, reproduced, to some extent, the previous results. After the difficulties meet in the synthesis of the carboxy or phosphonate amidines, the simpler amidine **31** was prepared. This compound also had the features ambitioned on the TS analogs for the carbohydrate processing enzymes (Figure 3-7).

The synthesis of amidine **31** was first carried out using neat trimethyl orthoformate, and HCl as the catalyst (Figure 3-7). This reaction provided the molecule **32** that had a very similar $^{1}$H NMR spectrum when compared with that of the expected compound **31**. Analysis of the reaction by MS and 500 MHz NMR resulted in identification of **32** as the diacylated compound.

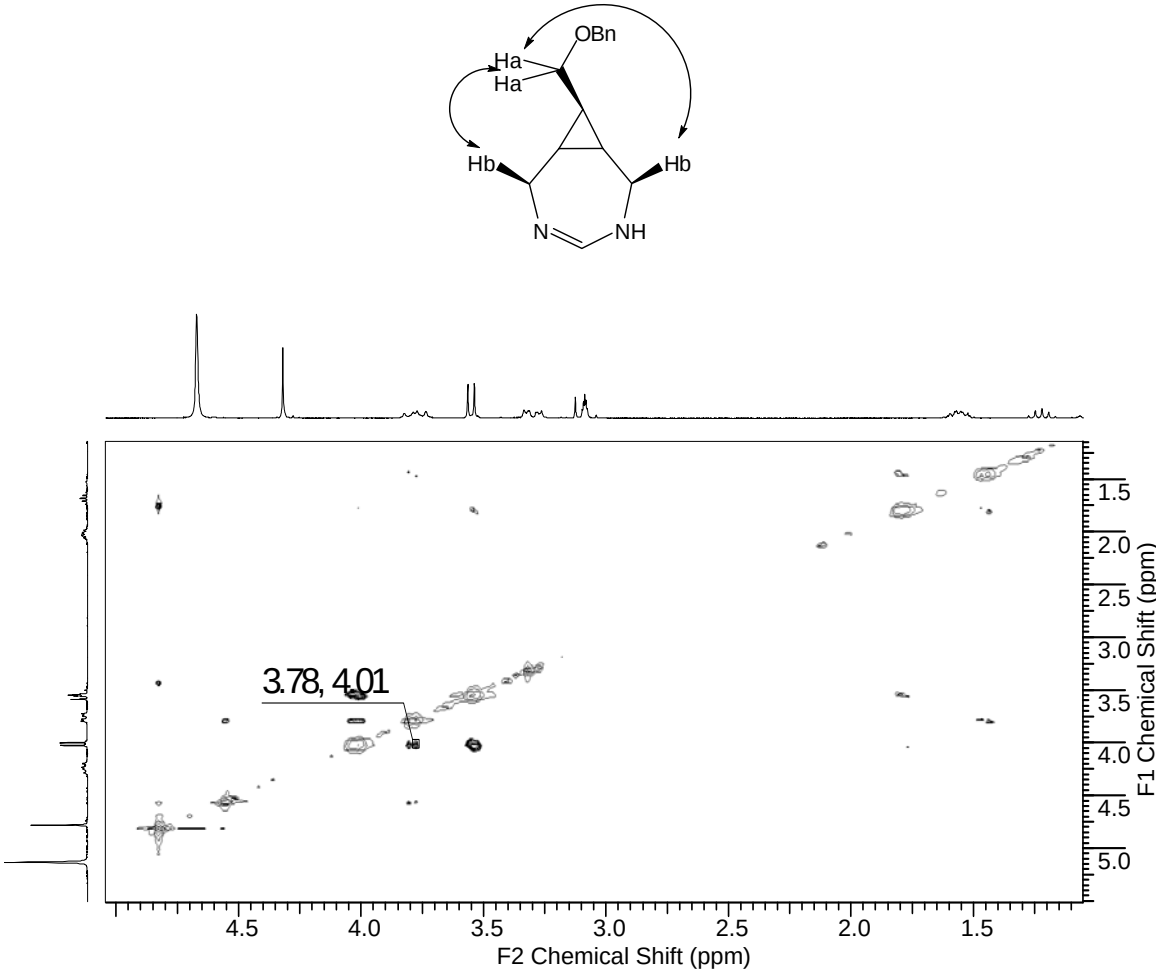


Figure 3-8. 2D-NOESY for amidine **31**

When p-toluenesulfonyl acid and one equivalent of trimethoxy orthoformate were utilized in this reaction, the desired compound **31** was obtained in 46% yield. Based on these results, it appears that the formation of the diacylated amine with $(CH_3O)_3CH/HCl$ was driven by the large excess of the orthoformate and the subsequent hydrolysis by the water present in the system. To improve the yield in the amidine reaction, compound **31** was synthesized by using ethyl formoimidate in EtOH. In this case, the amidine derivative was obtained as a white solid in 88% yield (Figure 3-7). This compound's stereochemistry was analyzed by NOESY 2D NMR in order to confirmed the desired all *cis* configuration. A crosspeak was observed between Ha ($\delta_{Ha}$ = 3.78 ppm) and Hb ($\delta_{Hb}$ = 4.01 ppm), indicated their proximity and was only consistent with an all *cis* cyclopropane geometry (Figure 3-8).

Removal of the benzyl protected group of compounds **31** and **23** was performed by conventional ammonium formate hydrogenation, giving in both cases quantitative conversion (Figure 3-9).

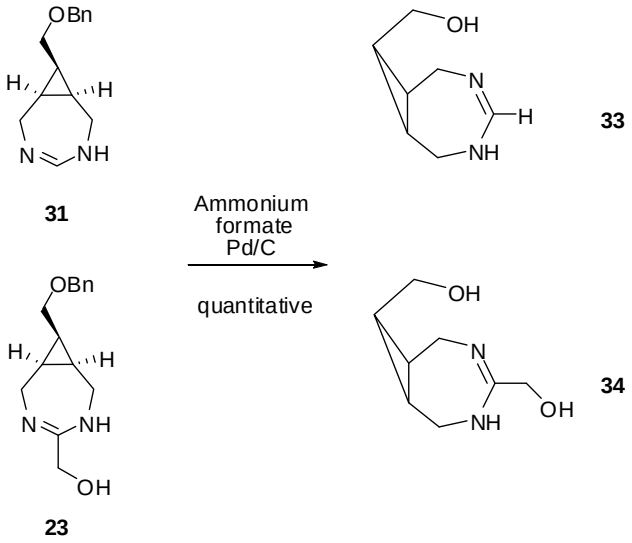


Figure 3-9. Deprotection of compounds **31** and **23** benzyl groups

**Synthesis of Five-Membered Ring Amidines Precursor**

An important step on the synthetic route of the five-member ring bicyclic TS analogs was to obtain the amine functionality directly attached to the cyclopropane ring. Starting from the cyclic lactone, this can be achieved by converting the ester into an amide and then, obtain the amine group by Hofmann rearrangement conditions. Another possibility is to perform a Curtius rearrangement on the carboxylic acid after opening the lactone in basic media (Figure 3-10).

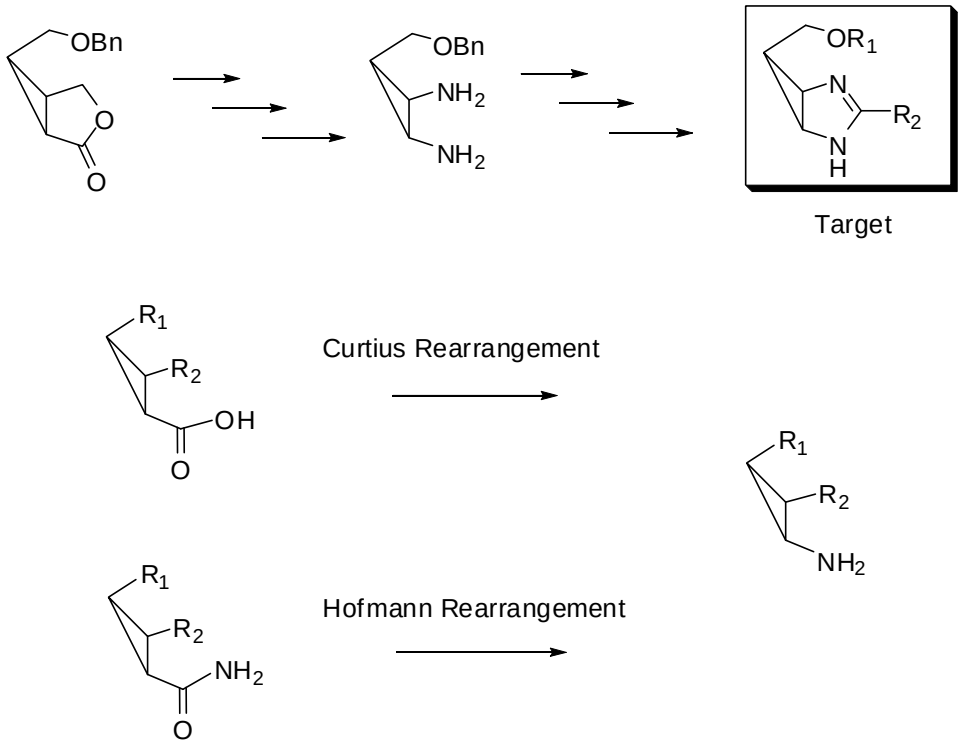


Figure 3-10. Products of Hofmann and Curtius rearrangements

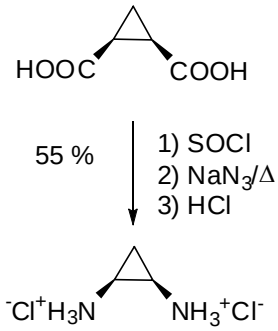


Figure 3-11. *Cis* diamine prepared by Guryn *et al.*[117]

Both reactions are suggested to proceed through a concerted mechanism in which there is a migration of a functional group to an electron-deficient nitrogen atom. This migrating group retains the starting stereochemical configuration. The product of these reactions is the corresponding isocyanate which can be hydrolyzed to the desired amine. There are several examples of these reactions in the literature.[118-125] One of them was the synthesis of cis-cyclopropanediamine by Guryn's group utilizing *cis*-cyclopropanedicarbonyl dichloride (Figure 3-11).[117] This was an important piece of evidence that the desired *cis* diamine synthon might be relatively easy to achieve.

Treatment of lactone **9** with a concentrated solution of ammonium hydroxide in MeOH afforded the cyclopropanecarboxamide **35** in a 78% yield. Before converting the amide group into the amine, compound **35**'s primary hydroxyl group was protected with TBDMSCl. From the different Hofmann reaction conditions examined, including $Pb(OAc)_4$[118,126] and $Br_2$ in NaOMe[123], the successful method utilized N-bromosuccinimide in MeOH in the presence of DBU (1,8-diazabicyclo[5.4.0]undec-7-ene) (Figure 3-12).

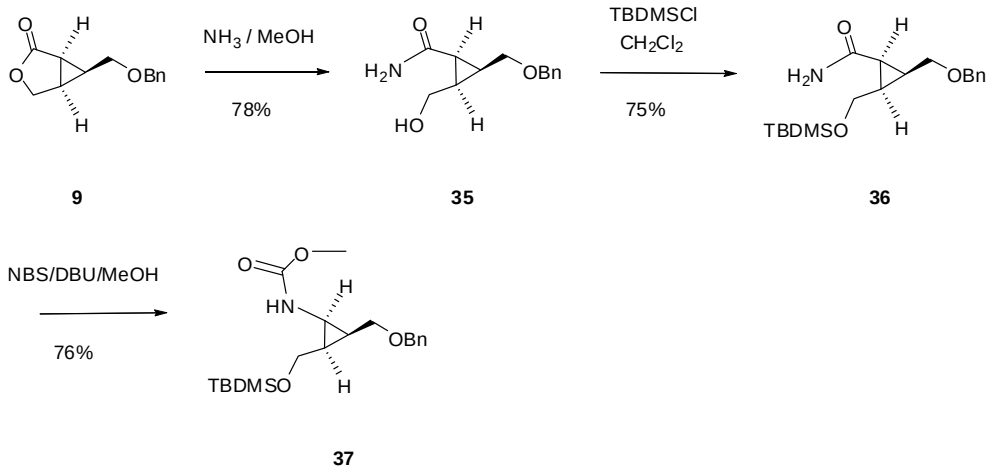


Figure 3-12. Synthetic route for carbamate **37**

The methyl cyclopropylcarbamate **37** was afforded in 76% yield. At this stage, compound **37**'s primary hydroxyl group needed to be transformed in a way to obtain the second amino

group directly connected to the cyclopropane ring. Thus, compound **37** was deblocked with tetrabutylammonium fluoride and subjected to different oxidative agents (Figure 3-13).

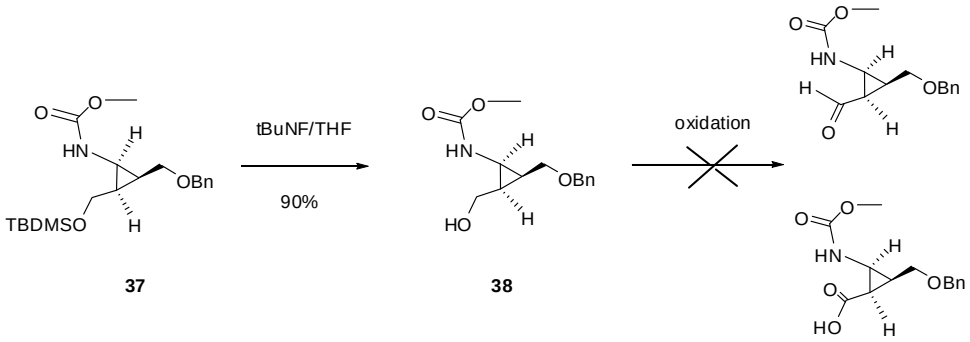


Figure 3-13. Oxidation of carbamate **38**

Attempted oxidations of alcohol **38** by classical Jones, PCC, tetra-n-propylammonium perruthenate (TPAP)/ N-methylmorpholine (NMO) and Swern reagents or even the mild $RuCl_3/NaIO_4$ could not generate the desired aldehyde or carboxylic acid. In all cases, degradation and spontaneous ring opening of the material was observed. The carbonyl (electro-withdrawing) group on one side of the cyclopropyl ring could act as a sink for the nitrogen electron pair, promoting the ring opening. As a result, a new synthetic approach was designed to avoid this problem. In the new pathway, the lactone ring was hydrolyzed in alkaline conditions, followed by esterification with diazomethane/Diazald which gave the hydroxyester **40** in a 76% overall yield. Subsequent oxidation of the free hydroxyl group with TPAP/NMO resulted in the unexpected *trans*-aldehyde **41** (Figure 3-14).

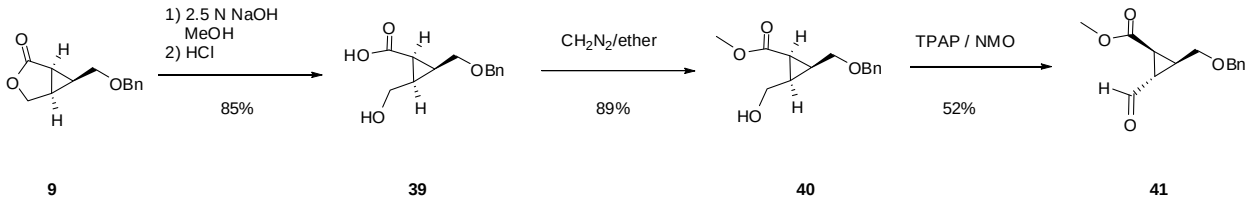


Figure 3-14. Reaction to prepare trans-aldehyde **41**

The 2D-NOESY characterization (Figure 3-15) of compound **41** exhibited crosspeaks between Ha-Hb ($\delta_{Ha}$ = 9.40 and $\delta_{Hb}$ = 2.46) and Ha-Hc ($\delta_{Hc}$ = 2.22). Then, Hd ($\delta_{Hd}$ = 2.55) displayed spatial interaction with the two He ($\delta_{He}$ = 3.80 and 3.65). From these results, it was believed that the aldehyde was undergoing epimerization due to the exposure to perruthenate basic media. Thus, the oxidation was carried out using the hypervalent iodine (V) of the Dess-Martin reagent instead. In this occasion, only the *cis*-aldehyde **42** was produced in a good 82% yield. Once again, the structure of this compound was assigned using 2D-NMR. For the aldehyde hydrogen Ha ($\delta_{Ha}$ = 9.73), a crosspeak with Hb ($\delta_{Hb}$ = 4.09) was observed. Then, the ester methyl group ($\delta_{CH3}$ = 3.71) displayed crosspeaks with Ha and the hydrogens on the phenyl ring ($\delta_{Ph}$ = 7.33) (Figure 3-16).

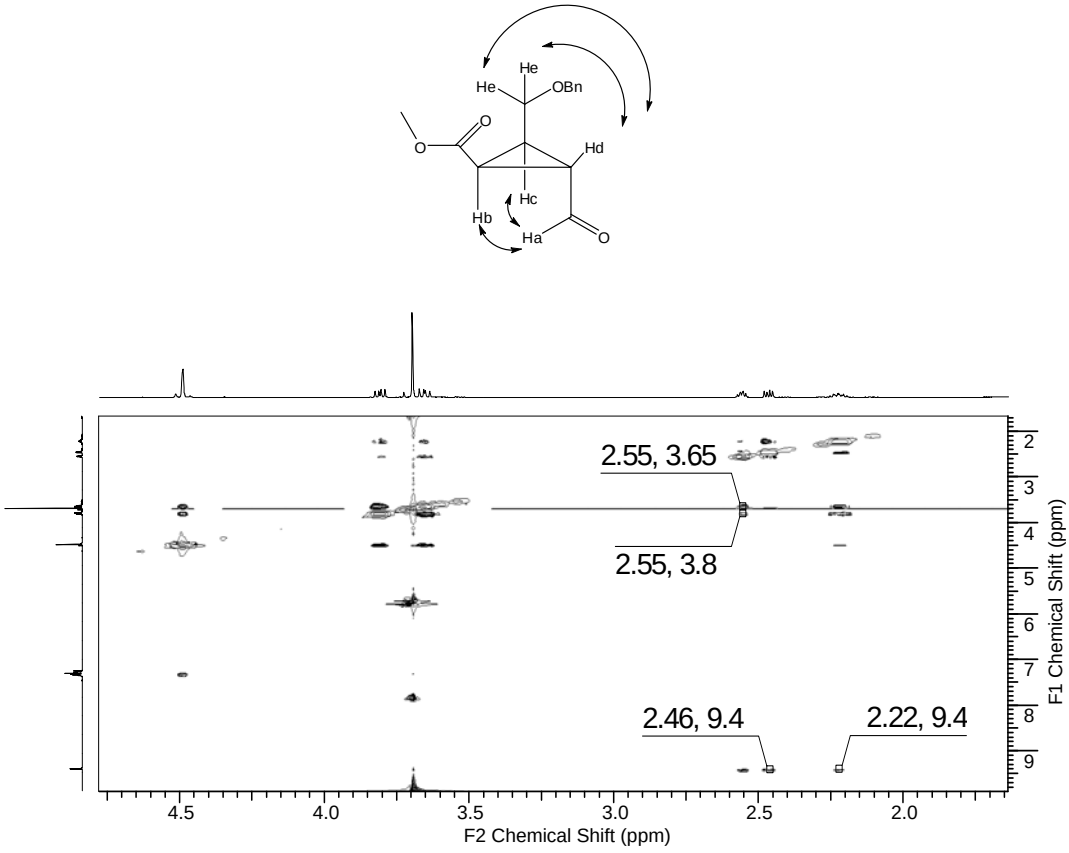


Figure 3-15. NOE interaction for trans-aldehyde **41**

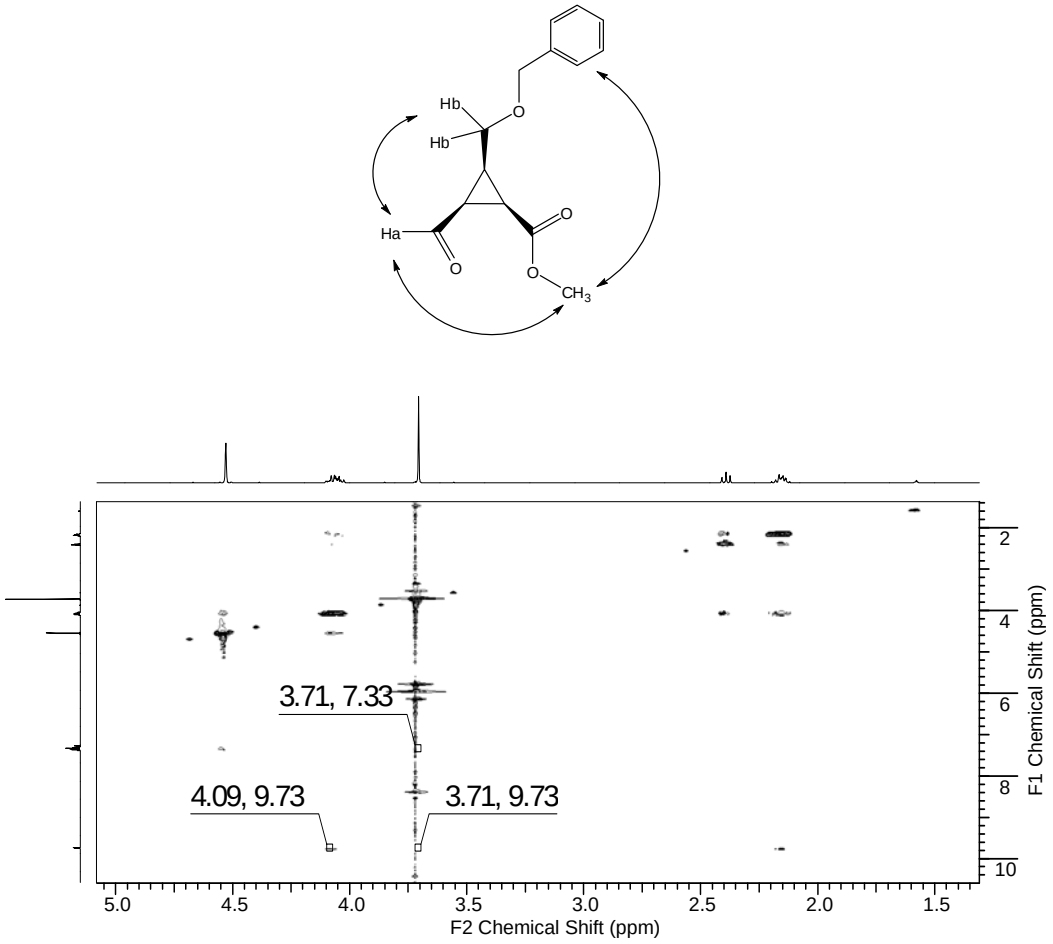


Figure 3-16. NOE interaction for trans-aldehyde **42**

Further oxidation of compound **42** with $NaClO_2/H_2O_2$ under buffered conditions,[127] gave the carboxylic acid **43** in 87% yield (Figure 3-17).

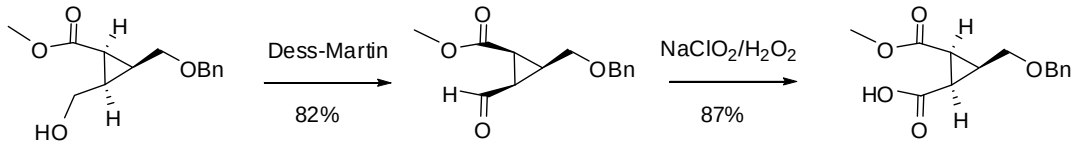


**40** **42** **43**

Figure 3-17. Synthesis of compound **43**

Then, the free carboxylic group of compound **43** was subjected to the Curtius reaction. Two methods were tested in this case. The first one utilized diphenylphosphoryl azide (DPPA) and triethylamine[118] and the second one used ethyl chloroformate and $NaN_3$.[125] The acyl azide

that is formed as an intermediate is hydrolyzed with t-BuOH. Neither stepwise procedure afforded the carbamate of interest (Figure 3-18).

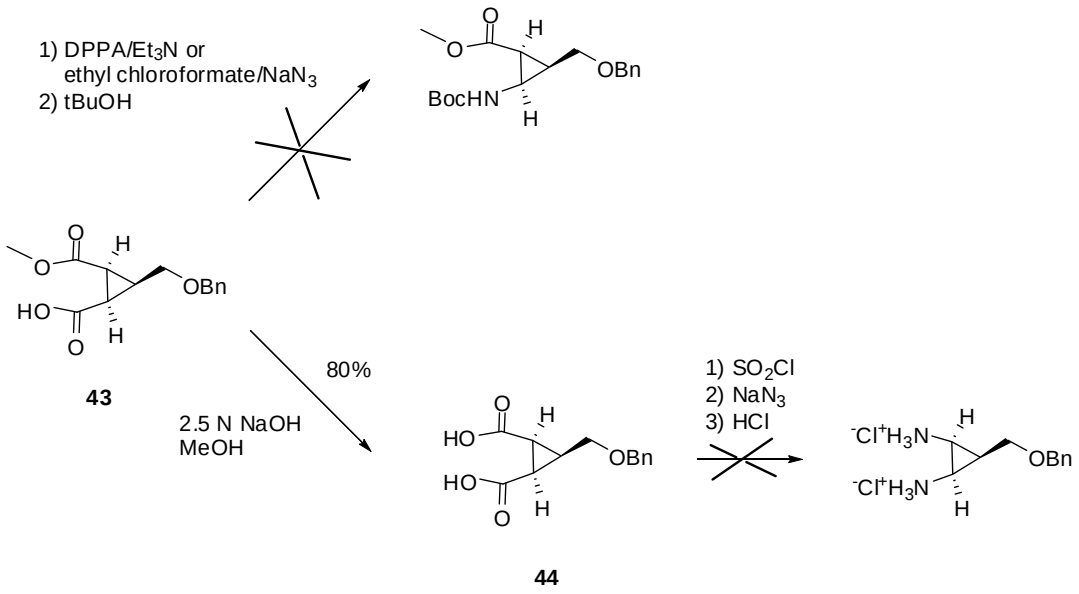


Figure 3-18. Synthesis of dicarboxylic acide **44**

In order to follow Guryn's synthetic procedure[117] for the cis-cyclopropanediamine, compound **43** methyl ester was hydrolyzed with aqueous 2.5 N NaOH. The diacid **44** was isolated from the organic extract without further purification in an 80% yield. The free cyclopropyl diacid was sequentially treated with thionyl chloride and a solution of $NaN_3$ in acetone/$H_2O$. After extracting the reaction mixture with ether, the crude mixture was dissolved in toluene and added dropwise to a solution of warmed 10% aqueous HCl. Characterization of the double Curtius reaction by $^1H$ NMR did not reveal any evidence for diamine formation (Figure 3-18). At this point, the synthesis of the *cis* cyclopropane diamine had turned out to be a very challenging task. Nevertheless, a last synthetic approach that involved a double Hofmann rearrangement of diamide **46** was pursued. In order to execute this synthesis, compound **43** was esterified with diazomethane which generated the diester **45** in an 88% yield. The diamide **46**

was successfully prepared by dissolving compound **45** in a ~16 M solution of $NH_3$/MeOH and letting it react in a pressure bottle for 4 days at 50 °C (Figure 3-19).[128,129]

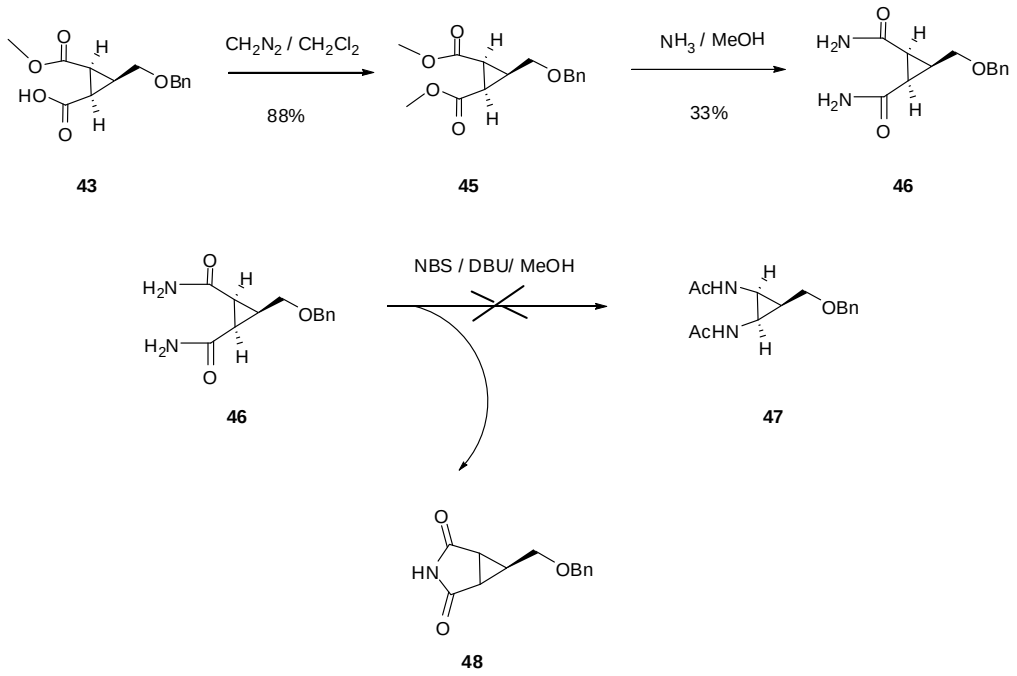


Figure 3-19. Synthesis of diamide **46**

Attemps to obtain the dicarbamate **47** by the Hofmann reaction with NBS/DBU, afforded a symmetric product which did not displayed the expected proton NMR chemicals shifts. Later on, this compound was identified by C18 HPLC/ESI-MS to be the succinimide **48** (Figure 3-19). Having in mind that the basic Hofmann reaction conditions might have promoted the amide intramolecular cyclization, the possibility of performing this reaction under acidic condition was investigated. Usually, iodoorganic reagents such us bis(trifluoroacetoxy)iodobenzene known as PIFA or iodobenzene diacetate (PIDA)[130-132] are utilized for the rearrangement of amides under mildly acid conditions. Unfortunately, after treatment of the diamide **46** with these iodo reagents, the synthesis of the diamine of interest could not be accomplished. In both cases mostly unreacted starting material and, in minor extent, decomposition products were observed by TLC and $^1$H NMR. Based on the Curtius and Hofmann rearrangement results, it is believed that the

presence of the bulky $CH_2OBn$ might have affected, by steric hindrance, the viability of these double rearrangement reactions.

**Synthesis of the Six-Member Ring Amidine Precursor**

The synthetic pathway for the diamine that gives rise to the six-member ring amidine started with the hydroxyamide **35** (Figure 3-20).

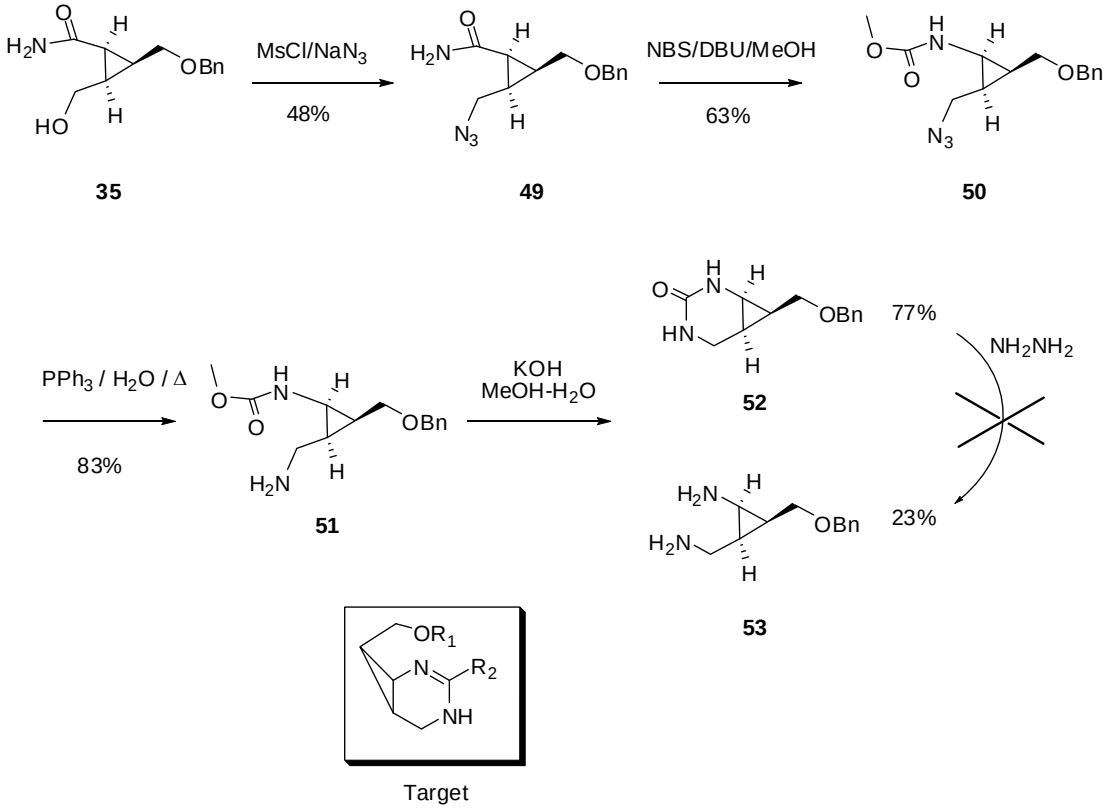


Figure 3-20. Synthesis of diamine **53**

The convertion of the primary alcohol to the azide group (compound **49**) was achieved by the two-step procedure involving MsCl and $NaN_3$. The overall yield was 48% after purification by flash chromatography. Transformation of the amide to give carbamate **50** was done using the Hofmann reaction, in a 63% yield. A challenge after synthesizing this compound resided in the purification. The desired product co-eluted with an impurity that was only detected when the TLC plate was visualized with the oxidant $KMnO_4$. After this discovery, compound **50** was

successfully purified by flash chromatography using petroleum ether/EtOAc (10:1 ratio) as the eluent. To synthesize the aminocyclopropylcarbamate, triphenylphosphine was employed as the reducing agent for the azide **50**. Deprotection of the methyl carbamate group of **51** with ethanolic KOH not only afforded the diamine of interest, but also the cyclization product **52** (Figure 3-20). The bicyclic urea **52** turned out to be very stable. Only starting material was observed by TLC when **52** was treated with hydrazine in attempts to open the ring. At this stage, it was necessary or either search for different solvents that could give a more labile carbamate at the Hofmann rearrangement step or deblock the amide by non alkaline conditions. Unfortunately, the efforts to trap the Hofmann isocyanate using other solvents such as $H_2O$ and tBuOH failed to give the desired product. In addition, decomposition of the starting material **50** was observed when a mixture of HCl/HOAc, 10% KOH/MeOH or iodotrimethylsilane (TMSI) were tested as carbamate deprotecting agents. In conclusion, improvements on the yield for the carbamate **51** deblocking reaction might be attained using other non-conventional reagents.

**Synthesis of the Six-Member Ring Oxazine Precursor**

To take advantage of the synthesis that lead to hydroxymethyl carbamate **38**, the preparation of the corresponding oxazine was considered (Figure 3-21).

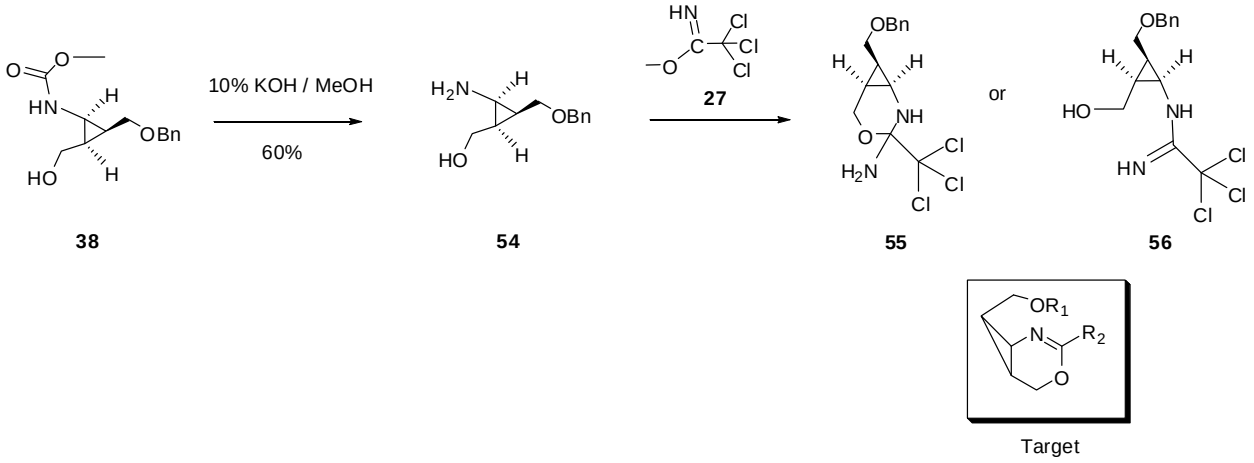


Figure 3-21. Synthesis to prepare aminoalcohol **54**

Accordingly, cyclopropylaminoalcohol **54** was obtained by alkaline deprotection of carbamate **38**, with a 60% yield after chromatographic purification using EtOAc/MeOH 10:1. Unfortunately, a preliminary trial to promote the oxazine ring closure with trichloroacetoimidate, finished up in compound **55** or **56** according to the m/z ion of 351 observed by ESI-FTICR mass spectrometry. Both compounds have the same MW and differ from the desired oxazine (MW = 334) in 17 mass units (possible $NH_3$). The $^1H$ NMR was similar to the starting material but with two extra broad singlets which integrated for 2H. This NMR analysis might point to the formation of compound **56** instead of **55**.

**Synthesis of Seven-Membered Ring Oxazepine**

In this case, the cyclopropyl carboxamide **35** was used as the starting material. After trying different reaction conditions and reagents for the amide reduction, the most efficient one turned out to be $LiAlH_4$ in THF in a stoichiometric ratio of 22:1 aluminum with respect to the amide. Compound **57** was obtained in a 51% yield after quenching the reaction with water, filtration through Celite and purification by flash chromatography (Figure 3-22).

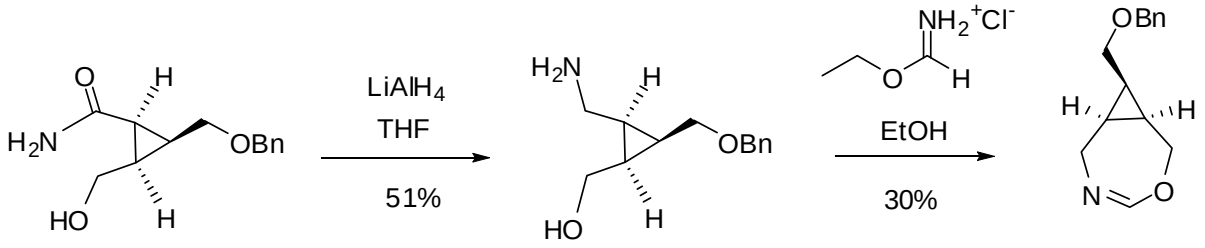


**35** **57** **58**

Figure 3-22. Synthesis of oxazepine **58**

Oxazepine **58** was obtained in a 30% yield using the same procedure as for compound **31**. Although MS analysis indicated the presence of contaminants, the major product of the reaction was oxazepine **58**. A more careful purification will be needed in future work with this compound.

**Synthesis of α-Functionalized Diazoacetate Esters**

One strategy to produce inhibitors with side chains attached to the cyclopropyl ring fusion carbons would be to use alpha-substituted diazo esters in the initial intermolecular cyclopropanation reaction. Introduction of the side chain to the acetoacetate ester **19** is outlined below (Figure 3-23). Compound **19** was treated with NaH followed by a solution of either allyl or benzyl bromide in dimethoxyethane (DME) to give alkylation products **59** and **60** in 73% and 61% yields, respectively (Figure 3-23). Subsequent diazo transfer reaction based on Collado's procedure[106] produced the corresponding α-functionalized diazoesters of interest without any difficulties. These two compounds are ready to be subjected to cyclopropanation reaction conditions with the purpose of generating **63** and **64**. These side chains could be further modified to prepare other TS analogs (Figure 3-23). For example, a variety of functionalizations could be performed on the allyl group of **64** including dihydroxylations and hydroxylation.

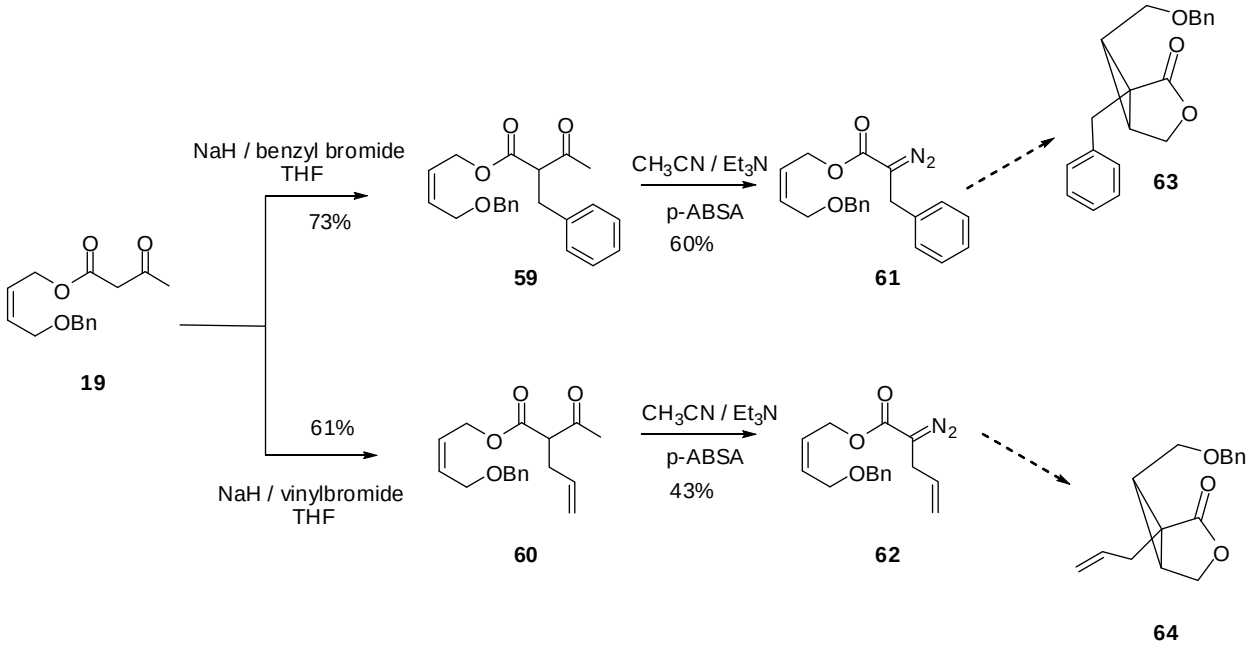


Figure 3-23. Synthesis of functionalized diazoacetates

**Synthesis of TS Nucleotide Analogs**

For the sialyltransferase TS analogs, the final step on the synthetic route involved conjugation of the molecule **33** with cytidine monophosphate (CMP). In order to accomplish this coupling, different methodologies can be followed.

The synthesis of oligo- and poly-nucleotides is one of the most challenging areas in the nucleic acids world due to the high number of possible side reactions that their chemistry involves. Among the difficulties that are needed to overcome, a matter of essential importance is the choice of the appropriate protecting groups not only for the nucleosides but also, for the internucleotide linkage. These groups should be able to be removed under conditions that will not affect other groups present in the rest of the molecule. Several methods have been developed in order to prepare oligonucleotides.[133] One of them is the called phosphoramidite approach. This method was introduced by Beaucage and Caruthers, in 1981, with the highly reactive intermediate phosphoramidite (Figure 3-24).[134]

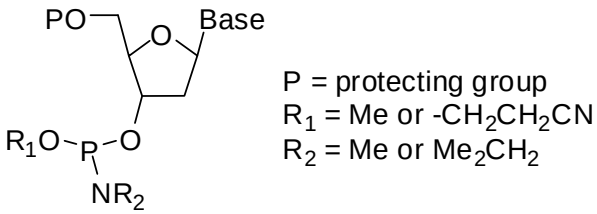


Figure 3-24. Nucleoside phosphoramidates

These nucleoside phosphoramidates are successfully utilized in solid phase synthesis of dinucleoside phosphates. The disadvantage of this approach, when applied in liquid phase synthesis, is the high moisture sensitivity of the reagents, which makes their handling extremely difficult. Another method that is widely used and was utilized in this thesis research is the phosphotriester approach.[133,135] A summary of the reagents and procedure applied in this synthesis is indicated in Figure 3-25.

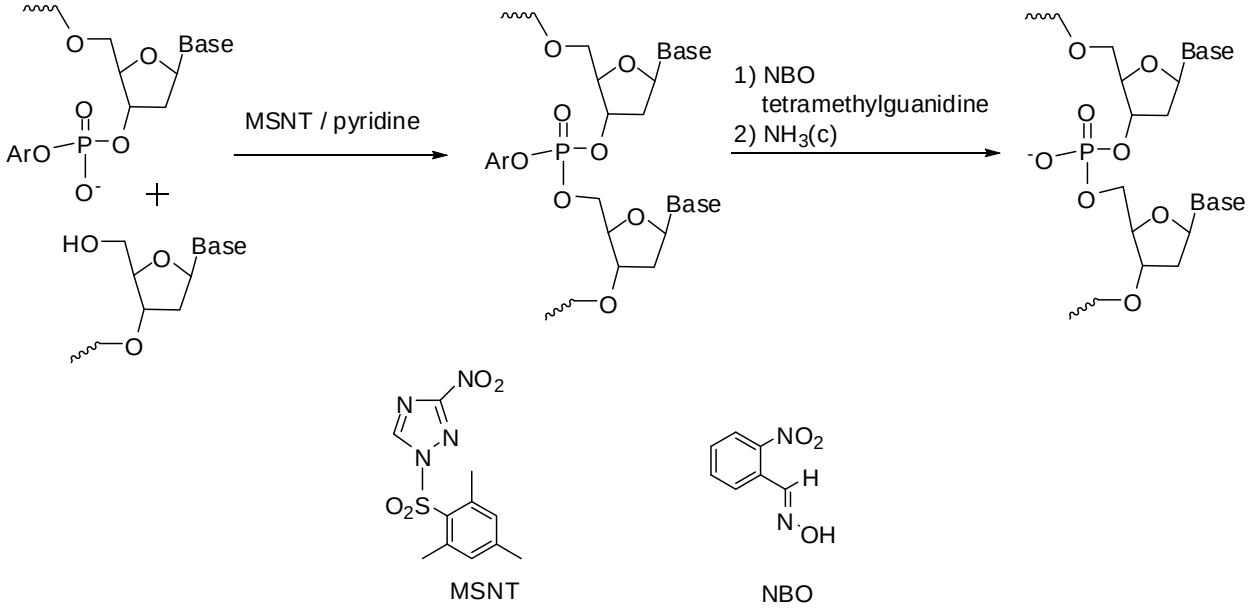


Figure 3-25. Phosphotriester approach reaction adapted from the article published by Reese, C. B. and Zhang, P. Z.[135]

With the idea of applying the phosphotriester approach in the synthesis of ST inhibitors, the triacetylated cytidine **68** was prepared as one of the building blocks (Figure 3-26). This compound was obtained by two different literature methods. The first one (Method A) involved the preparation of the acetyl dimethoxytrityl cytidine **66**.[136] This compound was converted to the desired product by a modified protocol in which the nucleoside secondary hydroxyl groups are acetylated and the 5' alcohol is deprotected in a one pot reaction. Compound **68** was obtained in 30% overall yield.

Following the two steps Halcomb *et al.* Procedure,[137] the triacetyl cytidine was achieved in a 25% total yield (Method B). In this case, t-butyldiphenylchlorosilane (TBDPSCl) is utilized as the 5' protecting reagent. Although, Method B afforded a slightly lower yield than Method A, the reaction was cleaner, which facilitated purification.

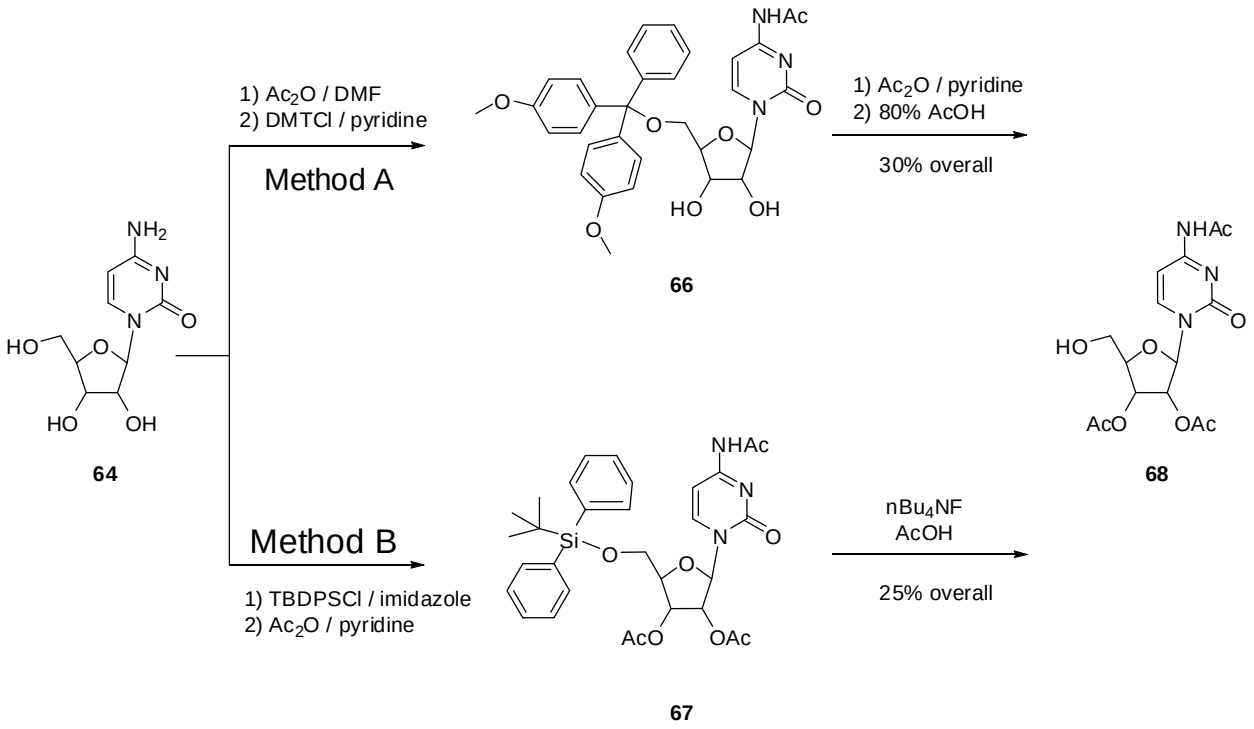


Figure 3-26. Synthesis of protected nucleoside **68**

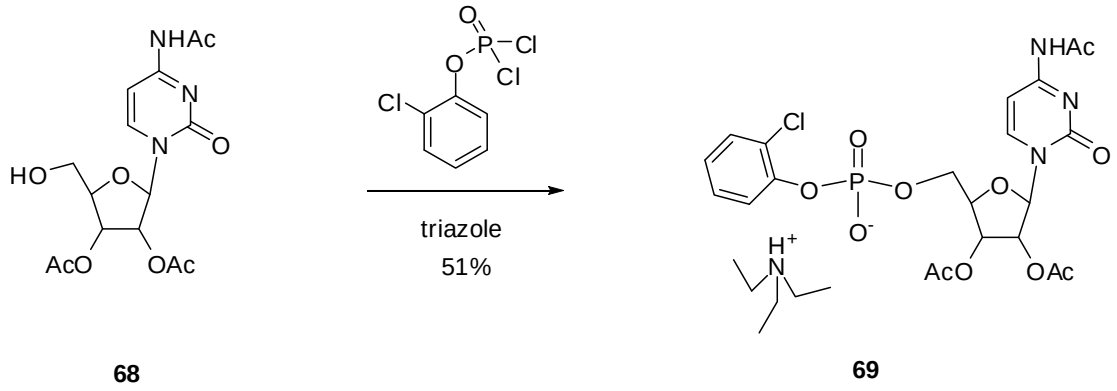


Figure 3-27. Synthesis of 2-chlorophenyl nucleoside **69**

Compound **69** was prepared in 51% yield using Reese 2-chlorophenyl dichlorophosphate reagent (Figure 3-27).[138,139] This phosphoester was used in the next reaction without further purification. The function of the 2-chorophenyl substituent is to protect the phosphate linkage from any imminent hydrolysis. A model coupling reaction between **69** and deprotected lactone **70** was successfully achieved utilizing 1-(mesityl-2-sulfonyl)-3-nitro-1*H*-1,2,4-triazole also

known as MSNT (Figure 3-28).[138,139] When the same coupling technique was tried on amidine **33**, the reaction did not afforded the desired compound **72**. The analysis of the complex crude sample by HPLC/ESI-MS did not even detected **72** as a minor component (Figure 3-29).

The last methodology employed to couple the amidine **33** with the cytidine nucleotide was the Khorana and coworkers phosphodiester approach.[140,141] In this case, the phosphodiester linkage is left completely unprotected. Either DCC or sulfonyl chlorides can be utilized as the coupling reagent. In order to follow this approach, the phosphorylation of amidine **33**'s primary hydroxyl group was first attempted. Several phosphorylating reagents were tried, such as tetrachloropyrophosphate ($P_2O_3Cl_4$), $POCl_3$/$PO(OEt)_3$,[142] dibenzylchlorophosphate/pyridine[143,144] (prepared from dibenzylphosphite) with subsequent benzyl removal, but the presence of high amounts of inorganic phosphate salts made the detection and the purification of the phosphoramidine impossible.

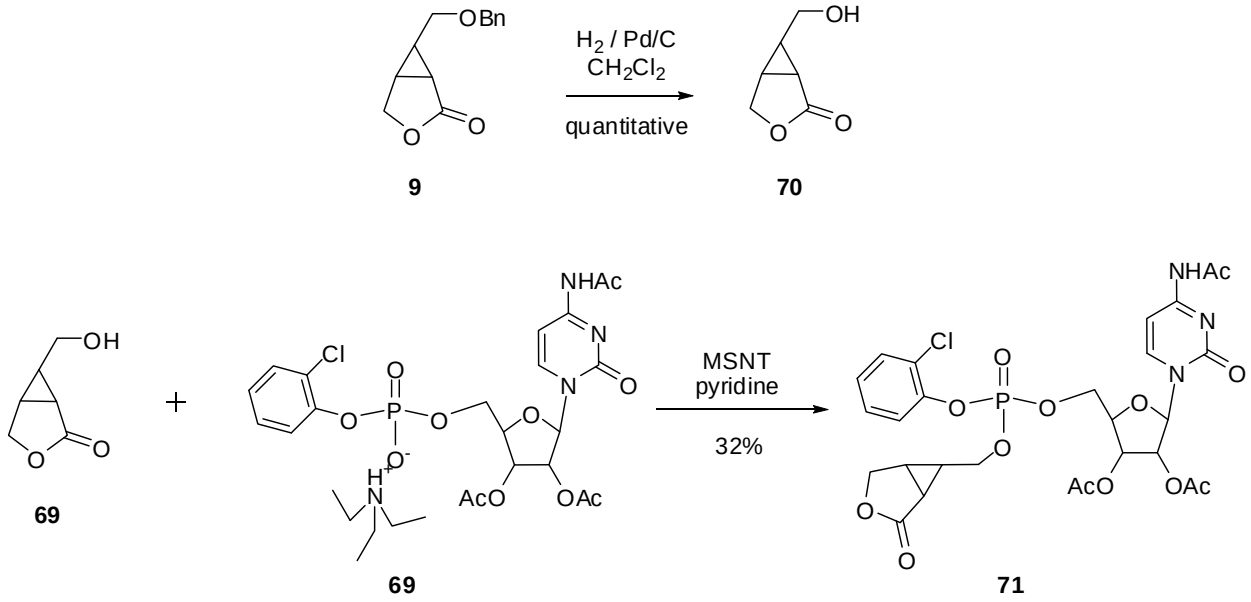


Figure 3-28. Synthesis of CMP-lactone **71**

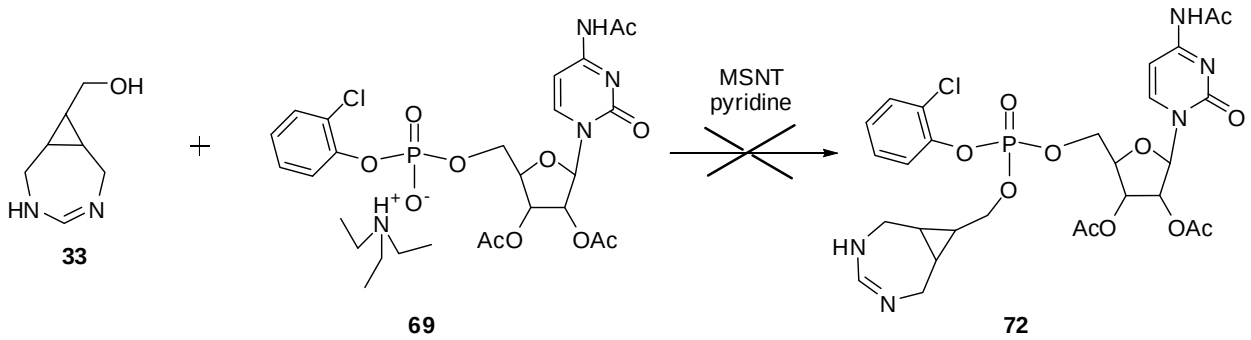


Figure 3-29. Coupling of amidine **33** by phosphotriester approach

Finally, the inverse reaction, in which the cytidine was the phosphate carrier, became the solution to the synthetic challenge. Treatment of a suspension of amidine **33** and cytidine-5'-monophosphate in pyridine with DCC,[140] resulted in the desired CMP-amidine **73** (Figure 3-30). Two difficulties found for this reaction were the low yield and tedious purification, which was carried out by C18 HPLC chromatography. After three consequtive HPLC purifications, the CMP-amidine was obtained in a 0.3% yield in 95% purity.

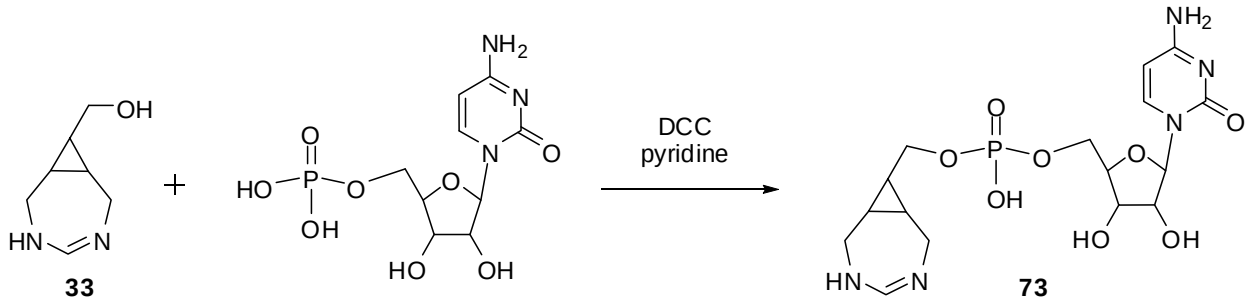


Figure 3-30. Synthesis of CMP-amidine **73**

In summary, the synthesis of the seven-membered ring diazabicyclic TS analogs was fruitfully accomplished in a relatively high yield. Consequently, compounds **23**, **29**, **31**, **33**, **34** and **73** will be tested for inhibition activity on different glycosidases and human recombinant α(2→6)ST. The set of compounds that will be evaluated as inhibitors is shown in Figure 3-31.

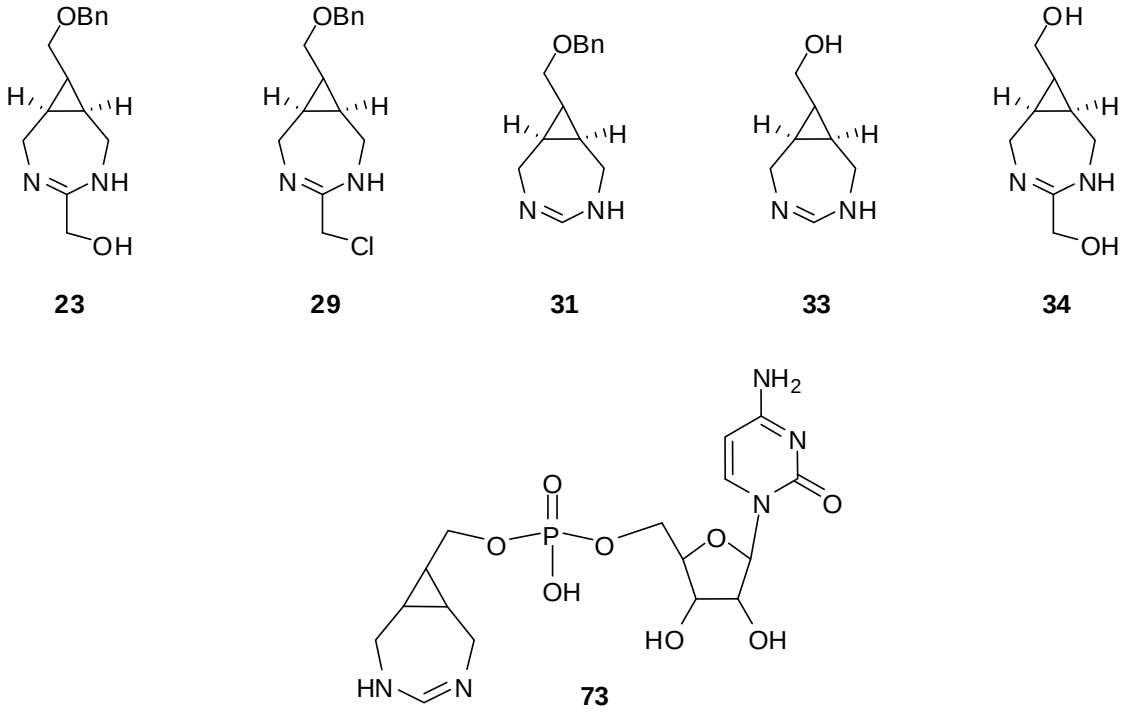


Figure 3-31. Diazabicyclic TS analogs

## Experimental Section

**General Methods.** Solvents and reagents were purchased from Aldrich Chemical Company and Acros Organics. The organic solvents were dried overnight over $CaH_2$ or 4 Å molecular sieves and freshly distilled before use. NMR spectra were obtained using VXR 300, Gemini 300 and 500, or Mercury 300 MHz spectrophotometers in appropriate deuterated solvents. Mass spectra were obtained on a Finningan MAT 95Q spectrometer operated in FAB, EI, CI or ESI modes. Infrared (IR) spectra were obtained by deposition of $CHCl_3$ solutions on NaCl plates followed by evaporation of the solvent. The HPLC column utilized was a Phenomenex C18 Synergi 10 μ Hydro-RP 80 Å (250 x 15 mm).

**((1R,2S,3S)-3-(benzyloxymethyl)cyclopropane-1,2-diyl)dimethanol 20.** Lactone **9** (1.0 g, 4.6 mmol) was added dropwise to a suspension of $LiAlH_4$ (1.6 g, 41 mmol) in dry THF (46 mL) at 0 °C. After 3 h, total consumption of lactone starting material was observed by TLC and

the reaction was quenched with a saturated aqueous solution of $NH_4Cl$. The reaction mixture was diluted with more THF and filtered through Celite. The organic layer was dried with $MgSO_4$. After evaporation of the solvent, the reaction mixture was purified by flash chromatography (silica, 2:1 petroleum ether/EtOAc). The yield of the reaction was 74% (0.8 g). $^1$H NMR ($CDCl_3$) δ ppm 1.49 (m, 3H), 2.55 (bs, 2H), 3.63 (d, 2H), 3.70 (dd, 2H), 3.78 (dd, 2H), 4.54 (s, 2H), 7.34 (m, 5H), $^{13}$C NMR ($CDCl_3$) δ (ppm) 138.0, 128.9, 128.3, 73.6, 66.6, 59.2, 22.2, 19.5. EI HRMS Calcd for $C_{13}H_{19}O_3$ $(M + H)^+$ : 223.1334, found: 223.1330.

**((((1S,2R,3S)-2,3-bis(azidomethyl)cyclopropyl)methoxy)methyl)benzene 21.** A mixture of diol **20** (0.4 g, 1.7 mmol) and $Et_3N$ (0.6 ml, 5.1 mmol) in $CH_2Cl_2$ (57 mL) was cooled to 0 °C. Then, freshly distilled methanesulfonyl chloride was added dropwise (0.4 ml, 5.1 mmol) and the resulting mixture was stirred at the same temperature for 20 min. After that time, all the diol starting material was consumed. The organic phase was washed with water and brine and dried over $MgSO_4$. The crude dimesylated product was dissolved in DMF (35 mL) and $NaN_3$ was added. The reaction was stirred at 60 °C for 4 h and the solvent was evaporated under reduced pressure. The residue was dissolved in EtOAc (150 mL) and washed with water (3 x 100 mL). The organic layer was dried with $MgSO_4$ and the solvent evaporated under vacuum. The product was purified by flash chromatography (silica, 20:1 petroleum ether/EtOAc) giving 0.3 g of **21** as a white solid in a 73% yield. $^1$H NMR ($CDCl_3$) δ ppm 1.48 (m, 2H), 1.55 (m, 1H), 3.34 (dd, 2H), 3.39 (dd, 2H), 3.56 (d, 2H), 4.50 (s, 2H), 7.32 (m, 5H). IR (NaCl) 2096 $cm^{-1}$. EI HRMS Calcd for $C_{13}H_{17}ON_6$ $(M + H)^+$ : 273.1464, found: 273.1388.

**((1R,2S,3S)-3-(benzyloxymethyl)cyclopropane-1,2-diyl)dimethanamine 22.** Triphenylphosphine (0.74 g, 2.84 mmol) was added to a solution of diazide **21** (0.19 g, 0.71 mmol) in dry $CH_2Cl_2$ (7.10 mL). The mixture was stirred at room temperature under argon for 24

h. Then, water (0.38 mL) was added and the mixture refluxed for 3 h. After the solvent was evaporated, the mixture was purified by column (silica, $CH_2Cl_2$:MeOH 1:1 then $CH_2Cl_2$:MeOH:$NH_4OH$ 1:1:0.01). The desired cycloproane diamine **22** was obtained as a white solid in 95% yield (0.15 g). $^1$H NMR ($CDCl_3$) δ ppm 1.17 (m, 2H), 1.30 (m, 1H), 1.81 (bs, 4H), 2.76 (d, 4H), 3.56 (d, 2H), 4.50 (s, 2H), 7.31 (m, 5H), $^{13}$C NMR ($CDCl_3$) δ (ppm) 138.6, 128.9, 128.2, 128.1, 73.5, 66.8, 37.9, 22.9, 18.5. EI HRMS Calcd for $C_{13}H_{21}ON_2$ $(M + H)^+$ : 221.1654, found: 221.1654.

**(Z)-(8-(benzyloxymethyl)-3,5-diazabicyclo[5.1.0]oct-4-en-4-yl)methanol 23.** Diamine **22** (0.5 g, 2.5 mmol) was dissolved in 13 mL of EtOH. Then, ethyl 2-hydroxyacetimidate hydrochloride **2** (0.3 g, 2.5 mmol) was added and the reaction mixture was stirred under reflux for 12 h. After the solvent was evaporated under vacuum, the residue was purified by flash chromatography (silica, $CH_2Cl_2$/MeOH 15:1) to give the hydroxymethyl amidine (0.5 g) as a white solid in a 70% yield. $^1$H NMR ($CDCl_3$) δ ppm 1.42 (m, 1H), 1.76 (m, 2H), 3.57 (dd, 2H), 3.77 (d, 2H), 3.95 (dd, 2H), 4.19 (s, 2H), 4.53 (s, 2H), 7.33 (m, 5H), $^{13}$C NMR ($CDCl_3$) δ (ppm) 166.9, 138.5, 128.5, 128.0, 127.9, 72.9, 65.4, 59.1, 40.3, 19.4, 17.6. ESI-FTICR (+) Calcd for $C_{15}H_{21}O_2N_2$ $(M + H)^+$: 261.1598, found: 261.1575.

**Methyl 2,2,2-trichloroacetimidate 27.** The title compound was synthesized using the literature procedure.[115] To a suspension of $K_2CO_3$ (0.3 g, 1.8 mmol) in anhydrous methanol (13 mL), trichloroacetonitrile (25 mL, 0.3 mol) was added slowly with stirring. Inmediately after the addition, the reaction mixture was distilled and the fraction that boiled around 151 °C was collected. The product was obtained as a clear liquid in a 38% yield (20 g). IR (NaCl) 1666 $cm^{-1}$, $^1$H NMR ($CDCl_3$) δ ppm 3.94 (s, 3H), 8.29 (bs, 1H), $^{13}$C NMR ($CDCl_3$) δ (ppm) 163.9, 91.5, 56.7. ESI-FTICR (+) Calcd for $C_3H_5Cl_3NO$ $(M + H)^+$: 176, found: 176.

**(Z)-8-(benzyloxymethyl)-4-(trichloromethyl)-3,5-diazabicyclo[5.1.0]oct-3-ene 28.** Trichloroacetoimidate **27** (0.11 g, 0.62 mmol) was added slowly to a suspension of diamine **22** (0.12 g, 0.56 mmol) in 1.86 mL of glacial acetic acid previously cooled to 0 °C. The ice bath was taken away and the reaction was stirred at room temperature until no more diamine **22** was observed by TLC. The mixture was diluted with a solution of 5% aqueous $Na_2CO_3$ (50 mL) and extracted with $CH_2Cl_2$ (3 x 30 mL). The organic layer was dried with $MgSO_4$ and the solvent evaporated under vacuum. The product was purified by flash chromatography (silica, $CH_2Cl_2$/MeOH 46:1) to give the trichloroamidine (78 mg) as a clear oil in a 40% yield. $^1$H NMR ($CDCl_3$) δ ppm 1.18 (m, 1H), 1.63 (m, 2H), 3.62 (m, 6H), 4.46 (s, 2H), 7.27 (m, 5H), $^{13}$C NMR ($CDCl_3$) δ (ppm) 152.4, 138.2, 128.7, 128.3, 128.1, 128.0, 96.6, 73.2, 66.1, 42.2, 18.0, 17.9. ESI-FTICR (+) Calcd for $C_{15}H_{18}ON_2Cl_3$ $(M + H)^+$: 347.0479, found: 347.0477.

**(Z)-8-(benzyloxymethyl)-4-(chloromethyl)-3,5-diazabicyclo[5.1.0]oct-3-ene 29.** Hydroxymethyl amidine **23** (0.4 g, 1.5 mmol) was added slowly to 8.0 mL of freshly distilled thionyl chloride. After the suspension was heated under reflux for 10 minutes, the amidine started to dissolve; thus the reaction was left for 2 h more. The unreacted thionyl chloride was evaporated under vacuum. The brown residue was purified by flash chromatography (silica, $CH_2Cl_2$/MeOH 20:1) to give the chloromethyl amidine **29** as a yellow solid in a 60% yield (0.3 g). $^1$H NMR ($CDCl_3$) δ ppm 1.25 (m, 1H), 1.41 (m, 1H), 1.78 (m, 1H), 3.56 (dd, 2H), 3.75 (d, 2H), 4.01 (dd, 2H), 4.24 (s, 2H), 4.52 (s, 2H), 7.32 (m, 5H), $^{13}$C NMR ($CDCl_3$) δ (ppm) 162.7, 138.4, 129.1, 128.4, 127.9, 127.8, 72.8, 62.3, 40.8, 40.5, 18.9, 17.1. ESI-FTICR (+) Calcd for $C_{15}H_{20}ON_2Cl$ $(M + H)^+$: 279.1259, found: 279.1256.

**(Z)-8-(benzyloxymethyl)-3,5-diazabicyclo[5.1.0]oct-3-ene 31.** Diamine **22** (0.5 g, 2.3 mmol) was dissolved in 20 mL of EtOH. Then, ethyl formimidate hydrochloride (0.3 g, 2.3

mmol) was added and the reaction mixture was stirred under reflux for 10 h. After the solvent was evaporated under vacuum, the residue was purified by flash chromatography (silica, $CH_2Cl_2$/MeOH 10:1) to give the amidine **31** as a white solid in a 88% yield (0.5 g). $^1$H NMR ($CD_3OD$) δ ppm 1.37 (m, 1H), 1.73 (m, 2H), 3.46 (dd, 2H), 3.70 (d, 2H), 3.93 (dd, 2H), 4.48 (s, 2H), 7.28 (m, 5H), 7.49 (s, 1H), $^{13}$C NMR ($CD_3OD$) δ (ppm) 154.4, 138.5, 128.4, 127.9, 127.8, 72.8, 65.4, 40.6, 19.7, 17.7. ESI-FTICR (+) Calcd for $C_{14}H_{19}ON_2$ $(M + H)^+$ : 231.1489, found: 231.1489.

**General procedure for the benzyl deprotection of cyclic amidines 33 and 34.** The amidine (1 mmol) is dissolved in 5 mL of freshly distilled MeOH. Ammonium formate (9 mmol) and 0.4 g of 10% Pd/C were added to the solution of amidine. The mixture was refluxed until no more amidine was observed. The black suspension was filtered through Celite. The celite bed was washed five times with MeOH to maximize product recovery. The solvent was evaporated under vacuum. All the products were used without further purification.

**(Z)-3,5-diazabicyclo[5.1.0]oct-4-en-8-ylmethanol 33.** This compound was obtained as previously described as a yellow solid in a 100% yield. $^1$H NMR ($CD_3OD$) δ ppm 1.29 (m, 1H), 1.70 (m, 2H), 3.48 (dd, 2H), 3.72 (d, 2H), 3.95 (dd, 2H), 7.49 (s, 1H), $^{13}$C NMR ($CD_3OD$) δ (ppm) 154.4, 56.9, 40.5, 22.1, 17.6. ESI-FTICR (+) Calcd for $C_7H_{13}ON_2$ $(M + H)^+$ : 141.1022, found: 141.1024.

**(Z)-3,5-diazabicyclo[5.1.0]oct-4-ene-4,8-diyldimethanol 34.** This compound was obtained as previously described as a white solid in a 100% yield. $^1$H NMR ($CD_3OD$) δ ppm 1.24 (m, 1H),1.65 (m, 2H), 3.52 (dd, 2H), 3.74 (d, 2H), 3.86 (dd, 2H), 4.14 (s, 2H), $^{13}$C NMR ($CD_3OD$) δ (ppm) 166.7, 59.0, 56.9, 40.1, 21.7, 17.5. ESI-FTICR (+) Calcd for $C_8H_{15}O_2N_2$ $(M + H)^+$ : 171.1128, found: 171.1138.

**(1R,2S,3R)-2-(benzyloxymethyl)-3-(hydroxymethyl)cyclopropanecarboxamide 35.** Lactone **9** (0.5 g, 2.3 mmol) was dissolved in a saturated solution of $NH_3$ gas in MeOH (23 mL). The reaction mixture was stirred for 48 h. The crude amide was purified by flash chromatography (silica, 1:5 petroleum ether/EtOAc) giving a colorless oil in 78% yield (0.4 g). $^1$H NMR ($CDCl_3$) δ ppm 1.67 (m, 2H), 1.81 (m, 1H), 3.18 (bs, 1H), 3.68 (m, 2H), 3.94 (m, 2H), 4.51 (s, 2H), 5.61 (bs, 1H), 6.19 (bs, 1H), 7.32 (m, 5H),$^{13}$C NMR ($CDCl_3$) δ (ppm) 173.2, 138.1, 128.9, 128.3, 73.7, 66.2, 58.7, 24.3, 23.8, 22.2. EI HRMS Calcd for $C_{13}H_{18}O_3N$ $(M + H)^+$ : 236.1287, found: 236.1287.

**(1S,2S,3R)-2-(benzyloxymethyl)-3-((tert-butyldimethylsilyloxy)methyl) cyclopropanecarboxamide 36.** Hydroxymethylamide **35** (0.6 g, 2.5 mmol) and imidazole (0.2 g, 2.8 mmol) were dissolved in dry $CH_2Cl_2$ (17 mL). Then, TBDMSCl (0.4 g, 2.8 mmol) in $CH_2Cl_2$ (10 mL) was added dropwise to the previous solution. After addition of this reagent, the reaction turned cloudy. The mixture was stirred at room temperature for 12 h. The organic phase was washed with saturated $NaHCO_3$ and brine. The crude product was purified by flash chromatography (silica, 1:1 petroleum ether/EtOAc) to give **36** in a 75% yield (0.7 g). $^1$H NMR ($CDCl_3$) δ ppm 0.06 (s, 3H), 0.06 (s, 3H), 0.07 (s, 3H), 0.89 (s, 9H), 1.58 (m, 2H), 1.84 (t, 1H), 3.72 (dd, 1H), 3.85 (dd, 2H), 3.98 (dd, 1H), 4.52 (dd, 2H), 5.24 (bs, 1H), 6.68 (bs, 1H), 7.33 (m, 5H),$^{13}$C NMR ($CDCl_3$) δ (ppm) 174.3, 138.1, 128.9, 128.3, 73.6, 66.8, 59.8, 26.4, 23.9, 21.3, 18.7. EI HRMS Calcd for $C_{19}H_{32}O_3NSi$ $(M + H)^+$ : 350.2151, found: 350.2139.

**Methyl(1S,2S,3R)-2-(benzyloxymethyl)-3-((tert-butyldimethylsilyloxy)methyl) cyclopropylcarbamate 37.** A solution of amide **36** (0.8 g, 2.2 mmol), DBU (9.9 μL, 6.6 mmol) and NBS (0.4 g, 2.2 mmol) in MeOH (22 mL) were heated to reflux for 15 min. Then, another equal amount of NBS (0.4 g, 2.2 mmol) was added and the reflux was continued for 10 min

more. The solvent was evaporated under vaccum and the residue dissolved in EtOAc. The solution was washed with 0.01 M HCl and saturated solution of $NaHCO_3$. The organic layer was dried over $MgSO_4$ and evaporated to give a yellow oil. The crude product was purified by flash chromatography (silica, 7:1 petroleum ether/EtOAc) to give 0.6 g of **37** in a 76% yield. $^1$H NMR ($CDCl_3$) δ ppm 0.02 (s, 6H), 0.83 (s, 9H), 1.38 (m, 2H), 2.76 (t, 1H), 3.55 (dd, 1H), 3.62 (s, 3H), 3.70 (dd, 2H), 3.80 (dd, 1H), 4.45 (s, 2H), 5.37 (bs, 1H), 7.28 (m, 5H),$^{13}$C NMR ($CDCl_3$) δ (ppm) 158.6, 138.6, 128.8, 128.2, 73.4, 66.1, 59.4, 52.7, 31.1, 26.3, 22.3, 20.6, 18.6. EI HRMS Calcd for $C_{20}H_{33}O_4NSiNa$ $(M + Na)^+$ : 402.2071, found: 402.2063.

**Methyl (1R,2S,3R)-2-(benzyloxymethyl)-3-(hydroxymethyl)cyclopropylcarbamate 38.** A solution of cyclopropylcarbamate **37** (0.7 g, 2.0 mmol) in dry THF (50 mL) was treated with a 1 M solution of tetrabuthylammmonium fluoride in THF (3.9 mL, 3.9 mmol). The reaction mixture was stirred at room temperature for 2 h until no more carbamate was observed by TLC. After this time, the solvent was evaporated under vaccum and the residue dissolved in EtOAc. The organic phase was washed with saturated saturated solution of $NaHCO_3$ and dried over $MgSO_4$. The colorless oil was purified by flash chromatography (silica, 3:2 petroleum ether/EtOAc) to give **38** in a 90% yield (0.5 g). $^1$H NMR ($CDCl_3$) δ ppm 1.49 (m, 2H), 2.76 (t, 1H), 3.47 (m, 3H), 3.69 (m and s, 5H), 4.50 (dd, 2H), 5.30 (bs, 1H), 7.34 (m, 5H),$^{13}$C NMR ($CDCl_3$) δ (ppm) 159.9, 138.1, 129.0, 128.3, 128.2, 73.5, 65.6, 57.8, 53.0, 30.2, 24.4, 19.4. EI HRMS Calcd for $C_{14}H_{19}O_4NNa$ $(M + Na)^+$ : 288.1206, found: 288.1204.

**2-(benzyloxymethyl)-3-(hydroxymethyl)cyclopropanecarboxylic acid 39.** To a solution of the lactone **9** (0.2 g, 0.9 mmol) in methanol (1.8 mL) was added an aqueous solution of 2.5 N NaOH (1.8 mL). The mixture was stirred at room temperature for 3 h. Then, the solvent was evaporated under vacuum and the solid dissolved in water (30 mL). The basic aqueous phase

was extracted with ether (3 x 30 mL) and afterwards it was acidified with HCl to reach pH of 1. Finally, the acidic aqueous layer was extracted with $CH_2Cl_2$ (4 x 30 mL). The organic phase obtained from extraction of the acidified aqueous phase was dried over $MgSO_4$ and evaporated under vacuum. The product was obtained as a white solid (0.2 g) in a 85% yield. $^1$H NMR ($CDCl_3$) δ ppm 1.84 (m, 2H), 1.90 (m, 1H), 3.92 (m, 4H), 4.51 (s, 2H), 7.34 (m, 5H), $^{13}$C NMR ($CDCl_3$) δ (ppm) 176.8, 138.0, 128.9, 128.3, 73.7, 64.8, 57.5, 26.6, 23.9, 21.4. EI HRMS Calcd for $C_{13}H_{16}O_4$ $(M + 2Na)^+$ : 281.0760, found: 281.0773.

**Methyl 2-(benzyloxymethyl)-3-(hydroxymethyl)cyclopropanecarboxylate 40.** The cyclopropyl carboxylic acid **39** (0.4 g, 1.9 mmol) was dissolved in an Erlenmeyer flask with a mixture of diethyl ether/$CH_2Cl_2$ (15 mL/5 mL) and cooled on an ice bath. Diazomethane was generated from Diazald (p-toluensulphonylmethylnitrosamide). It was assumed that 1 g of Diazald generated 3 mmol of diazomethane ($CH_2N_2$). In a filter flask that did not have any noticeable scratches on the walls, Diazald (2 g) was dissolved in EtOH (10 mL) and the mixture was stirred under flowing $N_2$ at 0 °C. This flask was connected to the reaction mixture Erlenmeyer by latex hoses. Then, a solution of 5 N NaOH was added drop wise from a septum with a plastic syringed until the Diazald was dissolved. The solution of NaOH was added until yellow color of $CH_2N_2$ persisted in the reaction mixture. After addition of $CH_2N_2$, the mixture was stirred for 1 h more and quenched with 3 drops of glacial acetic acid. The solvent was evaporated under vacuum and the residue purified by flash chromatography (silica, petroleum ether/EtOAc 3:1). The ester was obtained as a clear oil in a 89% yield (0.4 g). $^1$H NMR ($CDCl_3$) δ ppm 1.82 (m, 2H), 1.92 (m, 1H), 2.49 (bs, 1H), 3.65 (s, 3H), 3.82 (m, 2H), 4.02 (m, 2H), 4.54 (s, 2H), 7.34 (m, 5H), $^{13}$C NMR ($CDCl_3$) δ (ppm) 172.1, 138.0, 128.8, 128.2, 73.6, 64.8, 57.5, 52.1, 25.9, 23.1, 21.4. ESI-MS (+) Calcd for $C_{14}H_{18}O_4$ $(M + Na)^+$ : 273.1, found: 273.1.

**(1R,2R,3R)-methyl 2-(benzyloxymethyl)-3-formylcyclopropanecarboxylate 41.** Molecular sieves 4 (Å) (93 mg) were added to a solution of ester **40** (50 mg, 0.2 mmol) in dry $CH_2Cl_2$ (2.3 mL). This suspension was stirred at room temperature under argon for 5 minutes. Then, tetra-n-propylammonium perruthenate (TPAP) (2.0 mg, 5.1 μmol) and N-methylmorpholine N-oxide (NMO) (37 mg, 0.3 mmol) were added to the reaction mixture which was left stirring for 18 h. After filtering the solution through Celite, the solvent was evaporated under vacuum. The product was purified by flash chromatography (silica, petroleum ether/EtOAc 10:1). The *trans* cyclopropyl aldehyde **41** (26 mg) was obtained in a 52% yield as a clear oil. $^1$H NMR ($CDCl_3$) δ ppm 2.16 (m, 1H), 2.42 (m, 1H), 2.55 (m, 1H), 3.65 (m, 1H), 3.66 (s, 2H), 3.75 (m, 1H), 4.45 (s, 2H), 7.27 (m, 5H), 9.36 (d, 1H), $^{13}$C NMR ($CDCl_3$) δ (ppm) 197.8, 170.1, 138.2, 128.8, 128.1, 128.0, 73.4, 66.4, 52.6, 34.9, 28.5, 26.4. CI-MS (+) Calcd for $C_{14}H_{17}O_4$ $(M + H)^+$ : 249.1127, found: 249.1120.

**(1R,2R,3S)-methyl 2-(benzyloxymethyl)-3-formylcyclopropanecarboxylate 42.** Dess-Martin periodinane reagent (0.5 g, 1.2 mmol) was suspended in 3 mL of dry $CH_2Cl_2$. A solution of the ester **40** (0.2 g, 0.6 mmol) in dry $CH_2Cl_2$ (3 mL) was added drop wise to this suspension. The mixture was stirred for 45 minutes and quenched with 6 mL of aqueous 5% $NaHCO_3$ containing 98 mg of $Na_2S_2O_3$. The stirring continued for 10 more minutes and the aqueous mixture was extracted with $CH_2Cl_2$ (3 x 30 mL). The organic layer was dried over $MgSO_4$ and evaporated under vacuum. The all *cis* cyclopropyl aldehyde **42** was purified by flash chromatography (silica, petroleum ether/EtOAc 10:1) and obtained as a clear oil in a 82% yield (0.1 g). $^1$H NMR ($CDCl_3$) δ ppm 2.16 (m, 2H), 2.39 (m, 1H), 3.71 (s, 3H), 4.09 (m, 2H), 4.53 (s, 2H), 7.33 (m, 5H), 9.73 (d, 1H), $^{13}$C NMR ($CDCl_3$) δ (ppm) 198.9, 170.3, 138.1, 128.8, 128.2,

128.1, 73.5, 63.5, 52.7, 32.5, 27.2, 27.0. CI-MS (+) Calcd for $C_{14}H_{17}O_4$ $(M + H)^+$ : 249.1127, found: 249.1125.

**2-(benzyloxymethyl)-3-(methoxycarbonyl)cyclopropanecarboxylic acid 43.** To a solution of the *cis* aldehyde **42** (0.5 g, 2.0 mmol) in acetonitrile (20 mL) was added 30% $H_2O_2$ (0.5 mL, 4.8 mmol) and an aqueous solution of 0.65 M $NaH_2PO_4$ (8 mL). After this mixture was cooled to 0 °C, a 0.1 M solution of $NaClO_2$ (29 mL, 2.9 mmol) was added dropwise over 1.5 h. The reaction was stirred for 2 h more at 0 °C and then $Na_2SO_3$ (0.1 g, 0.8 mmol) was added to quench the excess of $NaClO_2$. The mixture was acidified to pH around 2 with 1M HCl. The aqueous phase was extracted with EtOAc (3 x 40 mL). The organic layer was dried with $MgSO_4$ and the solvent evaporated under vacuum. The product was purified by flash chromatography (silica, petroleum ether/EtOAc/HOAc 2:1:0.005). The acid **43** was obtained in a 87% yield (0.5 g) as a clear oil. $^1$H NMR ($CDCl_3$) δ ppm 1.95 (m, 1H), 2.23 (d, 2H), 3.67 (s, 3H), 3.97 (d, 2H), 4.50 (s, 2H), 7.30 (m, 5H), $^{13}$C NMR ($CDCl_3$) δ (ppm) 173.6, 169.9, 138.3, 128.7, 128.1, 128.0, 73.5, 64.8, 52.7, 24.6, 24.4. CI-MS (+) Calcd for $C_{14}H_{17}O_5$ $(M + H)^+$ : 265.1076, found: 265.1057.

**3-(benzyloxymethyl)cyclopropane-1,2-dicarboxylic acid 44.** This diacid was obtained in a similar manner as for acid **39**. The acid (0.1 g, 0.4 mmol) was dissolved in MeOH (0.7 mL). A solution of 2.5 N NaOH (1 mL) was added to the previous solution and the mixture stirred for 4 h at room temperature. After this time, the solvent was evaporated and the residue was dissolved in water (3 mL). This solution was acidified to pH of around 1 and extracted with EtOAc (3 x 30 mL). The organic layer was dried over $MgSO_4$ and the solvent evaporated under vacuum. The product was obtained in an 80% yield (80 mg) as a white solid and was considered pure enough to be used in the following step. $^1$H NMR ($CD_3OD$) δ ppm 1.77 (m, 1H), 2.14 (d, 2H), 3.93 (d,

2H), 4.40 (s, 2H), 7.23 (m, 5H), $^{13}$C NMR ($CD_3OD$) δ (ppm) 172.6, 139.7, 129.3, 128.8, 128.7, 74.0, 66.3, 25.0, 24.7. ESI-MS (+) Calcd for $C_{13}H_{15}O_5$ $(M + H)^+$: 251.0919, found: 251.0.952.

**Dimethyl 3-(benzyloxymethyl)cyclopropane-1,2-dicarboxylate 45.** This diester was obtained in a similar manner as for ester **40**. Compound **44** (0.3 g, 1.0 mmol) was dissolved in diethyl ether/$CH_2Cl_2$ (13 mL/8 mL) and cooled on ice. Diazomethane was freshly generated from Diazald (1.5 g, 4.0 mmol) which was suspended in 8 mL of EtOH. The mixture was stirred on ice for 1 h after yellow color of $CH_2N_2$ persisted in the reaction. Glacial acetic acid was used to quench the reaction. After the solvent was evaporated, the product was purified by flash chromatography (silica, petroleum ether/EtOAc 9:1). The diester **45** (0.2 g) was obtained in a 88% yield as a clear oil. $^1$H NMR ($CDCl_3$) δ ppm 1.88 (m, 1H), 2.21 (d, 2H), 3.70 (s, 6H), 4.02 (d, 2H), 4.51 (s, 2H), 7.33 (m, 5H), $^{13}$C NMR ($CDCl_3$) δ (ppm) 169.5, 138.7, 128.7, 128.0, 127.9, 73.4, 65.2, 52.4, 24.2, 24.1. CI-MS (+) Calcd for $C_{15}H_{19}O_5$ $(M + H)^+$ : 279.1248, found: 279.1250.

**3-(benzyloxymethyl)cyclopropane-1,2-dicarboxamide 46.** The diester cyclopropyl **45** (82 mg, 0.3 mmol) was dissolved in a ~16 M solution of ammonia in MeOH (4 mL). This solution was made by bubbling $NH_3$ gas into MeOH, previously cooled to -15 °C with an ice-salt bath. The reaction was performed in a pressure bottle and stirred for 4 days at 50 °C. After this time, the solvent was evaporated and the residue was purified by flash chromatography (silica, EtOAc/MeOH 5:1). The diamide was obtained in a 33% yield (25 mg) as a white solid. $^1$H NMR ($CD_3OD$) δ ppm 1.79 (m, 1H), 2.01 (d, 2H), 3.93 (d, 2H), 4.44 (s, 2H), 7.25 (m, 5H), $^{13}$C NMR ($CD_3OD$) δ (ppm) 172.9, 128.3, 127.9, 127.7, 73.0, 65.3, 25.1, 22.9. CI-MS (+) Calcd for $C_{13}H_{17}O_3N_2Na$ $(M + Na)^+$ : 271.1053, found: 271.1067.

**2-(azidomethyl)-3-(benzyloxymethyl)cyclopropanecarboxamide 49.** The hydroxylamide **35** (50 mg, 0.2 mmol) and triethylamine (44 μl, 0.3 mmol) were dissolved in dry $CH_2Cl_2$ (2.6 mL) and cooled to 0 °C. Methanesulfonyl chloride (25 μl, 0.3 mmol) was added dropwise to this mixture. The reaction was stirred at the same temperature for 30 minutes and more $CH_2Cl_2$ was added (10 mL). The organic layer was washed with $H_2O$ and brine. The solvent was evaporated under vacuum and the crude mixture dissolved in dry DMF (11 mL). Then, sodium azide (27 mg, 0.4 mmol) was added and the reaction stirred for 22 h at room temperature. Finally, DMF was evaporated under high vacuum. The residue was dissolved in $CH_2Cl_2$ and washed with $H_2O$ and brine. The organic layer was dried with $MgSO_4$ and the solvent evaporated under vacuum. The product **49** was purified by flash chromatography (silica, petroleum ether/EtOAc 4:1 then 1:1). The amide was obtained in a 48% yield (25 mg) as a white solid. IR (NaCl) 2102, 1667 $cm^{-1}$, $^1H$ NMR ($CDCl_3$) δ ppm 1.65 (m, 1H), 1.71 (m, 2H), 3.63 (dd, 1H), 3.79 (m, 2H), 3.91 (m, 1H), 4.49 (s, 2H), 5.69 (bs, 1H), 6.02 (bs, 1H), 7.31 (m, 5H), $^{13}C$ NMR ($CDCl_3$) δ (ppm) 172.4, 138.4, 128.8, 128.2, 128.1, 73.6, 65.0, 46.5, 23.0, 22.3, 22.1. ESI-FTICR (+) Calcd for $C_{13}H_{17}O_2N_4$ $(M + H)^+$: 261.1346, found: 261.1340.

**Methyl 2-(azidomethyl)-3-(benzyloxymethyl)cyclopropylcarbamate 50.** This compound was synthesized by the same procedure as **37**. In this case, the amide (0.2 g, 0.8 mmol), NBS (0.1 g, 0.8 mmol) and DBU (0.4 μL, 2.3 mmol) were dissolved in 8.3 mL of MeOH. The time and workup of the reaction were followed as described above for compound 37. The product was purified by flash chromatography (silica, petroleum ether/EtOAc 10:1). The carbamate **50** (0.2 g) was obtained in a 63% yield as colorless oil. IR (NaCl) 2102, 1731 $cm^{-1}$, $^1H$ NMR ($CDCl_3$) δ ppm 1.46 (m, 2H), 2.86 (t, 1H), 3.33 (dd, 1H), 3.52 (t, 2H), 3.67 (s, 3H), 3.74 (dd, 1H), 4.50 (s, 2H), 5.18 (bs, 1H), 7.33 (m, 5H), $^{13}C$ NMR ($CDCl_3$) δ (ppm) 158.4, 138.0, 128.9, 128.3, 128.1,

73.5, 65.8, 52.8, 47.1, 30.9, 20.1, 19.4. ESI-FTICR (+) Calcd for $C_{14}H_{18}O_3N_4Na$ $(M + Na)^+$: 313.1271, found: 313.1264.

**Methyl 2-(aminomethyl)-3-(benzyloxymethyl)cyclopropylcarbamate 51.** This compound was obtained by the same procedure as **22**. In this case, methyl carbamate (0.1 g, 0.4 mmol) was dissolved in 5.5 mL of $CH_2Cl_2$ and $PPh_3$ (0.2 g, 0.7 mmol) was added. After stirring the reaction for 22 h, 0.1 mL of $H_2O$ were added. The mixture was purified by flash chromatography (silica, $CH_2Cl_2$: MeOH: $NH_4OH$ 20:1:0.2). The desired amine **51** was obtained as a white solid in 83% yield (88 mg). $^1H$ NMR ($CDCl_3$) δ ppm 1.23 (m, 1H),1.43 (m, 1H), 2.55 (bs, 2H), 2.75 (t, 1H), 2.88 (m, 2H), 3.49 (t, 2H), 3.64 (s, 3H), 4.47 (s, 2H), 5.42 (bs, 1H), 7.31 (m, 5H), $^{13}C$ NMR ($CDCl_3$) δ (ppm) 159.0, 138.2, 128.9, 128.2, 128.1, 73.4, 65.8, 52.7, 36.8, 30.4, 23.7, 19.0. CI-HRMS (+) Calcd for $C_{14}H_{21}O_3N_2$ $(M + H)^+$: 265.1552, found: 265.1582.

**7-(benzyloxymethyl)-2,4-diazabicyclo[4.1.0]heptan-3-one 52.** Compound **51** (84 mg, 0.3 mmol) was dissolved in a solution of 10% KOH in MeOH-$H_2O$ (13 mL). The mixture was stirred under reflux for 4 h. The solvent was evaporated under vacuum and the residue was dissolved in $CH_2Cl_2$ and washed with water. The organic layer was dried with $MgSO_4$ and the solvent was evaporated under reduced pressure. The crude product was purified by flash chromatography (silica, $CH_2Cl_2$/MeOH 7:1 then $CH_2Cl_2$/MeOH/$NH_4OH$ 7:1:0.25) to give 54 mg of the bicyclic product **52** as a white solid in a 77% yield and the diamine **53** in a 23% yield (14 mg) as a clear oil. For diazabicyclo **52**: $^1H$ NMR ($CDCl_3$) δ ppm 1.23 (m, 1H), 1.49 (m, 1H), 2.93 (t, 1H), 3.36 (d, 1H), 3.57 (m, 3H), 4.49 (dd, 2H), 4.83 (bs, 1H), 5.17 (bs, 1H), 7.32 (m, 5H), $^{13}C$ NMR ($CDCl_3$) δ (ppm) 156.9, 138.4, 128.8, 128.2, 128.1, 73.7, 65.0, 37.2, 30.6, 22.1, 9.1. ESI-FTICR (+) Calcd for $C_{13}H_{17}O_2N_2$ $(M + H)^+$: 233.1285, found: 233.1284. For diamine

**53**: $^{1}$H NMR ($CDCl_3$) δ ppm 1.00 (m, 1H), 1.15 (m, 1H), 1.99 (bs, 4H), 2.60 (t, 1H), 2.92 (d, 2H), 3.70 (d, 2H), 4.51 (s, 2H), 7.32 (m, 5H).

**((1R,2R,3S)-2-amino-3-(benzyloxymethyl)cyclopropyl)methanol 54.** The cyclopropylcarbamate **38** (0.2 g, 0.8 mmol) was dissolved in a solution of 10% KOH in MeOH-$H_2O$ (7.5 mL). The mixture was stirred under reflux for 4 h. The solvent was evaporated under vacuum and the residue was dissolved in $CH_2Cl_2$ and washed with water. The organic layer was dried with $MgSO_4$ and the solvent was evaporated under reduced pressure. The crude product was purified by flash chromatography (silica, 15:1 EtOAc/MeOH) to give 99 mg of **54** in a 60% yield. $^{1}$H NMR ($CDCl_3$) δ ppm 1.26 (m, 2H), 1.78 (bs, 3H), 2.71 (m, 1H), 3.87 (dd, 4H), 4.56 (s, 2H), 7.35 (m, 5H). EI HRMS Calcd for $C_{12}H_{18}O_2N$ $(M + H)^+$ : 208.1332, found: 208.1332.

**((1S,2R,3R)-2-(aminomethyl)-3-(benzyloxymethyl)cyclopropyl)methanol 57.** A suspension of $LiAlH_4$ (0.2 g, 5.5 mmol) in dry THF (3 mL) was stirred at 0 °C under argon. Then, amide **35** (60 mg, 0.3 mmol) in dry THF (3 mL) was added dropwise. The reaction mixture was refluxed for 5 h. After that time, the reaction was diluted with more THF (15 mL) and water was added slowly, with caution (0.3 mL). The mixture was stirred at room temperature for 1 h and filtered through Celite. The organic solvent was evaporated under reduce pressure. The crude product was purified by flash chromatography (silica, 1:1 $CH_2Cl_2$:MeOH then 1:1:0.01 $CH_2Cl_2$:MeOH:$NH_4OH$) to give **56** in a 51% yield (34 mg). $^{1}$H NMR ($CDCl_3$) δ ppm 1.25 (m, 1H), 1.44 (m, 2H), 2.53 (t, 1H), 2.86 (bs, 3H), 3.16 (dd, 1H), 3.56 (m, 3H), 3.78 (dd, 1H), 4.50 (s, 2H), 7.33 (m, 5H), $^{13}$C NMR ($CDCl_3$) δ (ppm) 138.3, 128.8, 128.1, 73.3, 66.6, 58.8, 37.3, 21.7, 19.9. EI HRMS Calcd for $C_{13}H_{20}O_2N$ $(M + H)^+$ : 222.1489, found: 222.1482.

**(Z)-8-(benzyloxymethyl)-3-oxa-5-azabicyclo[5.1.0]oct-4-ene 58.** The hydroxylamine **57** (50 mg, 0.2 mmol) and ethyl formimidate (24 mg, 0.2 mmol) were dissolved in 2 mL of EtOH

and heated to reflux for 10 h. The material resulting from evaporation of the solvent was purified by flash chromatography (silica, $CH_2Cl_2$/MeOH 12:1 → 5:1) to give 14 mg of the oxazepine in a 30% yield. $^1$H NMR ($CD_3OD$) δ ppm 1.20 (m, 1H), 1.31 (m, 2H), 3.45 (m, 6H), 4.41 (s, 2H), 7.32 (m, 5H), 7.80 (s, 1H), $^{13}$C NMR ($CDCl_3$) δ (ppm) 154.2, 138.3, 128.4, 128.0, 127.8, 72.9, 65.8, 57.4, 37.8, 21.1, 18.7, 17.2. DIP-CI-MS (+) Calcd for $C_{14}H_{18}ON_2$ $(M + H)^+$: 232.1338, found: 232.1339.

**(Z)-4-(benzyloxy)but-2-enyl 2-benzyl-3-oxobutanoate 59.** To a suspension of NaH (60% in oil) (16 mg, 0.4 mmol) in dry dimethoxyethane (DME) (0.5 mL) was added a solution of acetoacetate (0.1 g, 0.4 mmol) in DME. The mixture was stirred at room temperature for 30 minutes under argon. After this time, benzyl bromide (91 μl, 0.8 mmol) was added and the mixture was left to react for 18 h. The solvent was evaporated under vacuum and the residue was dissolved in diethyl ether (20 mL). The mixture was extracted with water (3 x 20 mL). The organic phase was washed with saturated NaCl and dried over $MgSO_4$ and the ether was removed under reduced pressure. The crude product was purified by flash chromatography (silica, petroleum ether/AcEtO 20:1 to15:1 to 8:1) to give the functionalized acetoacetate **59** as a clear oil in a 73% yield (0.1 g). $^1$H NMR ($CDCl_3$) δ ppm 2.17 (s, 3H), 3.17 (d, 2H), 3.78 (t, 1H), 4.09 (d, 2H), 4.50 (s, 2H), 4.66 (d, 2H), 5.61 (m, 1H), 5.79 (m, 1H), 7.33 (m, 10H).

**(Z)-4-(benzyloxy)but-2-enyl 2-acetylpent-4-enoate 60.** This compound was obtained by the same procedure as **59**. In this case, allyl bomide (66 μl, 0.8 mmol) was used as alkylating agent. The amounts of the other reagents were kept the same as **59**. The crude product was purified by flash chromatography (silica, petroleum ether/AcEtO 20:1 then 8:1) to give the allyl functionalized acetoacetate **60** as a clear oil in a 61% yield (0.2 g). $^1$H NMR ($CDCl_3$) δ ppm 2.22

(s, 3H), 2.59 (t, 2H), 3.53 (t, 1H), 4.13 (d, 2H), 4.51 (s, 2H), 4.71 (d, 2H), 5.06 (m, 2H), 5.71 (m, 3H), 7.34 (m, 5H).

**(Z)-4-(benzyloxy)but-2-enyl 2-diazo-3-phenylpropanoate 61.** The title compound was synthesized using the procedure described for **8**. A solution of benzyl acetoacetate (90 mg, 0.3 mmol) and $Et_3N$ (47 μl, 0.3 mmol) in anhydrous acetonitrile (0.7 mL) were stirred at room temperature. Then a solution of p-ABSA (81 mg, 0.3 mmol) in acetonitrile (0.7 mL) was added dropwise over a 30 minutes period. After 3 h, an aqueous solution of 3 N LiOH (0.3 mL) was added. The work up of the mixture was the same as compound **8**. The crude product was purified by flash chromatography (silica, petroleum ether/EtOAc 20:1) to give 53 mg of benzyl azide as a yellow oil in a 53% yield. $^1$H NMR ($CDCl_3$) δ ppm 3.62 (s, 2H), 4.14 (d, 2H), 4.51 (s, 2H), 4.75 (d, 2H), 5.72 (m, 1H), 5.80 (m, 1H), 7.33 (m, 10H),$^{13}$C NMR ($CDCl_3$) δ (ppm) 167.3, 138.3, 137.4, 131.2, 129.2, 128.8, 128.7, 128.1, 128.1, 127.5, 127.1 72.8, 66.0, 61.0, 29.7. ESI-FTICR Calcd for $C_{20}H_{20}N_2O_3Na$ $(M + Na)^+$ : 359.1366, found: 359.1367.

**(Z)-4-(benzyloxy)but-2-enyl 2-diazopent-4-enoate 62.** This compound was prepared from allyl functionalized acetoacetate (63 mg, 0.2 mmol) using the same procedure used for synthesis of compounds **8** and **61**. The crude product was purified by flash chromatography (silica, petroleum ether/EtOAc 20:1) to give allyl azide as a yellow oil in a 32% yield (18 mg). $^1$H NMR ($CDCl_3$) δ ppm 3.04 (d, 2H), 4.14 (d, 2H), 4.51 (s, 2H), 4.73 (d, 2H), 5.12 (m, 2H), 5.81 (m, 3H), 7.33 (m, 5H). ESI-FTICR Calcd for $C_{16}H_{18}N_2O_3Na$ $(M + Na)^+$ : 309.1210, found: 309.1210.

**Method A. N4-Acetyl-5'-O-(4,4'-dimethoxytrityl)cytidine 66.** This compound was synthesized by literature procedure.[136] Cytidine **65** (5.0 g, 21 mmol) was suspended in dry DMF (42 mL). Freshly fractionally distilled $Ac_2O$ (2.1 mL, 23 mmol) was added to this suspension.

After the mixture was stirred at room temperature for 14 h, the organic solvent was removed by high vacuum. The residue was dissolved in pyridine (37 mL) and DMTCl (7.7 g, 23 mmol) was added slowly to that solution. The reaction was stirred at room temperature for 1 h and diluted with $CH_2Cl_2$ (150 mL). The organic phase was extracted with water (3 x 100 mL) and saturated $NaHCO_3$ (3 x 100 mL), dried with $MgSO_4$ and the solvent evaporated under vacuum. The product was purified by recrystallization with MeOH. The trityl cytidine **66** was obtained as a white solid in 44% yield (5.4 g) after two recrystallizations. $^1$H NMR ($CDCl_3$) δ ppm 2.23 (s, 3H), 3.48 (dd, 2H), 3.72 (bs, 1H), 3.79 (s, 6H), 4.39 (m, 3H), 5.83 (bs, 1H), 5.89 (d, 2H), 6.84 (m, 4H), 7.26 (m, 11H), 8.25 (d, 1H), 9.16 (bs, 1H). The NMR spectrum was consistent with the literature.

**2',3'-O,N$^4$-Triacetyl Cytidine 68.** Trityl N-acetyl cytidine (5.3 g, 9.1 mmol) was dissolved in dry pyridine (18 mL) and treated with $Ac_2O$ (3.0 mL, 32 mmol). After the mixture was stirred for 22 h, the solvent was evaporated under vacuum. The reaction was quenched slowly with saturated $NaHCO_3$ and, as soon as the evolution of gas ceased, it was extracted with $CH_2Cl_2$ (3 x 100 mL). The organic layer was dried with $MgSO_4$ and the solvent evaporated under vacuum. The product was pure enough by TLC ($CH_2Cl_2$/MeOH 9:1) to proceed with second step. The fully protected cytidine (6.7 g, 10 mmol) was treated with 90% solution of glacial acetic acid in water (55 mL) and let react at room temperature for 2 h. Then, the reaction was slowly neutralized with 5 N NaOH and extracted with $CH_2Cl_2$ (3 x 200 mL). The organic layer was dried with $MgSO_4$ and the solvent evaporated under vacuum. The product was purified by flash chromatography (silica, $CH_2Cl_2$/ MeOH 25:1) to give 2.3 g of the triacetyl cytidine **68** as a white solid in 68% yield for two steps. $^1$H NMR (DMSO) δ ppm 2.03 (s, 3H), 2.07 (s, 3H), 2.09 (s,

3H), 3.33 (s, 1H), 3.66 (dd, 2H), 4.18 (s, 1H), 5.37 (m, 2H), 6.01 (d, 1H), 7.22 (d, 1H), 8.31 (d, 1H), 10.95 (s, 1H). The NMR spectrum was consistent with the literature.

**Method B. 2',3'-O,$N^4$-Triacetyl-5'-tert-Buyldiphenylsilyl Cytidine 67.** This compound was synthetized by literature procedure.[137] Cytidine **65** (2.0 g, 8.2 mmol) was dissolved in DMF (34 mL) and imidazole (1.2 g, 18 mmol) and tert-Butyldiphenylchlorosilane (TBDPSCl) (2.6 mL, 9.9 mmol) were added. The reaction was stirred at room temperature for 20 h. Then, the reaction was diluted with pyridine (8 mL) and treated with $Ac_2O$ (4.0 mL, 43 mmol). After stirring for 12 h, the mixture was dissolved in EtOAc (100 mL) and washed with water (3 x 100 mL), saturated $NaHCO_3$ (3 x 100 mL) and brine (3 x 100 mL). The organic layer was dried with $MgSO_4$ and the solvent evaporated under vacuum. The product was purified by flash chromatography (silica, EtOAc/petroleum ether 2:1 to 9:1) to give 1.7 g of the protected cytidine **67** as a white solid in a 35% yield. $^1$H NMR ($CDCl_3$) δ ppm 1.10 (s, 9H), 2.04 (s, 3H), 2.06 (s, 3H), 2.26 (s, 3H), 3.80 (dd, 1H), 4.08 (m, 1H), 4.20 (dd, 1H), 5.43 (m, 2H), 6.29 (d, 1H), 7.23 (d, 1H), 7.43 (m, 6H), 7.64 (m, 4H), 8.16 (d, 1H), 10.48 (bs, 1H). The NMR spectrum was consistent with the literature.

**2',3'-O,$N^4$-Triacetyl Cytidine 68.** This compound was synthesized by the literature procedure.[137] To a solution of fully protected cytidine (1.8 g, 3.0 mmol) in dry THF (4.6 mL) was added glacial acetic acid (0.3 mL, 4.5 mmol) and a 1 M solution of n-$Bu_4NF$ in THF (15 mL, 15 mmol). After stirring the mixture 19 h at room temperature, 1 mL of acetic acid was added. The solvent was evaporated under vacuum. The product was purified by flash chromatography (silica, $CH_2Cl_2$/ MeOH 25:1) to give 8.0 g of the triacetylated cytidine **68** as a white solid in a 72% yield. The spectral data was consistent with literature and previously reported NMR.[137]

**Triethylammonium (5-(4-acetamido-2-oxopyrimidin-1(2H)-yl)-3,4-diacetoxy tetrahydrofuran-2-yl)methyl 2-chlorophenyl phosphate 69.** To a solution of 2-chlorophenyl dichlorophosphate (220 μL, 1.36 mmol) in anhydrous acetonitrile (2.80 mL) was added $Et_3N$ (376 μL, 2.71 mmol) and 1,2,4-triazole (0.24 g, 3.51 mmol). A white precipitate formed immediately and the mixture was stirred for 30 minutes at room temperature. A solution of triacetyl cytidine **68** (0.20 g, 0.54 mmol) in dry pyridine (2.70 mL) was added to the previous suspension. After stirring the solution for another 30 minutes, the reaction was quenched with a combination of $Et_3N$ (0.38 mL), water (0.1 mL) and pyridine (1 mL). This mixture was stirred for 15 minutes, diluted with 50 mL of saturated $NaHCO_3$ and extracted with $CHCl_3$ (8 x 20 mL). The organic layer was washed with more saturated $NaHCO_3$, dried with $MgSO_4$ and the solvent evaporated under vacuum. The residue was dissolved in a minimum amount of $CHCl_3$ and added dropwise to 50 mL of petroleum ether. The product **69** was collected by gravity filtration as a yellow powder in a 51% yield (0.18 g). The chlorophenyl triacetylated cytidine obtained was sufficiently pure enough to be used without further purification. $^1$H NMR (DMSO) δ ppm 1.92 (s, 3H), 1.95 (s, 3H), 2.12 (s, 3H), 4.23 (m, 3H), 5.32 (m, 2H), 6.16 (d, 1H), 7.23 (m, 5H), 8.23 (d, 1H), 11.42 (s, 1H), $^{31}$P NMR ($CDCl_3$) δ (ppm) -5.46. C18 HPLC/UV ESI-MS (-) Calcd for $C_{21}H_{22}O_{11}N_3ClP$ $(M - H)^-$ : 558, found: 558.

**6-(hydroxymethyl)-3-oxabicyclo[3.1.0]hexan-2-one 70.** Lactone **9** (0.2 g, 0.9 mmol) was dissolved in dry $CH_2Cl_2$ (35 mL). Then, 30 mg of 10% Pd activated with carbon were added. The reaction was stirred for 5 h at room temperature under $H_2$ (g) atmosphere. Then, the black suspension was filtered through Celite. The celite bed was washed five times with $CH_2Cl_2$ to maximize recovery of the product. The solvent was evaporated under vacuum. The product was obtained as a clear oil in 100% yield and was used without further purification. $^1$H NMR ($CDCl_3$)

δ ppm 1.85 (m, 1H), 1.95 (bs, 1H), 2.37 (dd, 1H), 2.45 (dd, 1H), 3.69 (dd, 1H), 3.84 (dd, 1H), 4.32 (dd, 1H), 4.46 (dd, 1H), $^{13}C$ NMR ($CDCl_3$) δ (ppm) 175.1, 66.7, 57.4, 23.8, 22.7.

**2-(4-acetamido-2-oxopyrimidin-1(2H)-yl)-5-(((2-chlorophenoxy)((2-oxo-3-oxabicyclo[3.1.0]hexan-6-yl)methoxy)phosphoryloxy)methyl)tetrahydrofuran-3,4-diyl diacetate 71.** A solution of lactone **70** (21 mg, 0.2 mmol) in dry pyridine (2.6 mL) was treated with 2-chlorophenyl phosphate cytidine (84 mg, 0.1 mmol) and 1-mesitylene-sulphonyl-3-nitro-1,2,4-triazole (MSNT) (0.3 g, 0.8 mmol). The reaction was stirred at room temperature until no more lactone starting material was observed by TLC (2 h). The mixture was diluted with a saturated solution of $NaHCO_3$ (20 mL) and extracted into $CHCl_3$ (8 x 20 mL). The organic layer was dried with $MgSO_4$ and the solvent evaporated under vacuum. The product was purified by flash chromatography (silica, $CH_2Cl_2$/ MeOH 50:1 then 25:1) to give 43 mg of the product **71** as a clear oil in a 32% yield. $^1H$ NMR (DMSO) δ ppm 1.97 (s, 1H), 2.07 (s, 6H), 2.23 (s, 3H), 2.44 (m, 2H), 4.39 (m, 7H), 5.41 (dd, 2H), 6.12 (dd, 1H), 7.31 (m, 5H), 7.88 (m, 1H), 9.68 (bs, 1H), $^{31}P$ NMR ($CDCl_3$) δ (ppm) -5.22, -5.56, -5.65, -5.97. ESI-TOF-MS (+) Calcd for $C_{27}H_{30}O_{13}N_3ClP$ $(M + H)^+$: 670.1199, found: 670.1177.

**(Z)-3,5-diazabicyclo[5.1.0]oct-4-en-8-ylmethyl (5-(4-amino-2-oxopyrimidin-1(2H)-yl)-3,4-dihydroxytetrahydrofuran-2-yl)methyl hydrogen phosphate 73.** Amidine **33** (0.1 g, 0.8 mmol) was suspended in a few milliliters of dry pyridine and evaporated under high vacuum. Then, a solution of cytidine-5'-monophosphate (0.3 g, 0.9 mmol) in 1 mL of pyridine was mixed with the amidine and again evaporated under vacuum. The white residue was suspended in 6.5 mL of dry pyridine and DCC (0.8 g, 3.8 mmol) was added. After the mixture was stirred for six days, water was added and the mixture was stirred for 1.5 h more and filtered. The solvents were evaporated and the crude reaction was partitioned in $H_2O/CHCl_3$. The organic phase was

discarded. Finally, the aqueous phase was concentrated and the resulting sample was purified by HPLC. The solvent utilized was a mixture 95% of $H_2O$/acetonitrile with a flow rate of 5.5 mL/min and the detector set it at 270 nm. Under this eluent solvent system, the CMP-amidine exhibit a retention time of 8.1 minutes. The desired amidine was obtained in a 0.3% yield as a white solid with a 95% purity. $^{1}H$ NMR ($D_2O$) δ ppm 1.44 (m, 1H), 1.77 (m, 2H), 3.56 (dt, 2H), 4.05 (m, 13H), 5.94 (d, 1H), 6.08 (d, 1H), 7.45 (s, 1H), 7.31 (m, 5H), 7.86 (d, 1H), $^{31}P$ NMR ($D_2O$) δ (ppm) 1.06. C18 HPLC/UV ESI-MS (+) Calcd for $C_{16}H_{25}O_8N_5P$ $(M + H)^+$: 446.4, found: 446.1.

CHAPTER 4
INHIBITION OF HUMAN SIALYLTRANFERASE AND GLYCOSIDASES BY DIAZABICYCLIC AMIDINES

## Introduction

The design and synthesis of enzymes specific and potent enzyme inhibitors is of considerable interest due to their possible applications in several research areas. For example, mechanism-based analogs are valuable tools in the examination of an enzyme catalyzed mechanism. In addition, they could serve to identify which amino acids could be involved in the substrate binding and recognition. The only disadvantage of this kind of inhibitor resides in the difficulty of preparing the synthetic products. In general, the ideal compound should display high binding affinity to the active site of the protein. This feature is frequently found in TS analogs with competitive binding. From diverse kinetic experiments, the best TS analog inhibitors interact with the enzymes $10^7$ to $10^{15}$ times tighter than the corresponding substrate does in the ground state.[145]

Compounds that possess the aza functionality are found among the most potent inhibitors for glycosidases and glycosyltransferases (see Chapter 1 for further discussion on these derivatives). One of the reasons is their ability to bind to enzyme active site by charge-charge interaction, as well as, by hydrogen bonding (Figure 4-1).

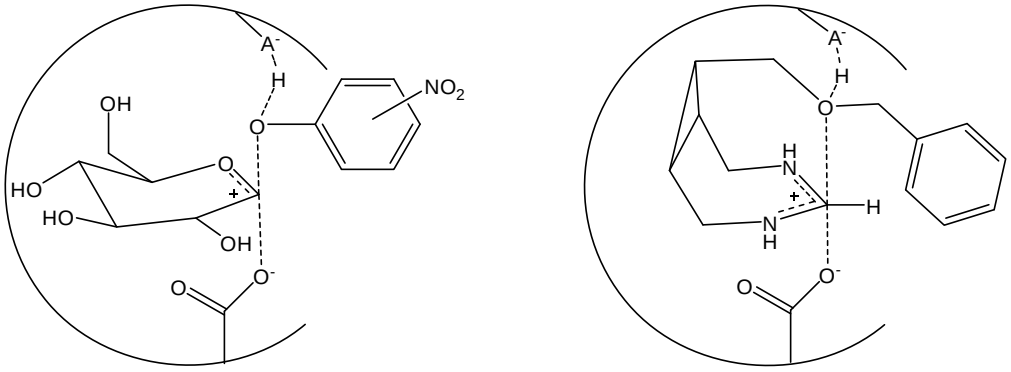


Figure 4-1. Transition State for glucosidase and amidine TS analog

With the intention to explore the general utility of the bicyclic amidines as mimics of oxocarbenium ion-like transition states, a small family of bicyclic amidines which differed in their substitution and mimicry of a leaving group (LG) moiety was tested on several glycosidases. In addition, CMP-amidine **73** was tested on human recombinant α(2→6)-sialyltranferase (α(2→6)-ST).

## Results and Discussion

### Glycosidases Kinetic Assay

The seven-membered ring amidines utilized for glycosidases screening are shown in Figure 4-2. They are divided in two classes. While the amidines that have a –OBn group (with Bn being benzyl) as the LG mimicry were meant to simulate the aglycon portion of the substrate, the ones that have hydroxyl group might mimic the attacking water molecule.

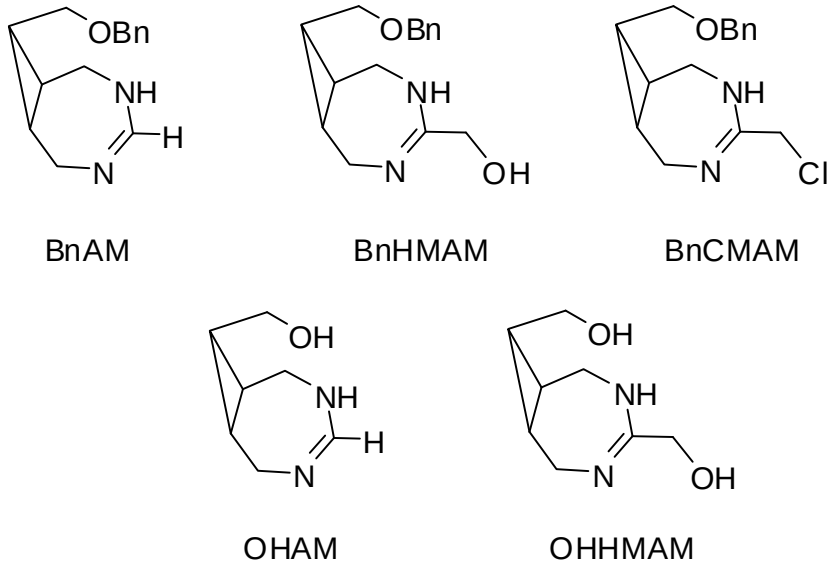


Figure 4-2. Library of glycosidases TS analogs

For the inhibitors' kinetic characterization, a continuous assay with a chromogenic substrate was utilized. A representation of this assay is shown in Figure 4-3.

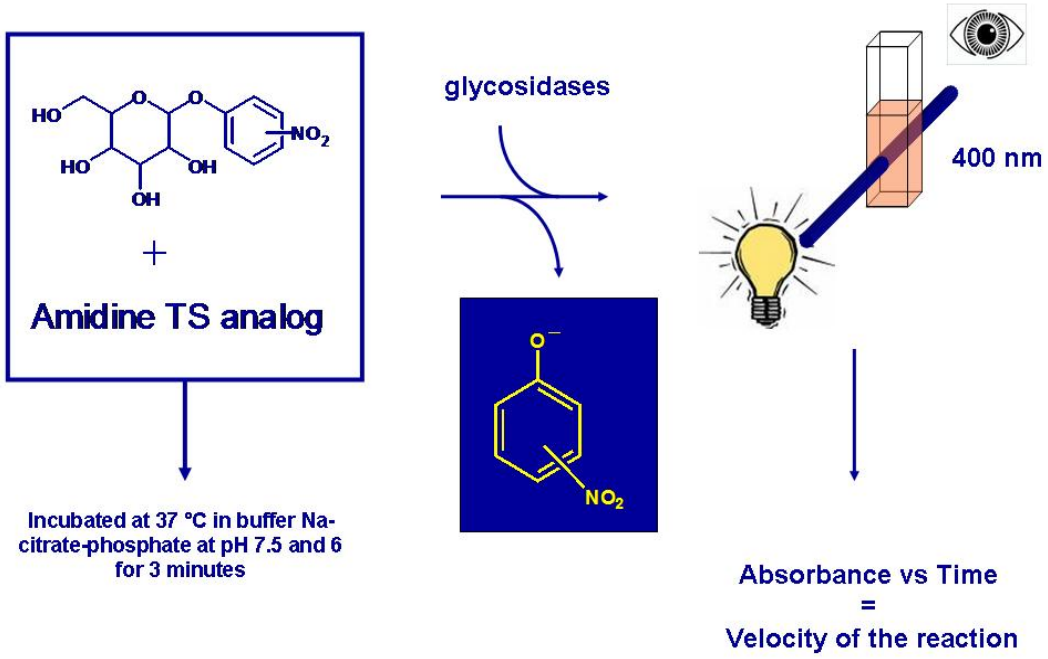


Figure 4-3. Kinetic assay for glycosidases

The commercially available o- or p-nitrophenyl α- or β-glycopyranosides were incubated with the inhibitor at 37 °C in a buffer of 50 mM Na-citrate-phosphate. After the mixture equilibrated to temperature, the appropriate amount of enzyme was added. The glycosidase hydrolyses the nitrophenol moiety which develops a yellow color in the solution. The continuous increase in the reaction absorbance is followed at 400 nm by a UV/VIS spectrophotometer. The velocity of the enzymatic reaction can be calculated from the absorbance vs time profile and the extinction coefficient of the nitrophenol, which was determined independantly. The inhibitor screening was performed at pH of 7.5 and 6. Any variations in the kinetic parameters with pH might provide a preliminary clue into the charge state of the inhibitor or inhibitor/enzyme complex.

**TS analogs screening**

The glycosidases utilized in these experiments were α-galactosidase from green coffee beans (α-gal), β-galactosidase from *Escherichia coli* (β-galEcoli), β-galactosidase from *Aspergillus orizae* (β-galAsp), α-glucosidase from *Saccharomyces cerevisiae* (α-glu) and β-glucosidase from sweet almonds (β-glu) which are all retaining enzymes.

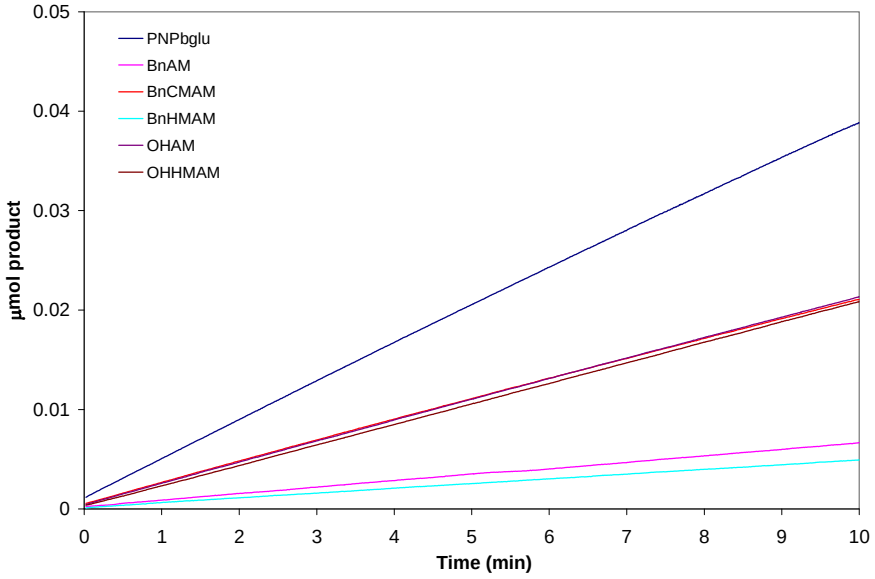


Figure 4-4. Kinetic assay for β-glu at pH 7.5 with all TS analogs

The kinetic screenings were accomplished under initial velocity conditions. In all cases the concentration of substrate and inhibitor were set close to the $K_m$ of the corresponding glycosidase. The reported $K_m$ data in the literature were the following: a) α-gal, 0.25 mM (pH 6.5),[146] b) α-glu , 0.3 mM(pH 7.0),[146] c) β-galAsp, 0.72 mM (pH 4.5),[147] d) β-galEcoli, 0.65 mM (pH 7.0),[146] and e) β-glu,1.3 mM(pH 5.0).[146] Consequently, the concentration of substrate and inhibitors utilized were 0.25 mM for α-gal, 0.3 mM for α-glu, 1 mM for β-galAsp and β-galEcoli and 2 mM for β-glu. The inhibitor screening with different glycosidases is reported in Table 4-1.

Table 4-1. Inhibition screening data (ni, no inhibition at those concentration of substrate and inhibitor)

| Compound | α-gal | | α-glu | | β-glaAps | | β-galEcoli | | β-glu | |
|---|---|---|---|---|---|---|---|---|---|---|
| | pH 7.5 | pH 6 | pH 7.5 | pH 6 | pH 7.5 | pH 6 | pH 7.5 | pH 6 | pH 7.5 | pH 6 |
| BnAM | 2% | ni | ni | ni | 16% | 16% | 10% | ni | 83% | 65% |
| OHAM | ni | 4% | 2% | ni | 11% | ni | 3% | ni | 45% | 24% |
| BnHMAM | 2% | ni | ni | 3% | 40% | 16% | 10% | 13% | 87% | 71% |
| OHHMAM | ni | 3% | ni | ni | 34% | ni | 10% | 5% | 46% | 26% |
| BnCMAM | ni | ni | ni | ni | 13% | ni | 51% | 12% | 46% | 29% |

The inhibition is presented as a percentage inhibition when the initial velocity of the reaction without inhibitors is compared with the enzymatic reaction in the presence of inhibitor. An example of the appearance of the velocity profile when inhibitors are tested against β-glu is presented in Figure 4-4 (PNPglu is p-nitrophenyl-β-glucopyranoside). The full set of kinetic inhibition assay plots can be found in Appendix B. Based on the kinetic screening of the different inhibitors, neither α-gal nor α-glu showed a significant decrease on activity at either pH 6 or 7.5. On the other hand, all three β-glycosidases tested showed selective responses to these molecules.

**TS analogs kinetic characterization**

The kinetic parameters ($K_m$, $V_{max}$ and $K_i$) for the most potent amidine inhibitors were determined by full steady state kinetic analysis. While $K_m$ and $V_{max}$ were obtained by the corresponding Linewearve-Burke plots, the $K_i$ data were estimated by fitting the Michaelis-Menten curves with Excel (a complete illustration of Michelis-Menten equations, Lineweaver-Burke plots and Michaelis-Menten curves are enclosed in Appendix B). The $K_m$ and $V_{max}$ determined were the following: a) for β-galAsp, 1.5 mM and 1.9 $\mu mol_{prod}/min.mg_{enz}$ ; b) for β-galEcoli, 0.08 mM and 446 $\mu mol_{prod}/min.mg_{enz}$; c) for β-glu, 3.8 mM and 25 $\mu mol_{prod}/min.mg_{enz}$. A summary of the $K_i$ obtained with the TS analogs is shown in Table 4-2.

Table 4-2. Inhibition constants ($K_i$ are in mM; because BnCMAM displayed a non-competitive mode of action two $K_i$ were determined)

| Compound | β-galAsp | β-galEcoli | β-glu |
|---|---|---|---|
| | pH 7.5 | pH 7.5 | pH 7.5 |
| BnAM | ----- | ----- | 0.27 |
| OHAM | ----- | ----- | ----- |
| BnHMAM | 0.76 | ----- | 0.15 |
| OHHMAM | 1.55 | ----- | ----- |
| BnCMAM | ----- | 0.80 and 0.56 | ----- |

For β-galAsp only the hydroxylmethyl amidines (BnHMAM and OHHMAM) displayed some inhibitory activity. This result implies that $CH_2OH$ functionality, next to the anomeric center mimic, might be forming a hydrogen bond to the active site nucleophilic carboxylate.[10-14] In addition, the amidine BnHMAM, which has the benzyl group as the mimic of the departing aglycon, was the most potent inhibitor for this β-galactosidase. Consequently, this amidine's higher inhibitory potency might be explained by a favorable hydrophobic interaction of its benzyl group with the aglycon binding portion of the enzyme active site. None of the molecules tested on β-galAps at pH 6 showed any significant inhibition, which suggests that there is a catalytic active residue that needs to be deprotonated in order to stabilize the transition state Titration of either BnAM or BnHMAM failed to reveal a pKa up to pH 10, indicating that the pH sensitivity of the inhibition data reflects an ionization on the enzyme.

A completely different inhibitory profile was observed with β-galEcoli. The only modest inhibitor was molecule BnCMAM that contains a chloromethyl functional group. Particularly, this molecule presented a mixed or non-competitive type of profile based on the Lineweaver-Burke plot (see appendix B). In addition, a slight curvature in the initial velocity data was observed, suggesting a time dependant inactivation mechanisms might be operative (Figure 4-5).

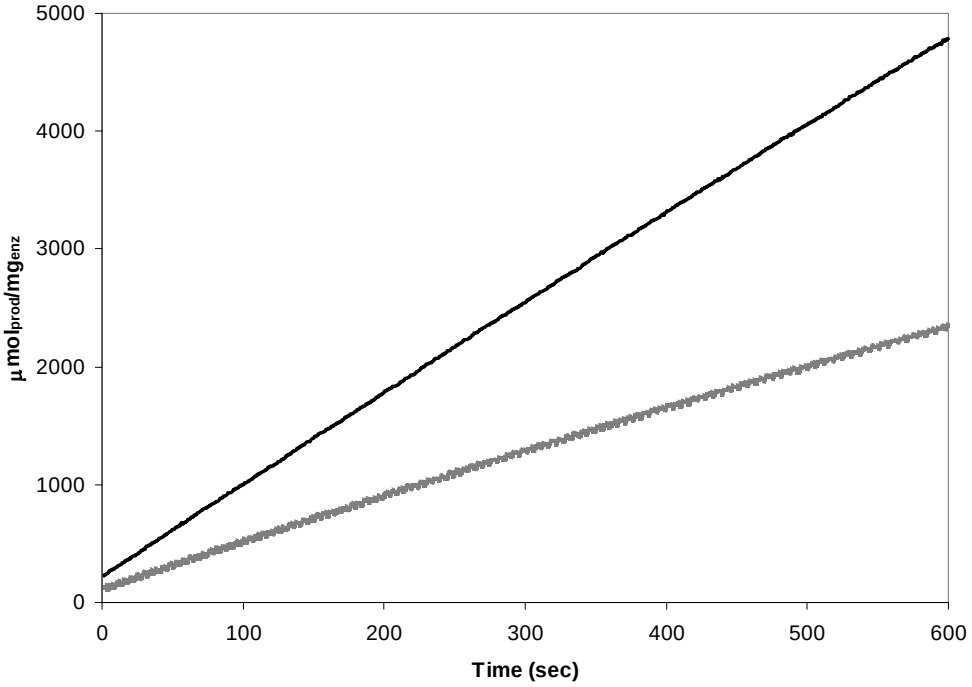


Figure 4-5. Inhibition of β-galEcoli by TS analog BnCMAM. Solid line is reaction without inhibitor; dashed line is enzymatic reaction with BnCMAM.

Because it was suspected that an attack to the chloromethyl center was occurring, thus, forming a covalent inhibitor-enzyme intermediate, an inactivation assay was performed on the β-galEcoli. This kind of nucleophilic attack from the enzyme was previously observed with glycosides that included reactive functional groups like triazenes and fluorine near the anomeric center.[148,149] The methyl triazene compounds acted as "affinity labels" generating a carbonium ion that irreversible inhibited β-galEcoli.[148] Alternatively, 2-deoxy-2-fluoro glycosyl molecules showed a decreased in the deglycosylation rate reaction and subsequent accumulation of glycosyl enzyme intermediate.[149] To test these hypotheses, β-galEcoli was incubated with the TS analog before adding the substrate. This experiment showed a curvature on the slope vs. time plot which suggested that the molecule not only inhibits the enzyme but also inactivates it (Figure 4-6).

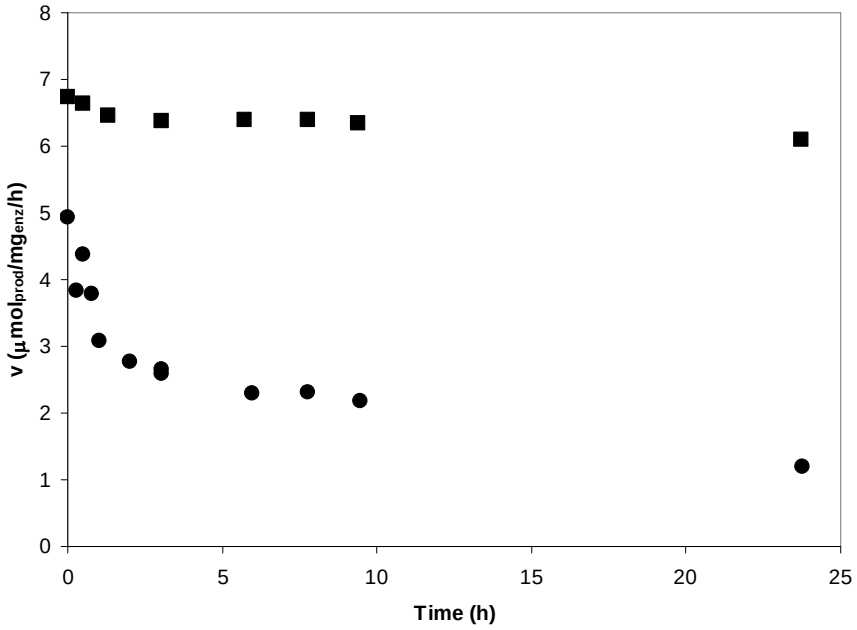


Figure 4-6. Inactivation of β-galEcoli by compound BnCMAM. The β-galactosidase was incubated with two chloromethyl amidine concentrations ■, 0 mM and ●, 0.6 mM, and the reaction started with 0.7 mM of ONPG.

Analysis of this data did not show pseudo first order kinetics which implied that a complex mechanism of inactivation is taking place. Specifically, after an initial, rapid inactivation phase, a slower rate of inactivation was observed, still in progress after 25 hours. This interaction needs to be further examined, and appears consistent with the chloromethyl group functioning as an alkylating agent.

Similar to the β-galAsp enzyme, β-galEcoli's best inhibition was observed at pH 7.5, which it is expected in an enzyme that has a catalytic amino acid side chain that needs to be deprotonated before the reaction occurs.

In this thesis research, β-galactosidases belonging to two different organisms (*A. oryzae* and *E. coli*) were studied. Surprisingly, they showed a different inhibitory profile when tested with this series of TS analogs. This result might suggest that these enzymes do not present a parallel arrangement of catalytic residues in their active sites.

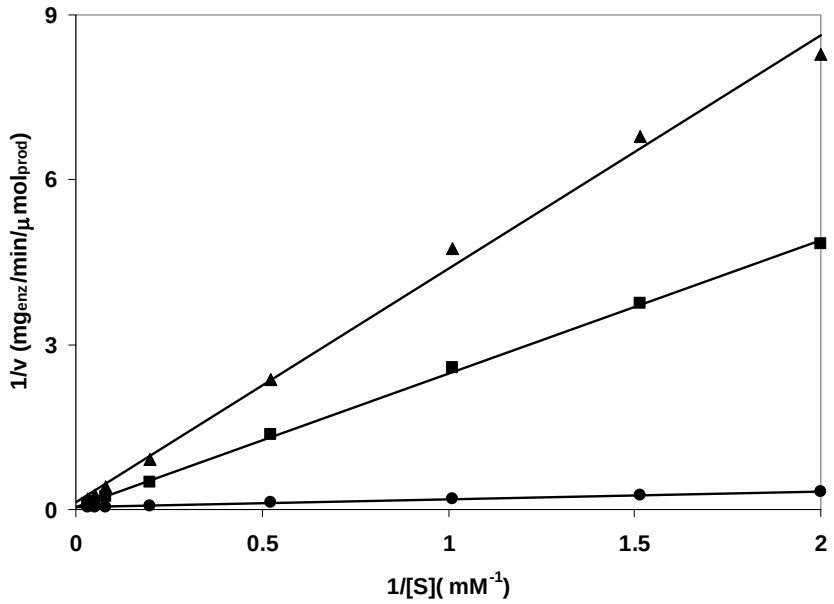


Figure 4-7. Lineweaver-Burke plot for (Z)-(8-(benzyloxymethyl)-3,5-diazabicyclo[5.1.0]oct-4-en-4-yl)methanol (BnHMAM). The concentrations of TS analogs were ▲, 4 mM; ■, 2 mM; ●, 0 mM.

Finally, β-glu was the most susceptible and the less selective enzyme to this set of TS analogs. All compounds showed a degree of inhibitory action, with BnAM and BnHMAm being the most potent inhibitors. The Lineweaver-Burke plot for β-glu against hydroxymethyl amidine BnHMAM is showed in Figure 4-7.

These compounds shared the common feature of a benzyl group which implies that the enzyme active site's aglycon region may also recognize hydrophobic residues. From the comparison of kinetic data for BnAM and BnHMAM, it is established that including a hydroxyl group only improved the potency of the amidine TS analog by a factor of 2. When performing the screening assays on β-glu at pH 6, it was observed that the inhibition only decreased 20% relative to the pH 7.5 data. This result was different from what was observed with the other enzymes, where the potency of the amidines at pH 7.5 was at least 30% higher than for pH 6. This effect is consistent with a β-glu pH-independent inhibition mode of action against some TS

analogs, also observed by other groups.[37,39,49] With respect to the relative contributions of a hydrophobic aglycon mimic, or the hydrophilic hydroxymethyl group to the potency of the inhibitors, it can be concluded that the hydrophobic aglycon mimic group was more effective than the hydroxymethyl group.

**α(2→6)-Sialyltransferase Inhibition Screen**

A point assay was utilized to perform the kinetic characterization of compound **73** as a ST inhibitor. The glycosyl donor substrate, cytidine monophosphate-N-acetylneuraminate (CMP-NeuAc) was $^{14}C$ radiolabeled at the N-acetyl group. Upon transfer of the NeuAc group to the acceptor saccharide N-acetyl lactosamine (LacNAc), the resulting $^{14}C$-labeled trisaccharide product was quantified with liquid scintillation counting (LSC) by passing time point aliquots through a Dowex-1 (Pi form) column, which retained unreacted starting material. The inhibition assay was carried out under initial velocity conditions utilizing a 200 μM concentration of CMP-amidine **73**, two different concentrations of CMP-NeuAc (43 μM and 100 μM) and the LacNAc concentration held at 4.6 mM. A control runs were also performed using the same concentrations of CMP-NeuAc and LacNAc but without the inhibitor. All the reaction mixtures were incubated at 30 °C for a short period of time before adding the enzyme. After initiating the reaction by addition of enzyme, time point aliquots at 5 and 10 minutes were applied to Dowex 1 (Pi) mini columns. The estimation of the $K_i$ was obtained by plotting the slope of the Lineawear-Burke plots againts the [I] and getting the x-axis intercept of these plot after linear regressions. Assuming competitive inhibition, CMP-amidine **73** exhibited a $K_i$ of ~ 50 μM. Clearly the analysis is preliminary with so few data collected, but it is clear that compound **73** is indeed a reasonable micromolar inhibitor. The inhibition constant estimated for compound **73** is comparable with the one exhibited by α(2→6)-ST from human serum in the presence of free

CMP ($K_i$ of 50 μM).[71] This result confirms the fact that the cytidine portion of the donor is required for enzyme recognition. On the other hand, the amidine fraction did not seem to have any significant contribution to binding. In addition, the previous generations of scorpio inhibitors obtained in our lab displayed 10 times lower $K_i$ when compared with amidine **73**. Although those molecules were tested on the rat α(2→3)- and α(2→6)-ST, it can be inferred that the inhibitory activity of the TS analog might have been affected by the greater size of the seven-membered ring amidine. These suggestions must be taken with caution, given the preliminary nature of the data. A more complete characterization of the inhibition kinetics of **73** and its selectivity profile for other sialyltransferases are required.

## Experimental Section

Solvents and reagents were purchased from Aldrich Chemical Company and Acros Organics. Glycosidase enzymes and nitrophenyl glycoside substrates were purchased from Sigma. UV/visible spectra were obtained in Beckman DU 640 and Agilent 8453 spectrophotometers. An Isotemp 210 from Fisher Scientific was used to maintain constant temperature.

### Inhibition Studies on Glycosidases

Initial velocities for enzyme catalyzed reactions were determined spectrophotometrically based on the appearance of nitrophenol produced by hydrolysis of the corresponding nitrophenyl hexopyranoside. The kinetic assays were performed at 37 °C at pH 6.0 and pH 7.5 using 50 mM Na-citrate-phosphate buffers with the exception of the β-galactosidase from E. coli, whose buffer contained also 10 mM $MgCl_2$. The glycosidases used were α-galactosidase from green coffee beans, β-galactosidase from *Escherichia coli*, β-galactosidase from *Aspergillus orizae*, α-glucosidase from *Saccharomyces cerevisiae* and β-glucosidase from sweet almonds. The substrate used for each enzyme were the following: p-nitrophenyl-α-galactopyranoside PNPgal

(α-galactosidase), p-nitrophenyl-α-glucopyranoside PNPαglu (α-glucosidase), p-nitrophenyl-β-glucopyranoside PNPβglu (β-glucosidase) and o-nitrophenyl-β-galactopyranoside ONPG (β-galactosidase). The concentrations of substrate and TS analog used were the following: 0.25 mM for α-galactosidase from green coffee beans, 0.3 mM for α-glucosidase from baker yeast, 1 mM for β-galactosidase from A. oryzae and β-galactosidase from E. coli and 2 mM for β-glucosidase from almonds. The enzymatic reaction were initiated by the addition of the following units and volumes of enzymes: 0.2 U of β-galactosidase (*Aspergillus orizae*) in 5 μL for both pHs; 0.2 U of α-galactosidase in 10 μL at pH 7.5 and 0.02 U in 15 μL at pH 6.0; 0.1 U of α-glucosidase in 5 uL at pH 7.5 and 0.2 U in 10 uL at pH 6.0; 0.3 U of β-galactosidase (*E.coli*) in 5 μL at pH 7.5 and 0.5 U in 10 μL at pH 6.0; 0.1 U of β-glucosidase in 5 μL at pH 7.5 and 0.01 U in 5 μL at pH 6.0. For the inhibition screening assays, the substrate concentration used was around $K_m$ and the amount of enzyme was adjusted to obtain less than 10% hydrolysis of the substrate over 5 or 10 minutes time courses. In all cases, 1 mL reaction mixtures were incubated at 37 °C for 3 minutes before enzyme addition. The increase of nitrophenol absorbtion was monitored at 400 nm after adding the enzyme. The reactions were followed for 5 to 10 minutes to obtain initial velocity data. The kinetic parameters ($K_m$, $V_{max}$, $K_i$) were determined using 5 to 8 substrate concentrations between 0.05 mM and 30 mM, and 3 different inhibitors concentrations between 0.3 mM and 4 mM. Velocity data were obtained from the slope of the plot μmol product vs. time (see Appendix B). The $K_m$ and $V_{max}$ were calculated by fitting the corresponding Michaelis-Menten curves and double reciprocal plots (Lineweaver-Burke reverse plots) (see Appendix B). The inhibition constants were obtained by fitting the different Michaelis-Menten curves with and without inhibitor with Excel. These constants were compared with the values obtained by

plotting the slope of the Lineawear-Burke plots againts the [I] and getting the x-axis intercept of these plot after linear regressions (Appendix B).

The extinction coefficient ε for o- and p-nitro phenol were calculated by the Beer-Lambert Law in 50 mM Na-citrate-phosphate buffer using known concentrations of the phenol. For p-nitrophenol, ε was 15059 and 2983 $cm^{-1}M^{-1}$ at pH 7.5 and 6 respectively. For o-nitro phenol, ε was 2558 and 1159 $cm^{-1}M^{-1}$ at pH 7.5 and 6 respectively.

**Inactivation of β-galactosidase from E.coli**

These experiments were carried out by incubating 1.5 U of enzyme in the presence of 0.6 mM (Z)-8-(benzyloxymethyl)-4-(chloromethyl)-3,5-diazabicyclo[5.1.0]oct-3-ene (BnCMAM) on an ice bath during a period of 25 h. In parallel to this mixture, another 1.5 U of enzyme were incubated without inhibitor under the same temperature and time conditions. The buffer used was 50 mM Na-citrate-phosphate containing 10 mM $MgCl_2$ at pH 7.5. A solution of 0.7 mM ONPG (~ 10 $K_m$) was equilibrated at 37 °C for 3 minutes. At appropriate intervals of time, 10 μL aliquots (0.05 U of enzyme) from the vial of enzyme with or without inhibitor were added to the solution of the substrate. The final volume for each reaction mixture was 1 mL. The hydrolysis of o-nitrophenyl-β-galactopyranoside was monitored at 400 nm.

**Inhibition Studies on α(2→6)-Sialyltransferase**

The α(2→6)-ST kinetic assays were performed at 30 °C using a 50 mM MES (pH = 7.2) buffer containing 0.05% Triton CF-54 and 0.1mg/mL BSA. The enzyme was a recombinant, human α(2→6)-ST (Calbiochem), lacking the N-terminal membrane spanning region which was expressed in *S. frugiperda* insect cells using a baculovirus expression system. The concentrations of substrate and TS analog used were 43 μM and 100 μM of CMP-NeuAc, 4.6 mM LacNAc and 200 μM of CMP-amidine **73**. The concentrations of CMP-NeuAc were

obtained by mixing 4 μL of a stock 273 μM solution of $^{14}$C-CMP-NeuAc (specific activity of $2.65x10^{-8}$ μmol/cpm) and the appropriate amount of a 720 μM solution of cold CMP-NeuAc. The enzymatic reactions were initiated by the addition of 1 μL of enzyme (1.43 mU). In all cases, the 210 μL reaction mixtures were incubated at 30 °C for approximately 2 minutes before enzyme addition. Two 100 μL aliquots were taken at 5 and 10 minutes and quenched in 500 μL of ice-cold 5 mM phosphate buffer (pH of 6.8). Then, 580 μL of the quenched mixtures were applied to the Dowex 1 (Pi) columns and eluted with 3.42 mL of 5 mM phosphate buffer. After collecting the columns eluate, the vials were filled with 10 mL of Scintisafe30 LSC fluid. The radioactivity of each vial was counted for 3 minutes.

The Dowex-1 (Pi) resin was prepared from the $Cl^-$ form by washing it first with 2 L of deionized water and 500 mL of EtOH. Then, the resin was treated with 1 L of 4 M NaOH. The $OH^-$ resin was washed with deionized water until the pH was approximately 7. The $OH^-$ resin was converted into the Pi by adding 1 L of a 4 M solution of 85% aqueous $H_3PO_4$. Finally, the Pi resin was extensively washed with deionized water until pH reached neutrality again.

# CHAPTER 5
# SYNTHESIS OF QUINUCLIDINE AND QUINUCLIDINONE DERIVATIVES AS NICOTINIC ACETYLCHOLINE RECEPTOR AGONISTS

## Introduction

In this chapter a study involving the synthesis of potential agonists for the nicotinic acetylcholine receptor (nAChR) is outlined. The goal of this work is to use these compounds to help define, and identify what constitutes the structural requirements for agonism of the human α7 receptor subtype. The following section provides background information to develop the ideas behind the design of the target quinuclidine compounds.

Neurons communicate intracellularly with each other through synapse, by passing an electric signal (action potential) or chemical signal. The electric potential across the plasma membrane is regulated primarily by opening and closing $K^+$, $Na^+$, $Cl^-$ and $Ca^{2+}$ ion channels. On the other hand, because the gap (synaptic cleft) between neurons sometimes is too large for a direct transmission, the communication between these cells is mediated by neurotransmitters. These molecules travel across the gap to the corresponding receptor where they bind and trigger an action potential on the other neuron. If the neuron is connected with a muscle cell, the signal transmission may induce muscle contraction. If the postsynaptic cell is part of glandular tissue, the action potential may induce a hormone secretion.[150]

One big family of synaptic receptor is the ionophores. This type of receptor molecule allows the diffusion of ions through the cell membrane. There are two classes of ionophores: carriers, which bind the ion on one side of the cell membrane and release it on the other side, and ion channels, which have the capability of opening a pore through which ions can go through.[8,150] The specificity of carriers is much broader than for the ion channel. In contrast, the transport of current through an ion channel is faster than the carriers. The ion selective channels open and close for a very short period of time in response to different cellular signals. This gated

mode of action is regulated by the binding of a variety of ligands located inside or outside the neuron or, by changes of the electrical potential across the plasma membrane. Consequently, the channels that are controlled by the interaction with a chemical transmitter are known as ligand-gated channels. On the other hand, ion channels that respond to an electrical gradient across the membrane are called voltage-gated channels.[8,63,150] One example of a voltage-gated channel is the $Na^+$ ion channel located in the membrane of both neurons and muscles. When the outside of the cell becomes negative (depolarization), positively charge *voltage-sensing $\alpha$ helixes* of this channel change position, allowing a flux of $Na^+$ through the membrane. The channel closes after a short period of time when the interior of the cell becomes negative again. At this stage, the $\alpha$ helixes return to the relaxed position and a *channel-inactivating segment* blocks the gate on the interior making the channel momentarily inactive. This guarantees that the action potential only moves in one direction.[150]

A large family of ligand-gated channels respond to the binding of acetylcholine (Ach). Biosynthesized from acetyl coenzyme A and choline, ACh (Figure 5-1) is accumulated next to the neuron presynaptic plasma membrane. The release of this neurotransmitter to the synaptic cleft is regulated by voltage-gated $Ca^{2+}$ ion channels. After traveling across the synapse, ACh binds to the acetylcholine receptor (AChR) located in the postsynaptic neuron. This interaction triggers a conformational change of the receptor which allows the entrance of alkali ions like $Na^+$ and $K^+$; thus effecting transfer of the electrical signal from cell to cell.[150]

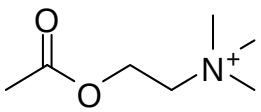


Figure 5-1. Acetylcholine, ACh

**Acetylcholine Receptor Family**

The acetylcholine ligand-gated channels are called cholinergic receptors and are divided into two major types. The ones that are sensitive to the mushroom alkaloid muscarine are the muscarinic acetylcholine receptors (mAChRs).[151,152] Some of these receptors are responsible for the entrance of $K^+$ in heart muscle, activation of phospholipases and inhibition of adenylyl cyclase. The other subfamily of acetylcholine receptors are the nicotinic acetylcholine receptors (nAChRs).[151,152] These ligand-gated channels are so named because they are susceptible to the alkaloid nicotine. Among the functions of this receptor, it was found that nAChRs are found at brain synapses and neuromuscular junctions. Being one of the first ion channels to be characterized and purified, they have served as a starting point for the study of the structure and mechanism of other receptors. Their importance also arises due to the fact that these ligand-gated channels are involved in several human neuronal diseases like Alzheimer's, schizophrenia and Tourette's syndrome (characterized by the development of a variety of vocal and motor tics).[151]

The nAChR belong to the super family of iontropic receptors that includes glycine, serotonin, and GABA receptors,[152] and they have been extensively studied due to their ready isolation from the electric organ of the Torpedo California (electric ray).[150,153,154] Moreover, the nAChR are strongly inhibited by two snake neurotoxins such as α-bungarotoxin and cobratoxin which facilitated their tagging and purification.[150] The muscle-type nAChR is composed of five different subunits, ε or γ, δ, β1 and 2 α1, being the α domains the binding sites for the acetylcholine neurotransmitter. Neuronal nAChRs are formed by an arrangement of α and β subunits (α2 through α6, β2 through β4) if they are heteromeric, or only α subunits (α7 through α10) if they are homomeric.[154,155]

**nAChR Structure**

The nAChR is a pentameric, integral membrane protein with a subunit molecular weight of approximately 250-270 kDa.[156] The amino acid sequence among subunits is considerably conserved, and they share a similar transmembrane topology: 1) a glycosylated N-terminal extracellular domain involved in agonist binding; 2) three short transmembrane fragments (M1, M2 and M3) connected to a fourth piece by an intracellular loop; and 3) a short extracellular C-teminal domain. It is believed that each M2 fragment folds into an α-helix followed by a loop. The five M2s (one from each subunit) are arranged to form the actual pore of the channel.[156] By electron microscopy it was possible to measure an outer pore diameter of approximately 25 Å (α-helix) that becomes ~ 7 Å in the interior of the channel (lower loop, Figure 5-2).[156] This narrow part of the ion channel provides selectivity towards the charge and size of the ions.

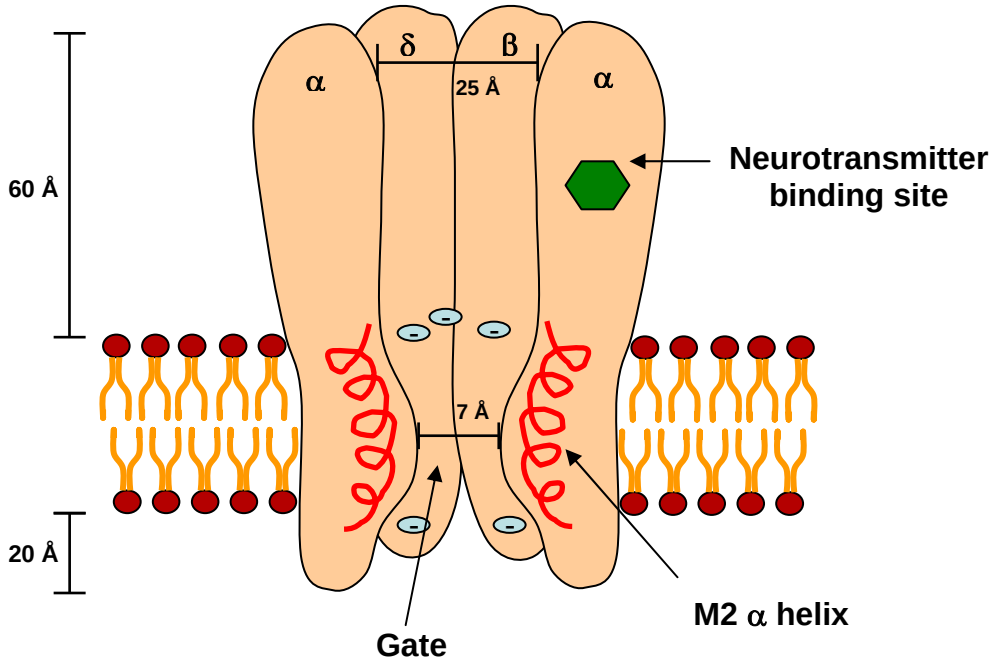


Figure 5-2. nAChR structure adapted from Lodish, H. F. and Darnell, J. E., *Molecular cell biology*; 3rd ed.[150]

Site directed mutagenesis and affinity labeling experiments support that the ion pore is organized by rings of amino acids which contribute to ion conductance.[154,157] First, the channel screens for cations with a ring of negatively charged residues like glutamate and aspartate, also found at the end of the channel. By studies with chloripromazin, it was found that the channel has two rings of serines and threonines in the middle region.[154] Finally, there are three more rings of leucines and valines that impart hydrophobicity to the pore. These residues may undergo an allosteric conformational change after acetylcholine binding, which make them twist and move away from the channel, allowing the passage of the cations.[158] Moreover, it was found that nAChRs permeability to positively charged ions increases when Leu251 is mutated to serine or threonine in nAChRs expressed in *Xenopus* oocytes.[157,159,160]

**Acetylcholine Binding Site**

Acetylcholine binds at the interface of the α subunit and an adjacent subunit. Based on the $\alpha_2$ stoichiometry of the channel, two molecules of neurotransmitter bind per oligomer (except for homopentamers like α7 that carry five acetylcholine-binding sites).[156] These two ACh binding sites do not neighbor each other and, even though both α-subunits are usually encoded by a single gene, they do not show exactly the same binding affinity for snake toxins.[154] The binding process is considered cooperative because the channel interaction with the first ACh increases the binding of the second. Acetylcholine-binding pockets are localized on the large N-teminus domain of the channel (Figure 5-2). It was observed that the binding site region is asymmetrically distributed, with a "principal section" on the α subunit and a "complementary section" on the neighbor subunits.[156] Studies on the electric organ and muscle nAChR revealed that the "principal section" of the binding site is constituted by a disulfide bridge of Cys192 and Cys193 and aromatic amino acids like Tyr93, Trp149 and Tyr190.[156,161] The "complementary

section" is constituted by residues including tryptophan, tyrosine and arginine.[156,161] From these experiments, it is observed that the nAChR contains a congregation of electron-rich aromatic residues on the ACh-binding site which are believed to stabilize the ACh quaternary ammonium positive charge. Specifically, an X-ray study of acetylcholinesterase from *Torpedo californica* suggested that the most potent cation-π interaction is given through the van der Waals contact between ACh quaternary ammonium and Trp84.[156]

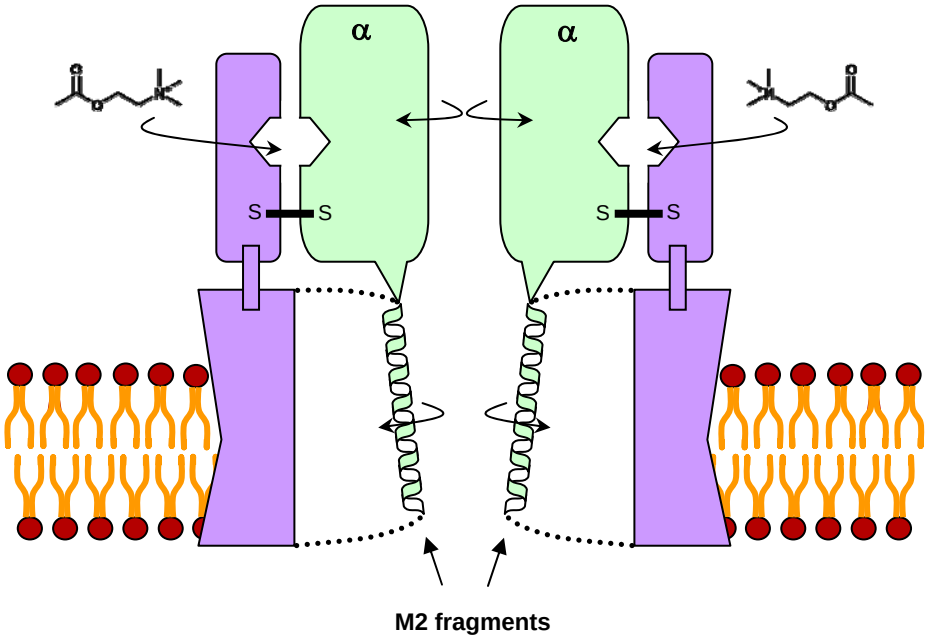


Figure 5-3. A model for acetylcholine induced gating of the nAChR receptor.The binding induces a twist on the α subunit that is transmitted to the M2 fragment. The M2 α helices assume a new conformation allowing the passage of ions. This figure was adapted from the article published by Miyazawa, A., Fujiyoshi, Y. and Unwin, N.[158]

More information about the acetylcholine binding site was obtained by electron microscopy of the electric organ membranes of the *Torpedo* electric ray and the snail acetylcholine binding protein (AChBP).[161] AChBP is a homopentameric protein, isolated from freshwater snail, and has a 26% homology with the N-terminus of the neuronal α7 nAChR. When the microscopy electron images of the nAChR from the electric ray were fitted by the AChBP β-sheet portion, it was observed that ACh binding induces a rotation of the α subunits β

barrels.[158] When this movement is transmitted to the M2 transmembrane fragment, the hydrophobic interaction among helices is disrupted and the channel becomes permeable to ions (Figure 5-3).[158] Despite the structural information briefly reviewed here, to our knowledge there does not yet exist even a single high resolution crystal structure of a pentameric nAChR suitable for the design of new agonists. Thus, as will be developed later in this chapter, structurally defined changes in known agonists, obtained through chemical synthesis, will be used to further probe the basis for agonist binding and the selectivity of agonists for one type of nAChR over another.

**Possible Roles of nAChRs in Human Diseases**

It is known that nAChR are involved in numerous inherited and acquired human diseases. Among the most common illnesses, myasthenia gravis (MG) is an autoantibody-mediated disorder in which the nicotinic receptor is the target of the antibodies.[151] The clinical manifestation is severe muscle weakness which is a consequence of reduced neuromuscular transmission. The diminution of postsynaptic currents is a result of the decrease in the number of nAChR arising from the autoimmune body response.[151] One of the treatments for MG includes immunosupresive drugs like oral antigens, but due to their lack of selectivity, they displayed generalized immunosuppression. Another choice for patients who have MG is plasma exchange, but there is a high risk of contracting transmitted diseases.[151]

A decrease in the number of nAChR is also observed in neurodegenerative diseases such as Alzheimer's (AD) and Parkinson's.[151,162] In the case of Alzheimer's, the pathology is showed by the lost of memory. For Parkinson's disease, the patient usually presents motor dysfunction and cognitive disorders. A major dimunition of nAChRs was observed in the cerebral cortex and hippocampus.[162] Different techniques, such as western-blot, immunohistochemical analysis or/and radiolabeled ligand binding, have helped to identify the primary nAChR subtypes

compromised in these diseases. Based on these analyses, the most affected nicotinic proteins are α7 and α4β2 subtypes.[162] Unfortunately, the exact mechanism that accounts for this loss still remains unclear. Until today, the main treatment utilized for AD is the administration of acetylcholinesterase inhibitors. These agents prevent the hydrolysis of ACh, resulting in a higher level of the neurotransmitter at the postsynaptic neuron terminal, which could compensate for the loss of brain cells. But their action was shown to be only temporary, losing their therapeutic effect at later stages on the disease. The discovery of agonists selective for α7 and α4β2 receptors has become one of the current challenges for the scientific community. Nowadays, GTS-21 (Figure 5-8) is under clinical trial for AD disease.[162,163]

Another typical neurological disease is schizophrenia.[151] Once more, the pathology affects primarily the α7-nAChR and in lesser extent the α4β2 subtypes. Some typical manifestations of this disease include auditory gating insufficiency and unpredictable eyes movements. Schizophrenics are not able to filter repeated auditory stimuli in the brain which could be reflected in their lack of concentration and hypervigilance. Nicotine helps to normalize the auditory response by stimulating the hippocampus cholinergic system. As a result, schizophrenic patients have a higher tendency to smoke that a normal person because they utilize the cigarette's nicotine as a self-medication.

**nAChR Ligands**

Several potent agonists and antagonists for the nAChR have been found so far, among them, α-bungarotoxin (α-Btx) from krait *Bungarus multicinctus* is an antagonist that binds tightly to muscle nAChR and α7-nAChRs.[151] This 76 amino acid peptide has been used for labeling experiments and purification of the receptor.

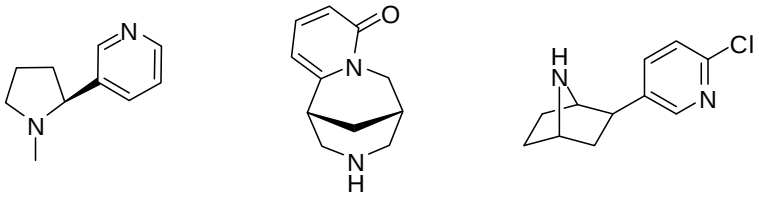

Nicotine Cytisine Epibatidine

**Agonists**

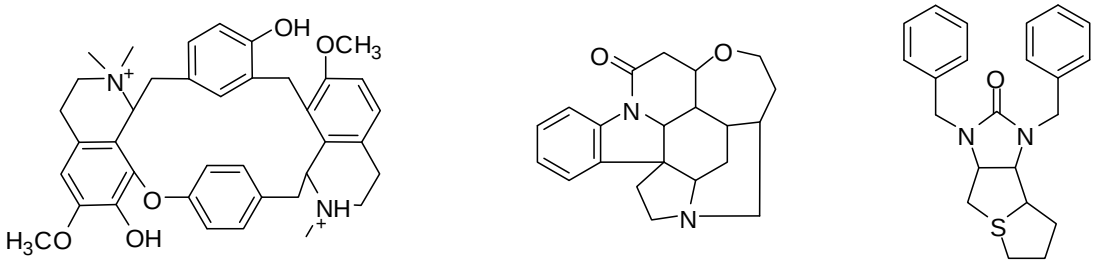

Tubocuranine Strychnine Trimethaphan

**Antagonists**

Figure 5-4. nAChR ligands[151]

Other examples are the curare alkaloids such as, tubocurarine and toxiferine (Figure 5-4). These compounds are nAChR antagonists and are known to be used as muscle relaxants.[151] Moreover, epibatidine an agonist alkaloid extracted from the Ecuadorian poison frog *Epipedobates tricolor*, has served to induce analgesia and has a high affinity for different neuronal nAChRs (Figure 5-4).[151,164] Another class of alkaloids that have high affinity for the α4β2-nAChR but low affinity for the α7 is nicotine and cytisine (Figure 5-4). With the help of radioligand binding and the numerous nAChR agonists and antagonists discovered, it is possible to define a pharmacophore for these ion channels. A pharmacophore is the minimal 3D arrangement of essential functional groups necessary to be recognized by the receptor.[151,165] These functional groups could be a particularly defined point (an atom) or a point of interaction

on the molecule, for example, a hydrogen-bond donor or acceptor. A number of groups have proposed different pharmacophore models, one of the first ones was presented by Barlow and colleagues where they considered that an onium feature is required and a flat hydrophobic area, at 4.5-6.5 Å from the onium point is necessary for activity.[166] After studying several nicotine analogs, it became evident that the position of the pyridine nitrogen atom was contributing in some way to receptor binding.[167] However, there are examples in the literature of compounds that still retain receptor affinity after the pyridine nitrogen is substituted by a carbon.[167] The Beers-Reich/Sheridan models suggested that the nAChR pharmacophore is defined by 3 points within the molecule.[168] By using different nicotinic agonist and antagonists like cytisine, strychnine, nicotine and trimethaphan (Figure 5-4), the first point, A, is given by the coulombic interaction between the quaternary (charged) nitrogen of the molecules and the receptor (Figure 5-5). The second point, B, will be the π-bonded electronegative atom that provides a hydrogen bond interaction. The distance between point A and B is at approximately 5.9 Å base on the Beer-Reich model or 4.8 Å based on Sheridan model. Finally, point C is identified as the other end of the local dipole moment set up by point B (for example C will be the carbon of a carbonyl group, Figure 5-5).[151,165,167,168]

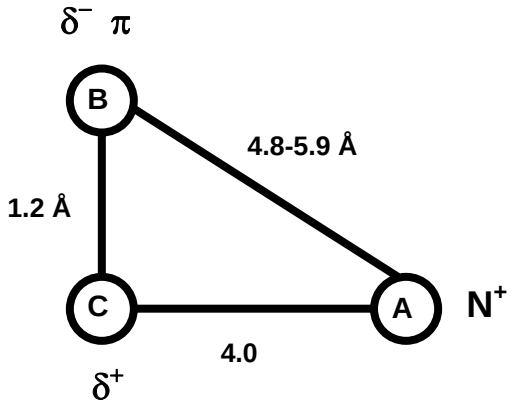


Figure 5-5. Pharmacophore representation adapted from the article published by Barrantes, F. J.[151]

However, it was observed by comparison of several nAChR agonists and antagonist that there is not a unique way of binding. Consequently, it became apparent that systematic structural changes on the molecules tested did not always result in the expected parallel affinity response on the receptor.[167] Moreover, it was found that choline and tetramethylammonium are also efficient agonists for α7 receptors which reduces the minimum pharmacophore structure to a quaternary nitrogen (Figure 5-6).[169] Based on these observations, it can be concluded that the point of hydrogen bond interaction is not a requisite for nAChR activation but it may be seen as a center that could provide binding affinity.[167]


Choline Tetramethylammonium

Figure 5-6. Other nAChR agonists[169]

**Anabaseine and Derivatives**

Anabaseine, a paralyzing toxin found in certain marine worms and ants, is a heterocyclic molecule related to nicotine (Figure 5-7).[170]

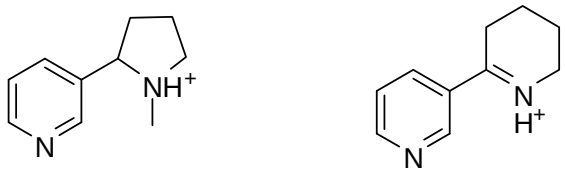


Nicotine Anabaseine

Figure 5-7. Nicotine and Anabaseine structures

Even though this compound displayed activity on several nAChR, it has a potent efficacy and affinity as agonist upon α7 nAChRs ($K_i$ of 58 nM and $EC_{50}$ 6.7 μM for rat α7) compared with nicotine ($K_i$ of 400 nM and $EC_{50}$ 47 μM for rat α7).[171] Although, nicotine and anabaseine share the common feature of having the positively charged ring nitrogen, these molecules differ

in the relative orientation of the pyridyl ring with respect to the ring bearing the charge. While the two rings of anabaseine are coplanar, because of the conjugation of the imine functionality with the pyridyl ring, the saturated ring of nicotine is twisted approximately 90° with respect to the aromatic ring (Figure 5-7). This structural difference may be reflected in their different mode of action against the nAChR subtypes.[171]

After discovering that neuronal α7-nAChR may be involved in neurodegenerative diseases like Alzheimer's,[162] the study of the possible therapeutic applications of anabaseine attracted the interest of numerous research groups. Several anabaseine derivatives have been synthesized and tested in order to identify nAChR subtype selectivity and reduce the toxicity of the parent compound.[172-175] One of these derivatives was 3-(2,4-dimethoxy)benzylidene-anabaseine (GTS-21) (Figure 5-8).

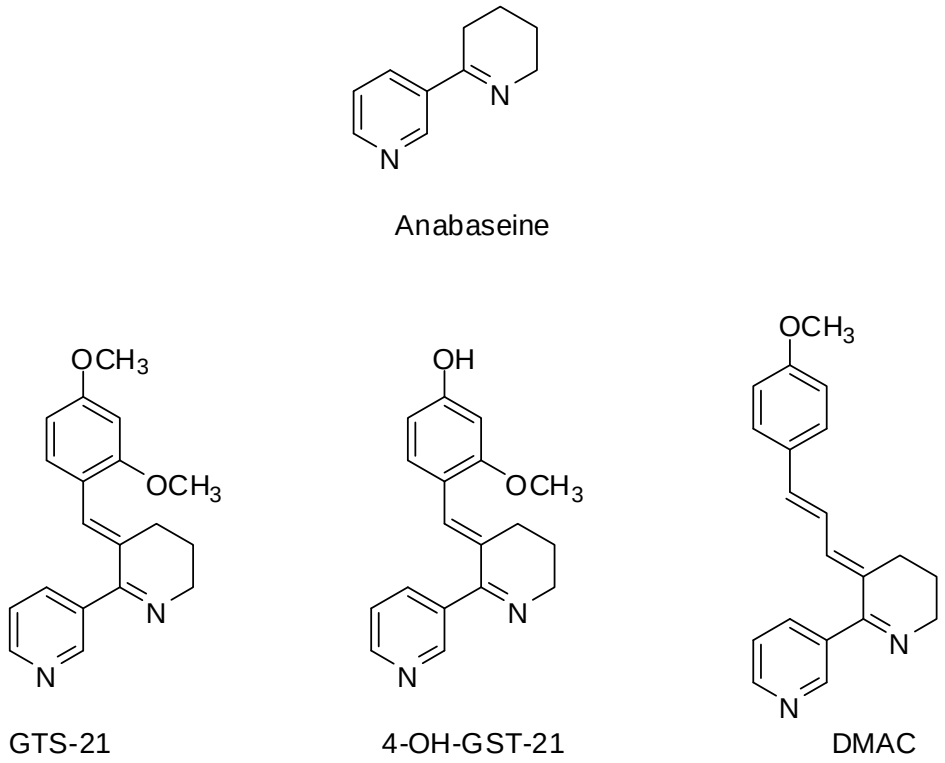


Figure 5-8. Anabaseine derivatives

Although this compound showed partial agonist selectivity for α7-nAChR, improving memory related behavior in primates and rodent species, it was much less efficient on human α7 receptor when it was compared with the parent agonist anabaseine.[163] The receptors dissimilar response to these two compounds may be a result of a specific interaction with the benzylidene ring.[175] Moreover, GTS-21 showed a α4β2 antagonist behavior when tested on rat receptors,[172] which could be a demonstration of the greater tolerance of agonist structure of the α7 towards activation when compared with α4β2. A different explanation to this antagonist action towards the receptor could be through channel blockade. When molecules of GTS-21 open the channel, additional binding of this compound to the receptor could cause the obstruction.[172] Another benzylidene anabaseine (BA), 4-OH-GST-21, displayed around 10 fold greater efficacy against both rat and human α7 receptor than for the nAChR constituted with β subunits (Figure 5-8).[163,176] Interestingly, 4OH-GST-21 is one of the main metabolites of GST-21 and is the first α7-nAChR agonist to exhibit cytoprotective activity on human cells.[163]

Another anabaseine derivative, 3-(4-dimethylamino) cinnamylidine (DMAC) (Figure 5-8), that has been studied by De Fiebre *et al.* showed very potent selective agonist activity of the rat brain α7-nAChR.[172] This compound bound to the receptor with a $K_i$ of 33 nM exceeding the potency of GTS-21 on this subtype of receptor.[172] Further, DMAC displayed an extremely poor agonist action not only on α4β2 but also on α4β4, α2β2, and α3β2.[172]

BA derivatives are considered to have two elements for receptor activation, the anabaseine center, which gives the nAChR recognition site to the molecules, and the benzylidene or cinnamylidene center, which might provide the selectivity for α7 subtype.

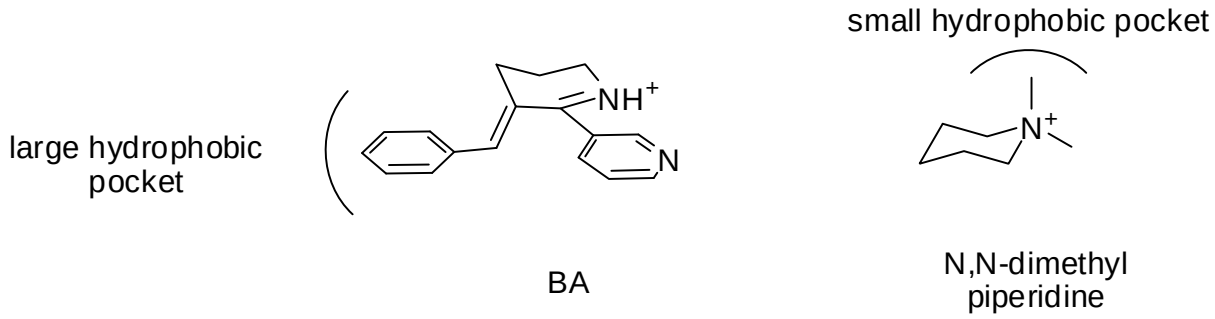


Figure 5-9. Proposed α7-binding pockets that confer selectivity

Nevertheless, in addition to this hydrophobic structural motif that imparts selectivity for the α7-nAChR, it has been found that the simple N,N-dimethyl piperidine is also selective towards this neuronal receptor.[177] Based on this experimental result, it was believed that another distinct hydrophobic pocket may be present nearby the quaternary nitrogen (Figure 5-9).

In the past few years, new kinds of nAChR agonists have been synthesized where a quinuclidine core structure is used for receptor activation. Among these compounds, the spirooxazolidinone (AR-R17779) (Figure 5-10) turned out to be the first full and most selective agonist reported for rat α7-nAChR.[178] This agonist displayed a great selectivity for rat α7-nAChR ($K_i$ of 92 nM) expressed on *Xenopus oocytes* but low when compared with α4β2 nicotinic receptor ($K_i$ of 16000 nM).[178] It has been noted though, that small structural changes on AR-R17779 provoked a drastic decrease of the α7 receptor affinity.[178]

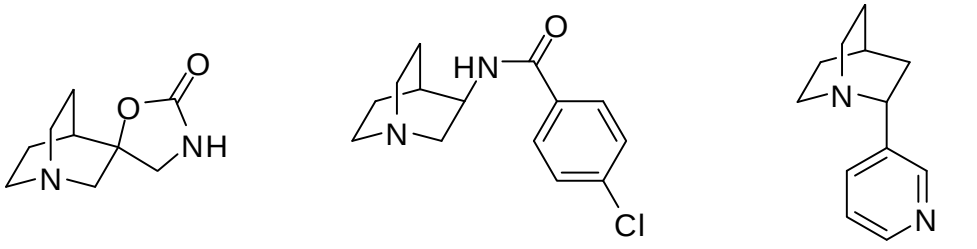


Figure 5-10. Compounds with quinuclidine core that are α7 selective agonists

Other two members of the quinuclidine nAChR-agonists family are TC-1698[179] and the 4-chlorobenzamidine PNU-282987[180] (Figure 5-10). From the PNU-282987 studies, it could be concluded that para-substituted benzamidines were the most potent, and the ortho substitution the worst.[180] It was also noticed that only the analogues that contained small substituents (chloro, fluoro, methoxy) on the para position were among the most potent.[180] A similar response for the α7-nAChR was found when TC-1698 was tested by Bencherif *et al.*.[179] This molecule displayed very low or no agonist effect when it was applied on the β-subunit-containing nAChR α4β2, α3β2, and α1β1εδ nicotinic subtypes.[179]

In order to find a better α7-nAChR agonist candidate, the quinuclidine and quinuclidinone core structures were utilized as a starting material for a new class of α7 analogs. With these kind of compounds it is possible not only to search for a novel therapeutic agent, but also to study the hypothesis of the dual hydrophobic motif present on α7 subtype of nicotinic receptors (Figure 5-11). This will be performed by incorporating aryl groups that will look like the BA α7-nAChR series or alkyl functionality that will resemble dialkyl piperidines. Something important to notice is that these compounds will not have the pyridyl H-bond acceptor present in anabaseine derivatives, a feature already noted as lacking in some α7 selective agonists.

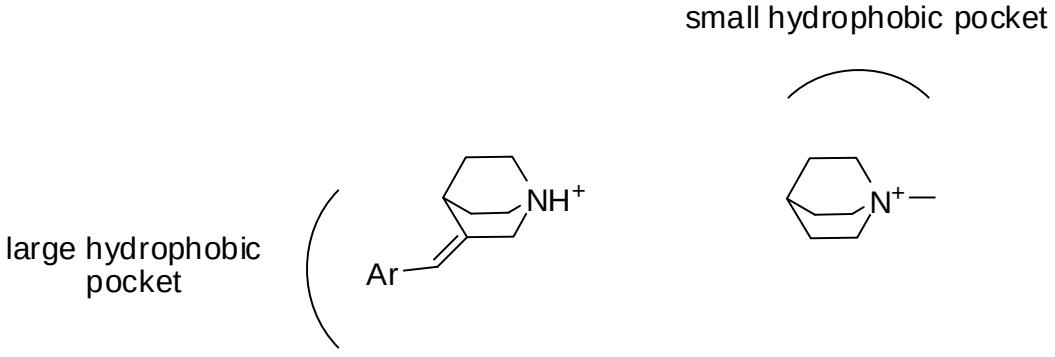


Figure 5-11. Proposed 3-arylidine and N-alkyl quinuclidines

## Results and Discussions

### Synthesis of Quinuclidine and Quinuclidinone Derivatives

Compounds **74** and **75** were synthesized and tested to study their selectivity as agonists of neuronal α7 and α4β2 nAChRs (Figure 5-12). To the best of our knowledge, surprisingly little has been reported regarding one step 3-benzylidene quinuclidine syntheses,[181] though olefination via organometallic additions to 3-quinuclidinone and dehydrative eliminations are known.[182] We envisioned a straightforward synthesis of the 3-benzylidine analogs of quinuclidine via Wittig-type olefinations and report the results of these studies.

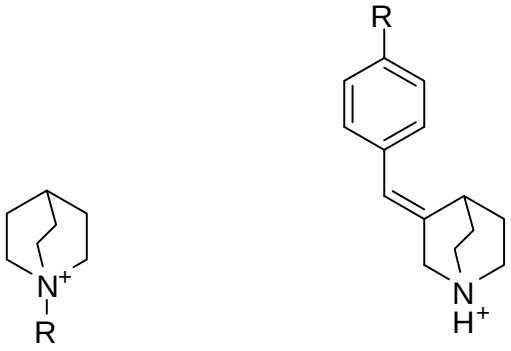


**74** a R= Me
b R= Et

**75** a R= H
b R= OMe

Figure 5-12. Target quinuclidines α7 agonists

Alkylation of quinuclidine hydrochloride with methyl or ethyl iodide in methanolic solution in the presence of $K_2CO_3$ afforded N-methyl and N-ethyl quinuclidines **74a** and **74b** in 99% and 90% yields, respectively (Figure 5-13).[183,184]

This method to quaternize amines is extensively used due to its selectivity, mild reaction conditions and high yields obtained. The desired compounds were obtained from the organic filtrate without needing further purification.

An initial attempt to synthesize 3-benzylidene quinuclidine **75a** utilized the Wittig[185,186] reaction between 3-quinuclidinone hydrochloride and the ylid derived from treatment of triphenyl benzyl phosphonium iodide with n-BuLi. Firstly, two equivalents of n-BuLi, one to deprotonate the amine and the second to form the ylid, were used, but base on $^1$H NMR spectroscopy no formation of the double bond was observed and quinuclidone was left unreacted. Then, the same reaction was performed on the free base quinuclidone. Unfortunately, only an 8% yield of an E/Z mixture of **75a** was obtained, with ~30% conversion of the starting 3-quinuclidinone based on $^1$H-NMR analysis of the crude reaction mixture. Based on this result, it was considered that the acidity of the 2-position in 3-quinuclidinone required a less basic olefination reagent.

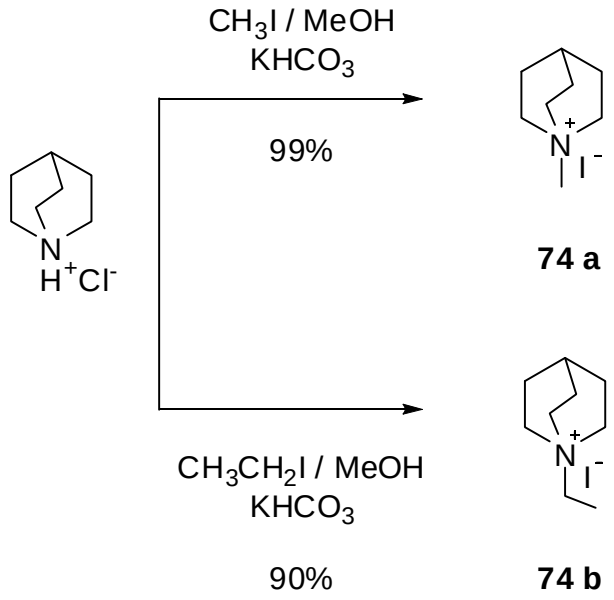


Figure 5-13. Alkylation of quinuclidine hydrochloride

Benzyl phosphonates were utilized in the Wadsworth-Emmons reaction to provide more satisfactory yields.[187] In this case, diethyl benzyl phosphonate for Z/E-**75a** and diethyl-4-methoxy benzyl phosphonate for Z/E-**75b** were used as olefination reagents (Figure 5-14). The best solvent for this reaction was found to be 1,2-dimethoxy ethane (DME).[188] Chromatographic

separation of the geometric isomers proved to be difficult, not only because the two isomers had very similar $R_f$ but also, because other amine containing side products were coeluting with the desired compounds. A variety of binary and ternary systems failed to provide a clean separation in a single step. After two successive chromatographic steps on silica in $CHCl_3$/MeOH/$Et_3N$ mixtures, the two isomers were obtained in pure form, providing **75a** in 46% yield[184] (Z:E ratio, 2:1). Compound **75b** was obtained in 23% yield with a Z:E ratio of 7:1 after chromatographic purification.[184]

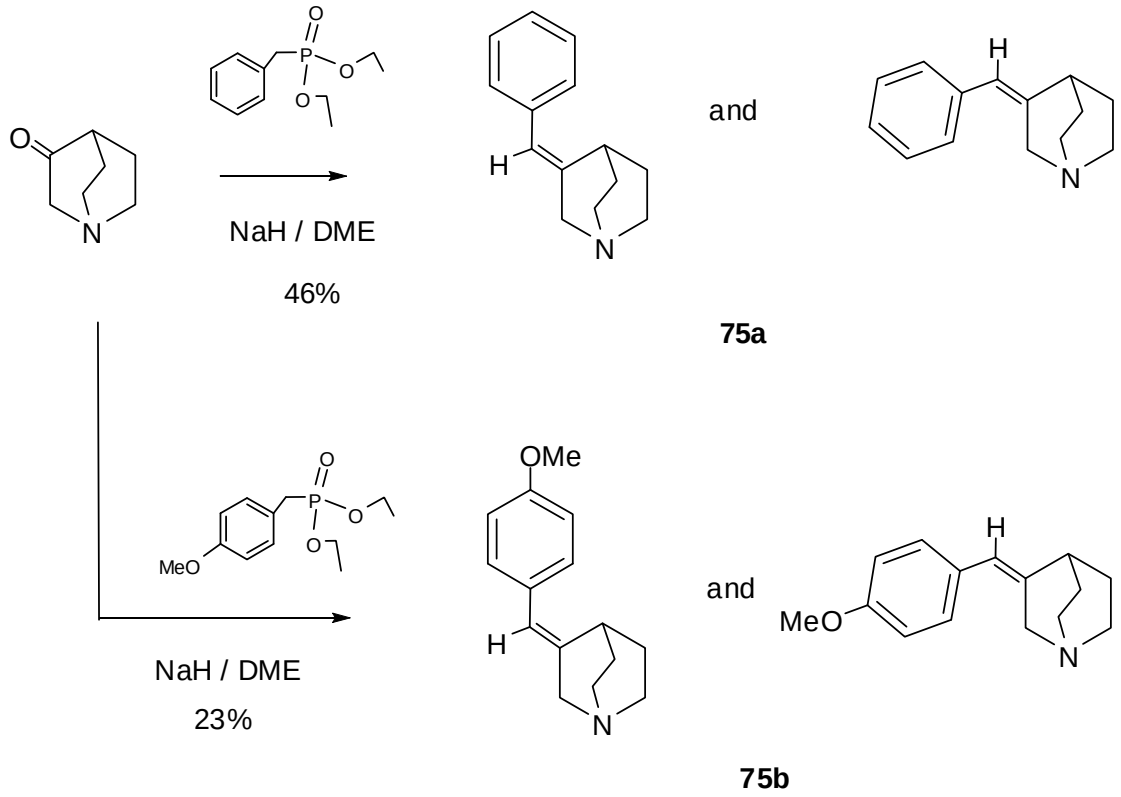


Figure 5-14. Synthesis of benzylidene quinuclidines

The olefin geometry for each isomer was unambiguously established based on analysis of NOESY spectra and analysis of chemical shifts (Figure 5-15). The NOESY spectrum for Z-**75b** revealed crosspeaks for interactions between $H_2$-$H_6$, and $H_4$-$H_5$. The E-isomer of **75b** presented a complementary set of data, with crosspeaks corresponding to interactions between $H_2$-$H_5$ and

$H_4$-$H_6$. The NOESY spectrum of Z-**75a** displayed crosspeaks for interactions between $H_2$-$H_6$, and $H_4$-$H_5$ as was observed for Z-**75b**. Finally, characteristic chemical shifts were identified for $H_2$ and $H_4$ depending on the isomer in question. Thus, for the E- isomers of **75a**,**b**, the chemical shift of $H_4$ was found downfield relative to the shift for $H_4$ of the Z-isomers, while in the case of the Z-isomers, $H_2$ was shifted downfield relative to the chemical shift of $H_2$ in the E-isomers. These effects may be attributed to deshielding from the phenyl ring.[184]

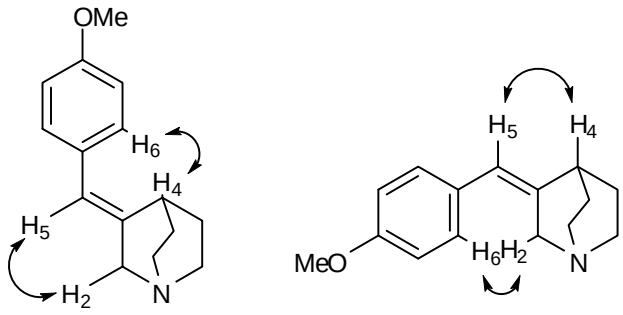


**E-75b** **Z-75b**

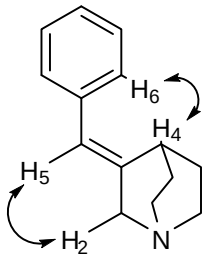


**E-75a**

Figure 5-15. NOE enhancements for assignment of olefin geometry of **75a** and **75b**

Finally, both benzyl quinuclidones were converted to their corresponding hydrochloride salts in order to improve their solubility in aqueous solution to facilitate their subsequent testing with nicotinic receptors.

With the purpose of further investigate the hypothesis of the dual hydrophobic pocket present in neuronal nAChR, Z and E-**75a** were N-methylated utilizing the method previously

described for the quinuclidines. The Z-N-methyl-**75a** was obtained in a 62% yield while the E isomer was isolated in a 94% yield (Figure 5-16).

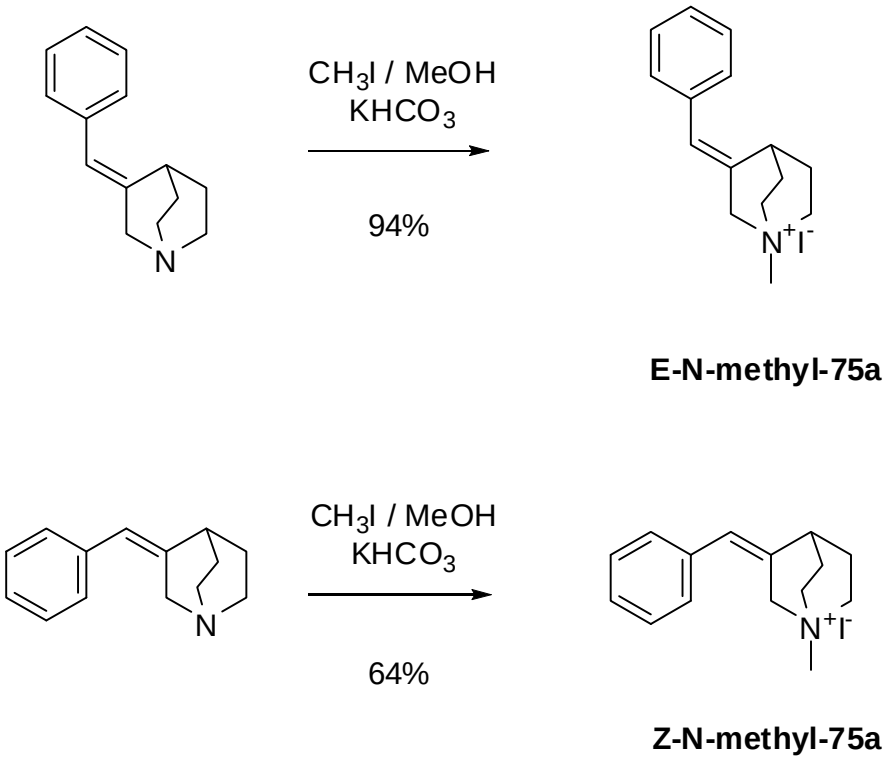


Figure 5-16. Methylation of Benzylidene quinuclidines

Furthermore, OH-Z-**75b** was synthesized by dealkylation reaction of Z-**75b**. This reaction could have been done by treating the methoxybenzylidene quinuclidone with trimethylsilyl iodide (TMSI).[189] In our case, TMSI was prepared from trimethylsilyl chloride and KI. This crude mixture was added to Z-**75b** but after leaving the reaction for 72 h at room temperature only unreacted Z-**75b** was observed by $^1$H NMR. Another conventional method to cleave the ether functionality is by using $BBr_3$[190-192] as a Lewis acid and performing the reaction at -60 °C under nitrogen atmosphere. Unluckily, $^1$H NMR and TLC characterizations of the crude mixture revealed the presence of a very complex mixture of products, leading to the abandonment of this synthetic route.

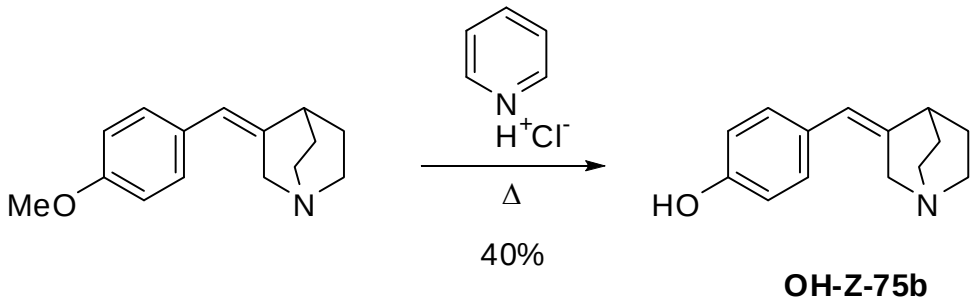


Figure 5-17. Methoxy Benzylidene quinuclidine demethylation

The desired OH-Z-**75b** was finally obtained when Z-**75b** was heated at 190 °C in the presence of pyridinium hydrochloride for 2 h.[193,194] After purifying the amine by flash column chromatography, OH-Z-**75b** was acquired in 40% yield (Figure 5-17). Unfortunately, neither Z or E-N-methyl-**75a** nor OH-Z-**75b** were tested for α7 and α4β2 nAChRs possible agonist activity. In both cases, the quantities and purity in hand were unsatisfactory to perform a reliable binding response experiment on the nicotinic ion channels.

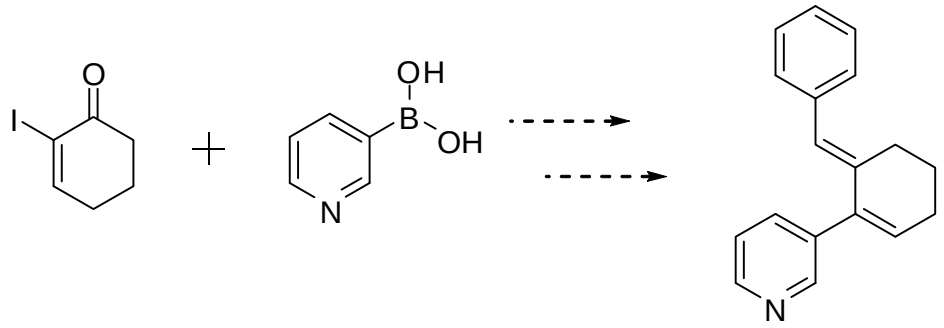


Figure 5-18. Proposed synthesis for BA analog **78**

With the observation that BA compounds can show considerable potency and efficacy for α7 activation, we considered the possibility that perhaps the hydrophobic group and its relative position in the tricyclic molecule might be sufficient in itself to produce receptor activation. Hence, compound **78** (Figure 5-18) was identified as a synthetic target. It lacks the ammonium

pharmacophore, but it otherwise identical to BA. In our attempts to synthesize this deaza BA analog (Figure 5-18), 2-iodocyclohex-2-enone was required as a precursor for the subsequent Suzuki coupling with pyridine boronic acid. This cyclohexenone was prepared by α-iodination of 2-cyclohexanone following Johnson's method but using DMAP as the base catalyst (Figure 5-19).[195,196] The α-iodoketone **76** was obtained in a 69% yield after chromatographic purification. The signals observed in the $^1$H NMR were consistent with the literature.[197]

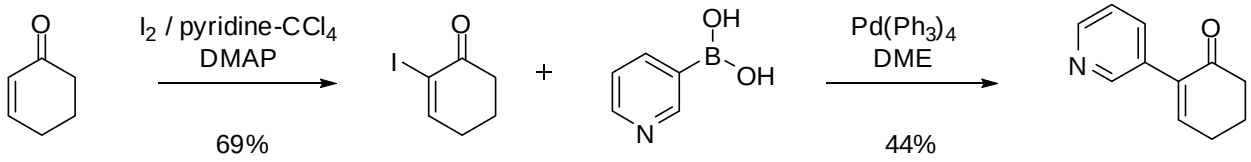


**76** **77**

Figure 5-19. Synthesis of α-pyridyl cyclohexenone **77**

Afterward, α-pyridyl cyclohexenone **77** was synthesized by the cross-coupling reaction known as Suzuki-Miyaura.[198] This reaction is one of the most used methods for carbon-carbon bond formation at sp2 centers. The reaction proceeds through conjugation of a haloalkene or haloalkynes with an arylboronic acid. Palladium catalysts are known to give the best results in this kind of reactions. Among them, the tertiary phosphines ligands are the most popular,[199] but recently, Felpin's research group observed that heterogeneous catalysis with Pd(0)/C could also produce coupling products in very good yields.[200] Initially, the heterogeneous Pd(0)/C Suzuki coupling was chosen for the synthesis of **77**. The previously prepared 2-iodocyclohex-2-enone and pyridine-3-boronic acid were utilized as vinyl halogen and aryl sources. In this case, the formation of the product was almost undetectable by $^1$H NMR. Under otherwise identical reaction conditions, Pd(0)/C was replaced with $Pd(Ph_3)_4$. Once again, the coupling reaction did not produce the desired product, leaving a large amount of unreacted α-iodoketone. In our case, the conditions that gave the best results were when $Pd(Ph_3)_4$ was first complexed with the

iodonone for 10 minutes, followed by the sequential addition of pyridine boronic acid and aqueous $Na_2CO_3$.[199] The product **77** was obtained as yellowish crystals in 44% yield.

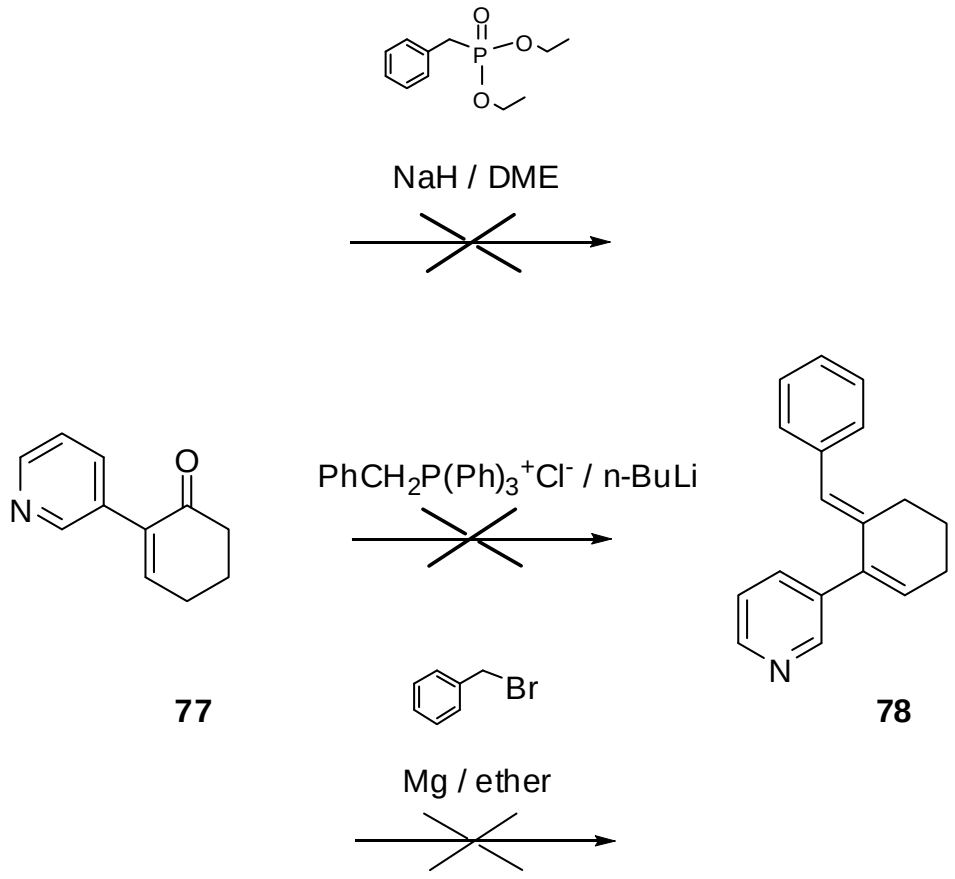


Figure 5-20. Synthesis route A for compound **78**

The first attempt in the synthesis of **78** utilized Wadsworth-Emmons reaction conditions already used for **75a** and **75b** (Synthesis route A (Figure 5-20)). The 2-pyridylcyclohexenone **77** was treated with diethyl benzyl phosphonate using NaH as the base. Analysis of the crude mixture by $^1$H NMR did not show evidence of either new double bond formation or pyridine hydrogen peaks. In a second effort to make this compound, triphenyl benzyl phosphonium chloride was used as the Wittig reagent precursor, but again, the reaction did not result in the desired product (Figure 5-20). The corresponding benzyl bromide Grignard reagent was prepared in a final attempt to produce this compound via the Synthetic route A. From the chromatographic

purification of the crude mixture a promising fraction was obtained. Unfortunately, the compound of interest was not present in the fraction mixture by analysis of the $^{1}$H NMR. One hypothesis for why this scheme was troublesome would be that deprotonation of the basic cyclohexenone γ-hydrogens was occurring with use of the relatively basic benzylidenating reagents discussed above. Thus, a new synthetic route was pursued. Based on the literature, conjugated dienes have been prepared by the reaction of an epoxide and the appropriate aldehyde or ketone in presence of tributylphosphine (Figure 5-21).[201]

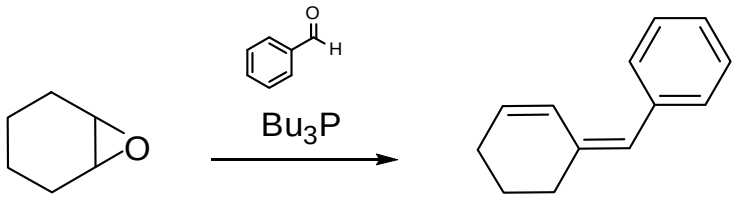


Figure 5-21. Example of the synthesis of conjugated dienes through an epoxide

In order to test this possibility, 3-cyclohexenylpyridine **82** was chosen as the epoxide precursor (Synthesis route B (Figure 5-22)). Unfortunately, efforts thus far at synthesizing **82** have been unsuccessful. First, 3-bromopyridine **79** was metallated with n-BuLi, and used for a carbonyl addition reaction with cyclohexanone. Despite spectroscopic evidence for the cyclohexanol intermediate in the crude product, attempts to dehydrate the crude mixture were unfruitful. Finally, it was believed that the Suzuki coupling between pyridine-3-boronic acid **80** and 1-chlorocyclohexene **81** could be the solution to the problem in hand (Figure 5-22). Unfortunately, this vinyl halide is not commercially available and attempts to synthesize this compound were unsuccesful. A third possibility, as yet untested might be to deoxygenate compound 77, above, via reduction of the corresponding thioketal.

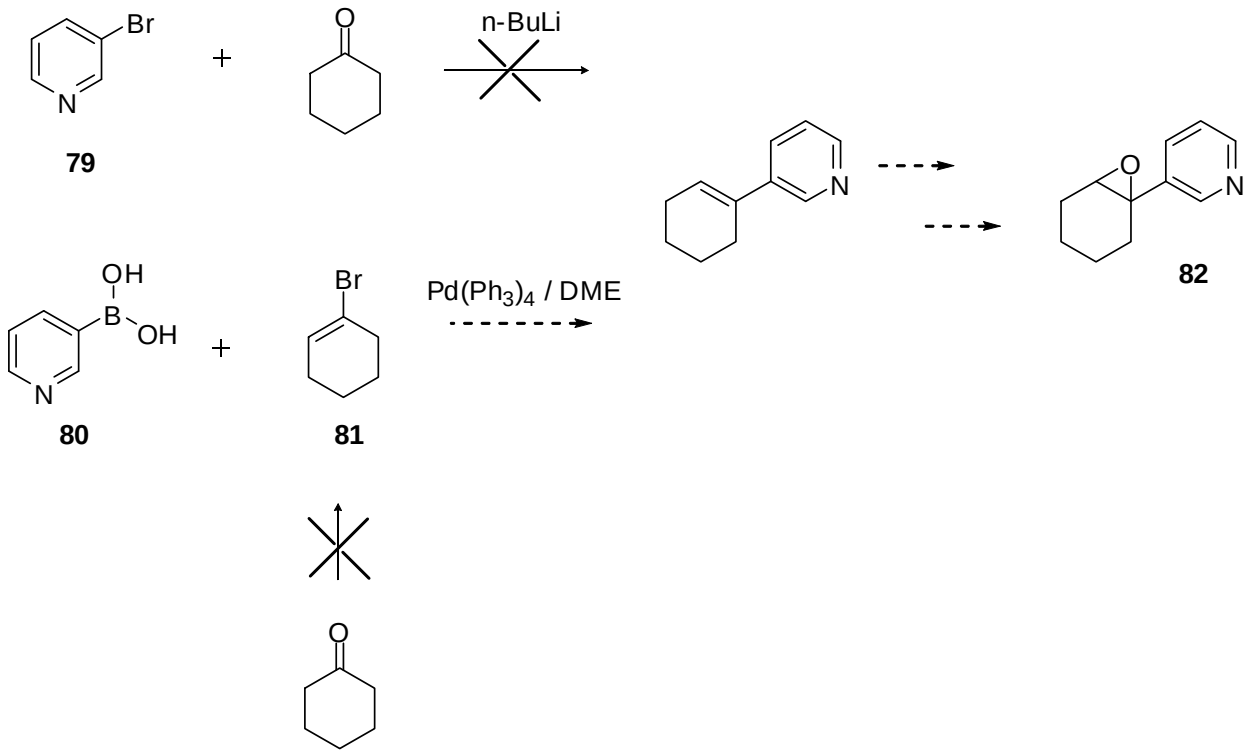


Figure 5-22. Proposed Synthetic route B for 3-cyclohenenylpyridine **82**

**Electrophysiological Evaluation of New Compounds**

*Xenopus* oocytes expressing mRNAs corresponding to α7, α3β4, or α4β2 subunits of nAChRs[177] were used by Dr. Roger Papke's group (UF Department of Pharmacology) to determine agonism of compounds **74a,b** and **75a,b**. The reference agonist was acetylcholine, applied at 300 μM, which produces a maximal channel current at this concentration. It was found that E-**75a** and E-**75b** were α7 selective partial agonists ($E_{max}$ ~ 40%) with respective $EC_{50}$'s of 1.5 and 1.3 μM. By comparison, 4OH-GTS-21 has an $EC_{50}$ of approximately 5 μM for human α7 and an $E_{max}$ of about 40% the maximum response produced by the full agonist ACh.

Compound **74a** was an α7-selective full agonist with an $EC_{50}$ of 40 μM, and the data for **74b** suggested it was a weak α7 selective agonist, but receptor-independent currents were observed upon application of the compound to oocytes making detailed interpretation of this

compound's activity difficult. Compounds E-**75a,b** and **74a,b** were tested in co-application experiments to see if they antagonized the activation of α3β4 or α4β2 receptors by ACh. When tested at a concentration of 10 μM, co-applied with ACh, E-**75b** produced a transient inhibition of the α3β4 receptor of approximately 50%, but otherwise there appeared to be no significant antagonist actions for the quinuclidine compounds at that concentration.

In summary, the results of these experiments are consistent with the proposed model for selectivity of α7 agonists, showing that selectivity and activity may be obtained with molecules possessing a charged nitrogen and suitable hydrophobic residue. It was believe the $EC_{50}$ values indicate that the binding site for the aryl group is tolerant of substitution and therefore amenable to further development of agonists. Further details of the biological activity of these and other quinuclidine compounds will be reported elsewhere.

## Experimental Section

**General Methods.** Solvents and reagents were purchased from Aldrich Chemical Company and Acros Organics. The organic solvents were dried overnight over $CaH_2$ or 4 Å molecular sieves and freshly distilled before use. NMR spectra were obtained using VXR 300, Gemini 300 and 500, or Mercury 300 and 500 MHz spectrophotometers in appropriate deuterated solvents. Mass spectra were obtained on a Finningan MAT 95Q spectrometer operated in FAB, CI, ESI or EI modes.

**1-methyl-1-azoniabicyclo[2.2.2]octane iodide 74a.**[183] A mixture of methyl iodide (0.54 mL), $KHCO_3$ (0.34 g) and quinuclidine hydrochloride (50 mg) was stirred in methanol at room temperature for 12 h. Then, solvent was evaporated and $CHCl_3$ was added and stirred overnight. The mixture was filtered and solvent evaporated under vacuum giving methyl quinuclidine as a white solid in 99% yield (85 mg). The solid started to decompose at temperatures greater than

230 °C. $^{1}$H NMR ($D_2O$) δ ppm 1.96 (m, 6H), 2.17 (m, 1H), 2.90 (s, 3H), 3.37 (t, 6H),$^{13}$C NMR ($D_2O$) δ (ppm) 57.4, 52.3, 23.9, 19.1. EI Calcd for $C_8H_{16}IN$ $(M-I)^+$: 126.1277, found: 126.1286.

**1-ethyl-1-azoniabicyclo[2.2.2]octane iodide 74b.**[183] This compound was synthesized by the same procedure explained above using 0.55 mL of ethyl iodide. The reaction gave the ethyl quinuclidine as a white solid in a 90% yield (81 mg). The solid started to decompose at temperatures greater than 210 °C. $^{1}$H NMR ($D_2O$) δ ppm 1.30 (t, 3H), 1.99 (m, 6H), 2.20 (m, 1H), 3.21 (q, 2H), 3.38 (t, 6H),$^{13}$C NMR ($D_2O$) δ (ppm) 60.0, 54.5, 23.8, 19.5, 7.6. ESI-FT-ICR Calcd for $C_9H_{18}IN$ $(2M+I)^+$: 407.1918, found: 407.1921.

**3-benzylidene-1-azoniabicyclo[2.2.2]octane chloride 75a**. To a suspension of NaH (60% in mineral oil, 0.23 g, 5.8 mmol) in 1,2-dimethoxy ethane (DME) (6.4 mL) was added dropwise a solution of diethyl benzyl phosphonate (1.3 g, 5.8 mmol) in DME (2 mL) at room temperature under argon. After this addition, a solution of quinuclidone (0.41 g, 2.54 mmol) in DME (1.78 mL) was injected slowly. The reaction mixture was refluxed for 1.5 h. Then, the mixture was quenched carefully with water (30 mL) and DME evaporated under reduced pressure. The aqueous phase was extracted with $CH_2Cl_2$ (3 x 30 mL) and the organic layer dried over $MgSO_4$ and evaporated under vacuum. The crude oil was purified by flash chromatography on silica gel using $CH_2Cl_2$: MeOH: $Et_3N$ 20:1:0.1 as eluent system to give the Z isomer in a 30% yield (0.15 g) and E isomer in a 16% yield (81 mg).

The hydrochloride salts of these isomers were obtained by adding ether-HCl to a solution of the bases in a mixture of $CH_2Cl_2$/ether. Both isomers were obtained as white solids, which decomposed at temperatures above 200 °C.

The free base quinuclidone used in the preceeding syntheses was obtained by treating quinuclidone hydrochloride with a 2 M aqueous solution of $K_2CO_3$ (20 mL). Then, this solution

was extracted three times with ether (30 mL), dried over $MgSO_4$ and, the solvent was evaporated under reduced pressure.

For the Z isomer: $^1$H NMR ($CDCl_3$) δ ppm 2.06 (td, 4H), 2.78 (m, 1H), 3.28 (m, 2H), 3.33 (m, 2H), 4.15 (s, 2H), 6.45 (t, 1H), 7.17-7.37 (m, 5H), $^{13}$C NMR ($CDCl_3$) δ (ppm) 145.3, 137.7, 130.2, 128.8, 128.7, 126.5, 120.5, 56.9, 48.1, 27.5, 26.1. ESI-FT-ICR Calcd for $C_{14}H_{18}N$ $(M)^+$: 200.1439, found: 200.1423.

For the E isomer: $^1$H NMR ($CDCl_3$) δ ppm 2.06 (td, 4H), 3.39 (m, 5H), 4.05 (s, 2H), 6.48 (t, 1H), 7.19-7.36 (m, 5H),$^{13}$C NMR ($CDCl_3$) δ (ppm) 144.5, 137.6, 128.9, 128.7, 126.7, 122.0, 56.0, 47.9, 34.1, 28.1. ESI-FT-ICR Calcd for $C_{14}H_{18}N$ $(M)^+$: 200.1439, found: 200.1423.

**3-(4-methoxybenzylidene)-1-azoniabicyclo[2.2.2]octane chloride 75b.** These compounds were synthesized using the same procedure explained above. A suspension of NaH (60% in mineral oil, 0.87 g, 22 mmol) in DME (24 mL) was stirred at room temperature under argon. A solution of diethyl –4-methoxy benzylphosphonate (3.6 mL, 21 mmol) in DME (7 mL) was added dropwise to that solution. After this, a solution of quinuclidone as a free base (1.1 g, 9.0 mmol) in DME (6 mL) was added dropwise. The reaction mixture was refluxed for 1.5 h and quenched with water. The DME was evaporated under vacuum and the residue dissolved with dichloromethane and washed with water. Then, the organic layer was washed with brine and dried over $MgSO_4$.The mixture was purified by flash chromatography (silica gel, $CH_2Cl_2$:MeOH 35 :1). The two isomers where isolated as free bases giving the Z- isomer in 20% yield (0.41 g) and the E- isomer in 3% yield (61 mg).

For the Z isomer: $^1$H NMR ($CDCl_3$) δ ppm 2.10 (td, 4H), 2.80 (m, 1H), 3.31 (dt, 2H), 3.39 (dt, 2H), 3.83 (s, 3H), 4.19 (s, 2H), 6.42 (t, 1H), 6.88 (d, 2H), 7.08 (d, 2H),$^{13}$C NMR ($CDCl_3$) δ

(ppm) 159.3, 131.1, 130.0, 128.2, 125.2, 114.6, 55.7, 54.4, 47.1, 32.2, 25.3. EI Calcd for $C_{15}H_{19}NO$ $(M)^+$: 229.1467, found: 229.1475.

For the E isomer: $^1$H NMR ($CDCl_3$) δ ppm 2.04 (td, 4H), 3.35 (m, 5H), 3.82 (s, 3H), 3.99 (s, 2H), 6.40 (t, 1H), 6.91 (d, 2H), 7.11 (d, 2H),$^{13}$C NMR ($CDCl_3$) δ (ppm) 159.3, 131.1, 129.9, 127.9, 125.5, 114.4, 55.7, 54.7, 47.0, 24.7, 24.2. EI Calcd for $C_{15}H_{19}NO$ $(M)^+$: 229.1467, found: 229.1475.

**3-benzylidene-1-methyl-1-azoniabicyclo[2.2.2]octane iodide (N-methyl-75a).** A mixture of methyl iodide (16 mmol), $KHCO_3$ (10 mmol) and Z or E-benzylidene quinuclidones (1 mmol) were stirred in methanol at room temperature for 12 h. Then, the solvent was evaporated and $CHCl_3$ was added and stirred overnight. The mixture was filtered and solvent evaporated under vacuum. The Z isomer was obtained in a 64% yield (80 mg) and the E in a 94% yield (26 mg).

For the Z isomer: $^1$H NMR ($D_2O$) δ ppm 2.17 (m, 4H), 2.91 (m, 1H), 3.06 (s, 3H), 3.48 (m, 4H), 4.45 (s, 2H), 6.61 (s, 1H), 7.28-7.44 (m, 5H).

For the E isomer: $^1$H NMR ($D_2O$) δ ppm 2.14 (m, 4H), 3.11 (s, 3H), 3.39 (m, 1H), 3.58 (m, 4H), 4.27 (s, 2H), 6.55 (s, 1H), 7.30-7.49 (m, 5H).

**(Z)-4-(quinuclidin-3-ylidenemethyl)phenol (OH-Z-75b).** Pyridinium hydrochloride (0.13 g, 0.88 mmol) and Z-**75b** (29.8 mg, 0.13 mmol) were heated at 190 °C under argon atmosphere for 2 h. After the crude mixture was poured into an ice-cooled saturated solution of sodium chloride, the reaction was neutralized with a solution of 1 M ammonium hydroxide to pH 7-8 and extracted into $CH_2Cl_2$ (3 x 10 mL). The organic phase was dried over $Na_2SO_4$ and the solvent evaporated under vacuum. The crude product was purified by flash chromatography (silica gel, $CH_2Cl_2$:MeOH 9:1). The product was isolated as the free base (11 mg) giving the OH-Z-**75b** in a 40% yield.$^1$H NMR ($CDCl_3$) δ ppm 1.94 (m, 4H), 2.59 (m, 1H), 3.11 (m, 4H), 4.03 (s,

2H), 6.29 (s, 1H), 6.76 (d, 2H), 7.04 (d, 2H). EI Calcd for $C_{14}H_{17}NO$ $(M)^+$: 215.1310, found: 215.1292.

**2-iodocyclohex-2-enone 76.**[195,196] 2-cyclohexe-1-one (2.1 mL, 21 mmol) was dissolved in a mixture of 1:1 pyridine/$CCl_4$ (100 mL) and the solution was cooled to 0 °C. Then, a catalytic amount of DMAP (51 mg, 0.42 mmol) and iodine (13 g, 52 mmol) in pyridine/$CCl_4$ (1:1, 60 mL) were added. After stirring the mixture at room temperature for 24 h, the reaction was quenched with 50 mL of 20% aqueous $Na_2S_2O_3$ solution. The aqueous phase was extracted with ether (3 x 100 mL). The combined organic layers were dried over $MgSO_4$ and the solvent evaporated under vacuum. The crude was purified by flash chromatography (silica gel, petroleum ether:EtOAc 25 :1). The α-iodoketone (3.2 g, 69% yield) was obtained as a yellow oil.$^1$H NMR ($CDCl_3$) δ ppm 2.08 (m, 2H), 2.42 (q, 2H), 2.66 (t, 2H), 7.76 (t, 1H). The $^1$H NMR was consistent with the literature.[197]

**2-(pyridin-3-yl)cyclohex-2-enone 77.** Iodoenone (2 g, 9 mmol) was added to a suspension of $Pd(Ph_3)_4$ (0.31 g, 0.27 mmol) in dimethoxyethane (DME) (27 mL). After stirring this mixture for 10 min at rt, pyridine boronic acid (1.65 g, 13.5 mmol) dissolved in a minimum amount of EtOH followed by a 2 M aqueous solution of $Na_2CO_3$ (2.2 mL, 4.4 mmol) were added. The reaction was heated under reflux for 6 h. The crude mixture was diluted with 5% aqueous $Na_2CO_3$ and extracted four times with EtOAc. The collected organic extracts were dried with $MgSO_4$ and concentrated under reduced pressure. Purification of **77** by flash chromatography (silica gel, petroleum ether:EtOAc 2:1) gave 2-pyridylcyclohexenone (0.7 g, 44% yield) as yellowish crystals.$^1$H NMR ($CDCl_3$) δ ppm 2.13 (m, 2H), 2.59 (m, 4H), 7.11 (t, 1H), 7.27 (m, 1H), 7.98 (dt, 1H), 8.52 (d, 2H). $^{13}$C NMR ($CDCl_3$) δ (ppm) 197.7, 149.5, 149.4, 148.9, 137.6, 136.6, 132.5, 123.0, 39.1, 26.9, 23.1. EI Calcd for $C_{11}H_{11}NO$ $(M)^+$: 173.0549, found: 173.0564.

# CHAPTER 6
# CONCLUSIONS AND FUTURE WORK

This dissertation work has resulted in the synthesis of a new class of TS analogs for glycosidases and glycosyltransferases where the apical geometry of the leaving group is held over the plane of atoms that present the oxocarbenium charge mimicry, using an all *cis* trisubstituted cyclopropyl ring fused to a second amidine containing ring

The synthesis of the seven-membered ring diaza analogs was successfully accomplished in a relatively good overall yield following a short multistep pathway. The design of the synthetic route also allows the preparation of amidines with a variety of side groups attached. As already demonstrated in this work, this can be accomplished using the corresponding imidate derivative in the last step of the synthesis. Other amidines differing in the "nucleophile" moiety could then be tested for glycosidases inhibitory activity. Moreover, the portion of the analogs that mimic the departing leaving group might as well be modified by changing the substituent of the cyclopropane bridging oxygen. Alterations of these two features may help to improve the molecules inhibitory potency and/or to explore new enzyme-TS analogs binding contacts. This synthetic pathway might be suitable to obtain inhibitors for other enzymes. For example, substitution of the amidine's benzyl group with a small oligosaccharide might convert the compound into a TS analog for endoglycosidases which have several pockets for binding a long polysaccharide chain.

Although the amidines lacked the hydroxyl groups present in the sugars backbone that are known to facilitate favorable enzyme-substrate interaction, they still displayed $K_i$ values on the high μM range. Based on Bleriot *et al.*[37] results, the incorporation of hydroxyl groups on glycosidases TS analogs increased the inhibitory power of the molecule. Thus, the incorporation

of hydroxyl groups on future amidine designs should also be investigated in order to increase the binding interactions of these compounds.

With the exception of the chloromethyl amidine **29** (BnCMAM), all the diaza compounds presented a competitive mode of inhibition which was expected for a TS analog. Amidine **23** (BnHMAM) was the best inhibitor from the library of analogs with a $K_i$ of 150 μM against β-glucosidase from sweet almonds. Consequently, BnHMAM binds almost 25 times tighter to the enzyme than the substrate PNPβglu. This result may be an indication that the BnHMAM **23** shape resembles, in some way, the geometry of glycosidases TS. Only BnCMAM displayed a mixed or non-competitive mode of inhibition. This unpredicted result may be explained by a possible interaction of BnCMAM with other sites in the enzyme. Further kinetic experiments will be necessary in order to clarify this hypothesis. Moreover, it might be concluded that the analogs were selective for the β-glycosidases because none of the α glycosidases were significantly inhibited. The significance of this observation remains to be explored.

For the series of α(2→6)-ST TS analogs, the final step on these multi-step synthetic route involved conjugation of the molecules with CMP. Analysis of the coupling reaction of compound **33** and CMP by mass spectrometry and NMR proved the presence of CMP-amidine **73**. The desired compound was obtained with 95% purity after purification by reverse phase HPLC. The estimated $K_i$ for CMP-amidine **73** on human recombinant α(2→6)-ST was ~50 μM. This TS analogs inhibitory activity turned out to be comparable with the one displayed by free CMP and higher than those observed for previous generation scorpio inhibitors. The modest activity might be a reflection of the size of the amidine ring which could situate the amidine center in a less favorable position for binding with respect to the leaving group mimic.

The all *cis* trisubstituted cyclopropanes, synthesized during the course of this study, may also find use in other applications. For example, they could serve as chiral ligand frameworks for asymmetric catalysis that could provide enantiomerically enriched compounds. In addition, they could be utilized as building blocks for targeting other proteins such as G-protein-coupled receptors (P2Y).[202] An example of a known antagonist for this receptor is shown in Figure 6-1.

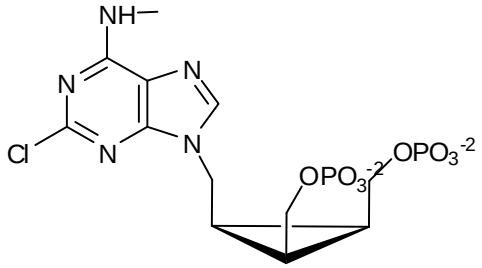


Figure 6-1. Antagonist for $P2Y_1$ receptor[202]

Finally, for the study of α7 nAChR agonists, quinuclidine and quinuclidinone derivatives were synthesized. By their agonist activity profiles, they supported the requirement for a charged nitrogen center but also, they supported the hypothesis that selectivity may be achieved with hydrophobic moieties having two very different sizes and spatial relationship with respect to the ammonium center. An ongoing work involves synthesis of functionalized tropanes to further investigate the selectivity filter of the α7 nAChR.

# APPENDIX A
# NMR SPECTRA FROM SYNTHESIZED COMPOUNDS

The NMR spectra of the synthesized compounds are shown in this Appendix. While the structure and number of the compound is shown in the spectra, the name of the molecule is described at the bottom of the page.

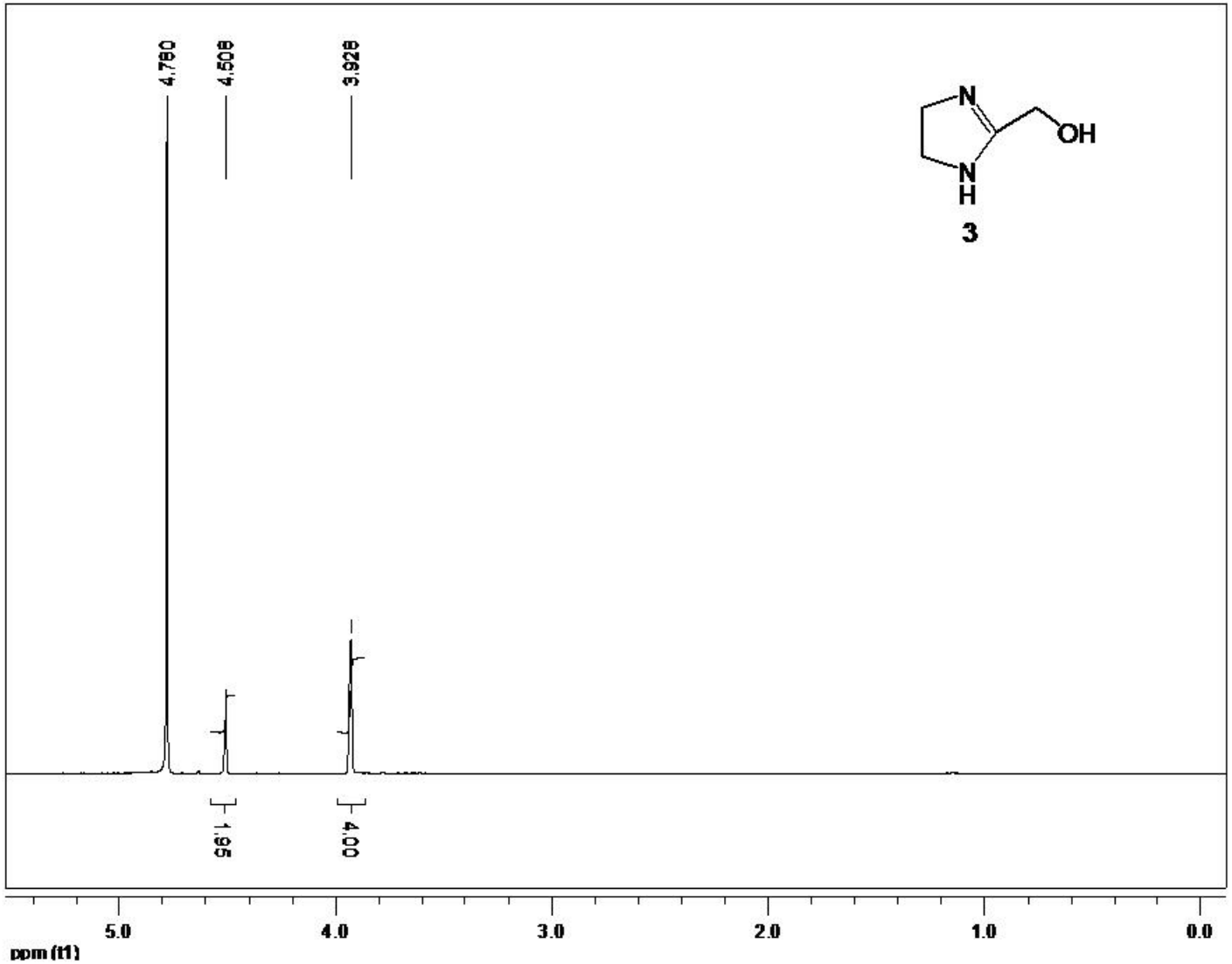


**Figure A-1. (4,5-Dihydro-1H-imidazol-2-yl)-methanol**

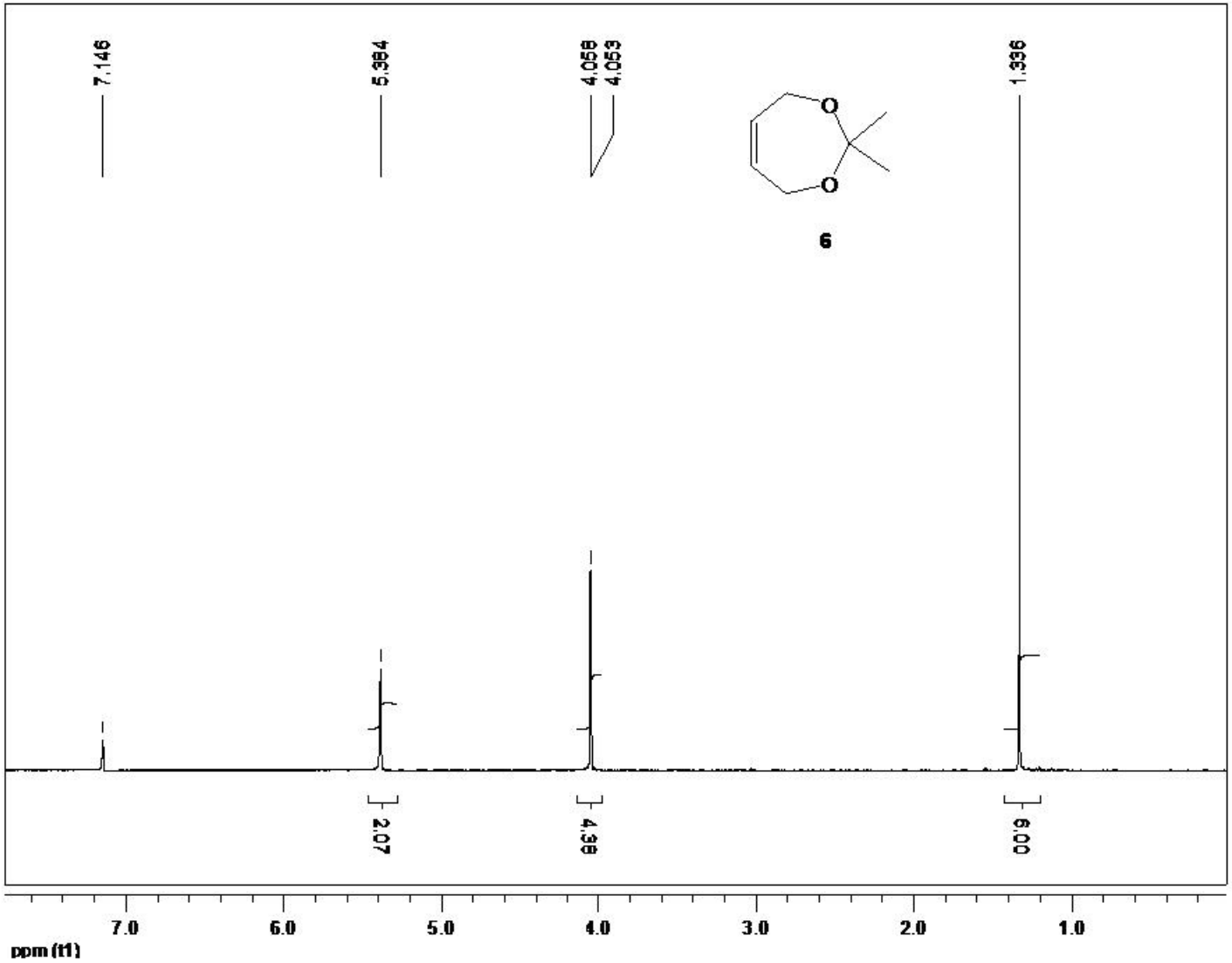


**Figure A-2. 2,2-Dimethyl-1,3-dioxocyclohept-5-ene**

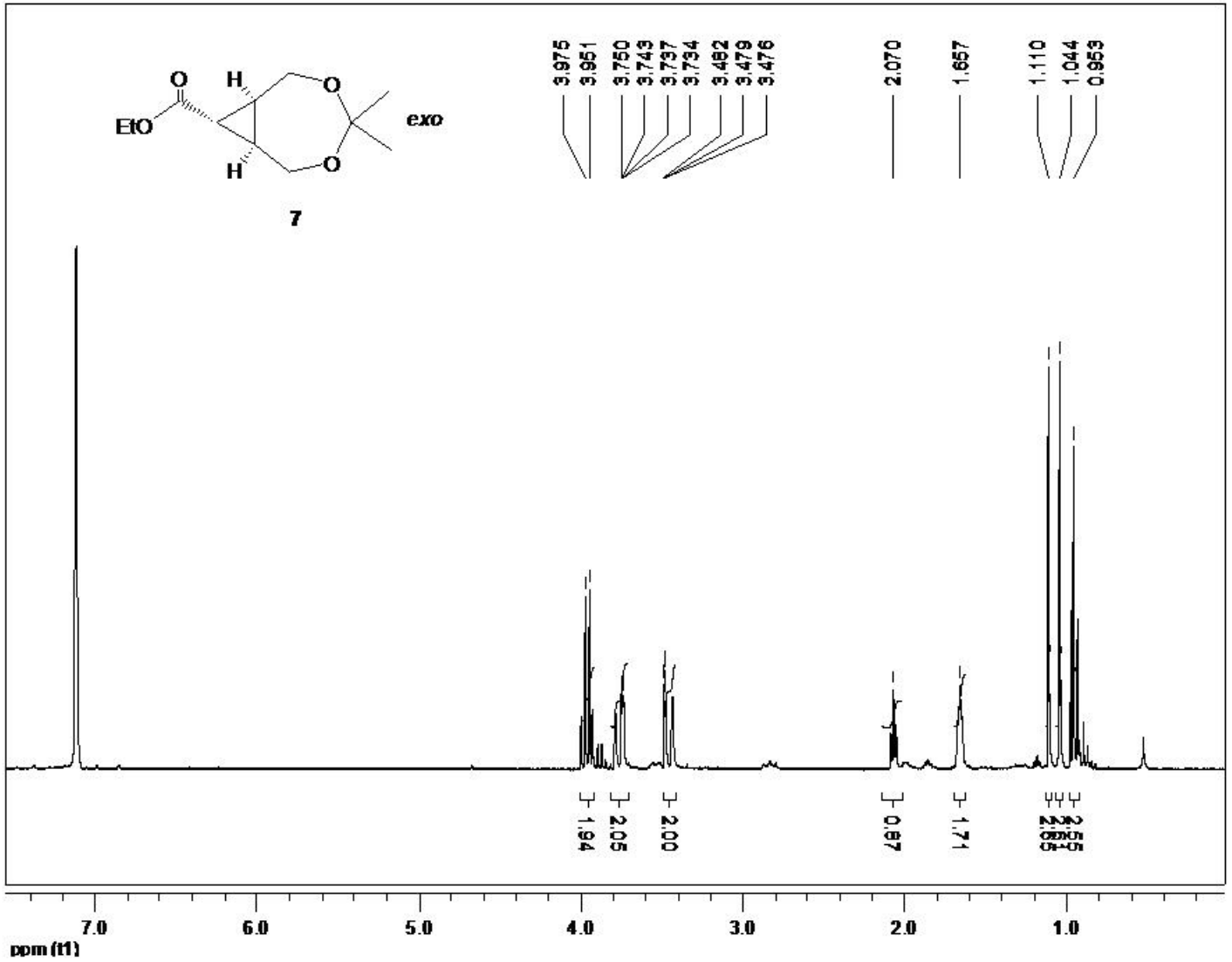


**Figure A-3. 4,4-Dimethy-8-ethylformyl-3,5-dioxa-bicyclo[5.1.0]octane**

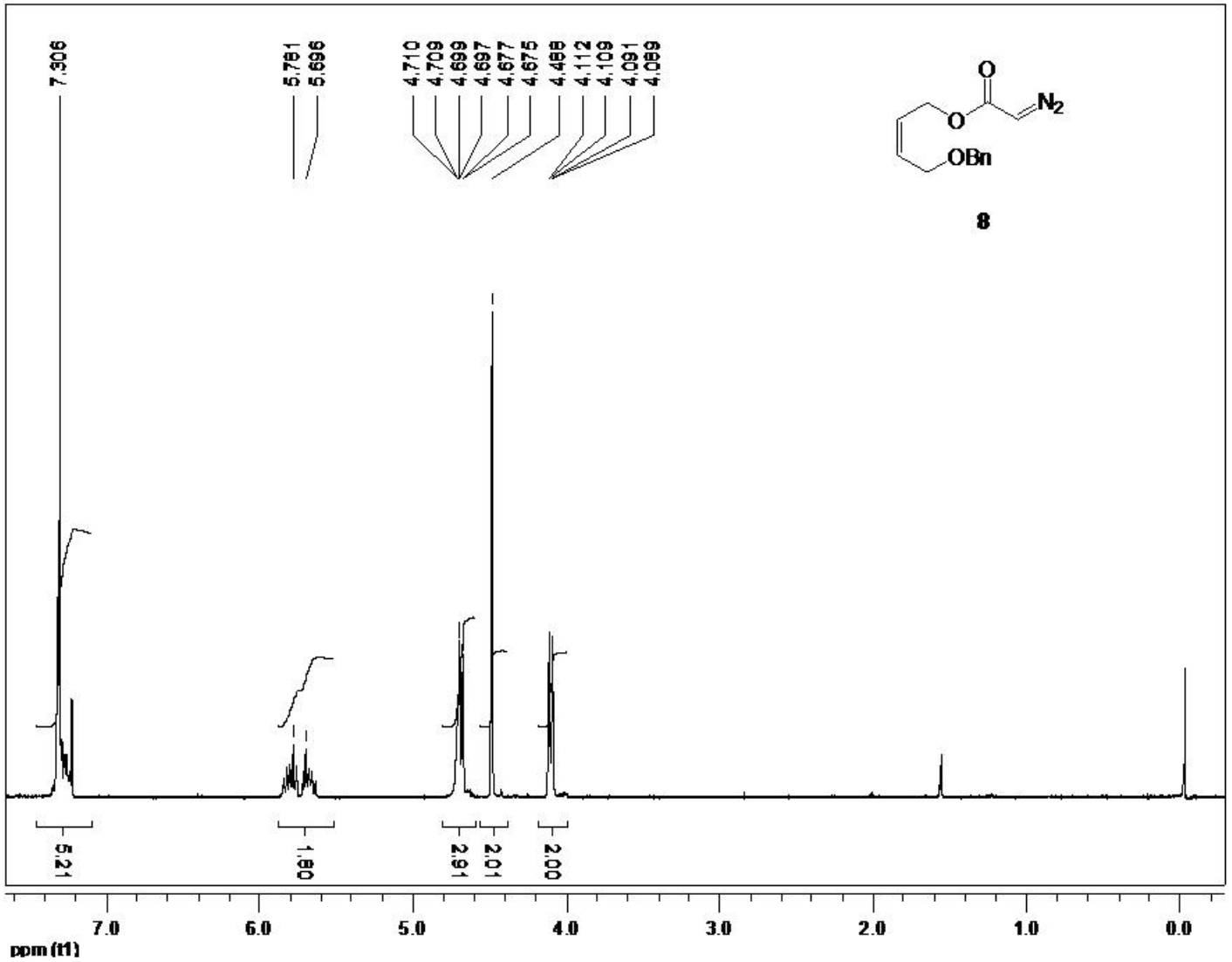


**Figure A-4. Diazo-acetic acid 4-benzyloxy-but-2-enyl ester**

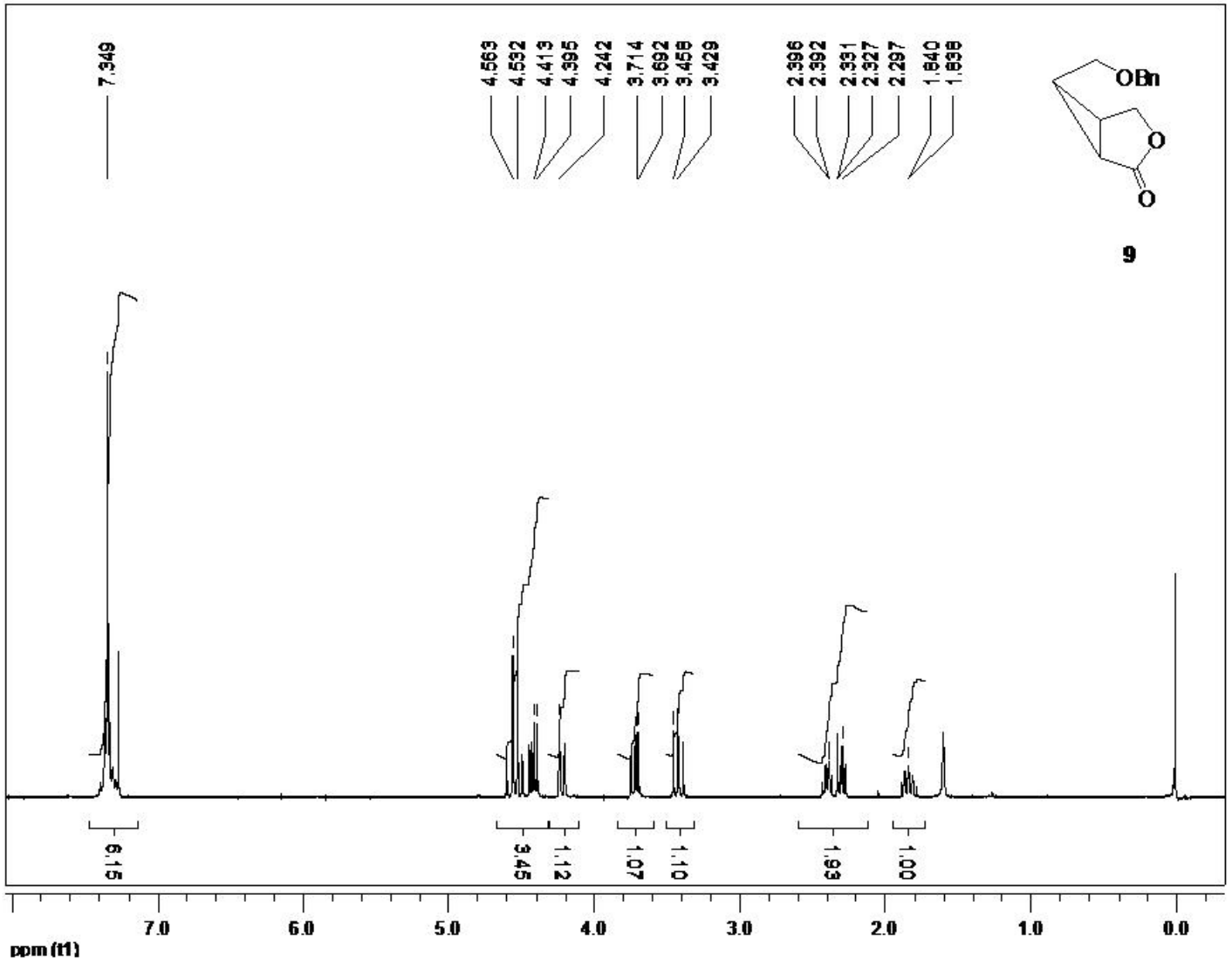


**Figure A-5. 6-Benzyloxymethyl-3-oxa-bicyclo[3.1.0]hexan-2-one**

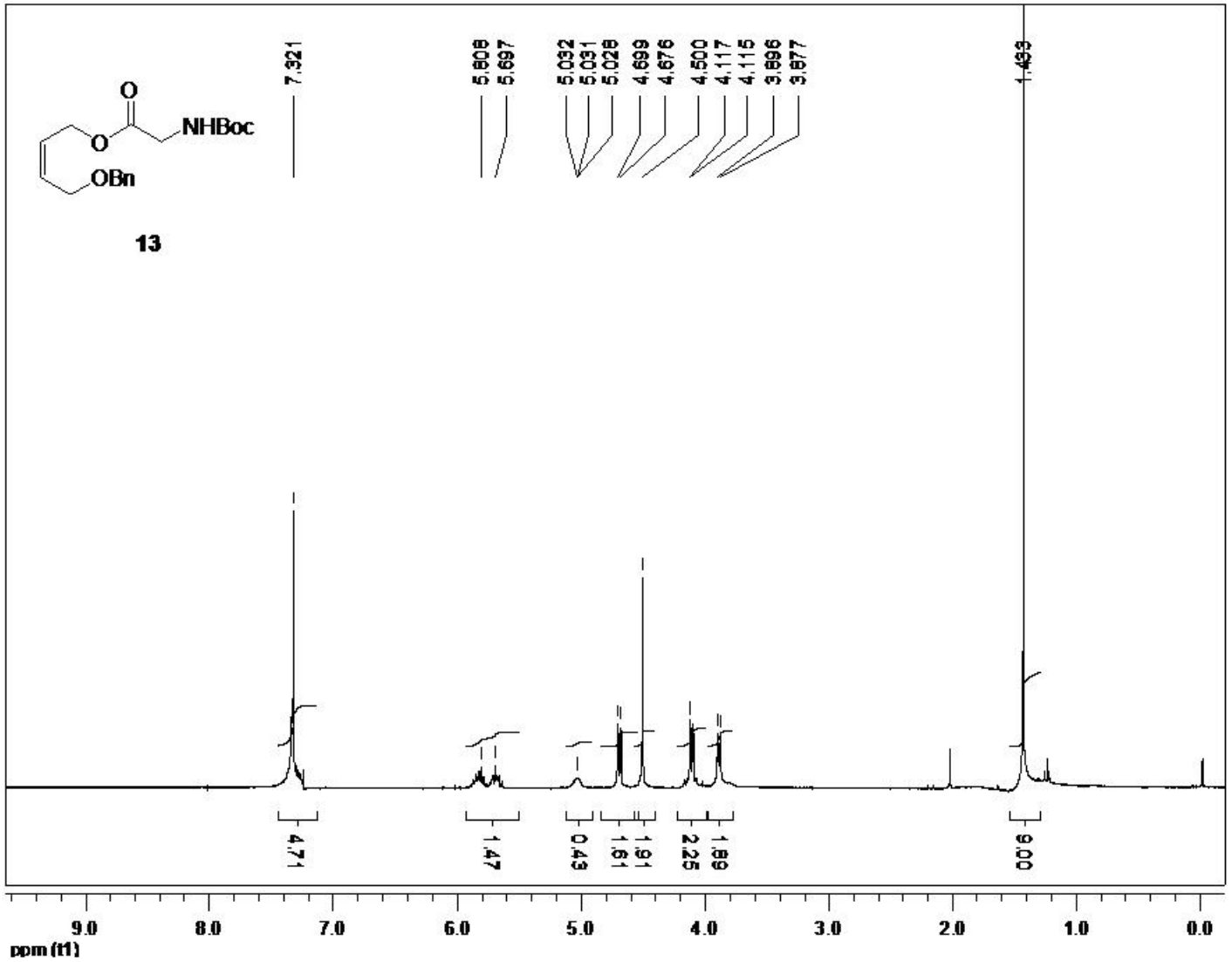


**Figure A-6. tert-Butoxycarbonylamino-acetic acid 4-benzyloxy-but-2-enyl ester**

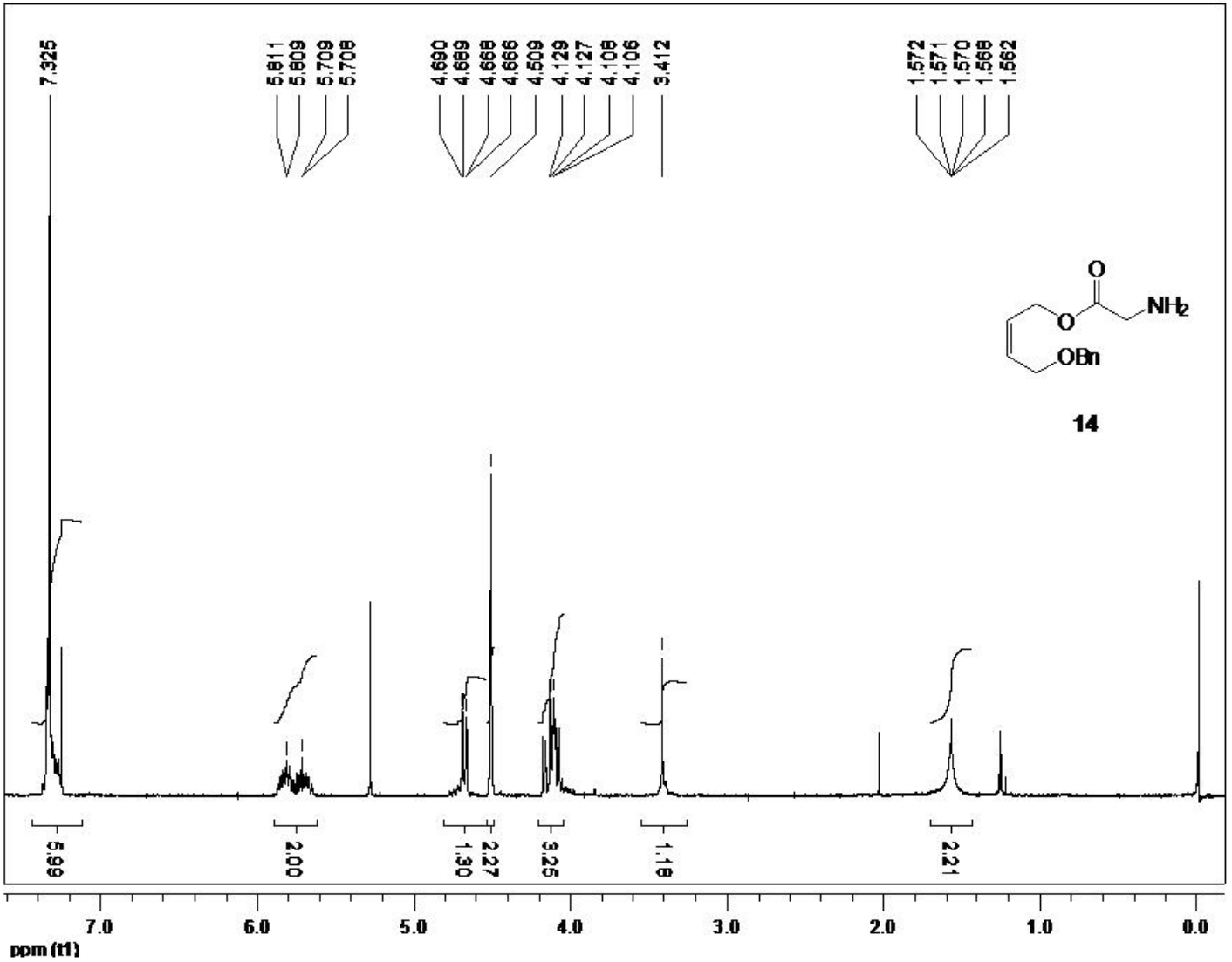


**Figure A-7. Amino-acetic acid 4-benzyloxy-but-2-enyl ester**

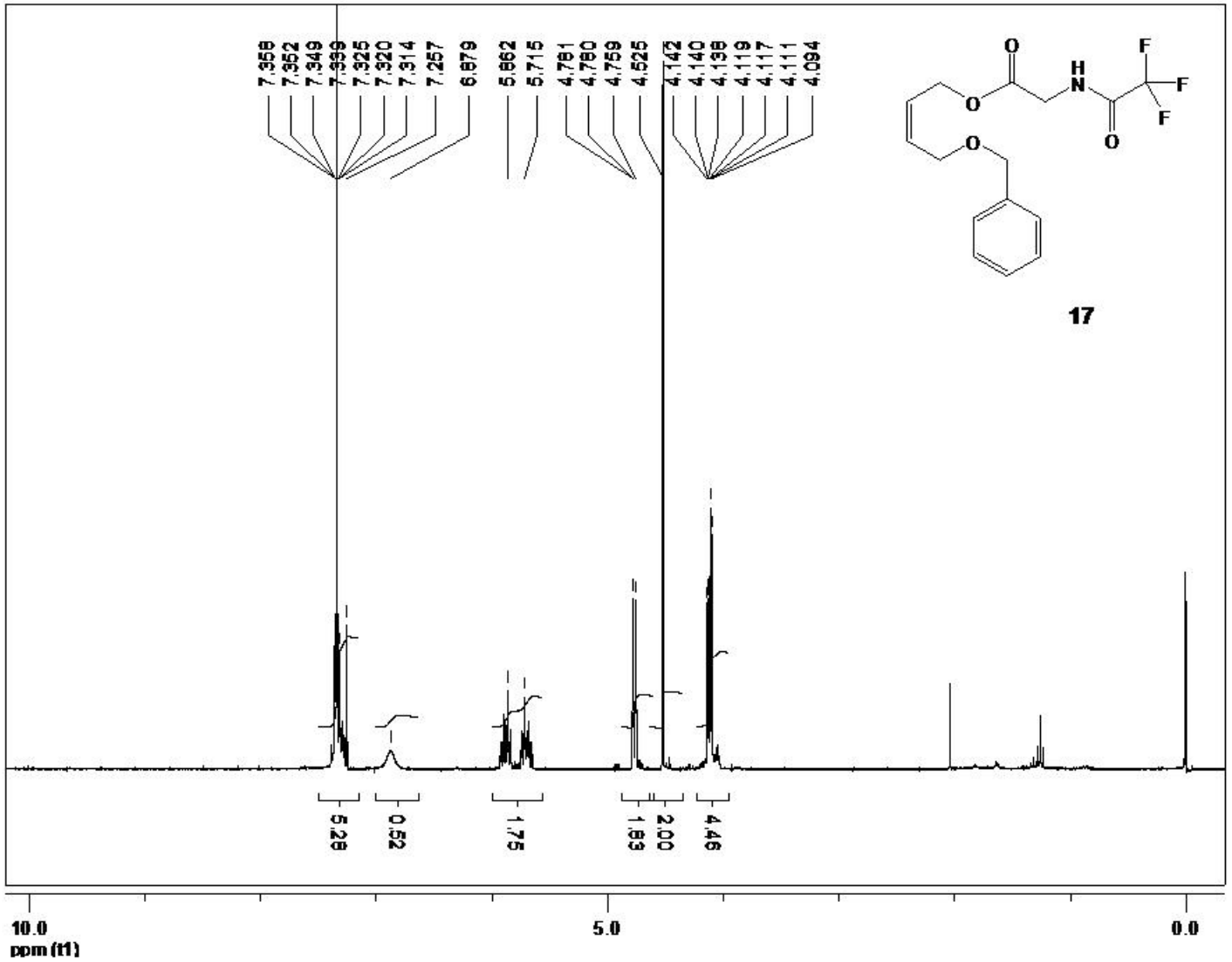


**Figure A-8. (Z)-4-(benzyloxy)but-2-enyl 2-(2,2,2-trifluoroacetamido)acetate**

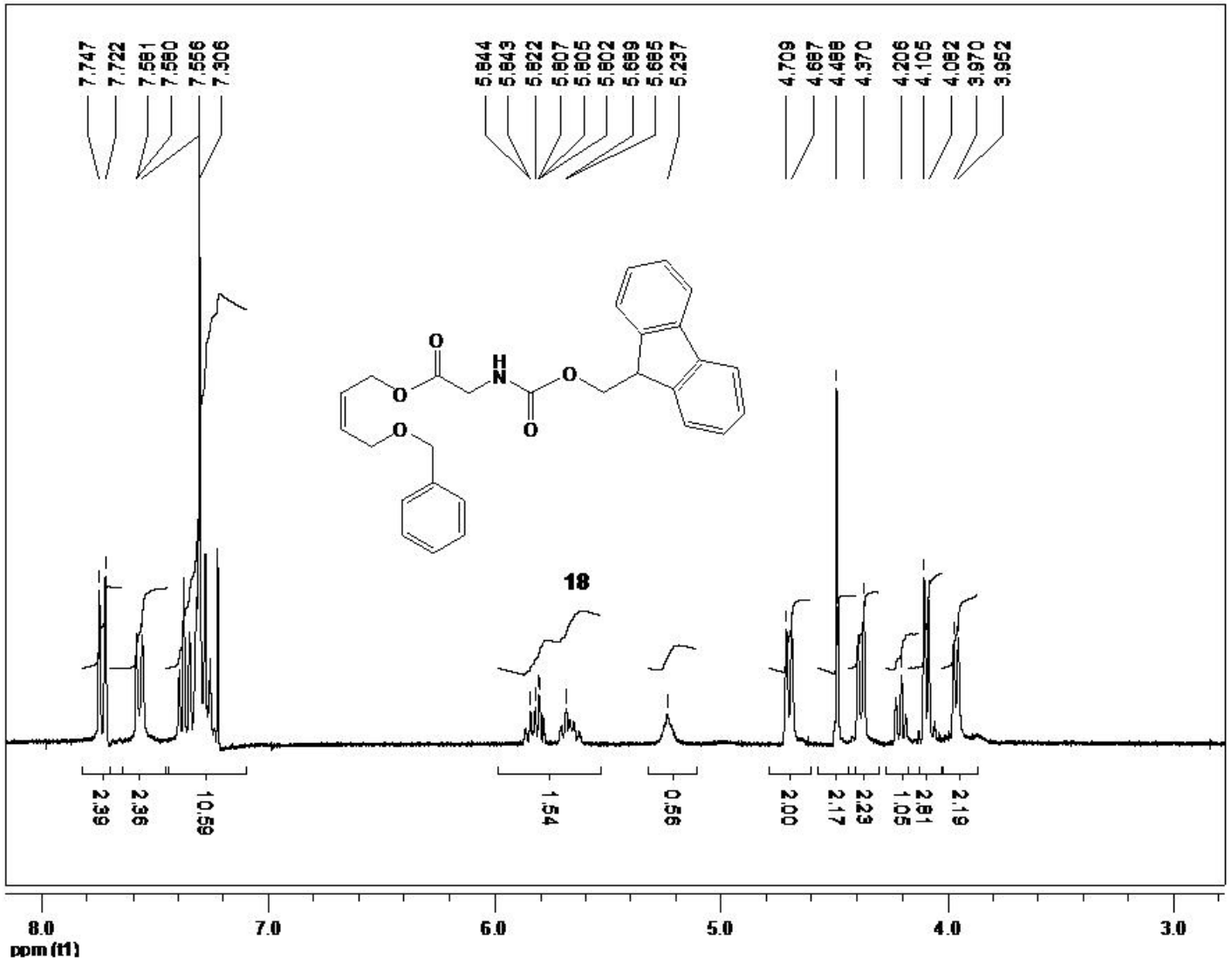


**Figure A-9. (Z)-4-(benzyloxy)but-2-enyl 2-(((9H-fluoren-9-yl)methoxy)carbonylamino)acetate**

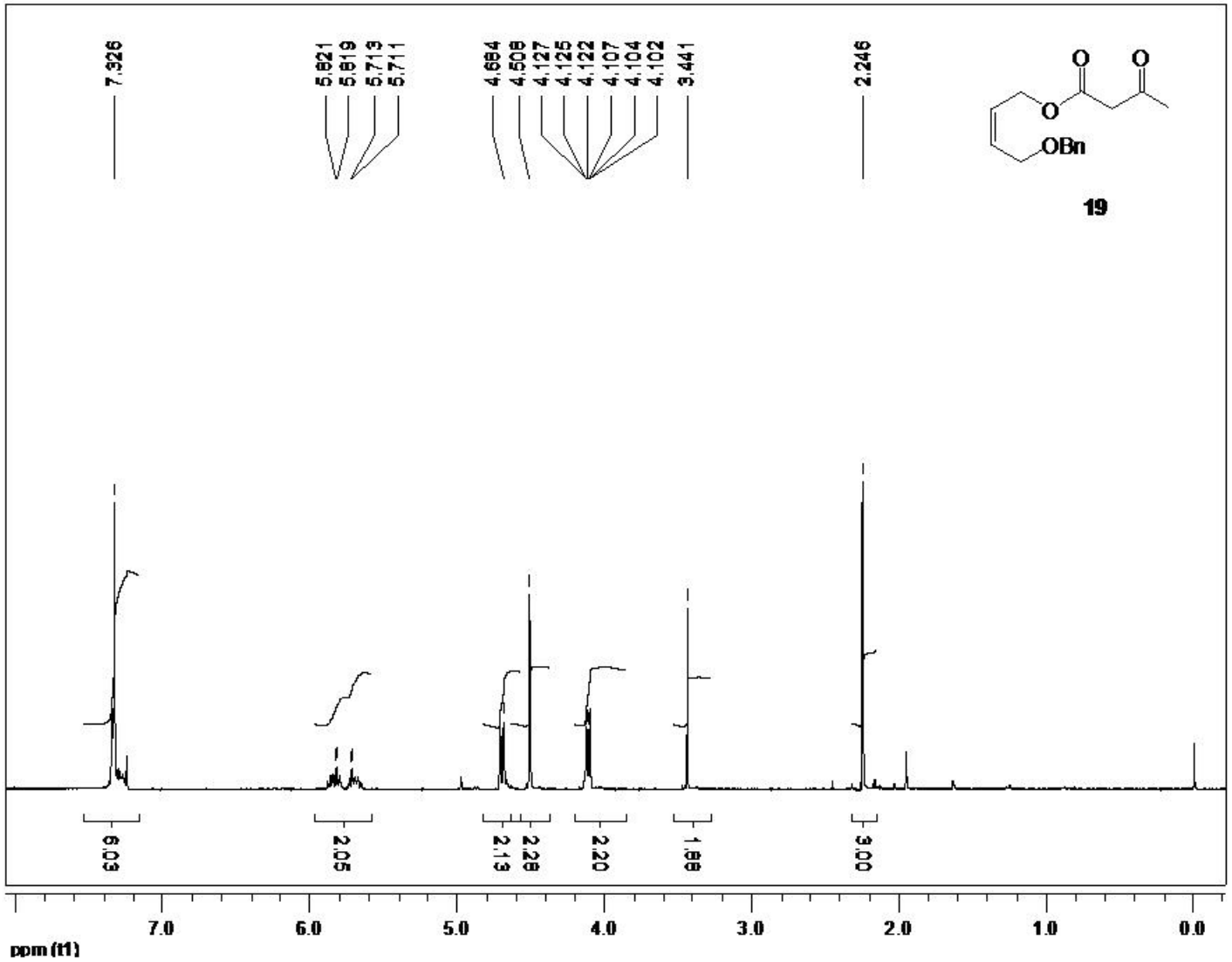


**Figure A-10. (Z)-4-(benzyloxy)but-2-enyl 3-oxobutanoate**

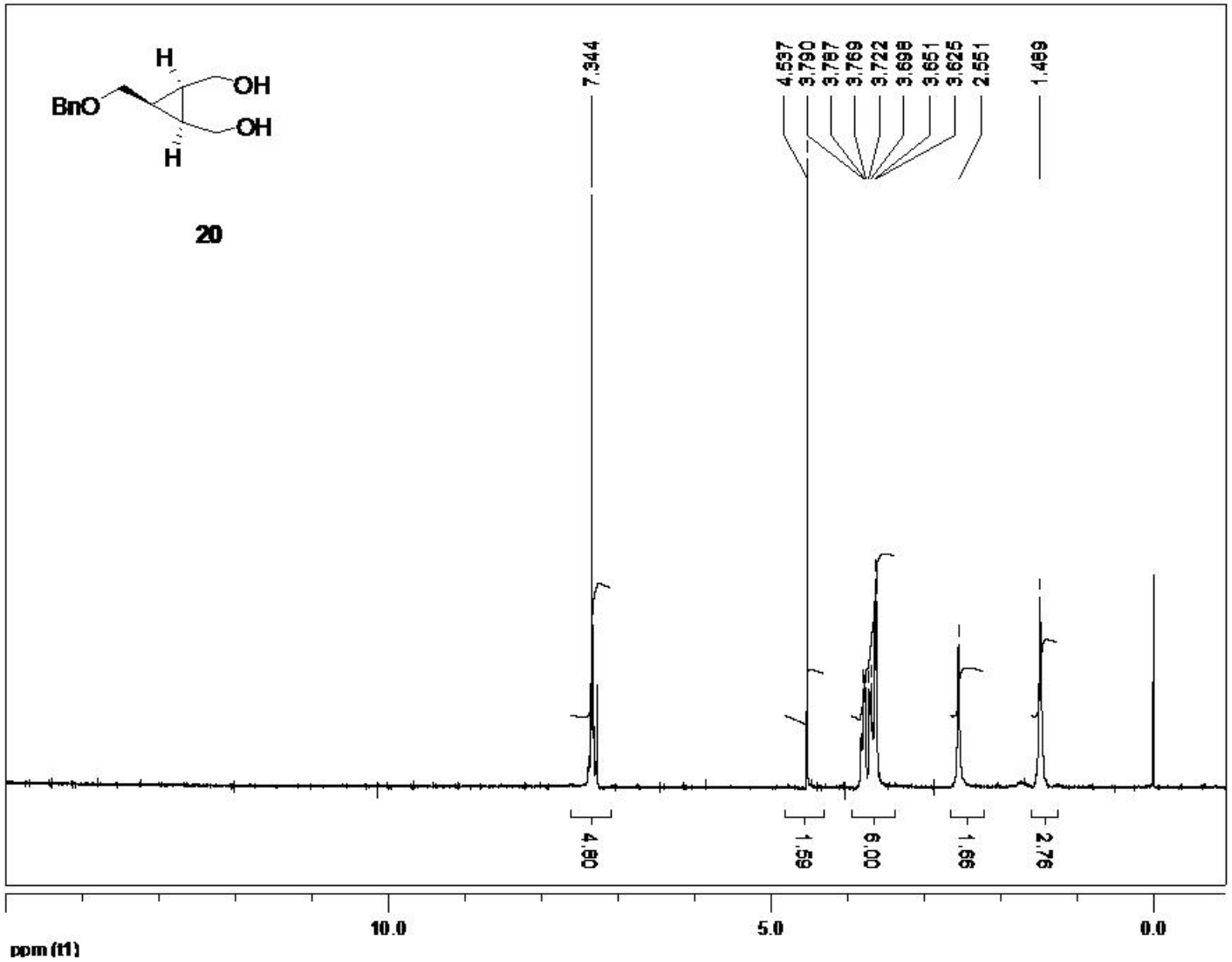


**Figure A-11. ((1R,2S,3s)-3-(benzyloxymethyl)cyclopropane-1,2-diyl)dimethanol**

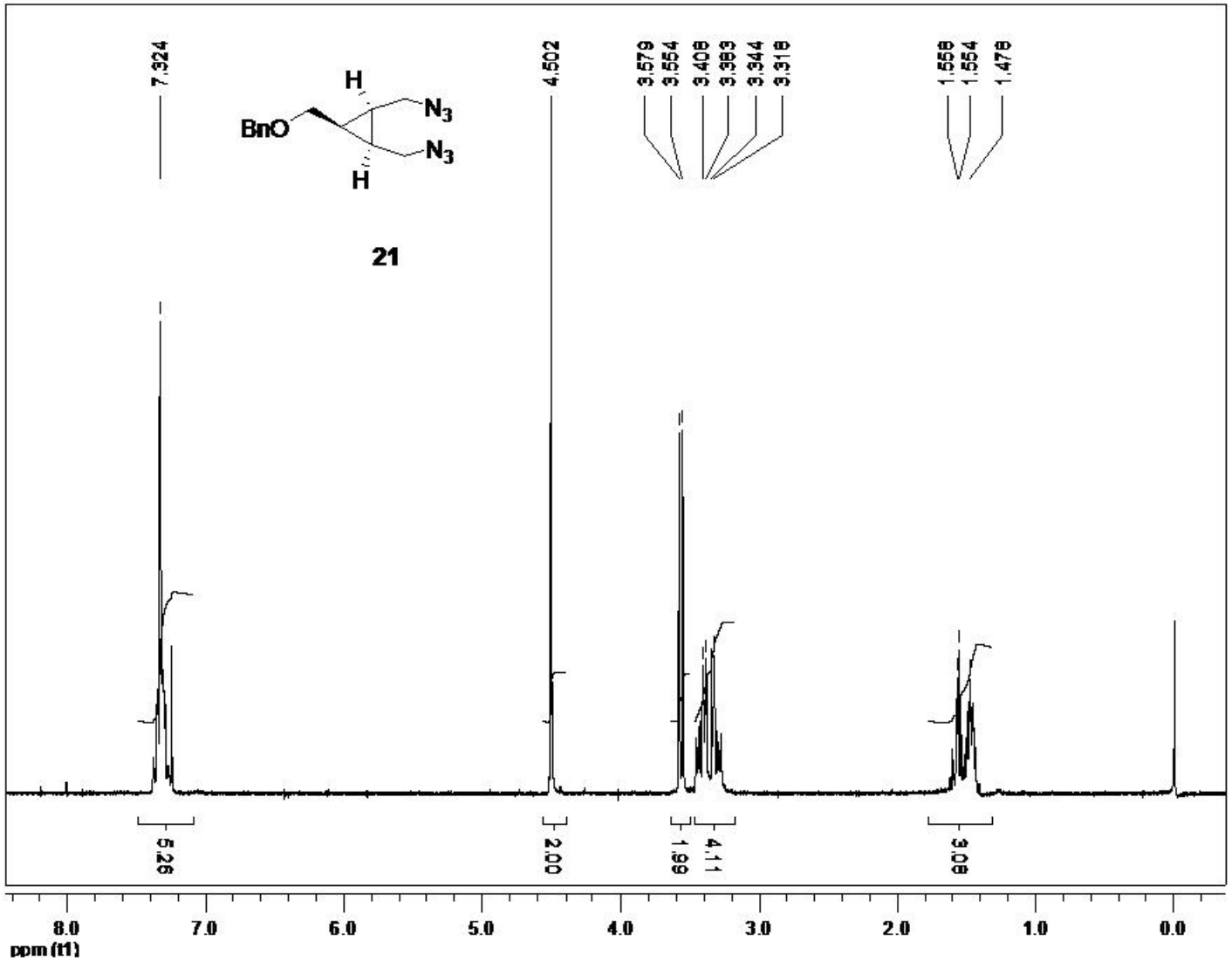


**Figure A-12. ((((1s,2R,3S)-2,3-bis(azidomethyl)cyclopropyl)methoxy)methyl)benzene**

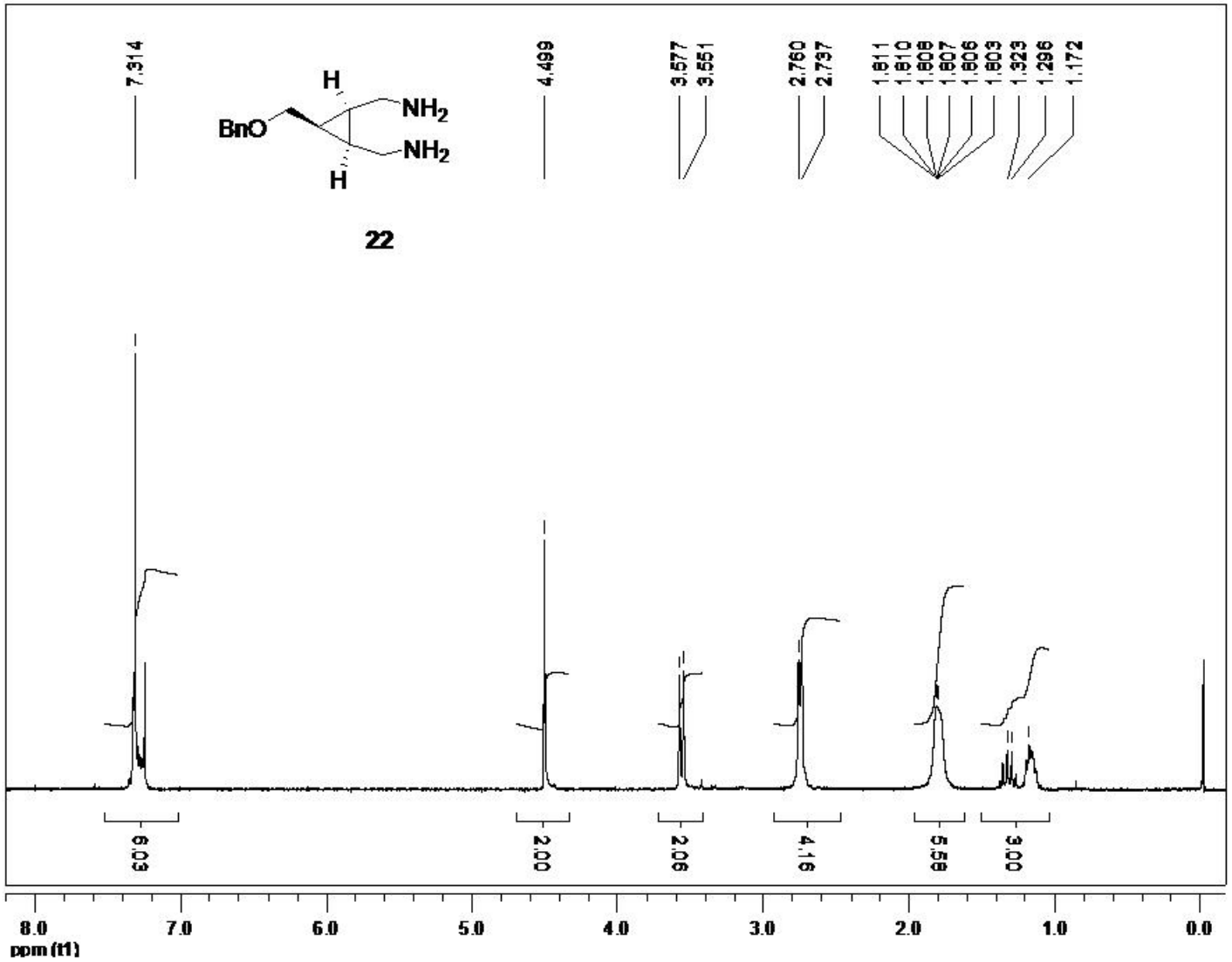


**Figure A-13. ((1R,2S,3s)-3-(benzyloxymethyl)cyclopropane-1,2-diyl)dimethanamine**

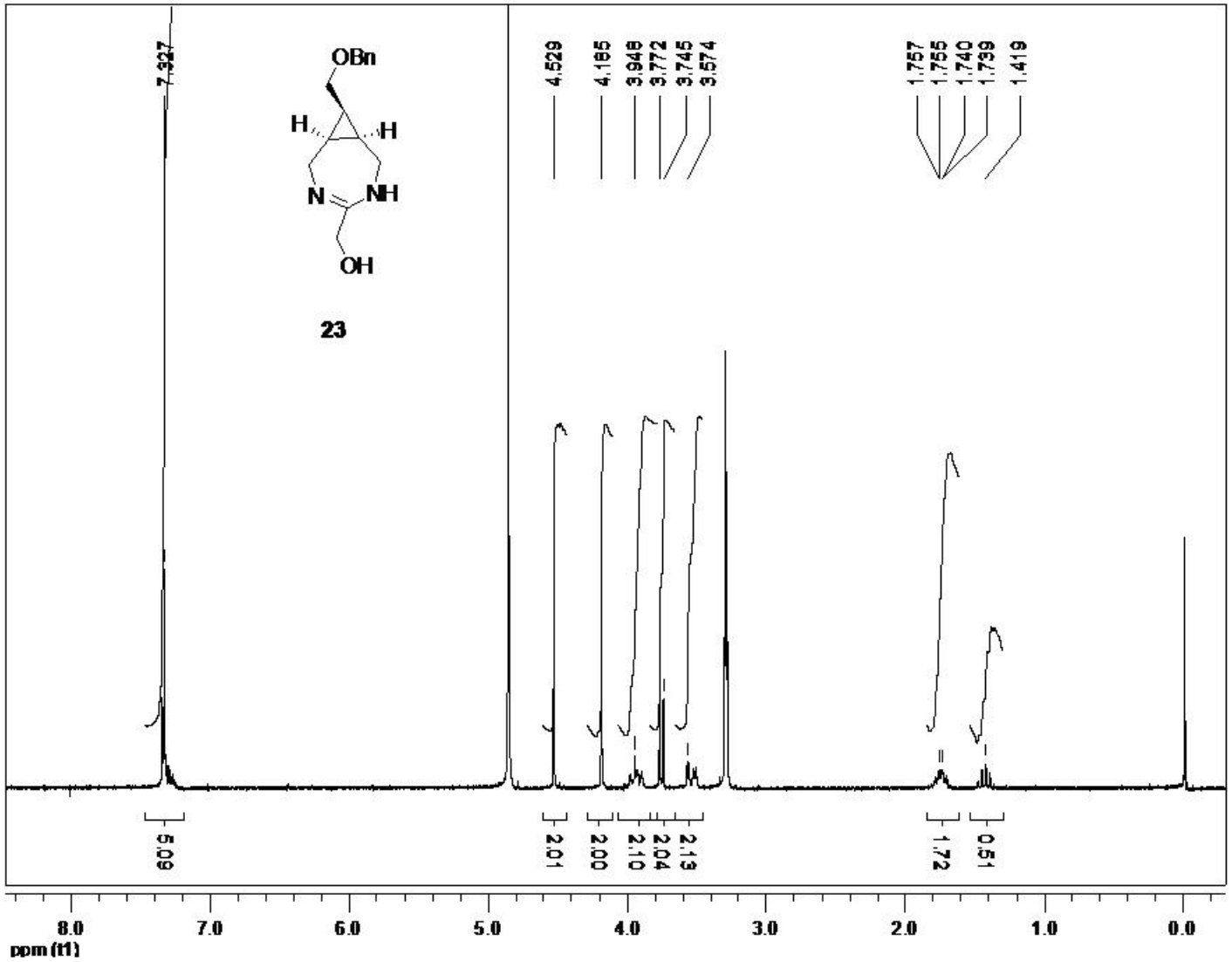


**Figure A-14. (Z)-(8-(benzyloxymethyl)-3,5-diazabicyclo[5.1.0]oct-4-en-4-yl)methanol**

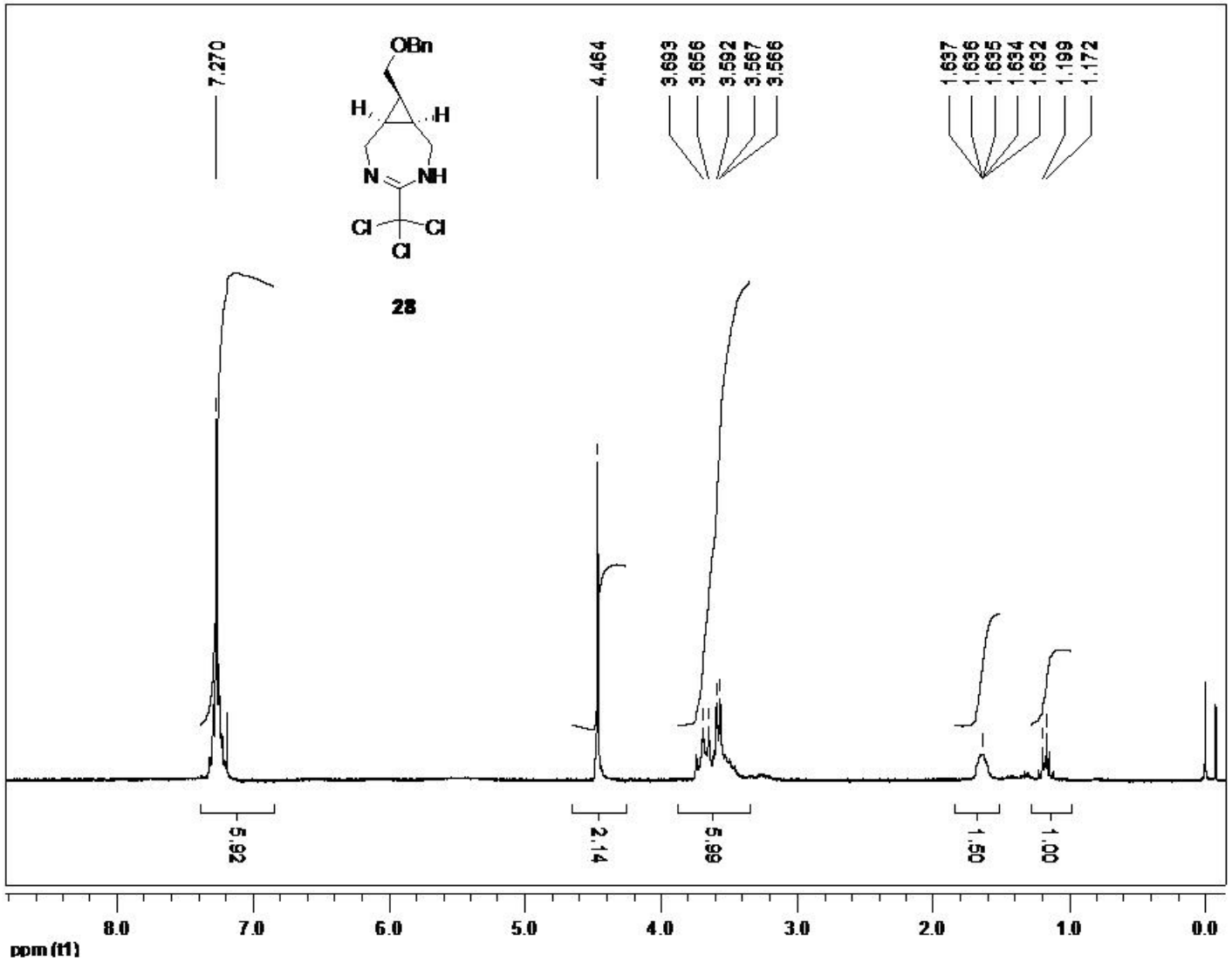


**Figure A-15. (Z)-8-(benzyloxymethyl)-4-(trichloromethyl)-3,5-diazabicyclo[5.1.0]oct-3-ene**

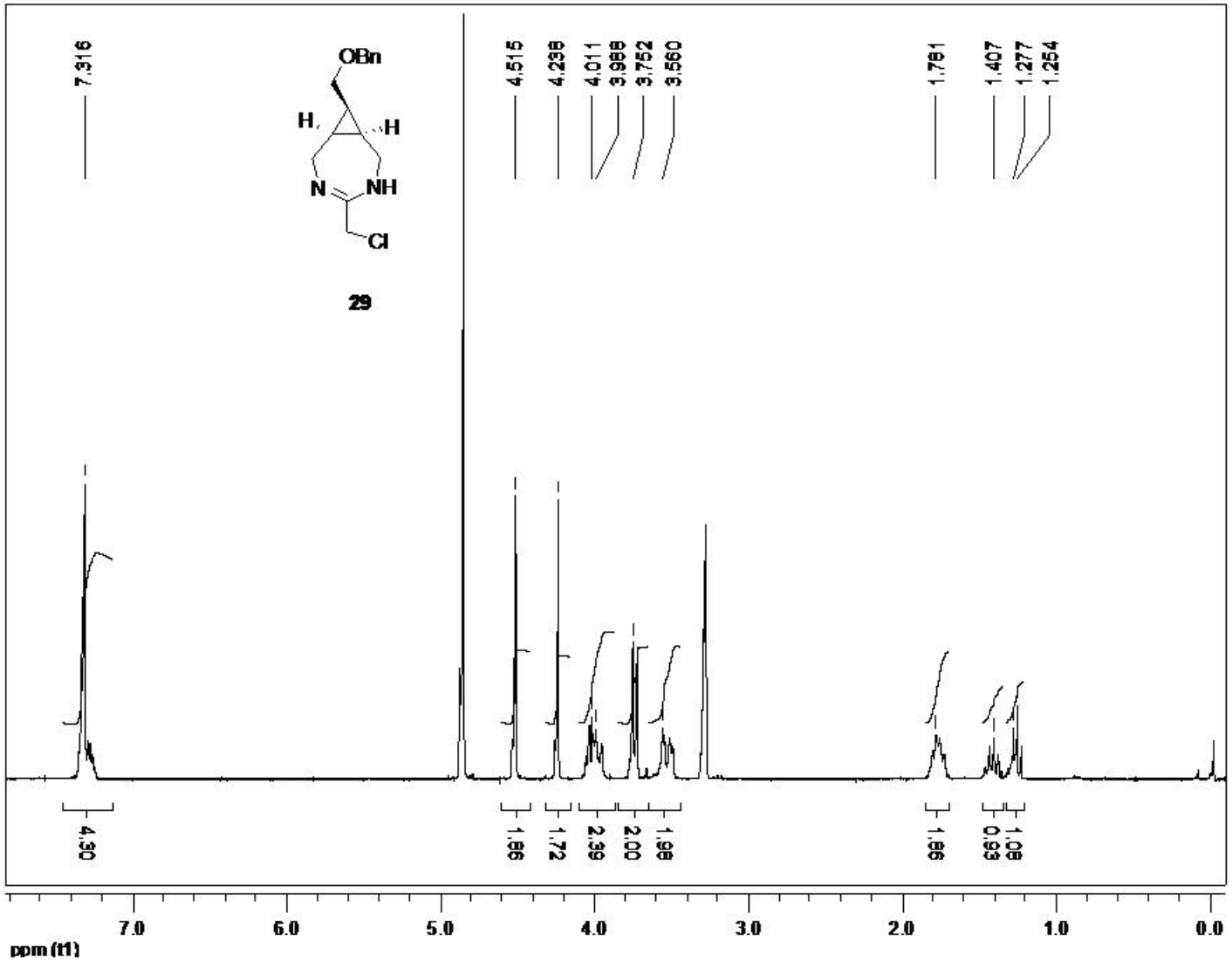


**Figure A-16. (Z)-8-(benzyloxymethyl)-4-(chloromethyl)-3,5-diazabicyclo[5.1.0]oct-3-ene**

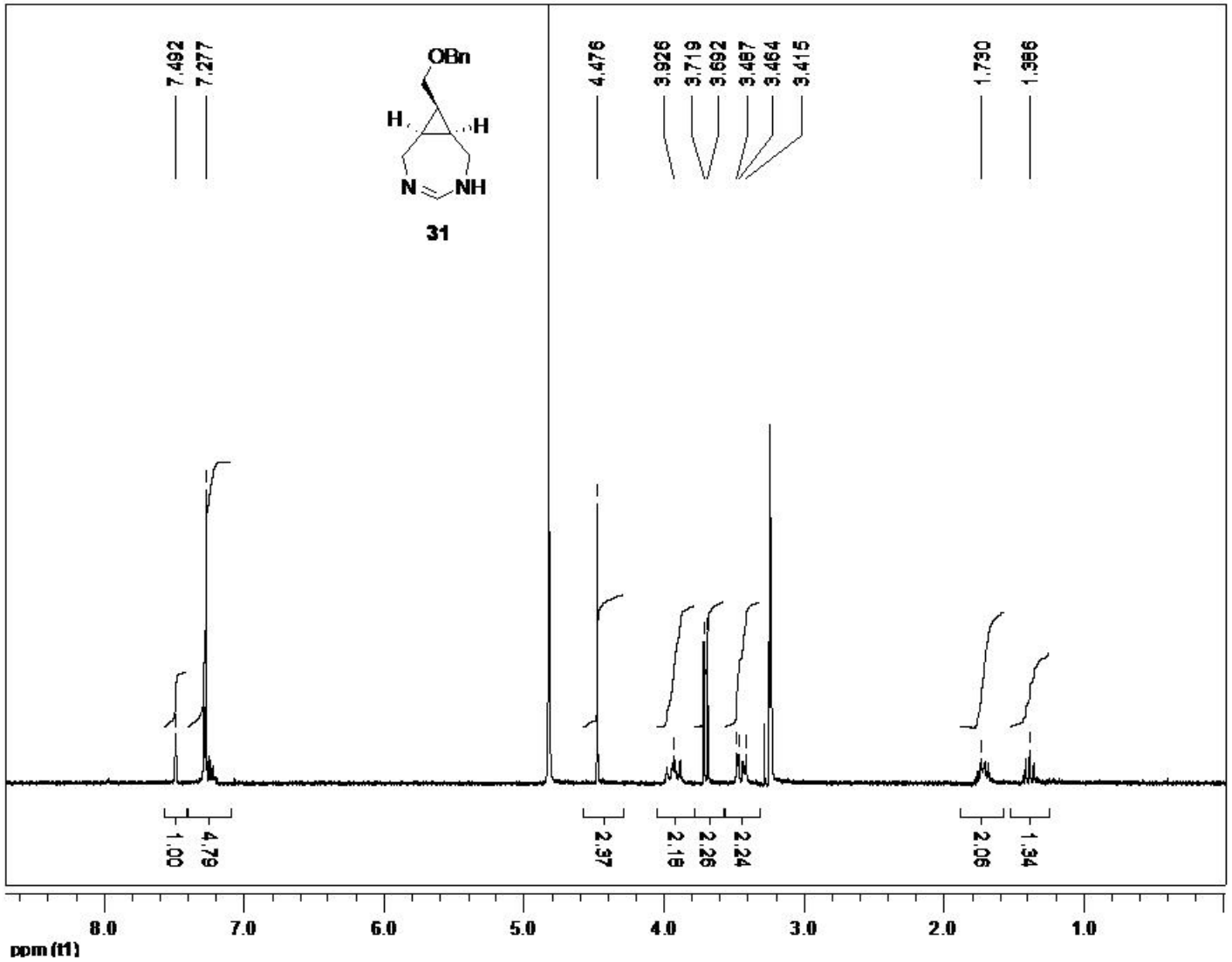


**Figure A-17. (Z)-8-(benzyloxymethyl)-3,5-diazabicyclo[5.1.0]oct-3-ene**

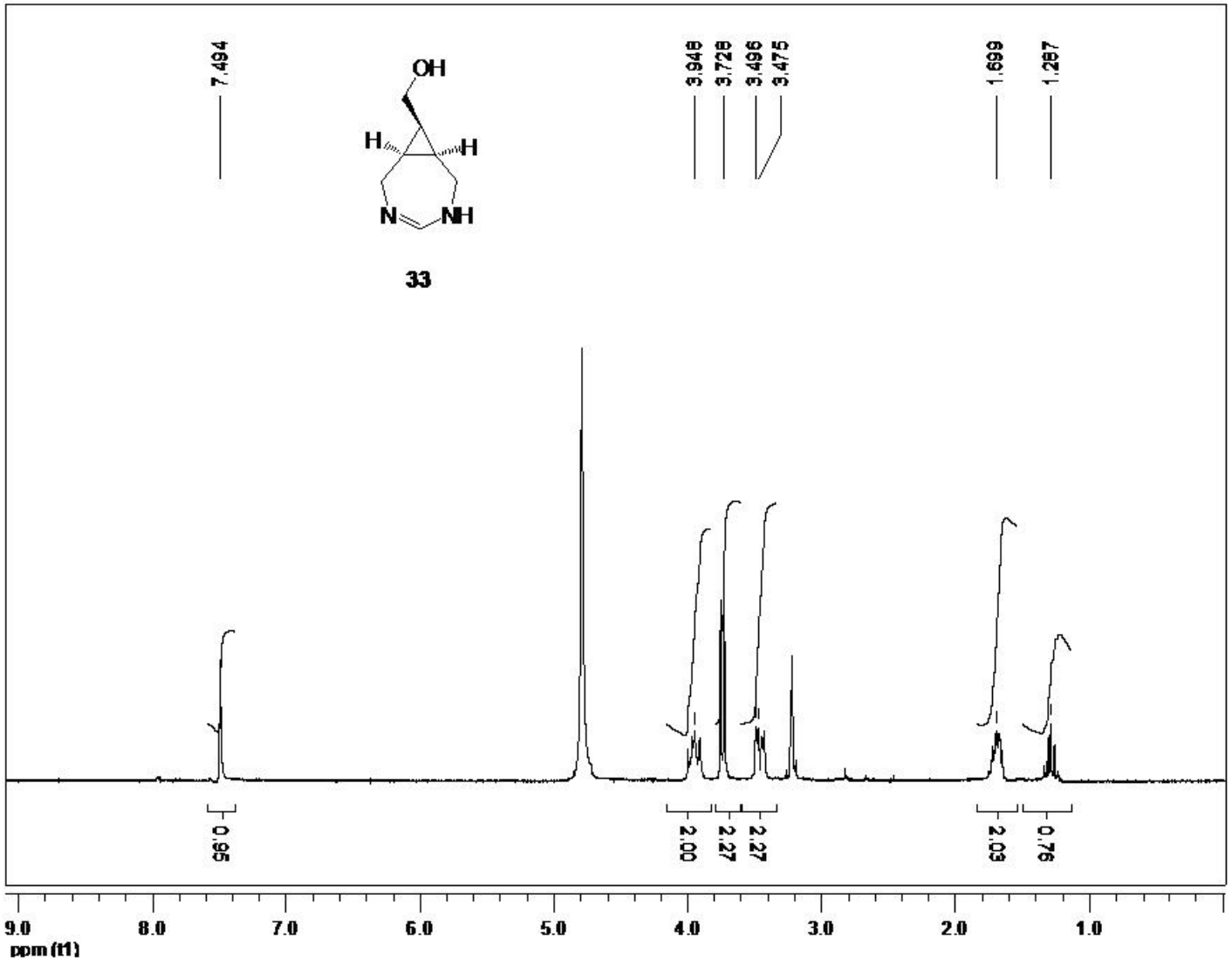


**Figure A-18. (Z)-3,5-diazabicyclo[5.1.0]oct-4-en-8-ylmethanol**

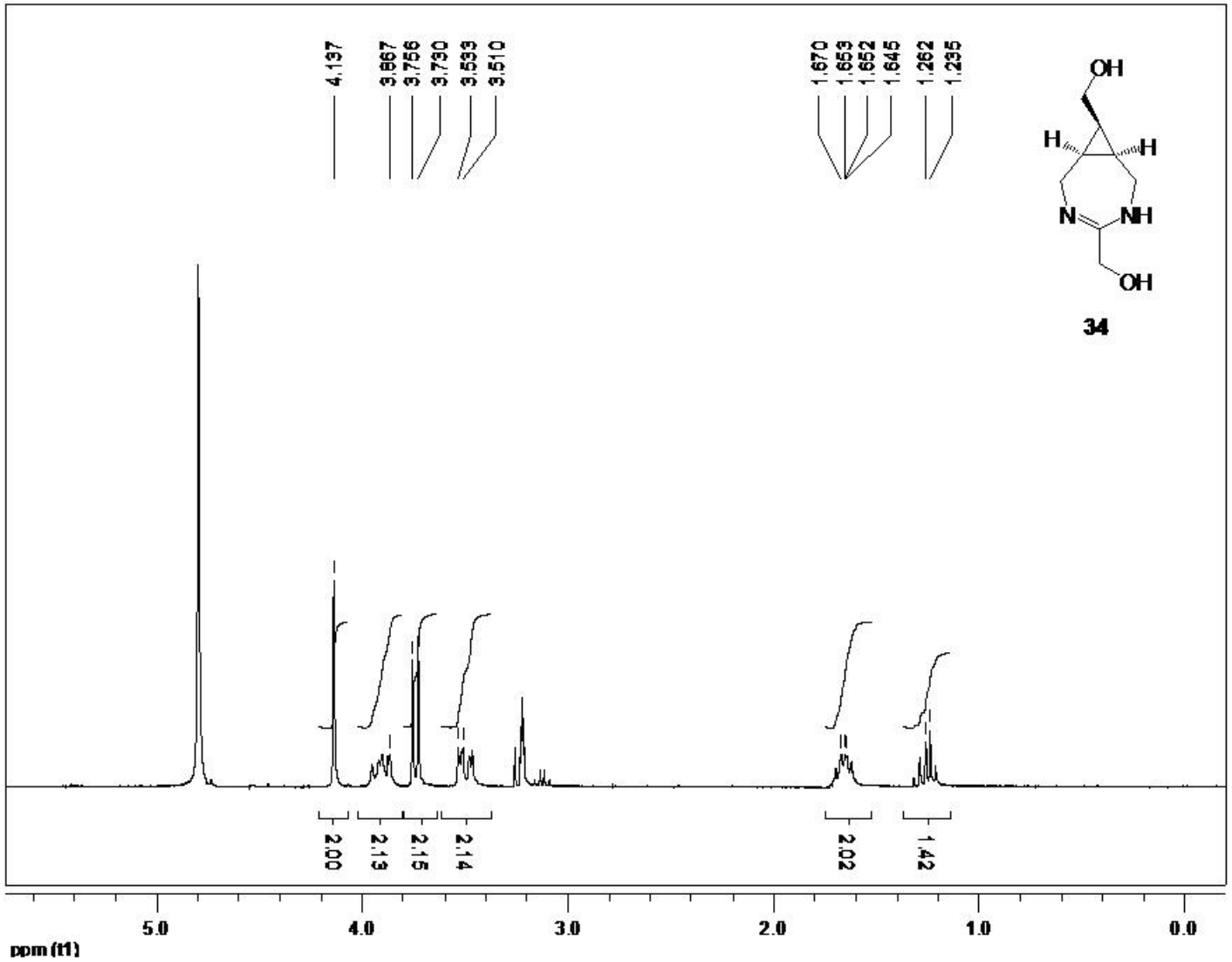


**Figure A-19. (Z)-3,5-diazabicyclo[5.1.0]oct-4-ene-4,8-diyldimethanol**

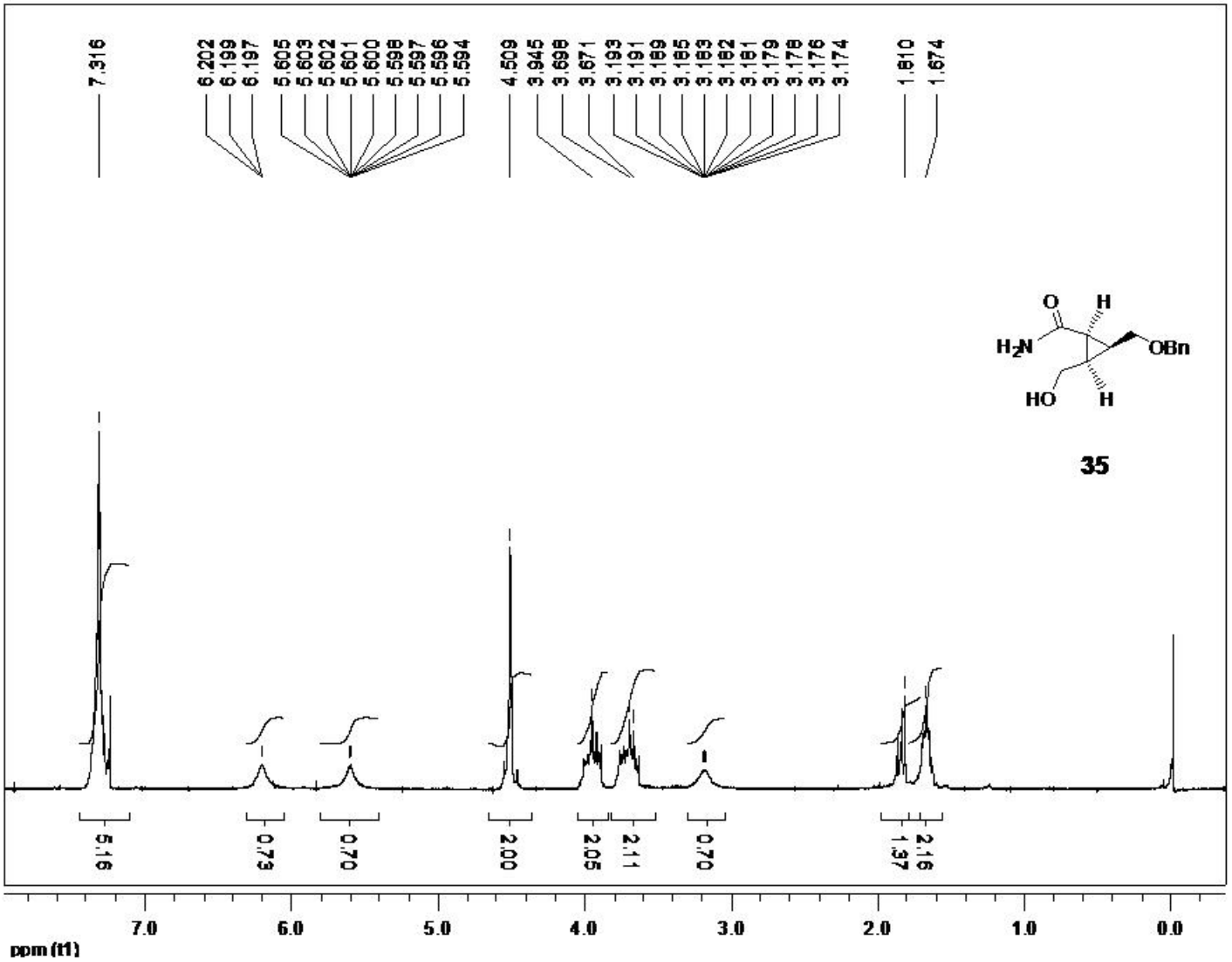


**Figure A-20. (1R,2S,3R)-2-(benzyloxymethyl)-3-(hydroxymethyl)cyclopropanecarboxamide**

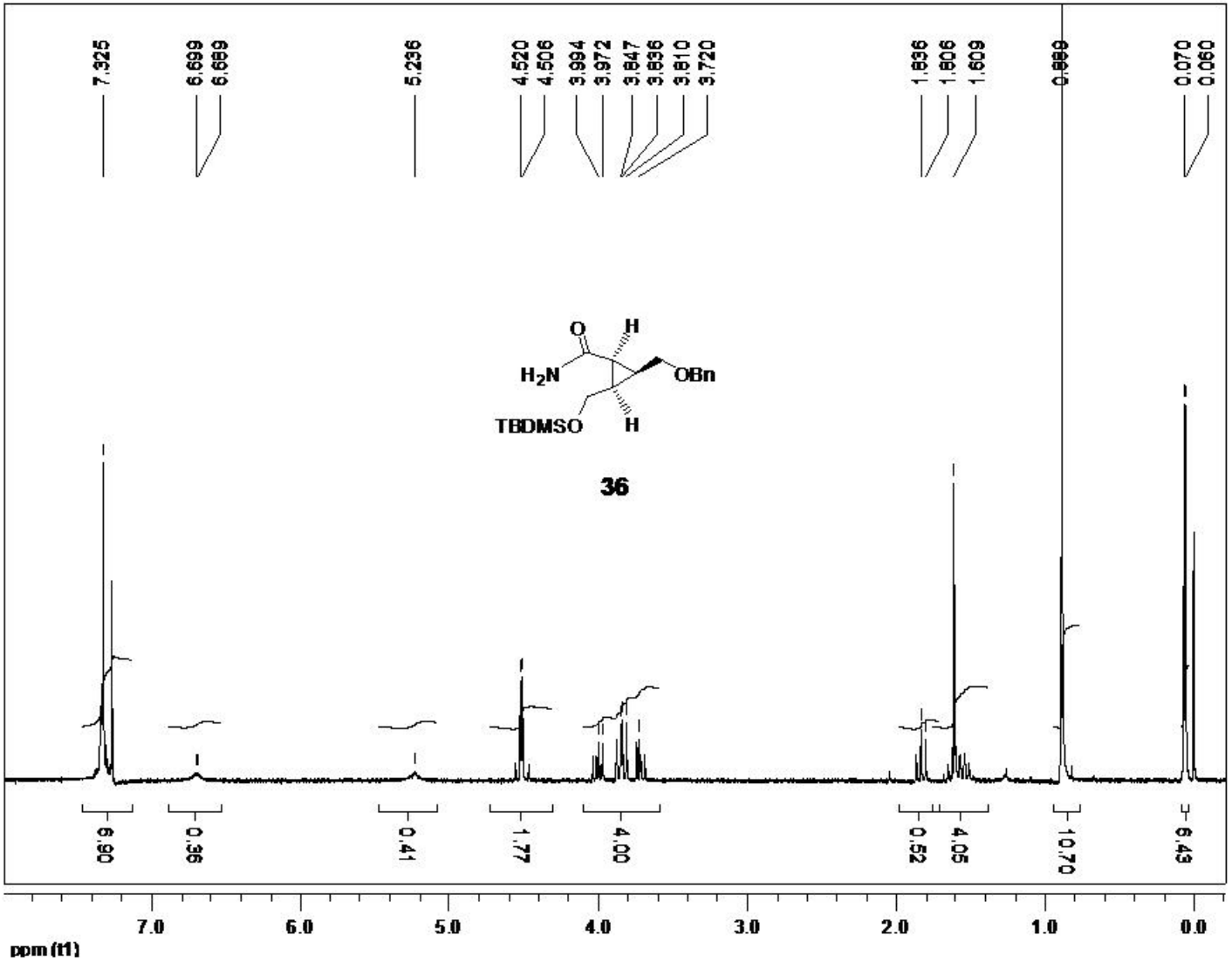


**Figure A-21. (1S,2S,3R)-2-(benzyloxymethyl)-3-((tert-butyldimethylsilyloxy)methyl) cyclopropanecarboxamide**

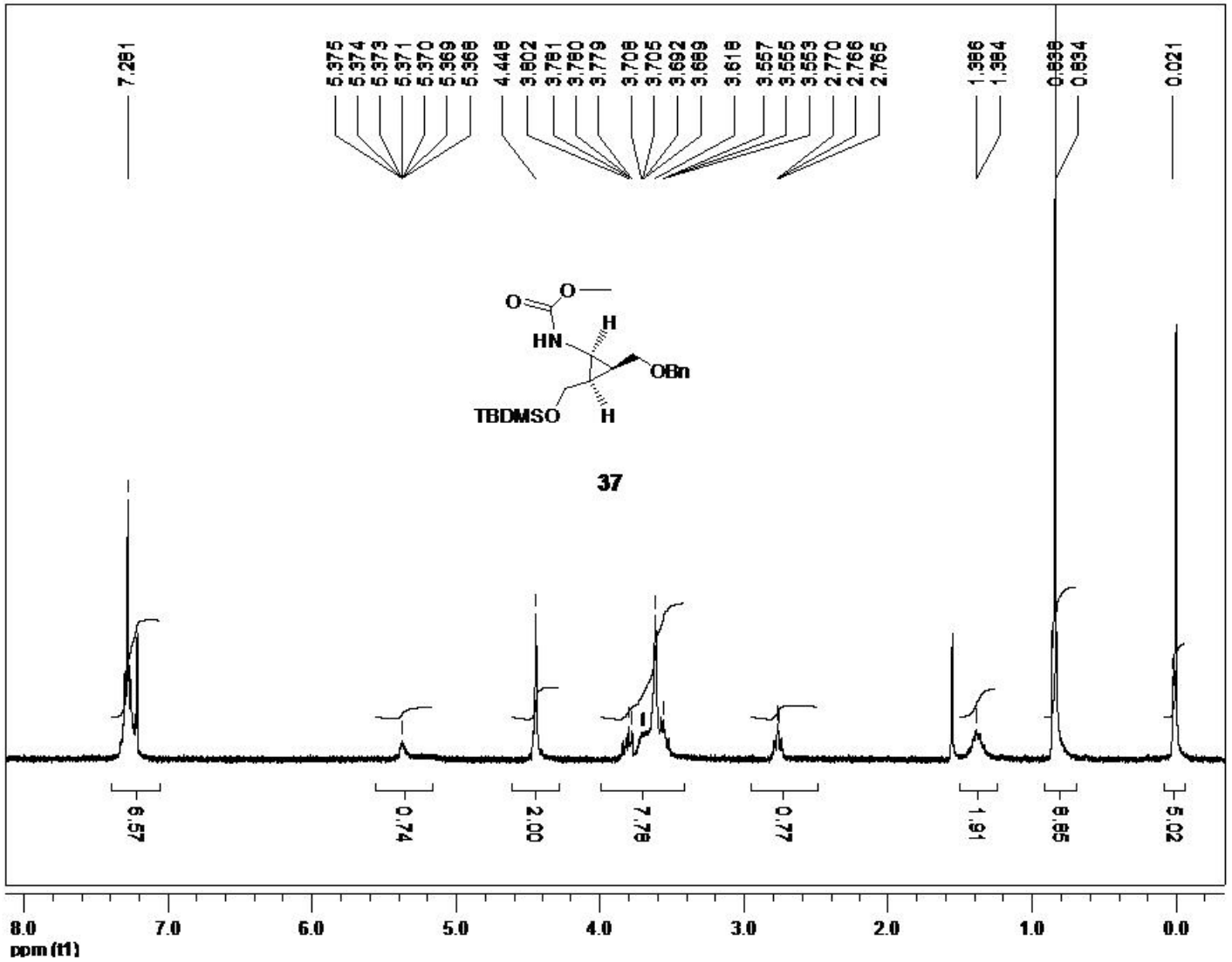


**Figure A-22. Methyl(1S,2S,3R)-2-(benzyloxymethyl)-3-((tert-butyldimethylsilyloxy)methyl) cyclopropylcarbamate**

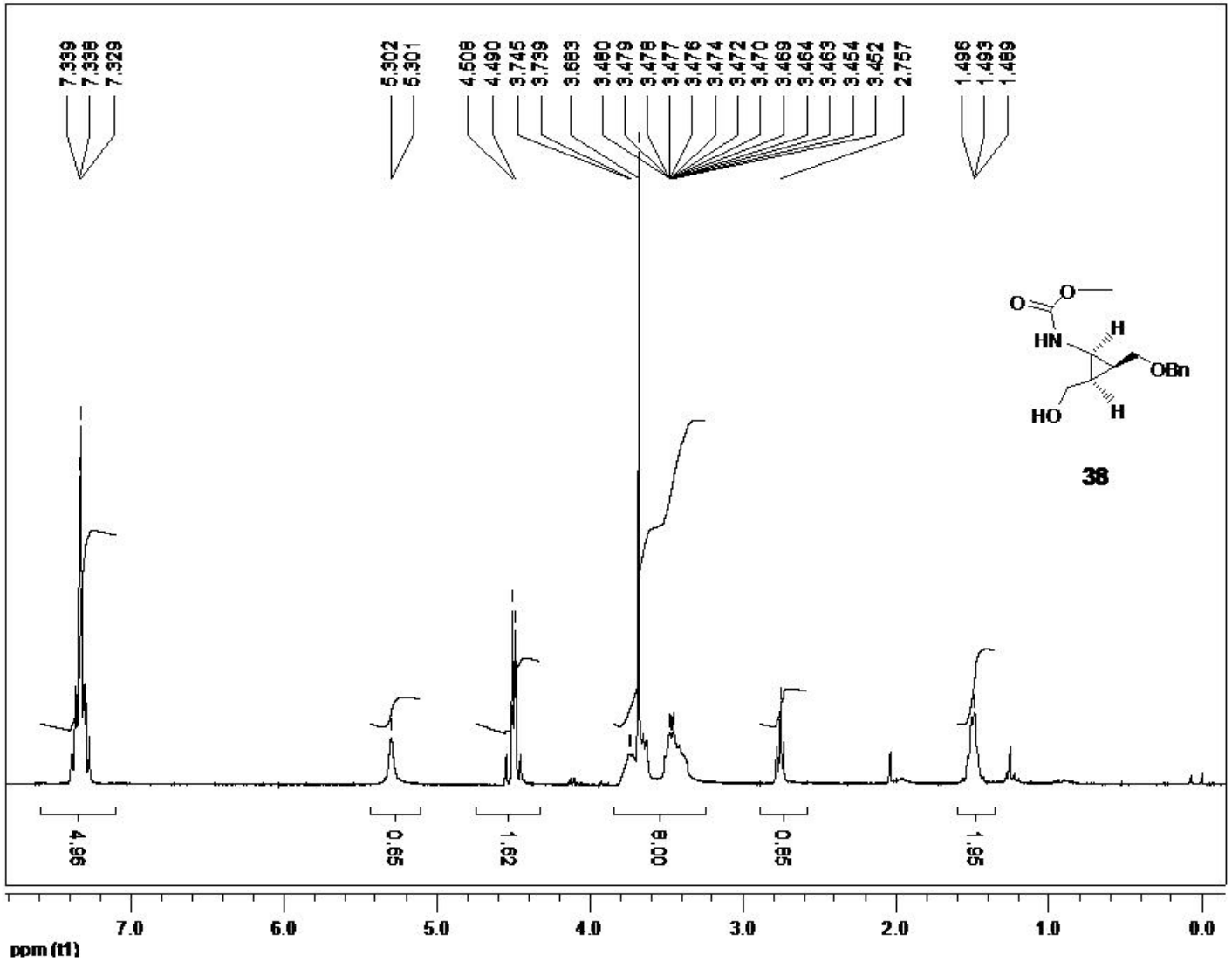


**Figure A-23. Methyl (1R,2S,3R)-2-(benzyloxymethyl)-3-(hydroxymethyl)cyclopropylcarbamate**

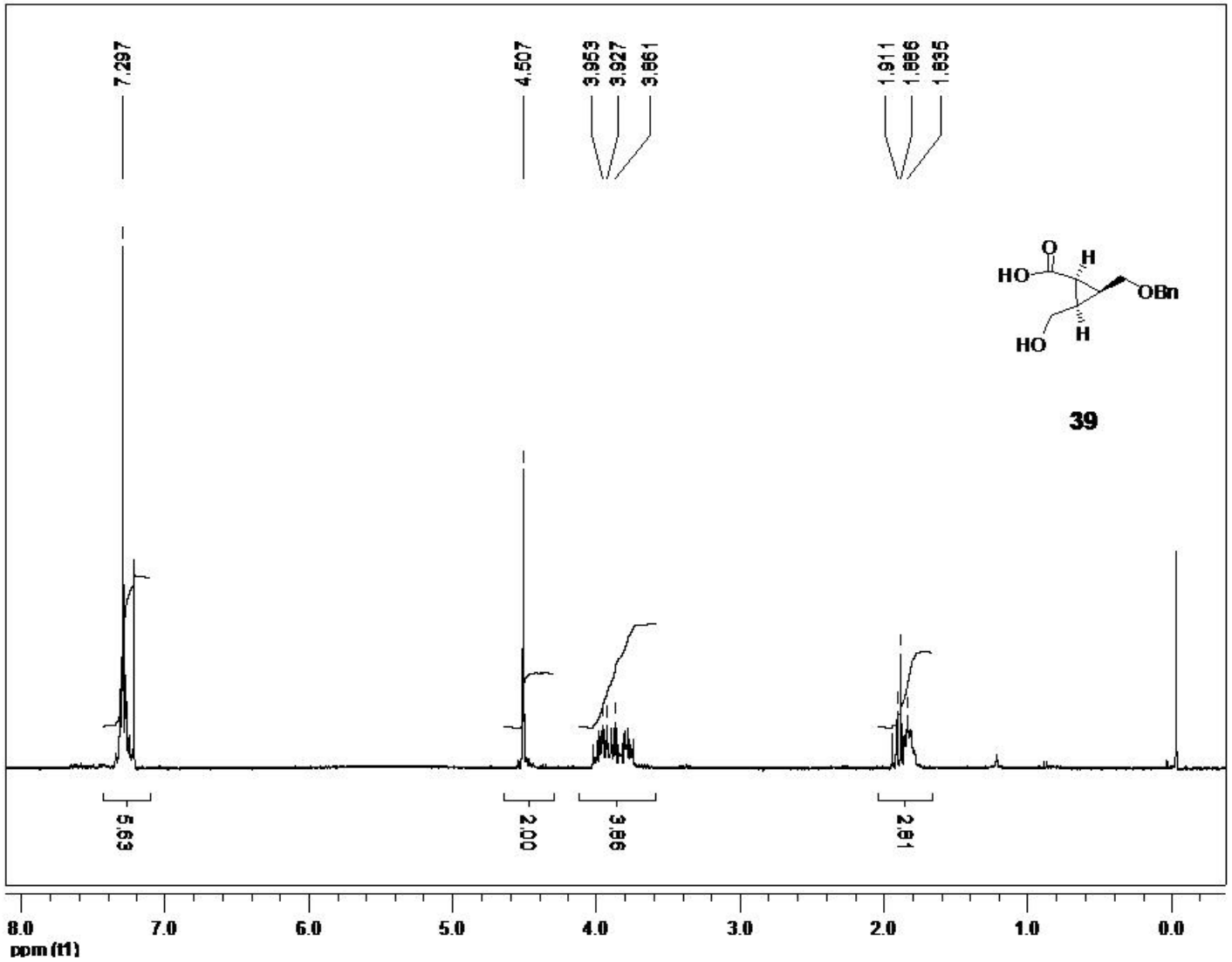


**Figure A-24. 2-(benzyloxymethyl)-3-(hydroxymethyl)cyclopropanecarboxylic acid**

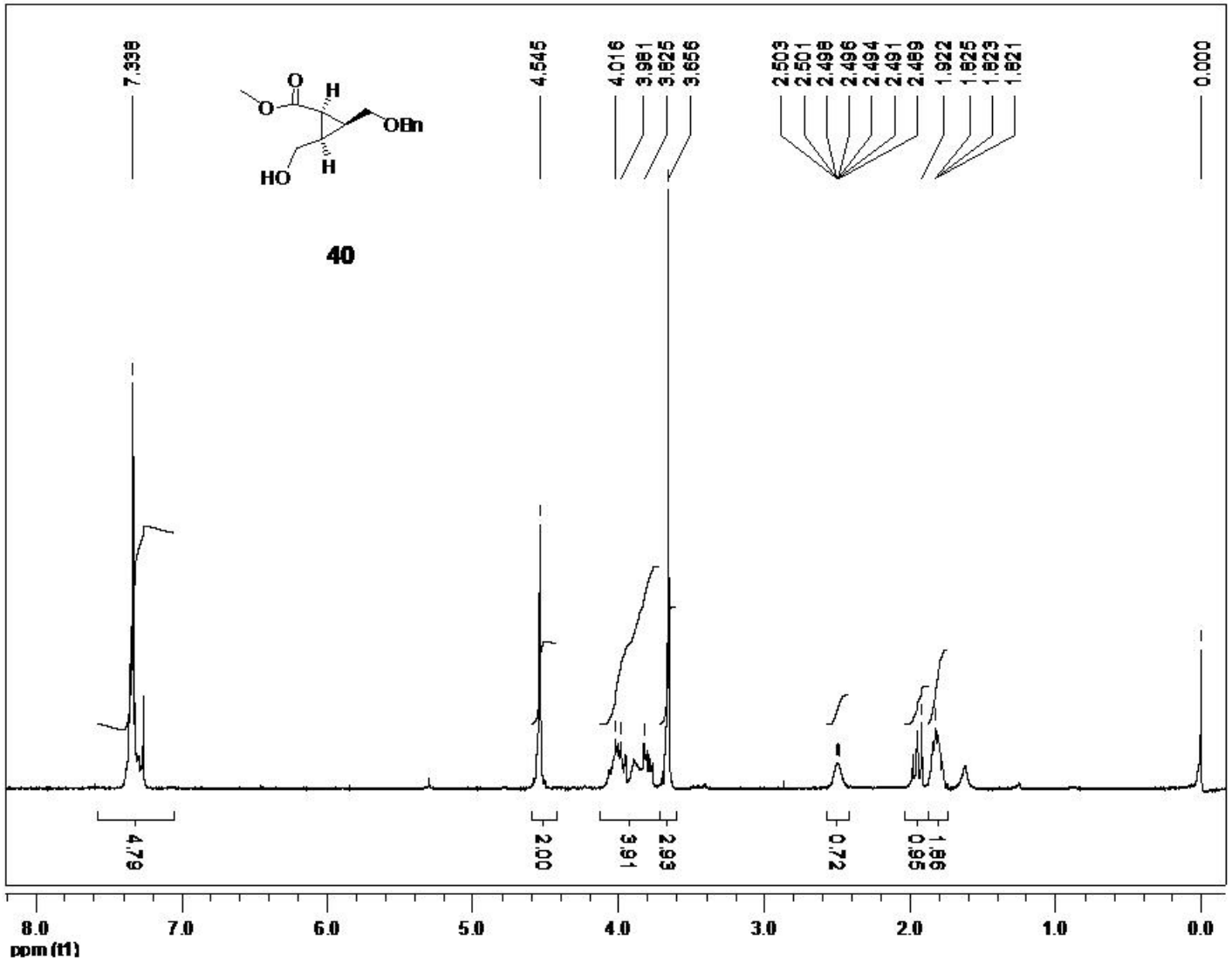


**Figure A-25. Methyl 2-(benzyloxymethyl)-3-(hydroxymethyl)cyclopropanecarboxylate**

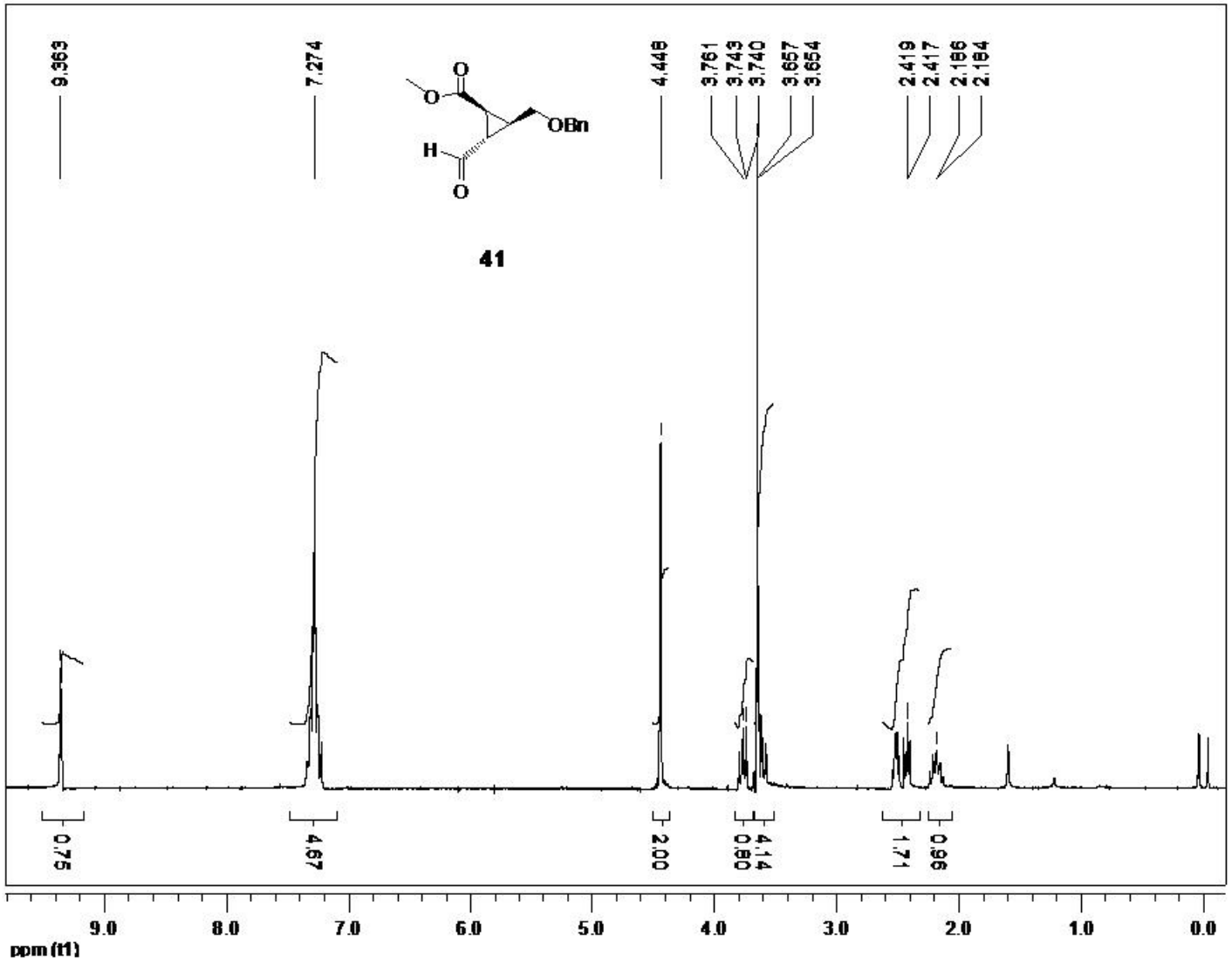


**Figure A-26. (1R,2R,3R)-methyl 2-(benzyloxymethyl)-3-formylcyclopropanecarboxylate**

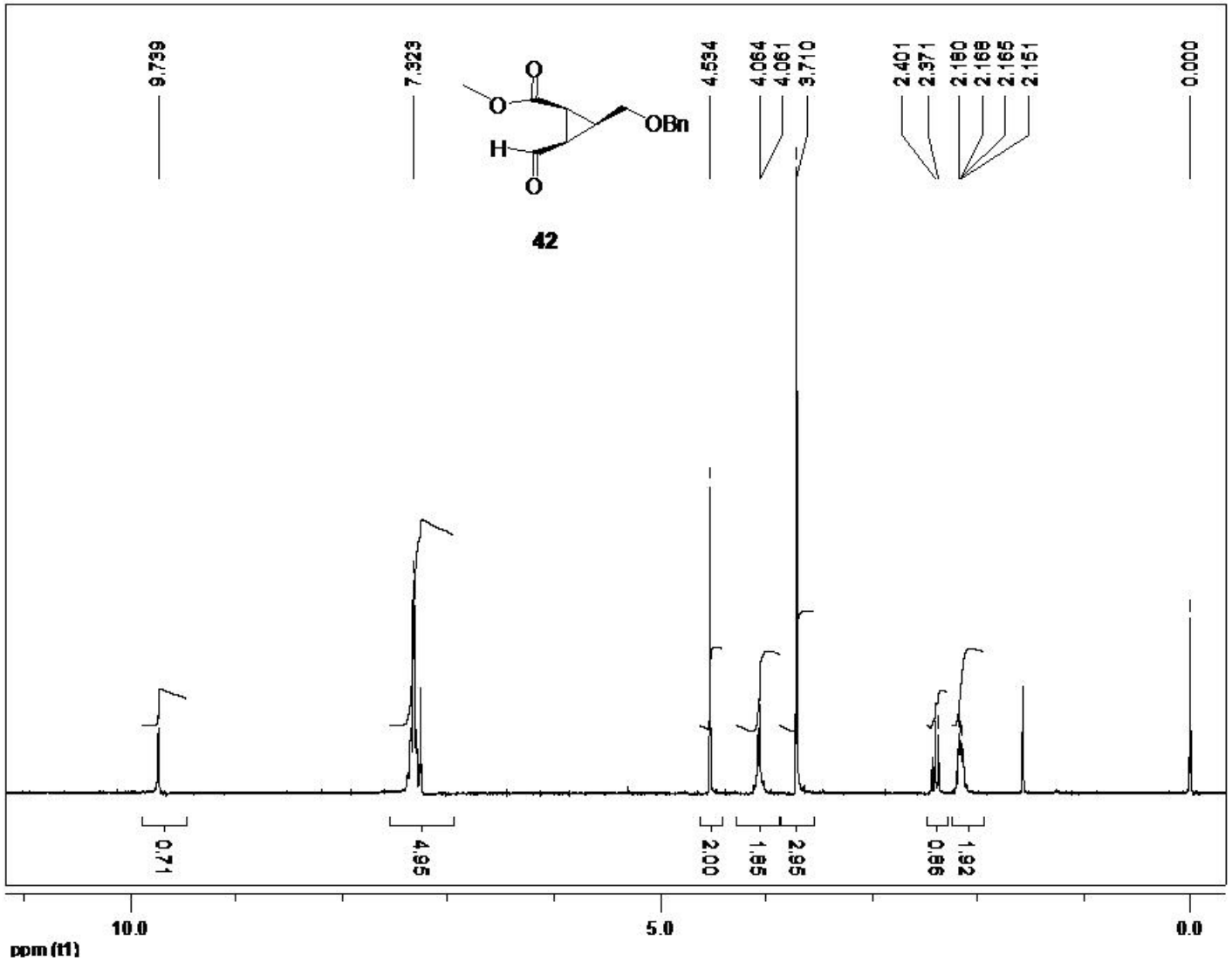


**Figure A-27. (1R,2R,3S)-methyl 2-(benzyloxymethyl)-3-formylcyclopropanecarboxylate**

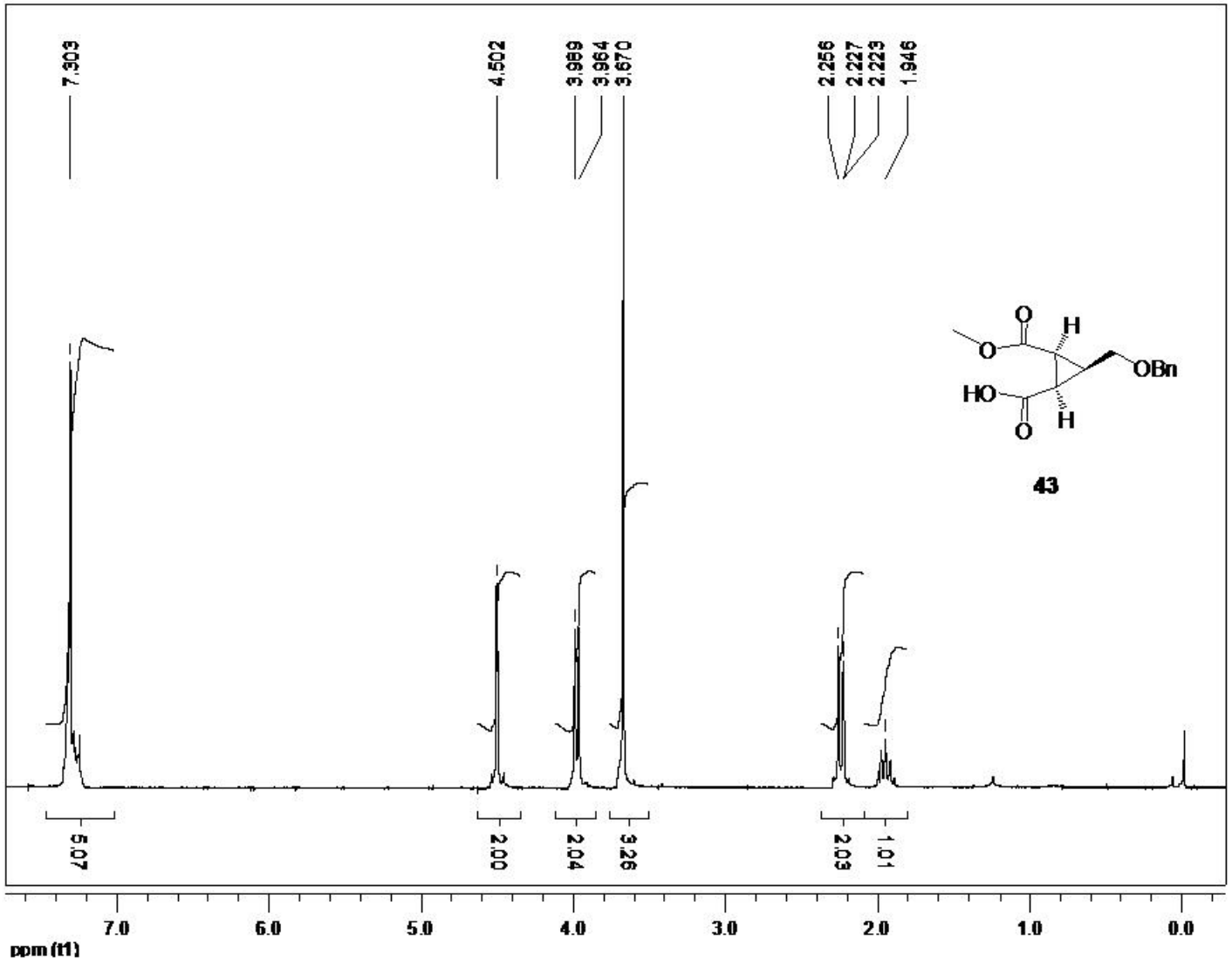


**Figure A-28. 2-(benzyloxymethyl)-3-(methoxycarbonyl)cyclopropanecarboxylic acid**

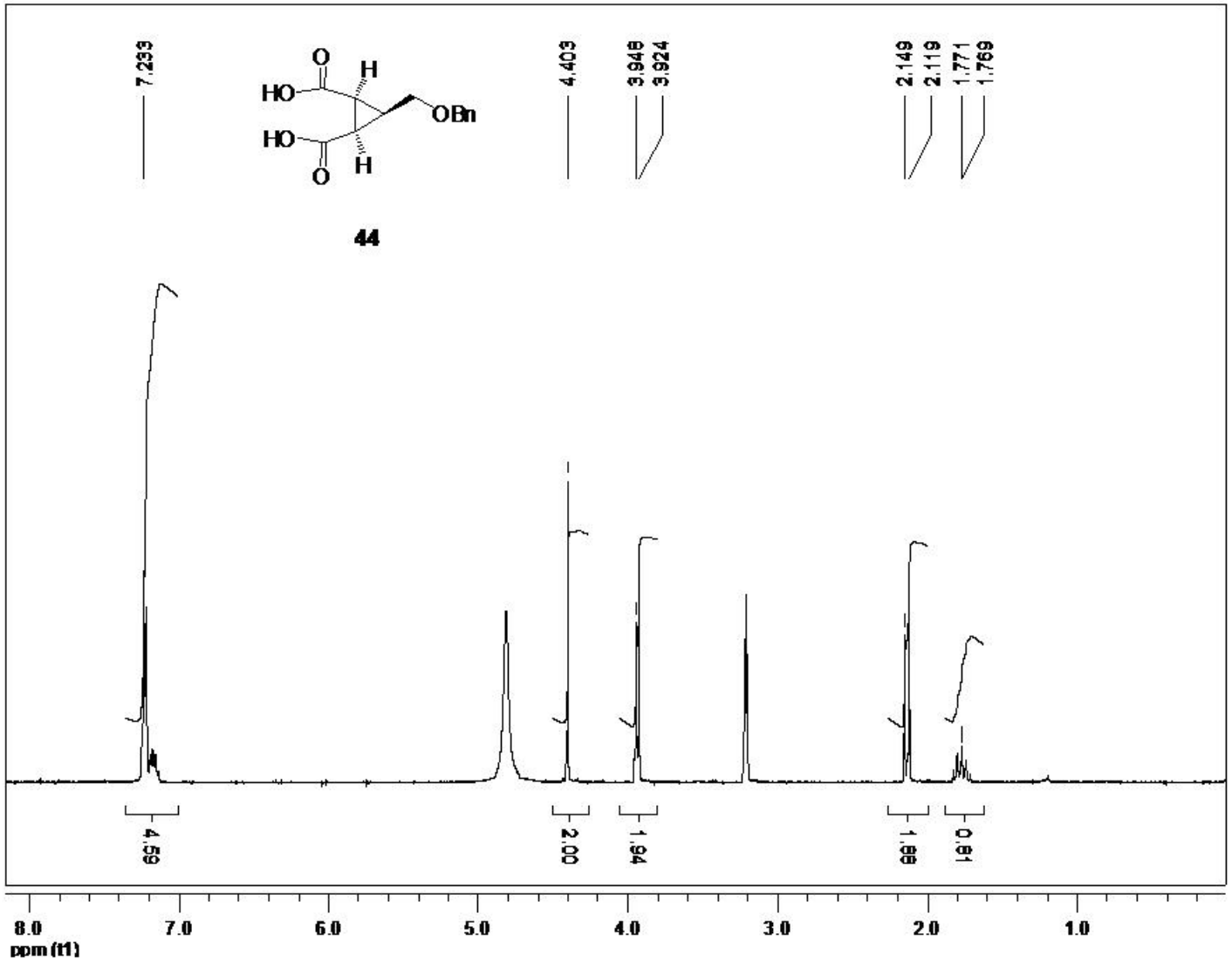


**Figure A-29. 3-(benzyloxymethyl)cyclopropane-1,2-dicarboxylic acid**

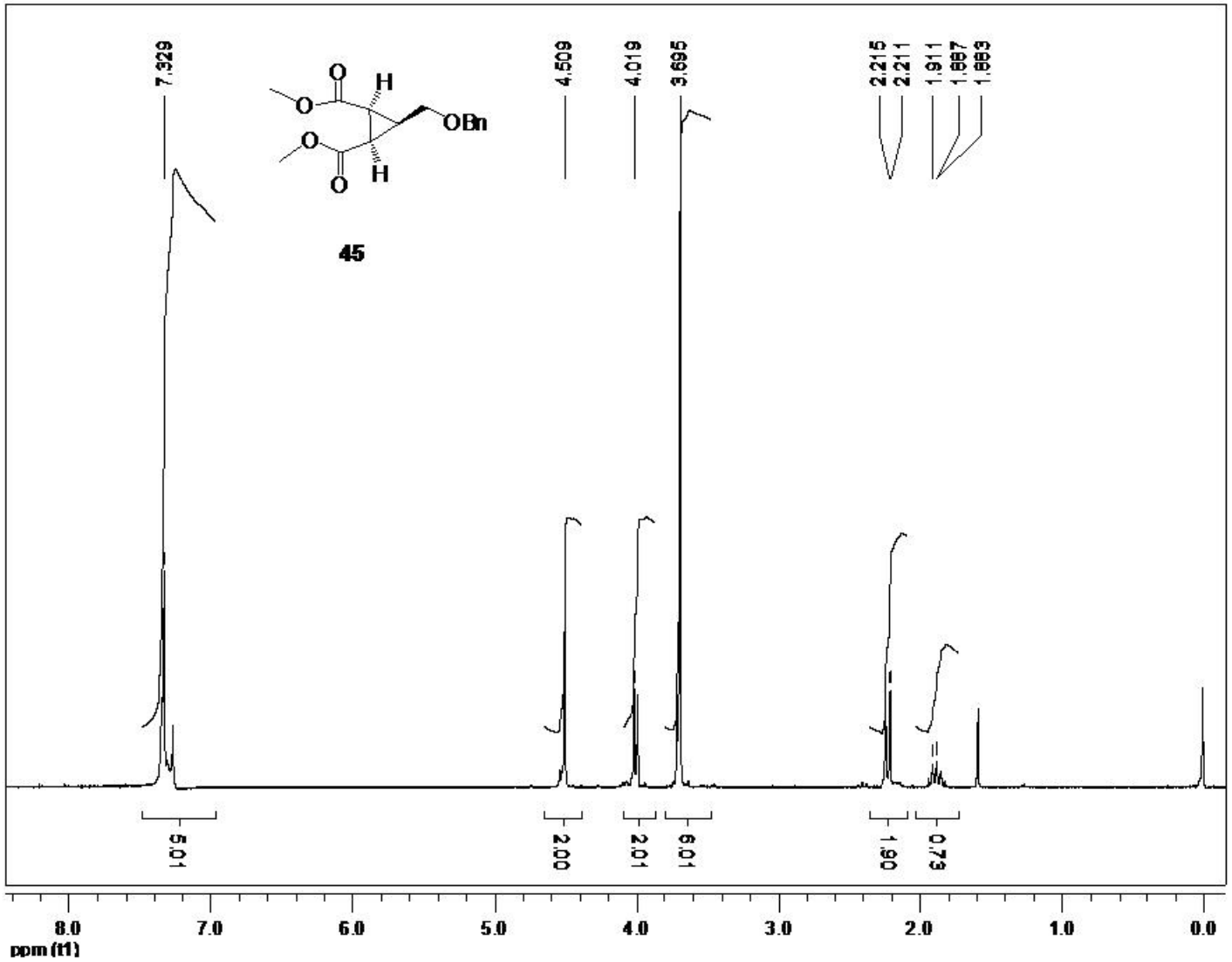


**Figure A-30. Dimethyl 3-(benzyloxymethyl)cyclopropane-1,2-dicarboxylate**

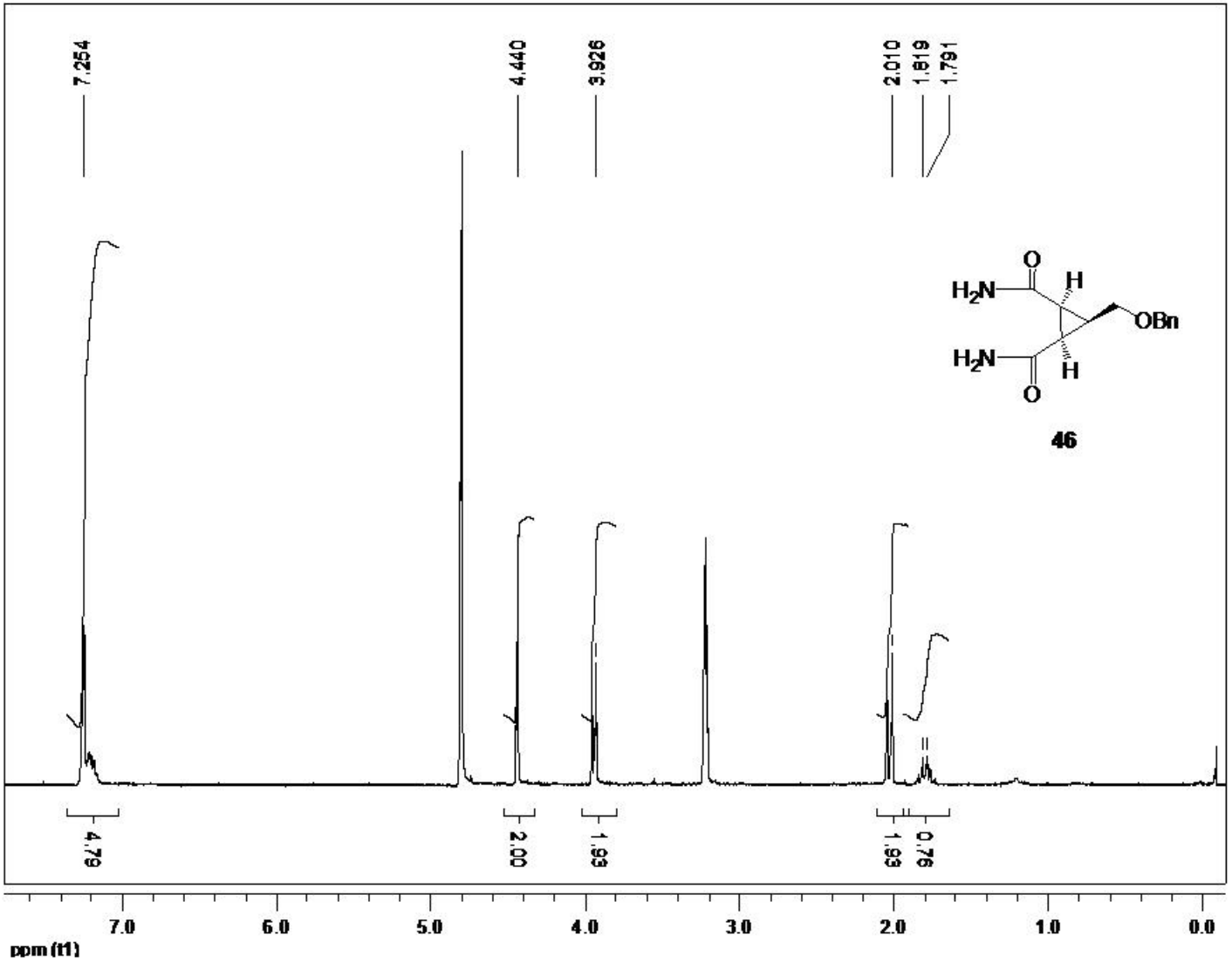


**Figure A-31. 3-(benzyloxymethyl)cyclopropane-1,2-dicarboxamide**

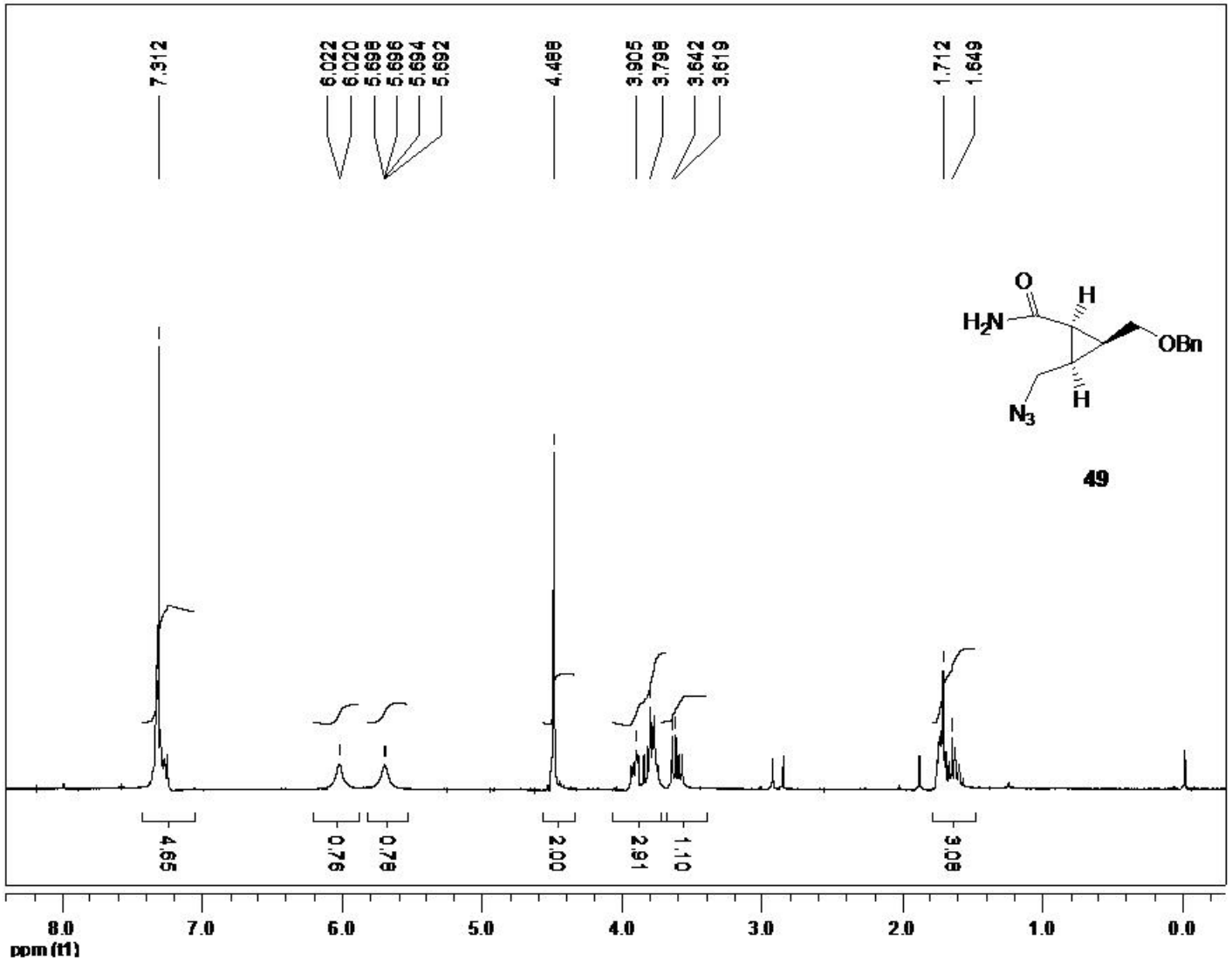


**Figure A-32. 2-(azidomethyl)-3-(benzyloxymethyl)cyclopropanecarboxamide**

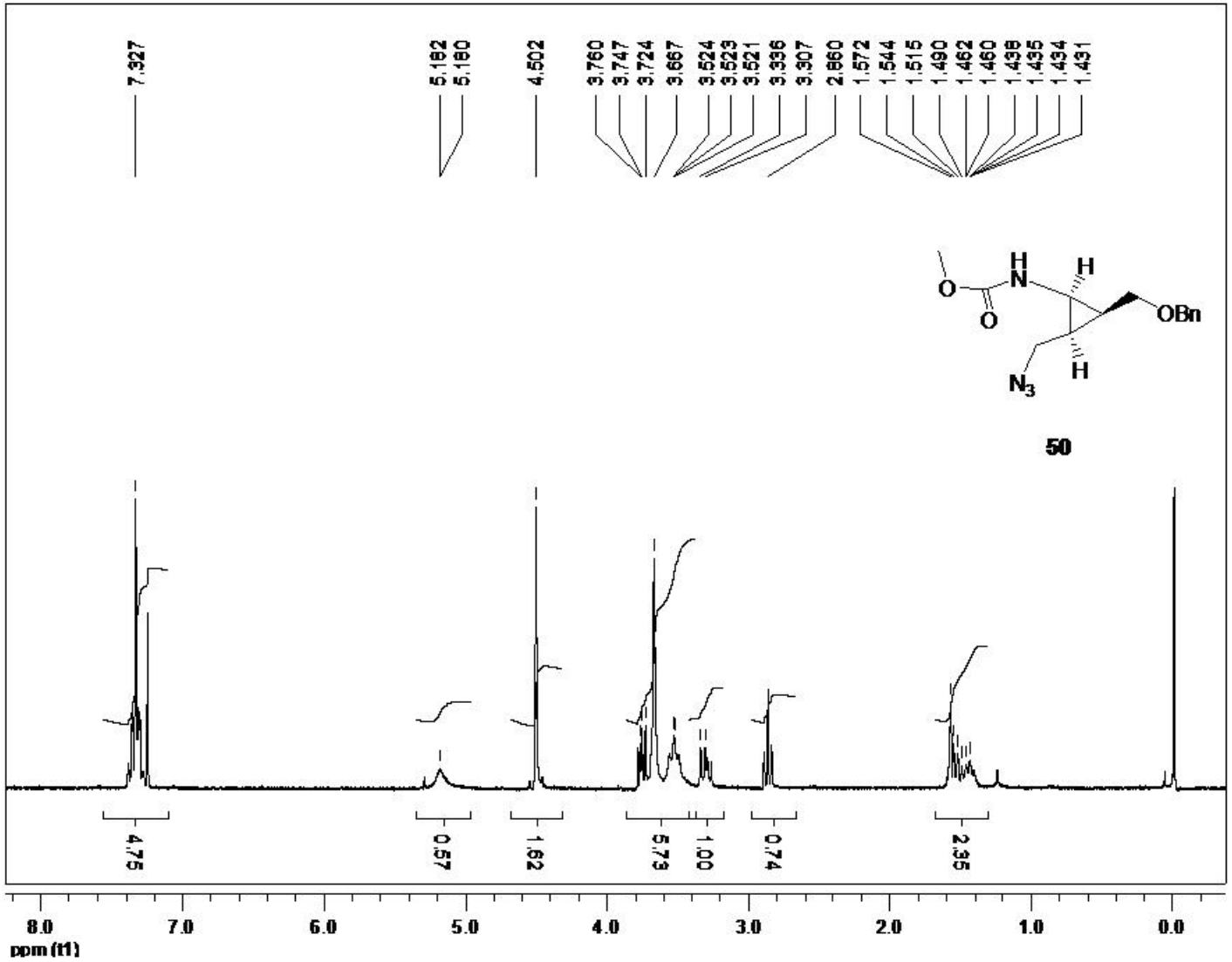


**Figure A-33. Methyl 2-(azidomethyl)-3-(benzyloxymethyl)cyclopropylcarbamate**

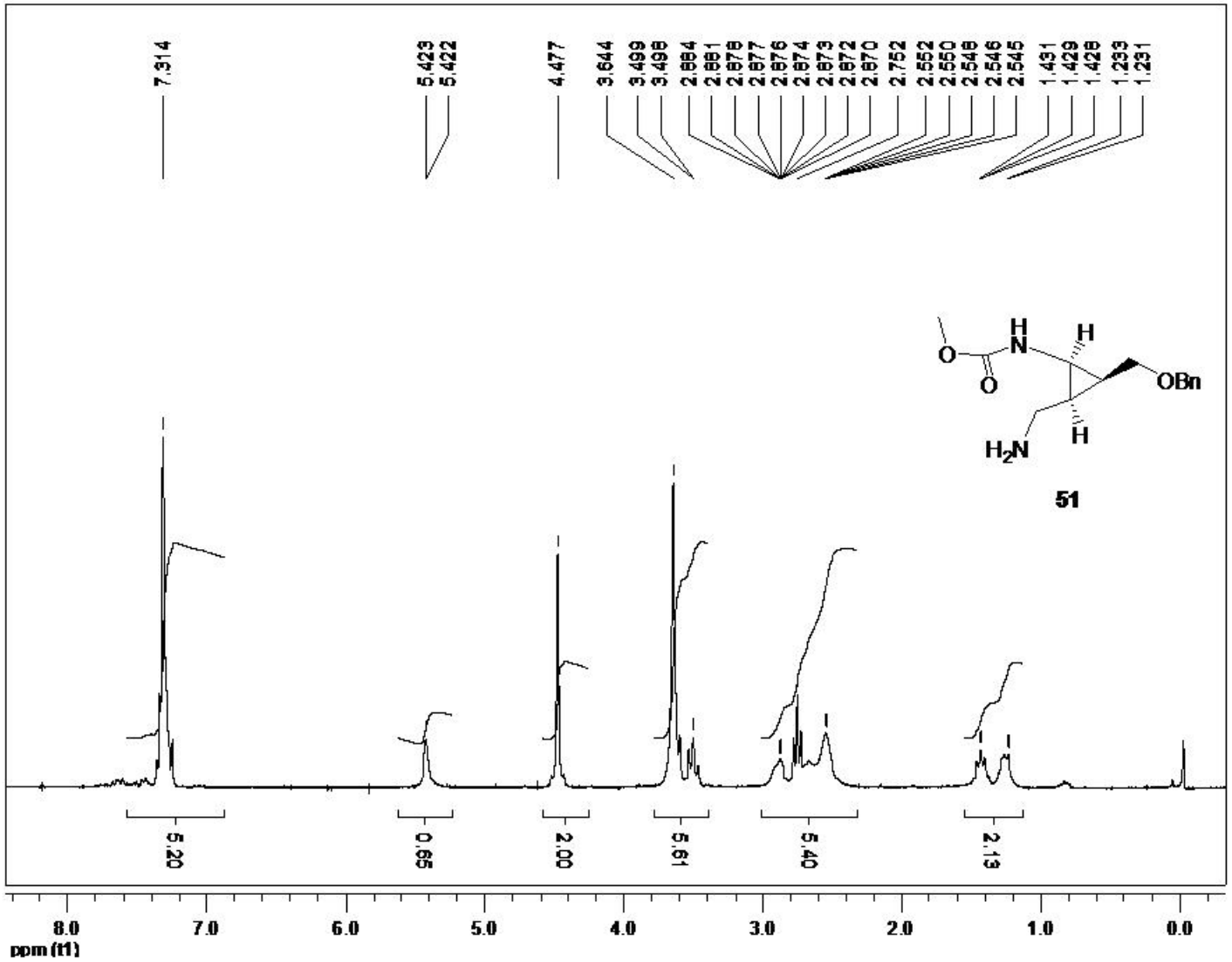


**Figure A-34. Methyl 2-(aminomethyl)-3-(benzyloxymethyl)cyclopropylcarbamate**

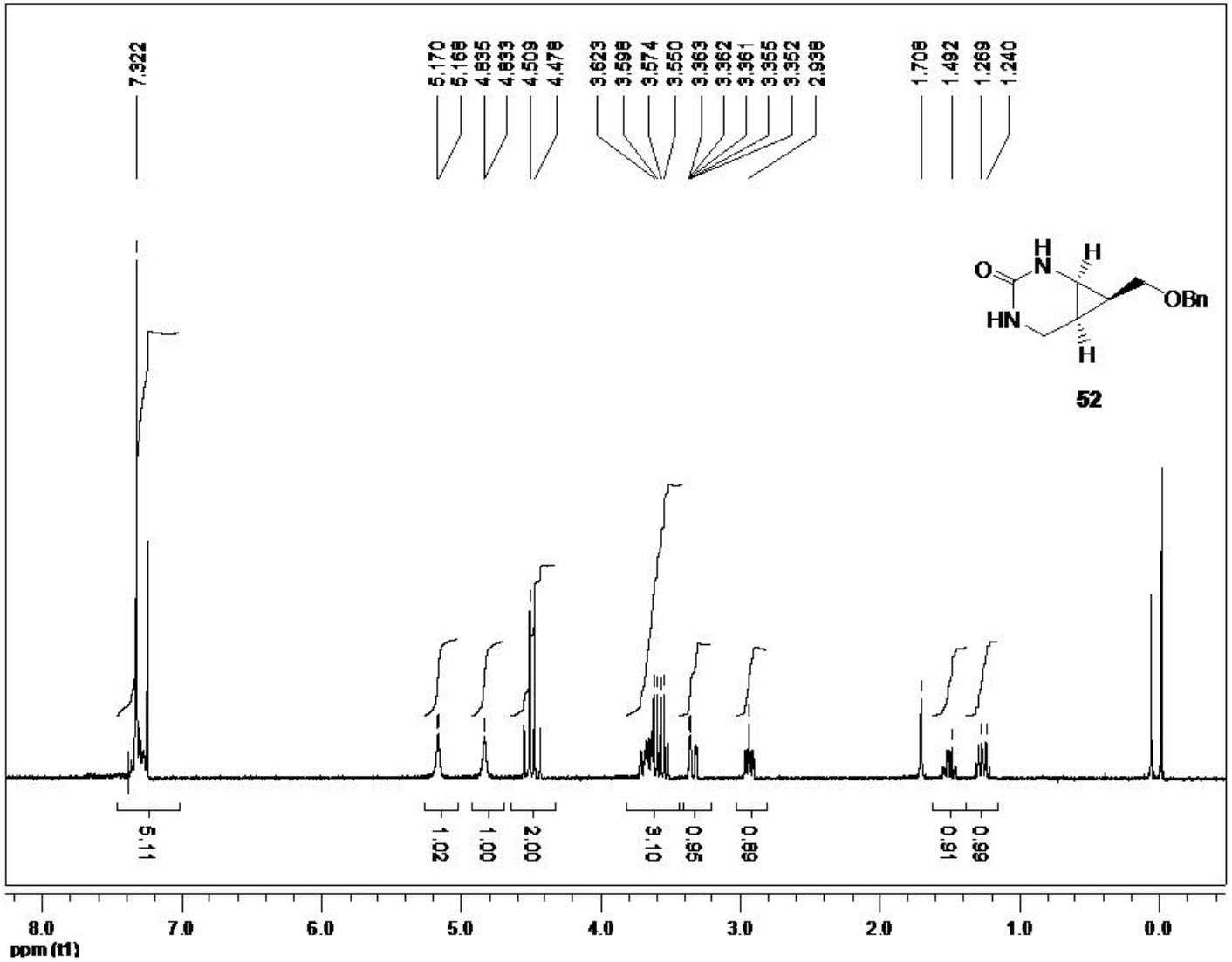


**Figure A-35. 7-(benzyloxymethyl)-2,4-diazabicyclo[4.1.0]heptan-3-one**

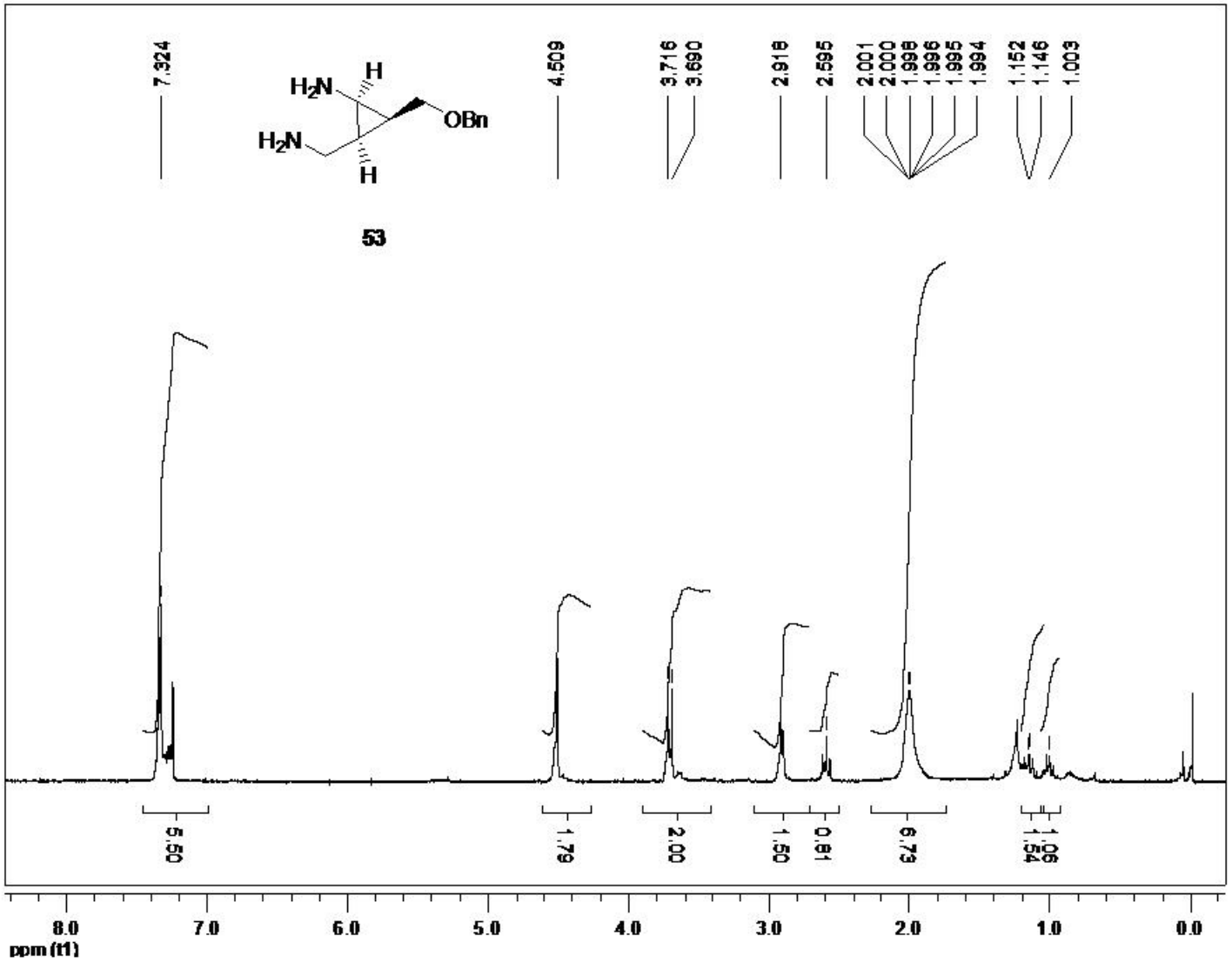


**Figure A-36. (1R,2S,3S)-2-(aminomethyl)-3-(benzyloxymethyl)cyclopropanamine**

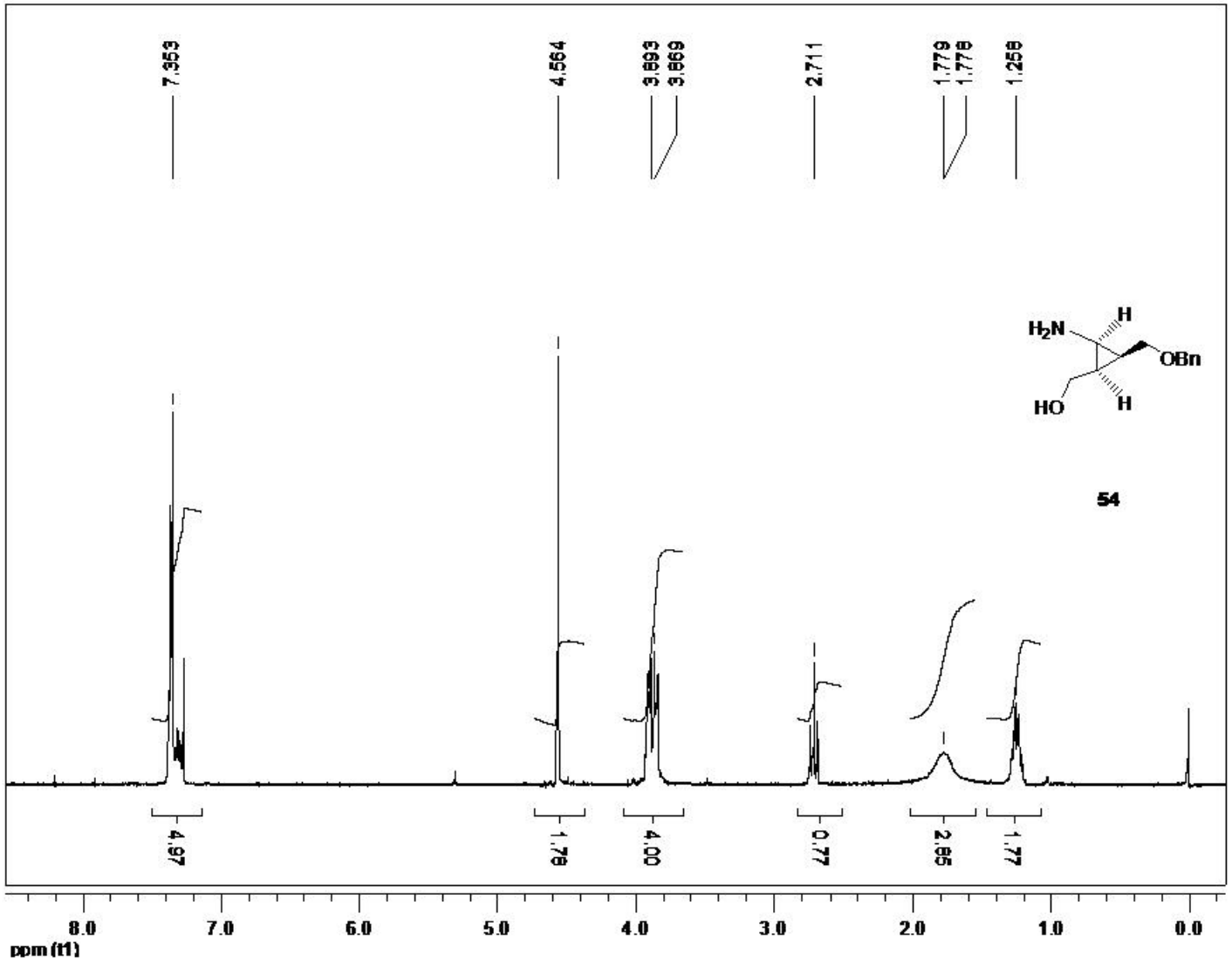


**Figure A-37. ((1R,2R,3S)-2-amino-3-(benzyloxymethyl)cyclopropyl)methanol**

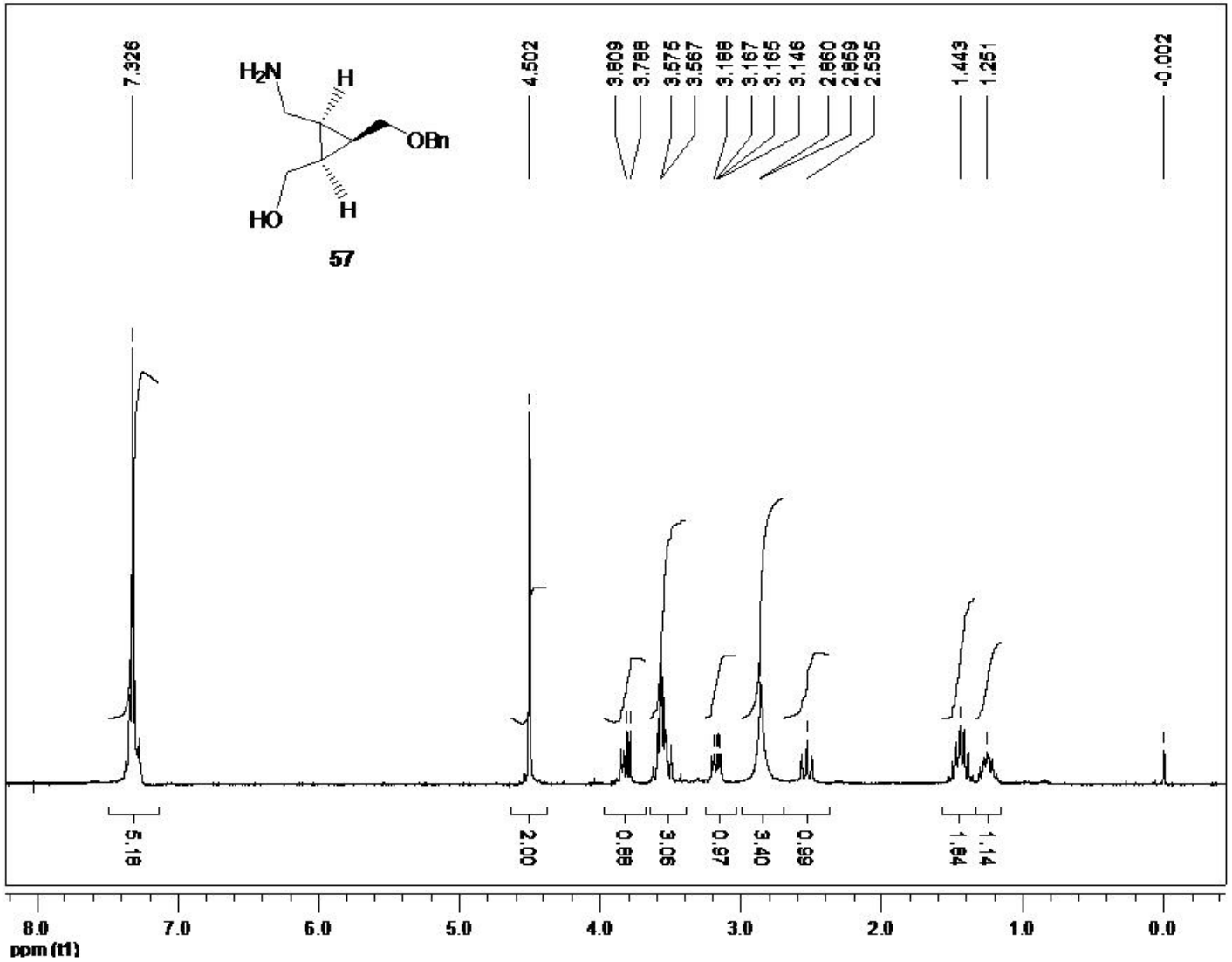


**Figure A-38. ((1S,2R,3R)-2-(aminomethyl)-3-(benzyloxymethyl)cyclopropyl)methanol**

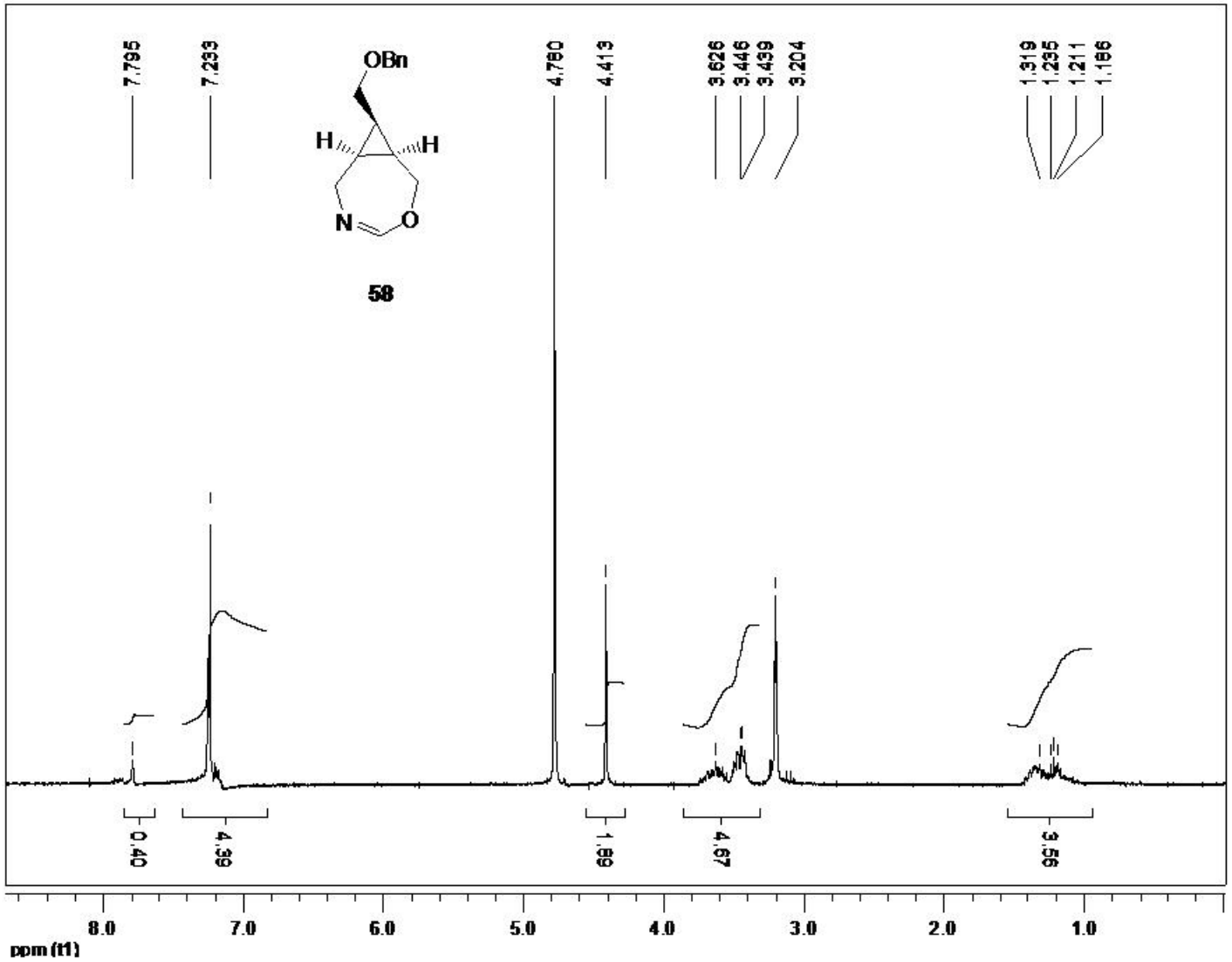


**Figure A-39. (Z)-8-(benzyloxymethyl)-3-oxa-5-azabicyclo[5.1.0]oct-4-ene**

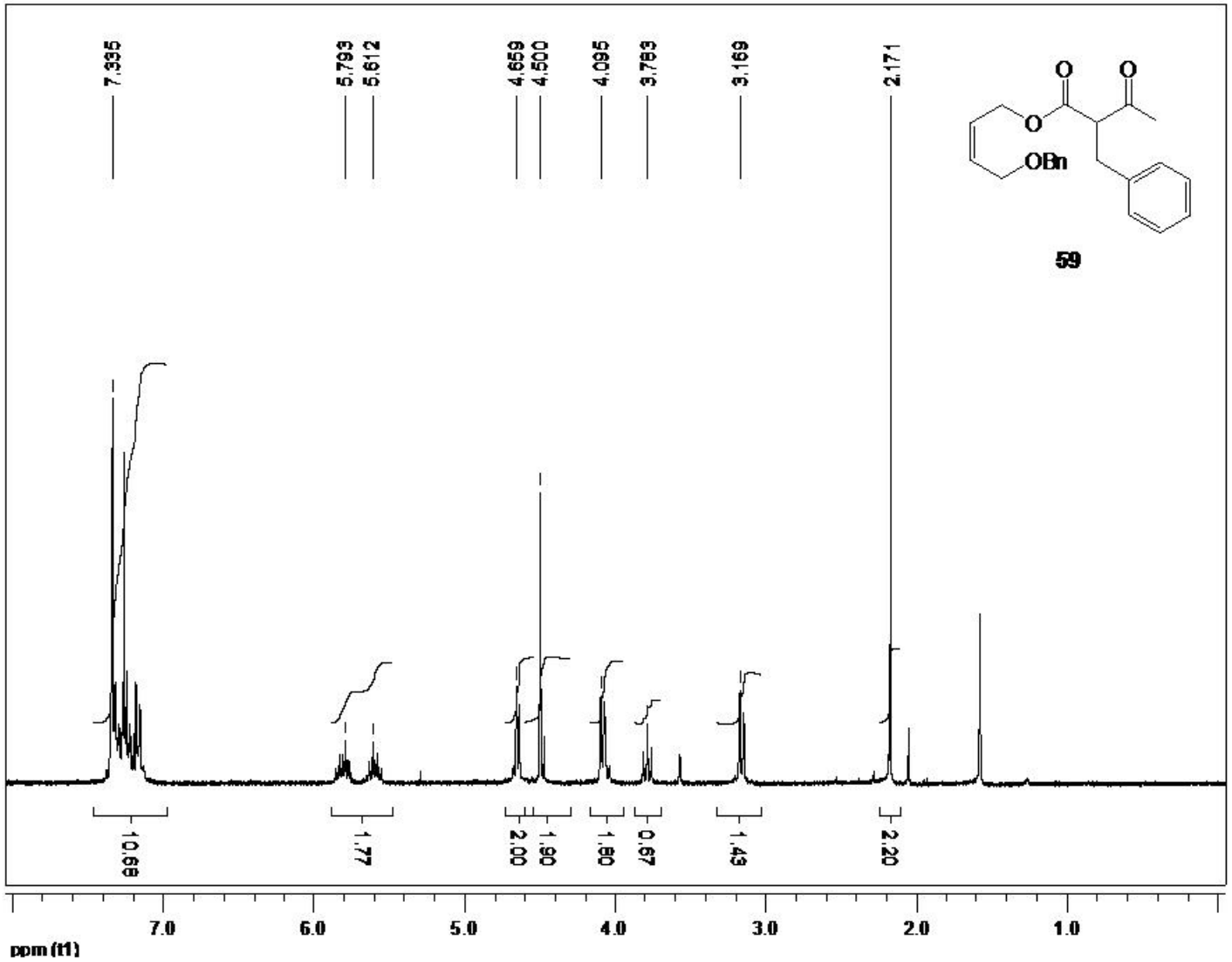


**Figure A-40. (Z)-4-(benzyloxy)but-2-enyl 2-benzyl-3-oxobutanoate**

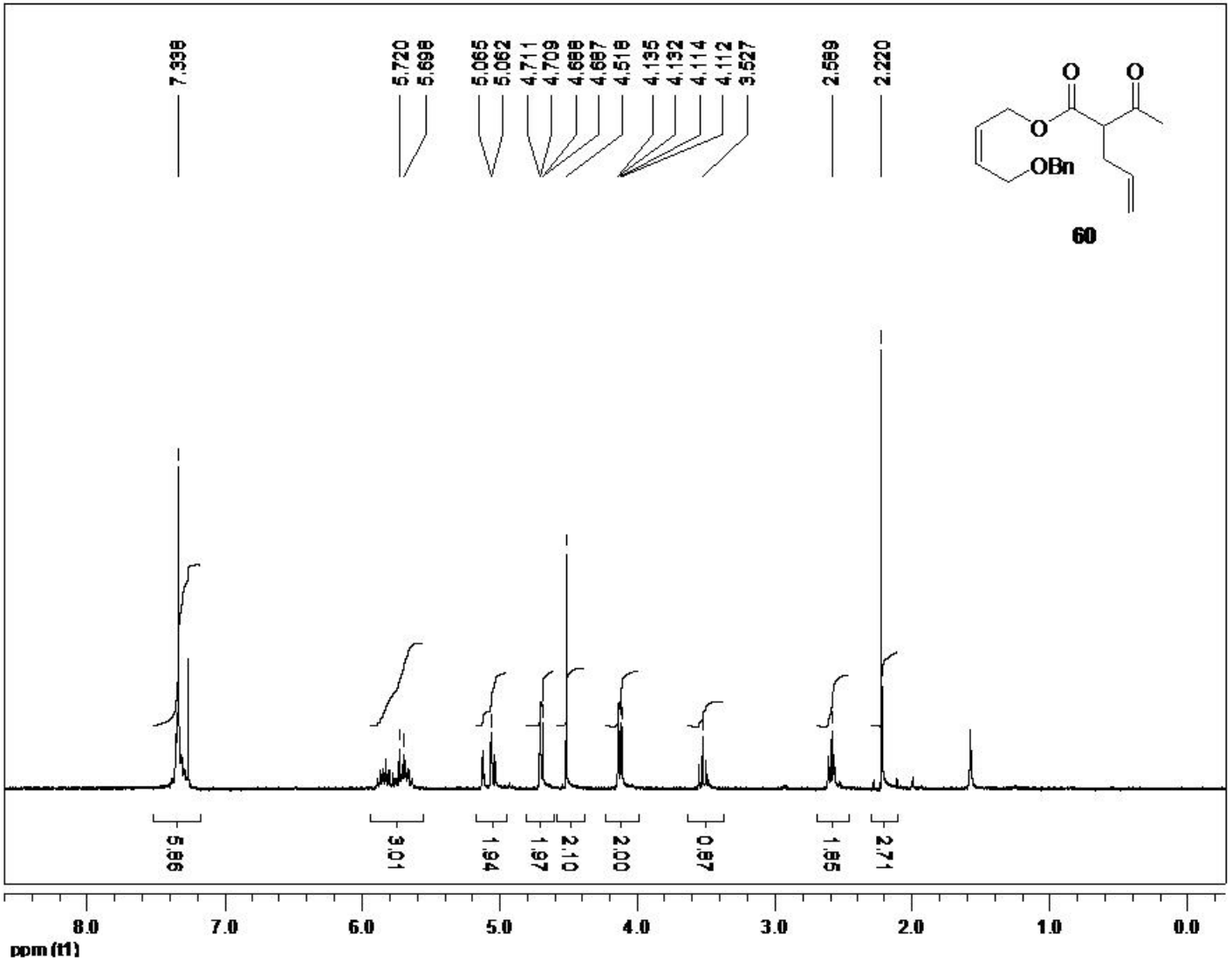


**Figure A-41. (Z)-4-(benzyloxy)but-2-enyl 2-acetylpent-4-enoate**

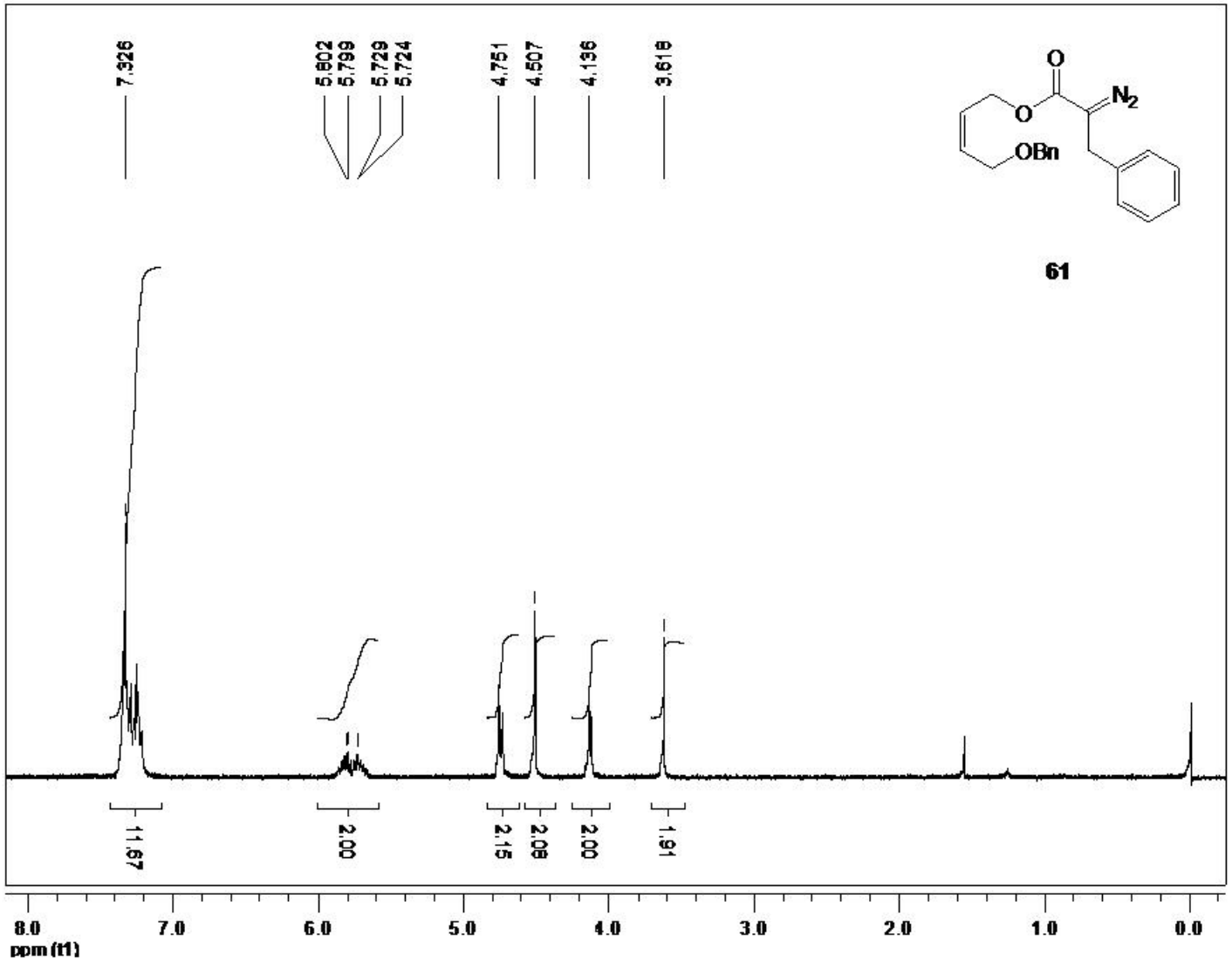


**Figure A-42. (Z)-4-(benzyloxy)but-2-enyl 2-diazo-3-phenylpropanoate**

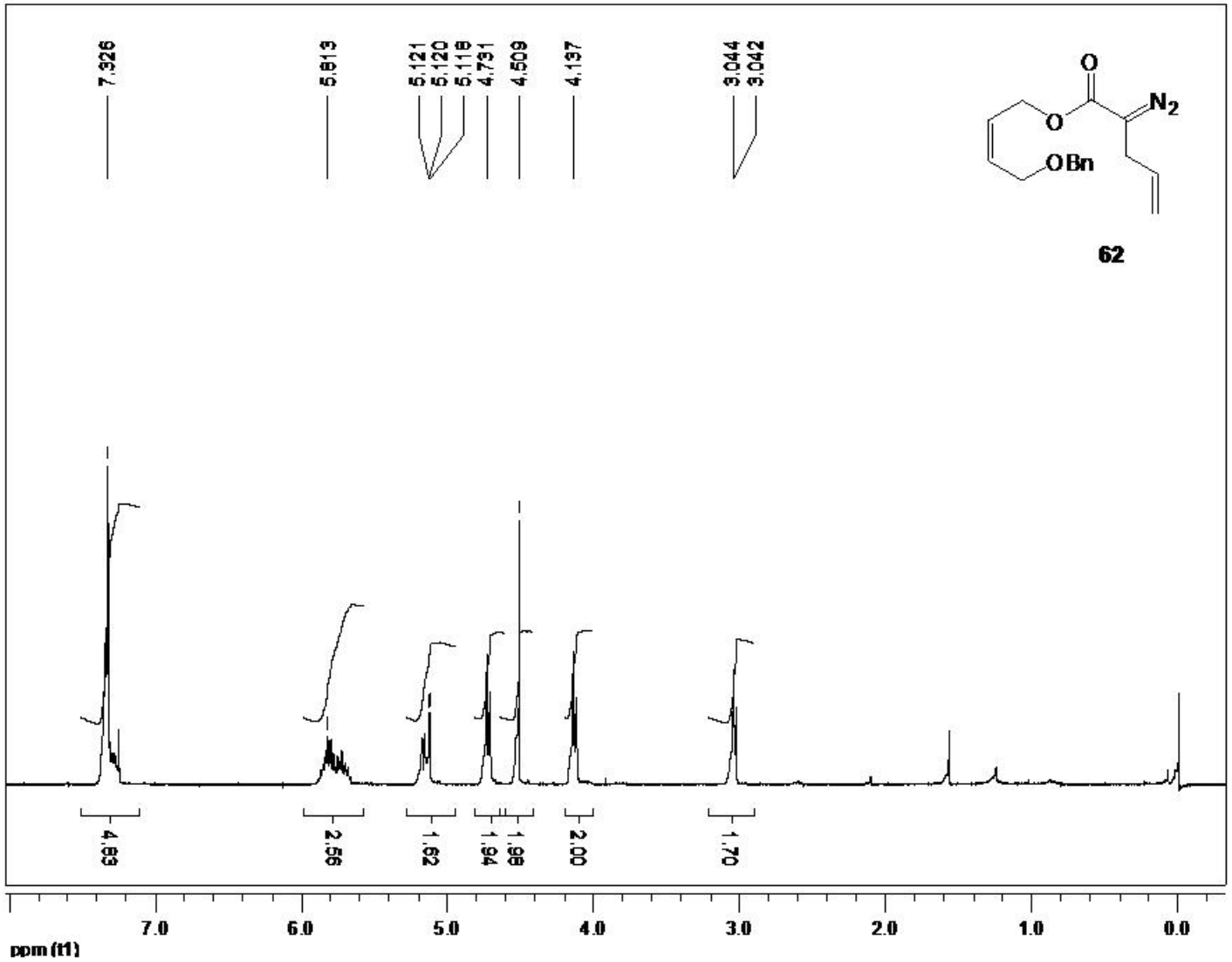


**Figure A-43. (Z)-4-(benzyloxy)but-2-enyl 2-diazopent-4-enoate**

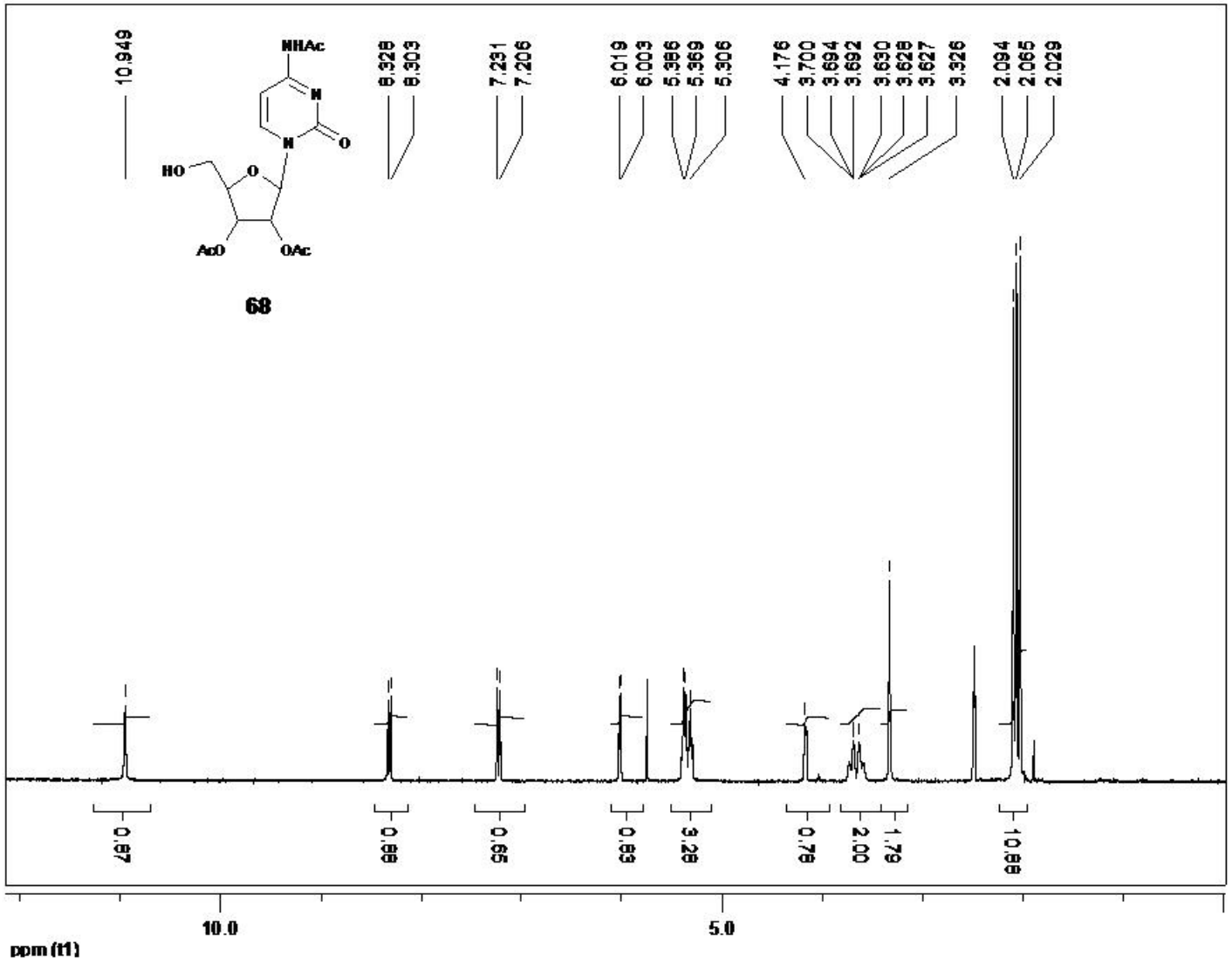


**Figure A-44. 2',3'-O,$N^4$-Triacetyl Cytidine**

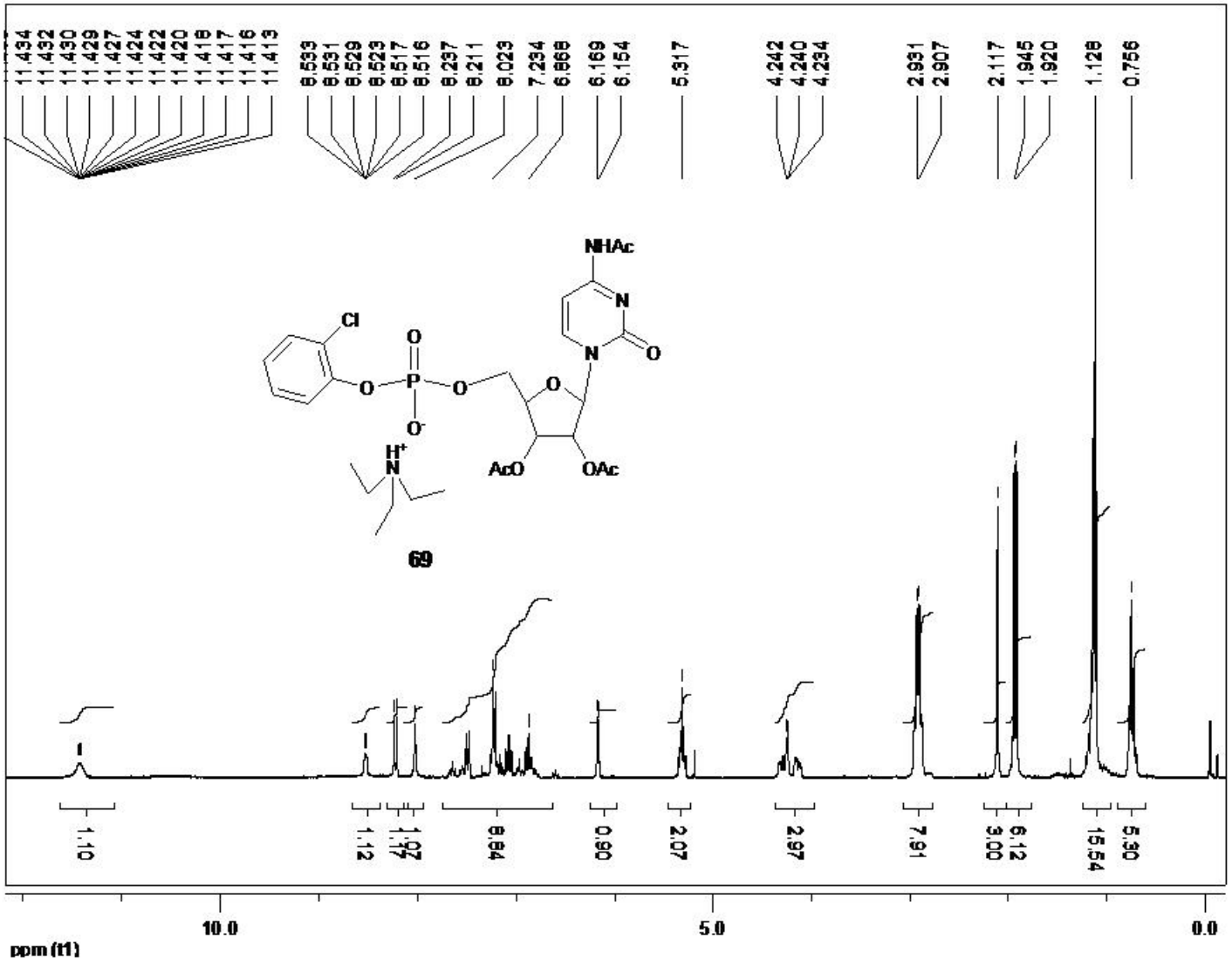


**Figure A-45. Triethylammonium (5-(4-acetamido-2-oxopyrimidin-1(2H)-yl)-3,4-diacetoxy tetrahydrofuran-2-yl)methyl 2-chlorophenyl phosphate**

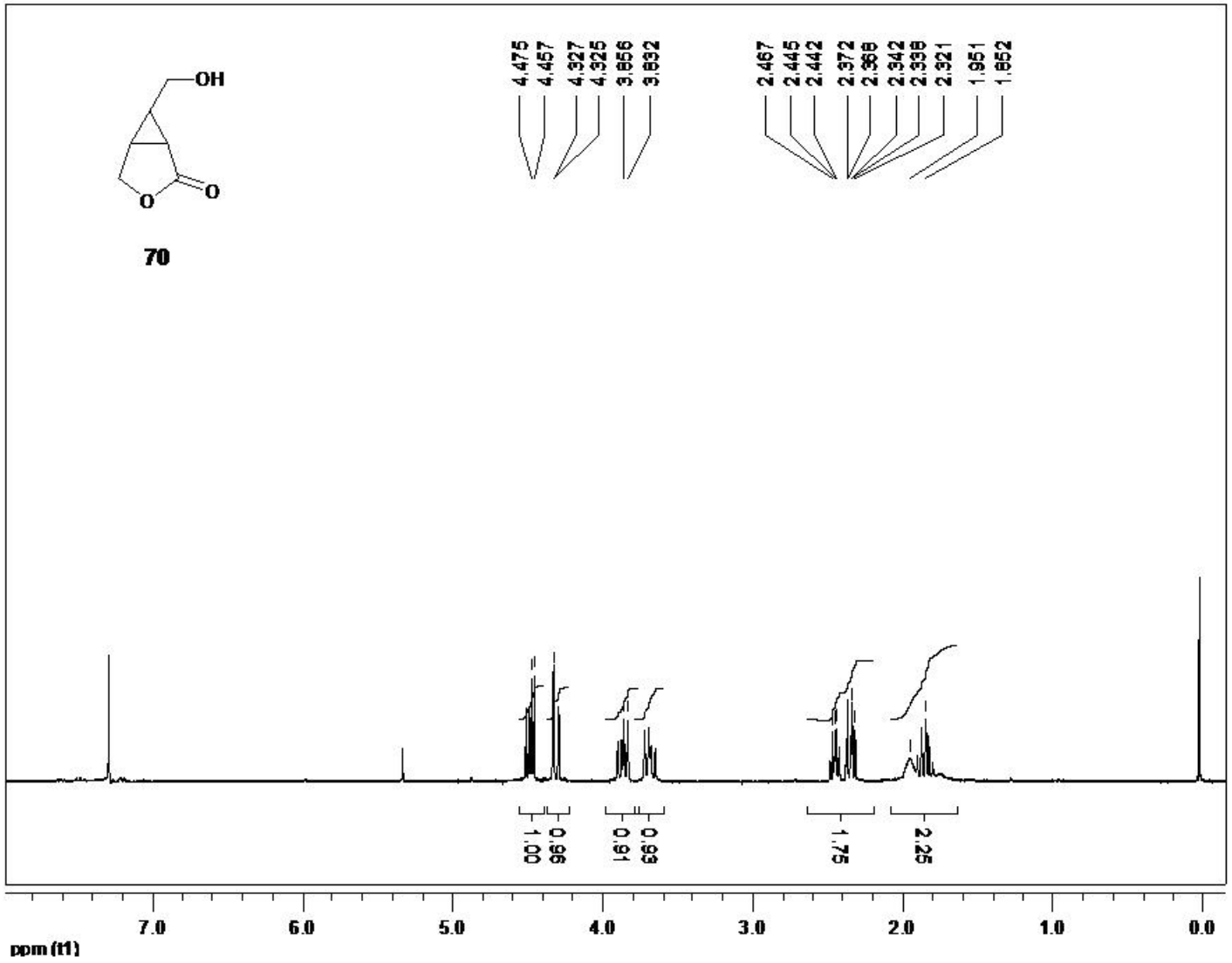


**Figure A-46. 6-(hydroxymethyl)-3-oxabicyclo[3.1.0]hexan-2-one**

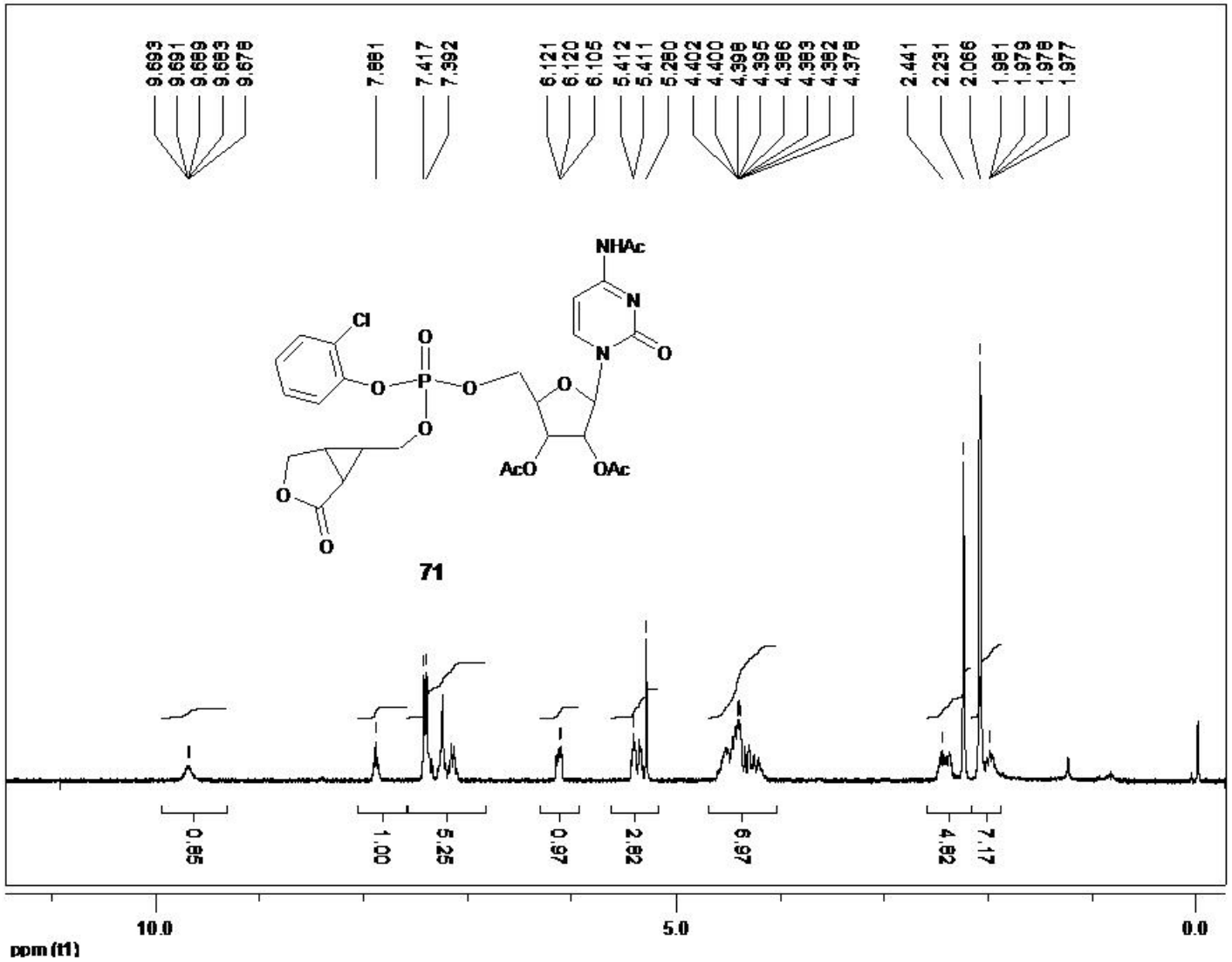


**Figure A-47. 2-(4-acetamido-2-oxopyrimidin-1(2H)-yl)-5-(((2-chlorophenoxy)((2-oxo-3-oxabicyclo[3.1.0]hexan-6-yl)methoxy)phosphoryloxy)methyl)tetrahydrofuran-3,4-diyl diacetate**

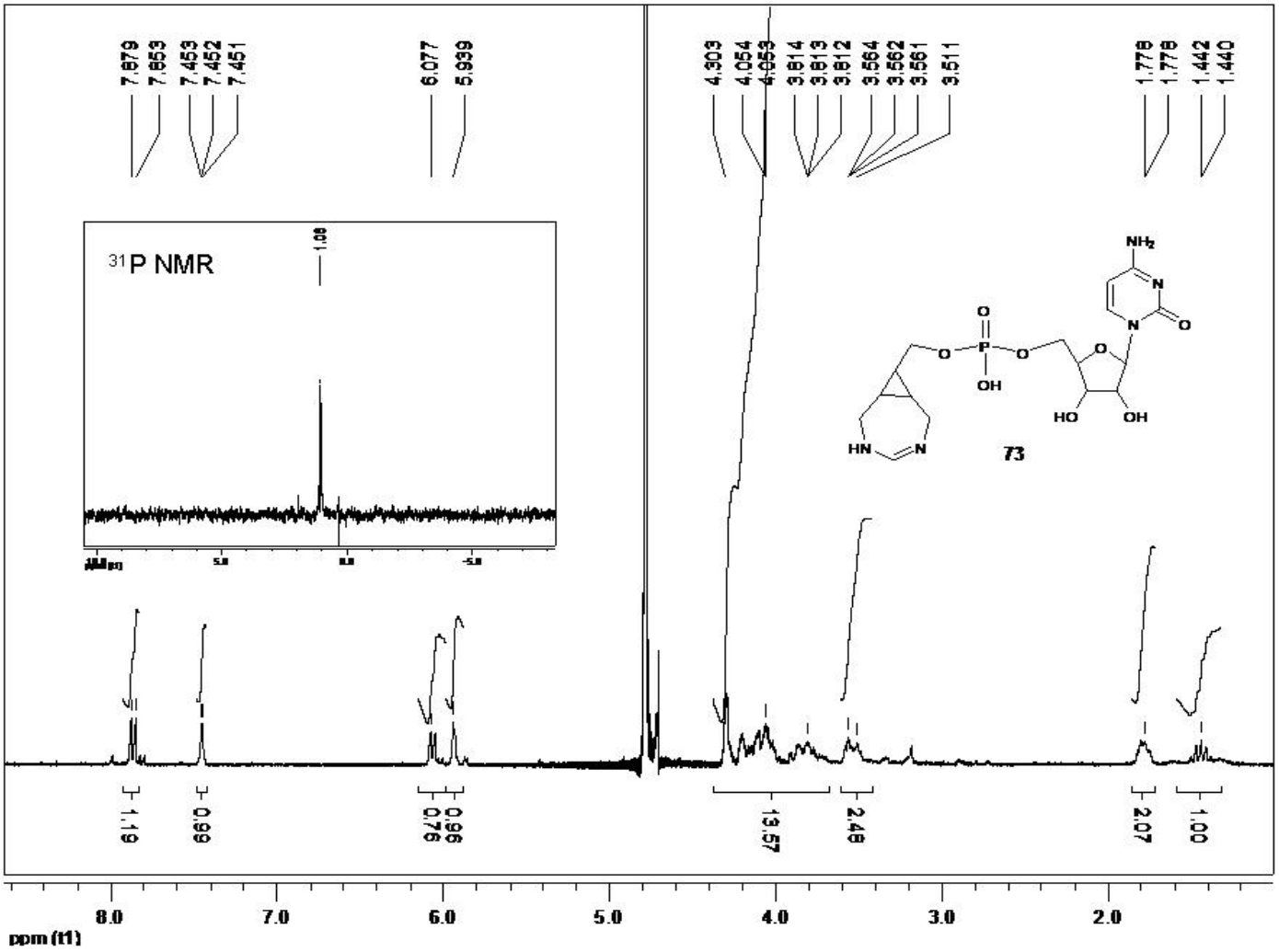


**Figure A-48. (Z)-3,5-diazabicyclo[5.1.0]oct-4-en-8-ylmethyl (5-(4-amino-2-oxopyrimidin-1(2H)-yl)-3,4-dihydroxytetrahydrofuran-2-yl)methyl hydrogen phosphate**

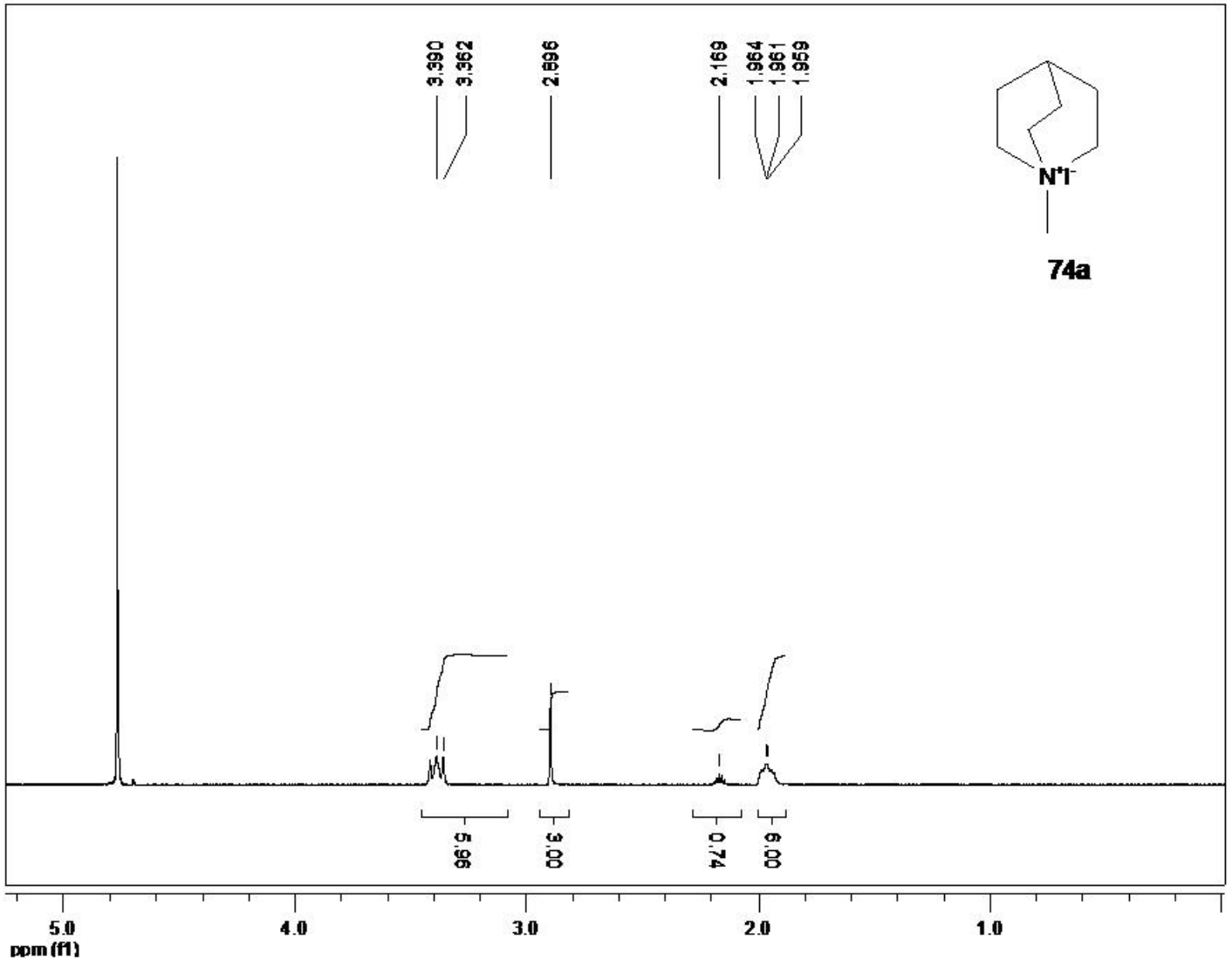


**Figure A-49. 1-methyl-1-azoniabicyclo[2.2.2]octane iodide**

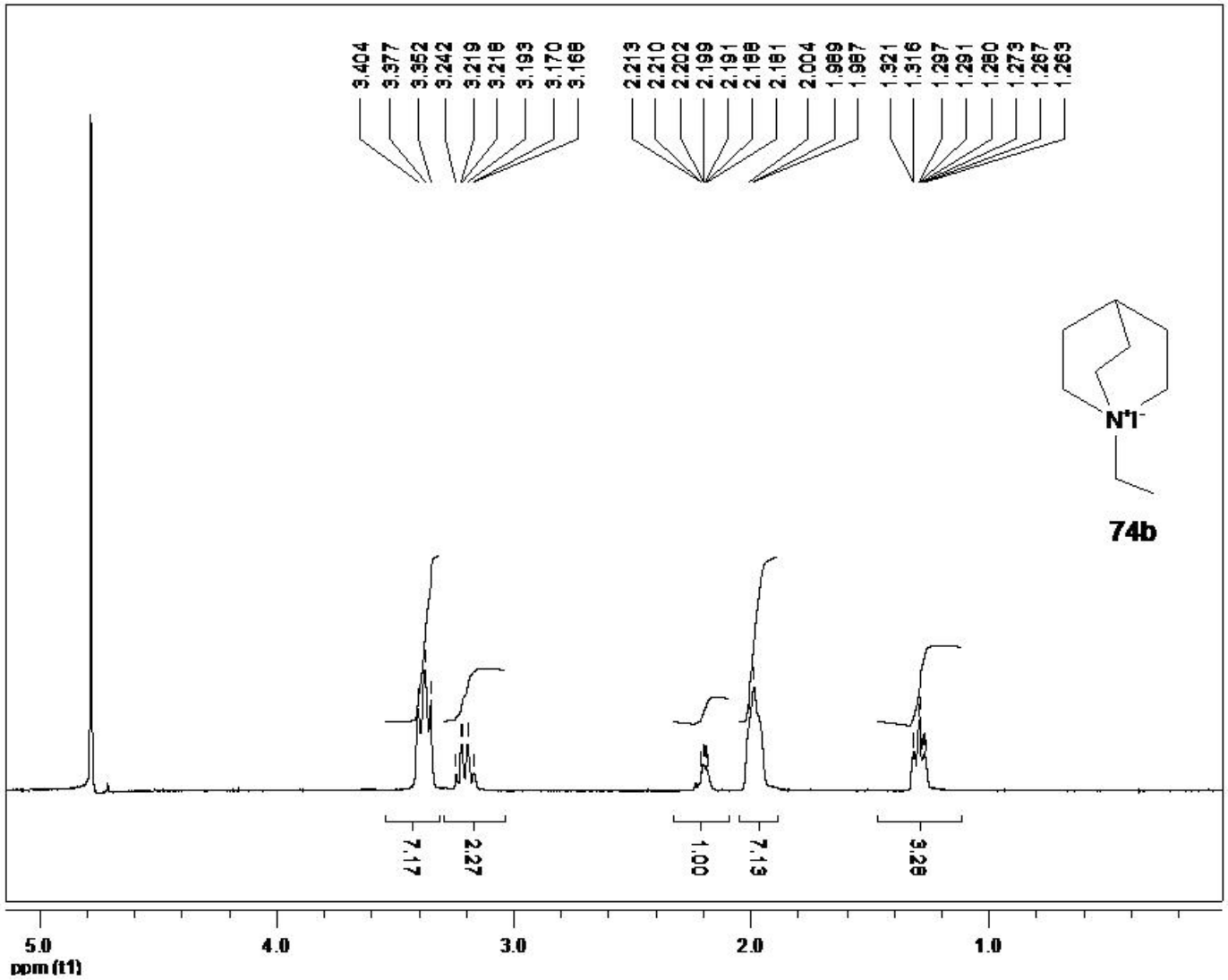


**Figure A-50. 1-ethyl-1-azoniabicyclo[2.2.2]octane iodide**

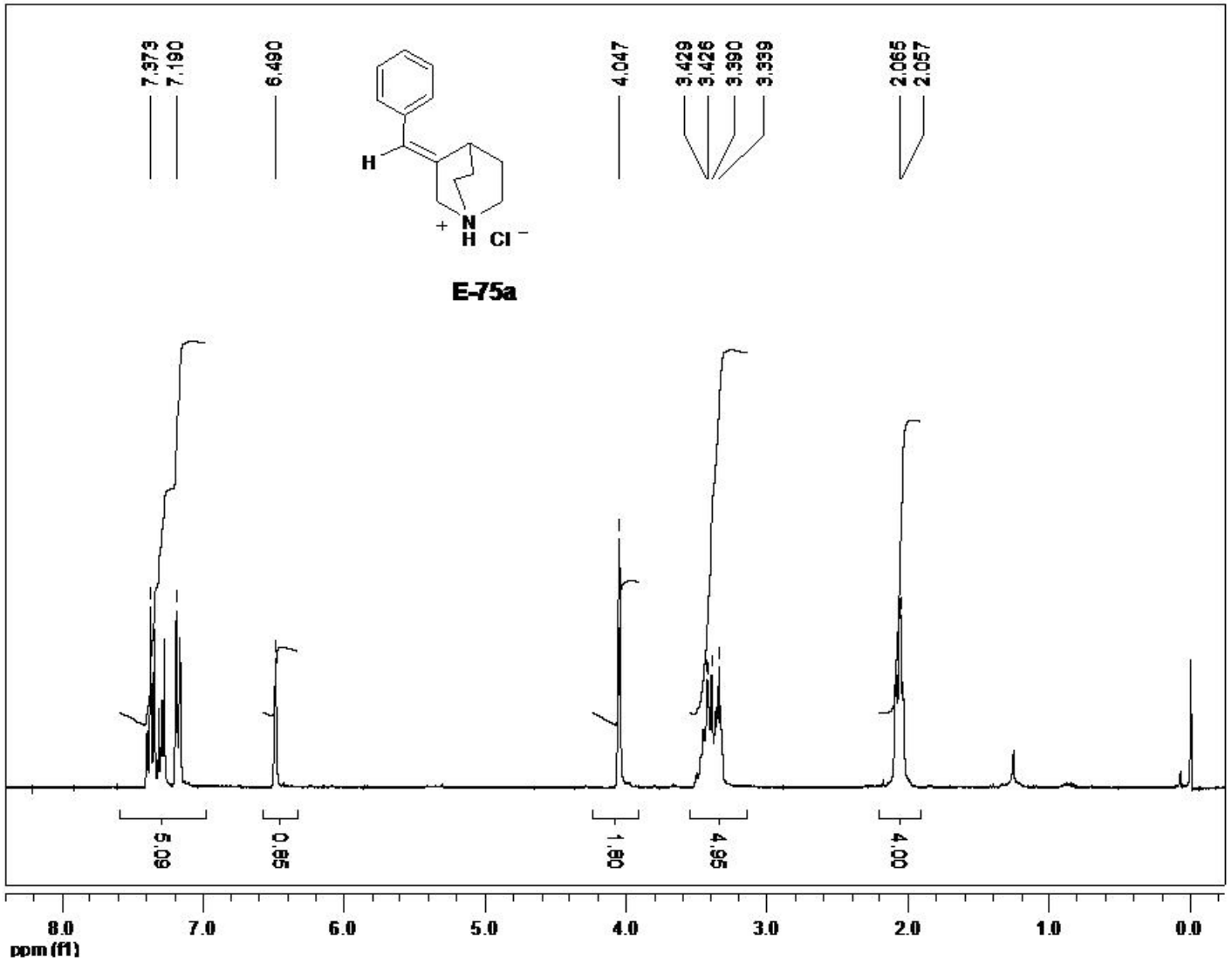


**Figure A-51. E-3-benzylidene-1-azoniabicyclo[2.2.2]octane chloride**

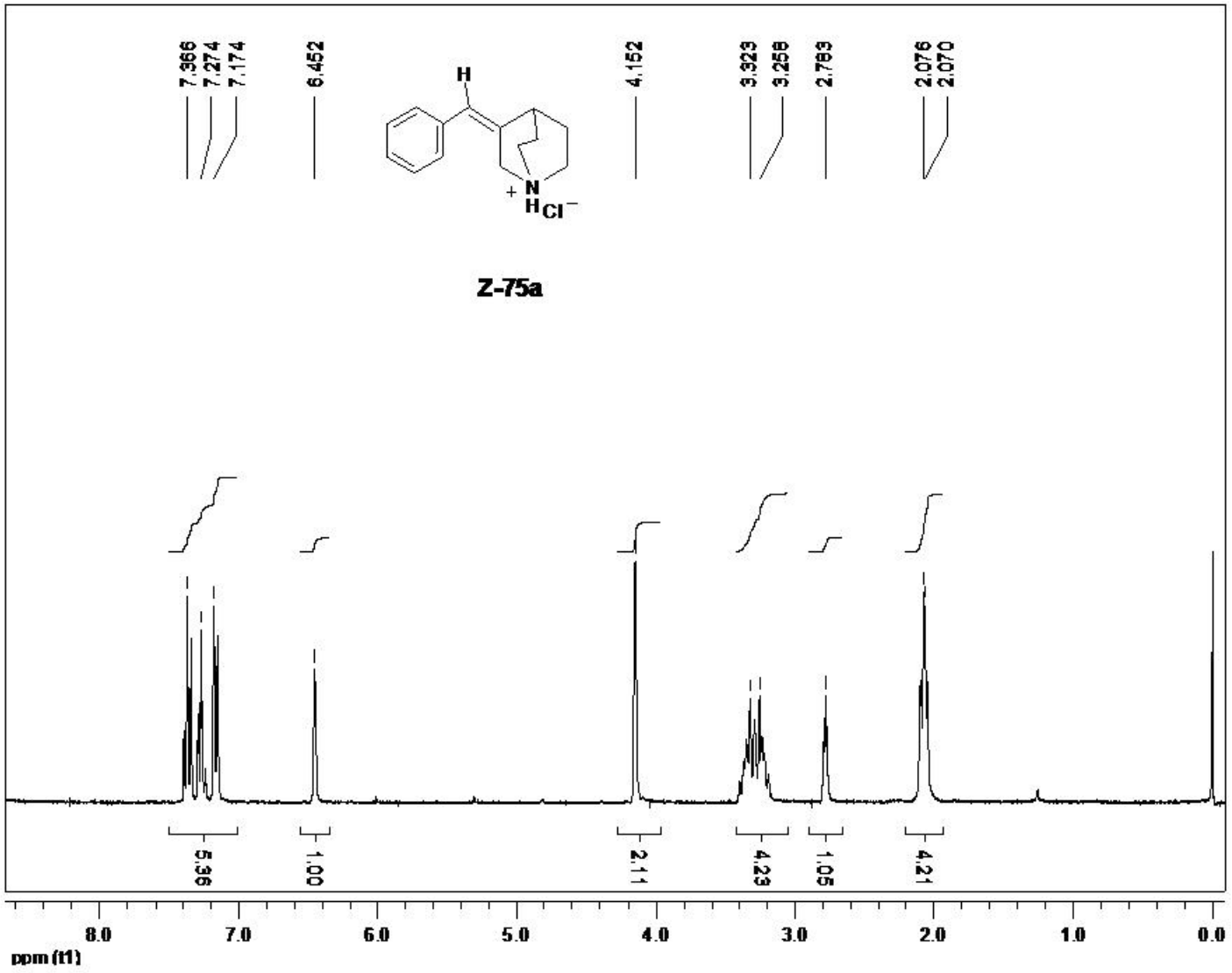


**Figure A-52. Z-3-benzylidene-1-azoniabicyclo[2.2.2]octane chloride**

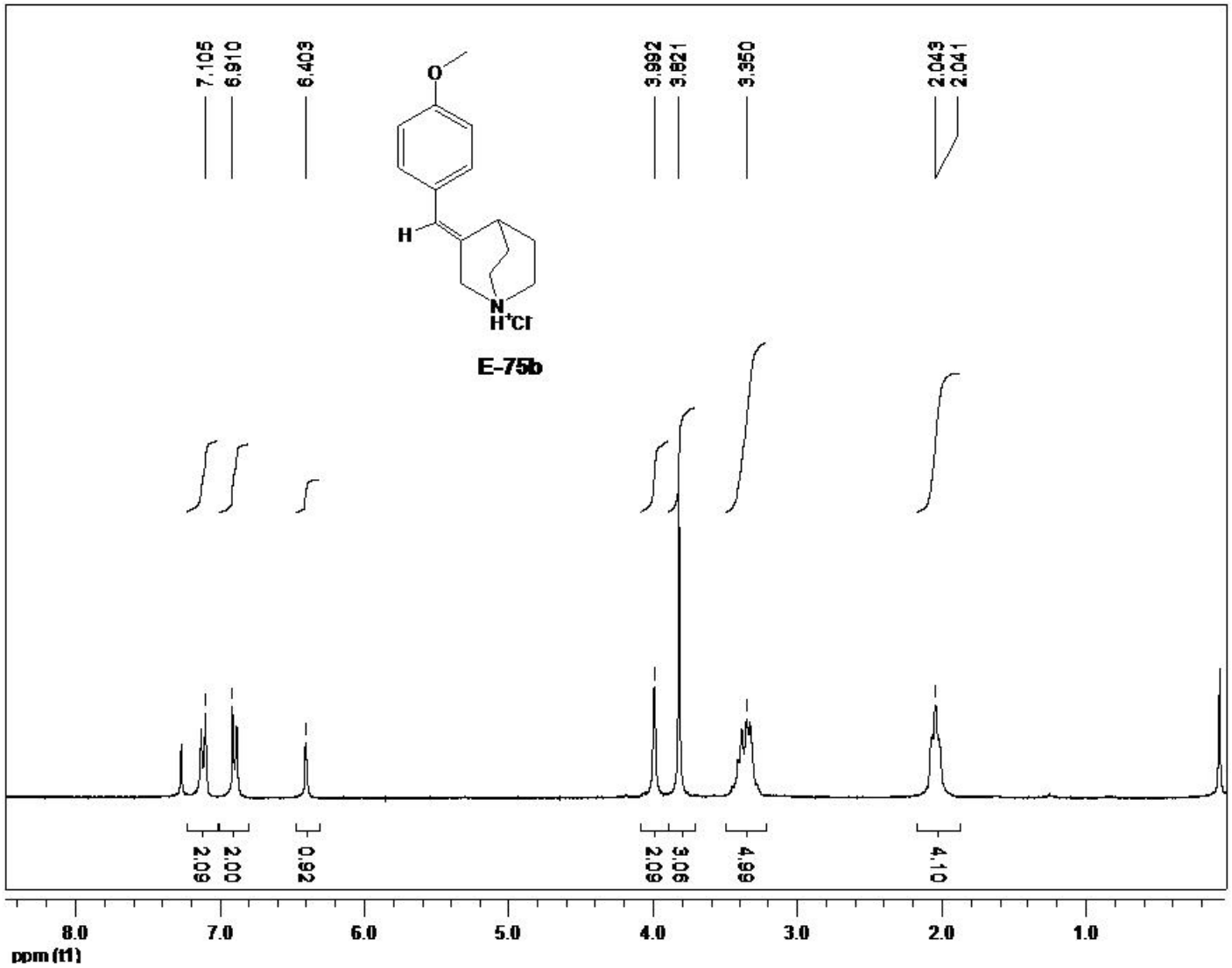


**Figure A-53. E-3-(4-methoxybenzylidene)-1-azoniabicyclo[2.2.2]octane chloride**

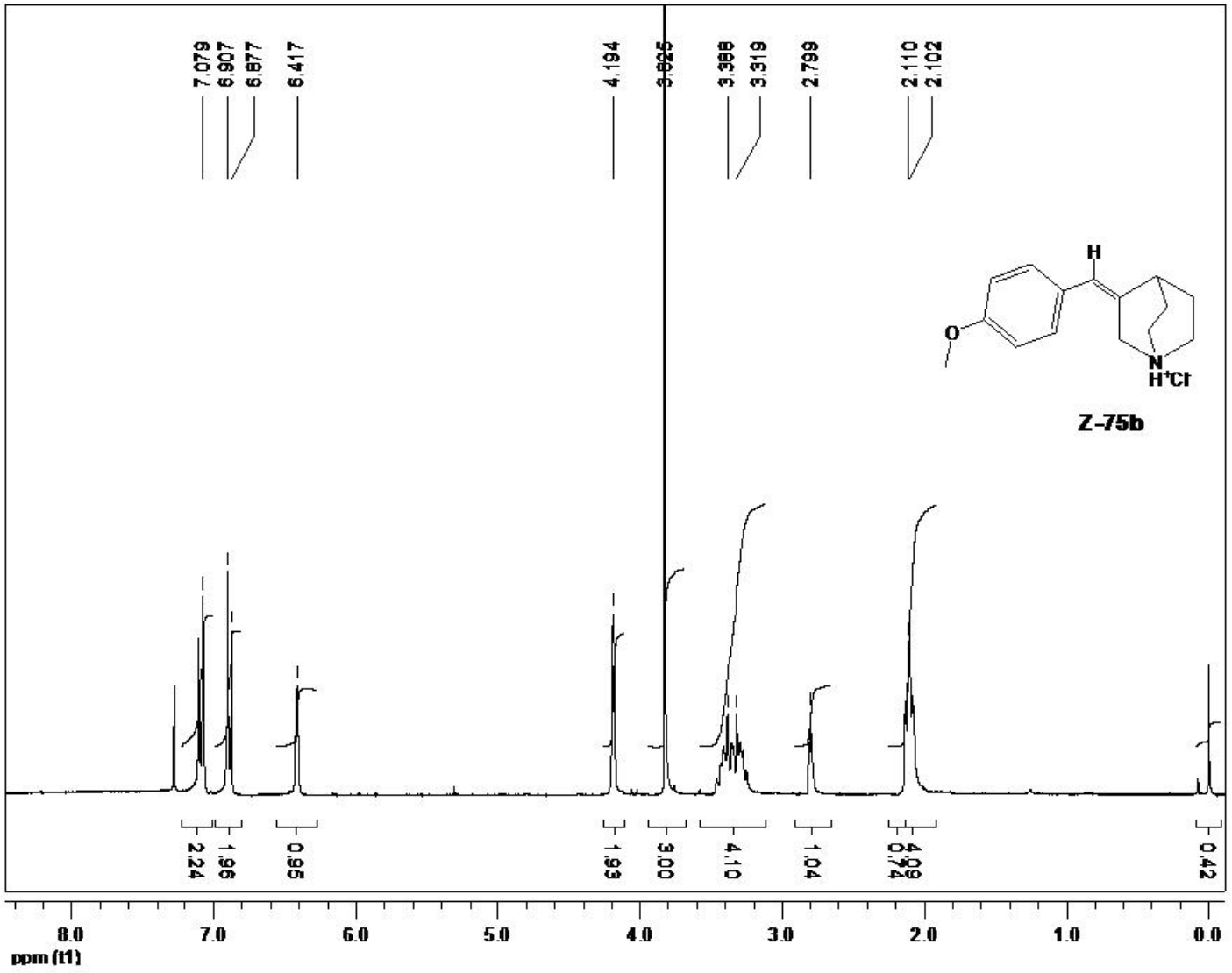


**Figure A-54. Z-3-(4-methoxybenzylidene)-1-azoniabicyclo[2.2.2]octane chloride**

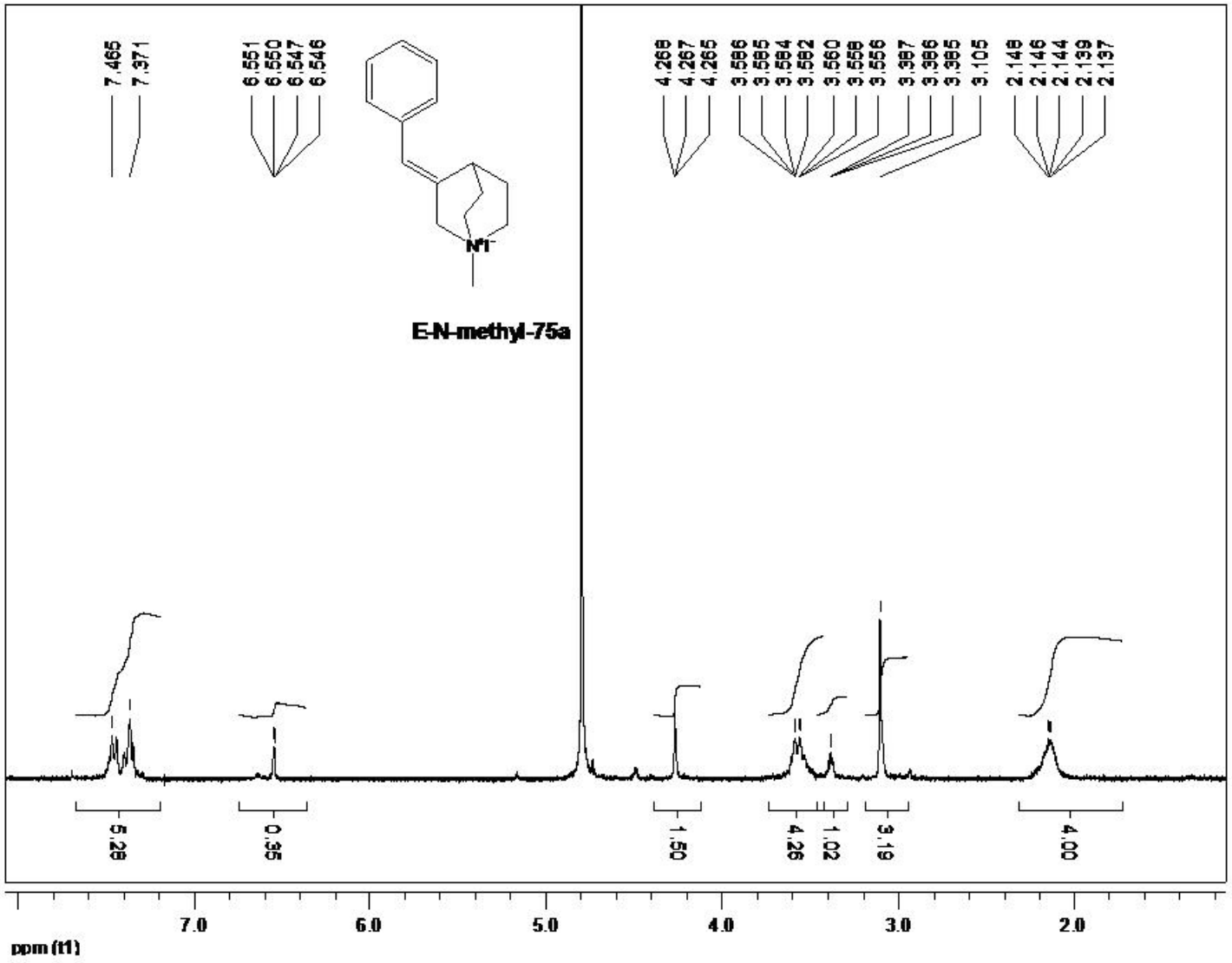


**Figure A-55. E-3-benzylidene-1-methyl-1-azoniabicyclo[2.2.2]octane iodide**

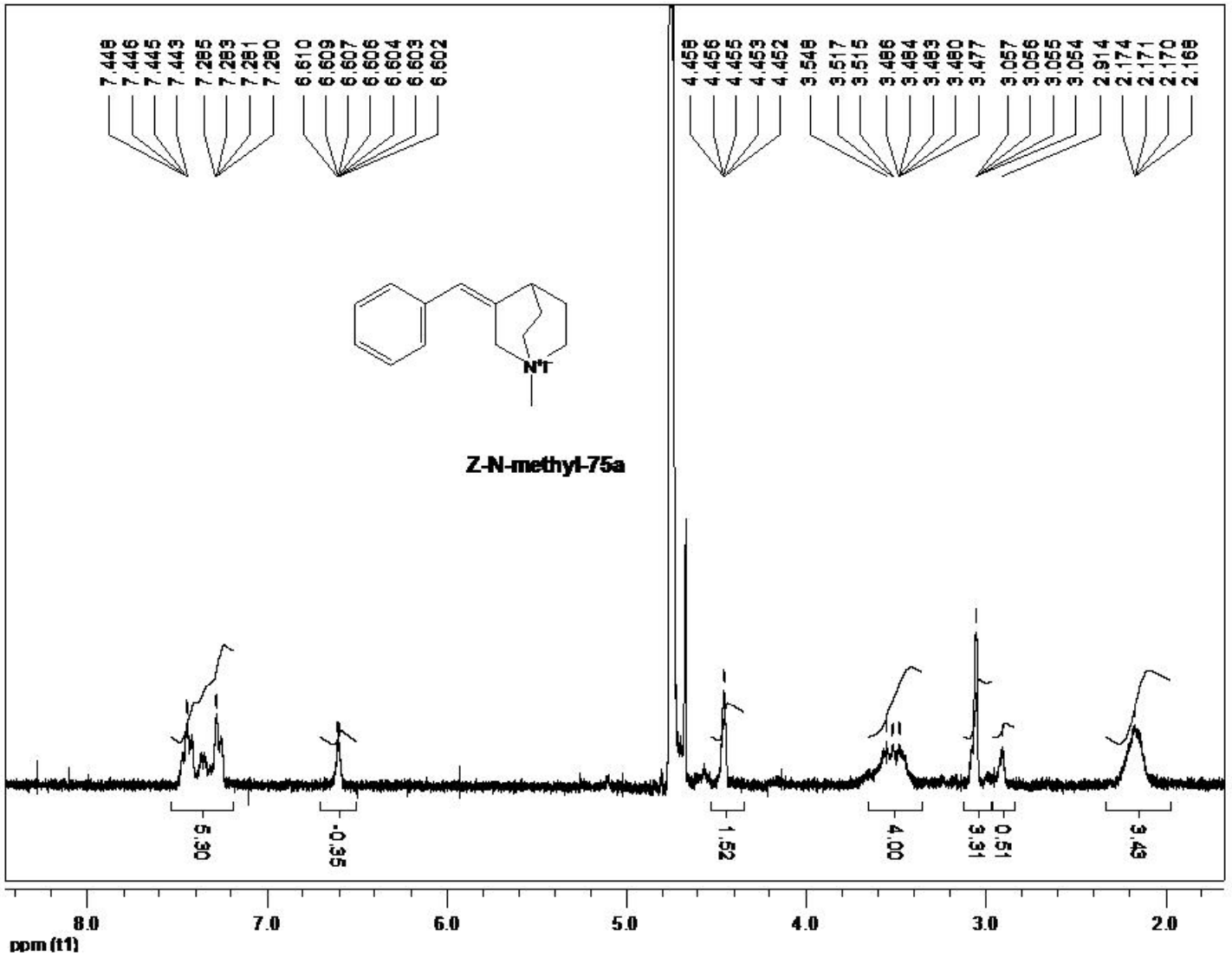


**Figure A-56. Z-3-benzylidene-1-methyl-1-azoniabicyclo[2.2.2]octane iodide**

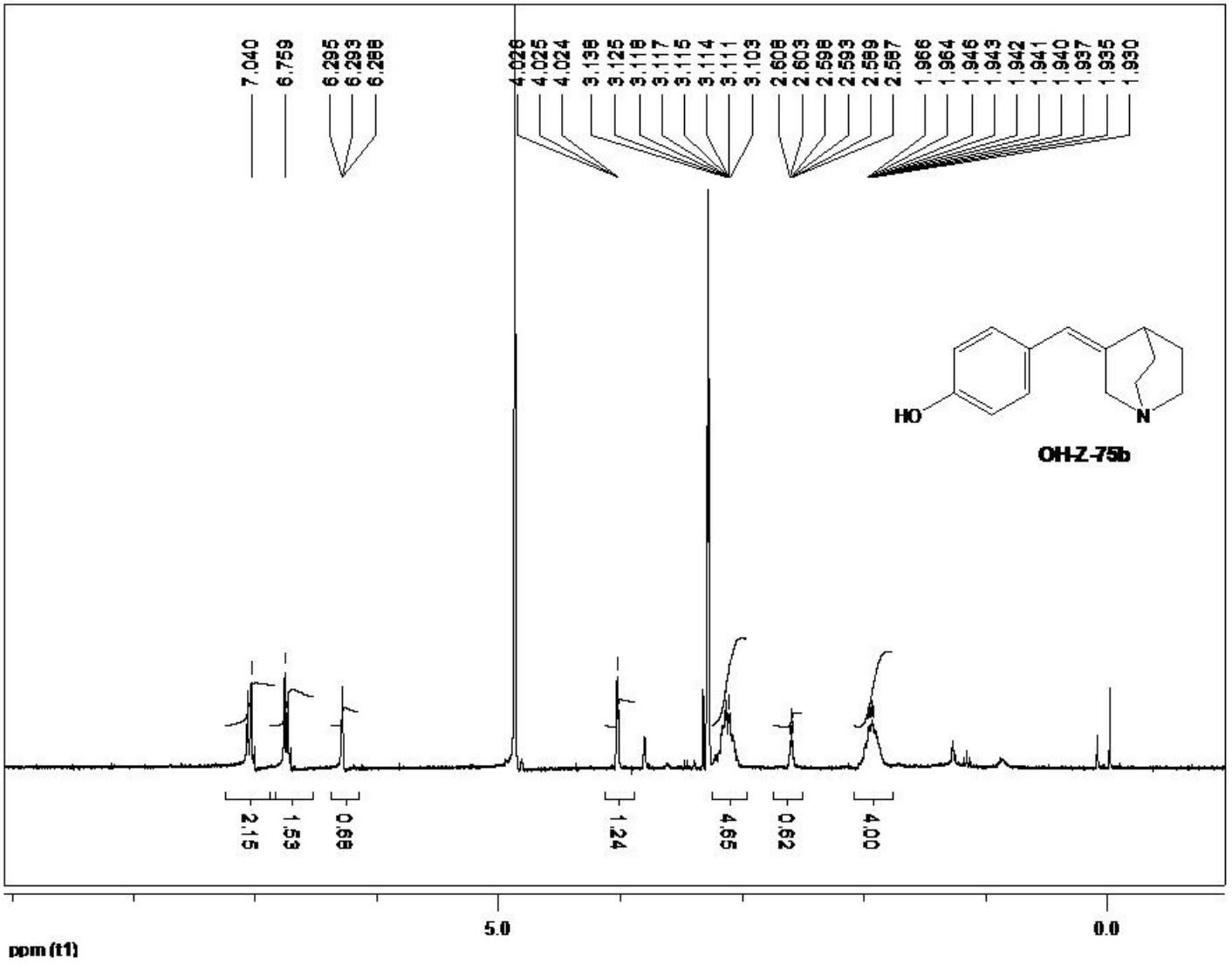


**Figure A-57. (Z)-4-(quinuclidin-3-ylidenemethyl)phenol**

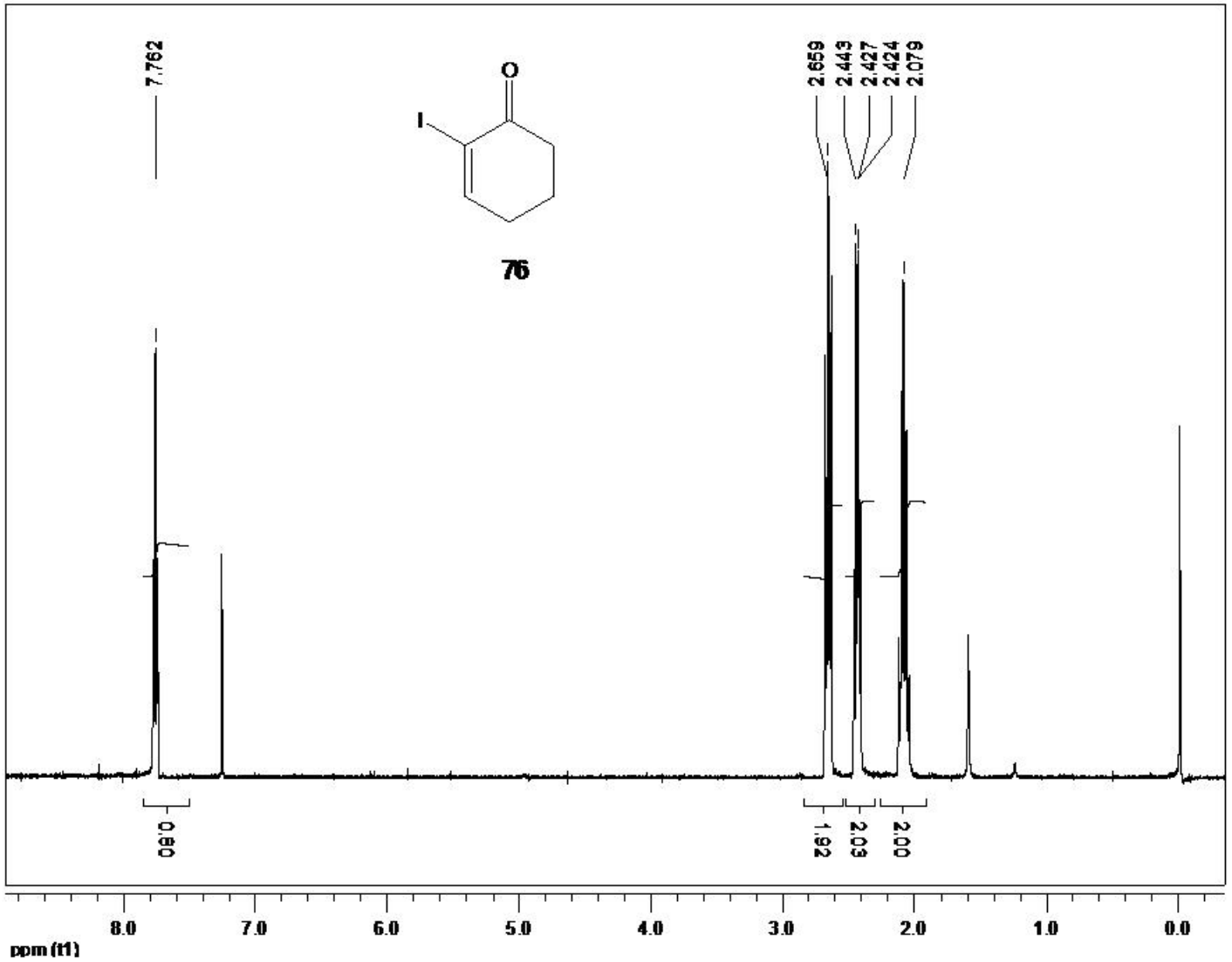


**Figure A-58. 2-iodocyclohex-2-enone**

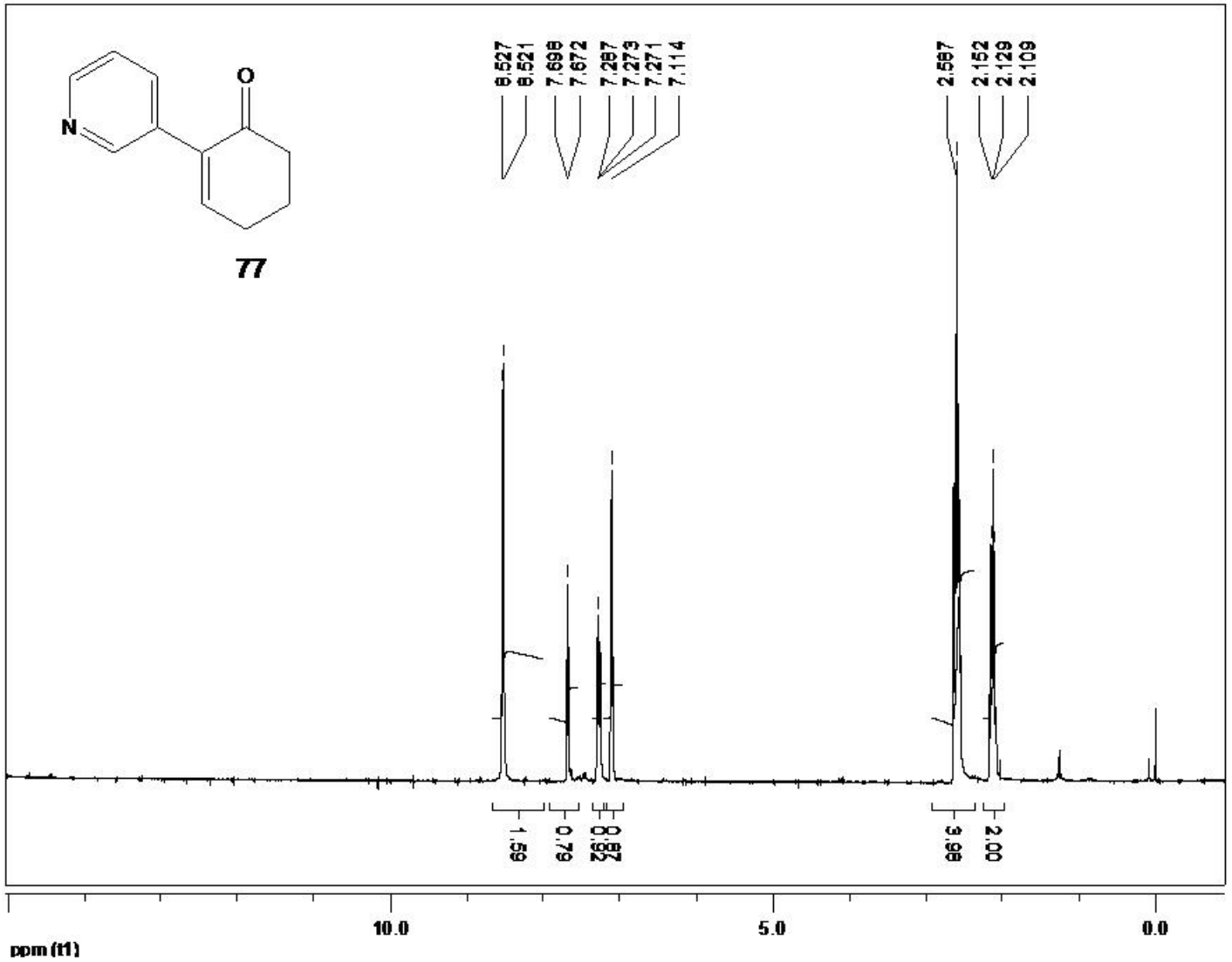


**Figure A-59. 2-(pyridin-3-yl)cyclohex-2-enone**

APPENDIX B
KINETIC ASSAY AND ANALYSIS FOR GLYCOSIDASES WITH DIAZABICYCLIC AMIDINES

The inhibitors screening graphics are displayed bellow. Assuming competitive and mixed or non-competitive inhibition, the models utilize to analyze the data were the following[6]:

- Competitive inhibition

$$K_i = \frac{[E][I]}{[EI]}$$

$$[E]_T = [E] + [EI] + [ES]$$

$$[E] = \frac{K_M[ES]}{[S]}$$

$$[EI] = \frac{K_M[ES][I]}{[S]K_i}$$

$$[E]_T = [ES]\left\{\frac{K_M}{[S]}\left(1+\frac{[I]}{K_i}\right)+1\right\}$$

$$[ES] = \frac{[E]_T[S]}{K_M\left(1+\frac{[I]}{K_i}\right)+[S]}$$

$$v_0 = k_2[ES] = \frac{k_2[E]_T[S]}{K_M\left(1+\frac{[I]}{K_i}\right)+[S]}$$

$$v_{\max} = k_2[E]_T$$

$$v_0 = \frac{v_{\max}[S]}{\left(1+\frac{[I]}{K_i}\right)K_M+[S]}$$

$v_0$ and $v_{\max}$ are initial velocity and maximal velocity respectively

For the Lineweaver-Burke reverse plots, the competitive inhibition reciprocal ecuation is:

$$\frac{1}{v_0} = \left[\left(1+\frac{[I]}{K_i}\right)\frac{K_M}{v_{\max}}\right]\frac{1}{[S]} + \frac{1}{v_{\max}}$$

- Mixed or non-competitive inhibition

$$K_i = \frac{[E][I]}{[EI]} \qquad K'_i = \frac{[ES][I]}{[ESI]}$$

$$[E]_T = [E]+[EI]+[ES]+[ESI]$$

$$[E]_T = [E]\left(1+\frac{[I]}{K_i}\right)+[ES]\left(1+\frac{[I]}{K'_i}\right)$$

$$\text{If } [E] = \frac{K_M[ES]}{[S]} \text{ then } [E]_T = [ES]\left[\left(1+\frac{[I]}{K_i}\right)\frac{K_M}{[S]}+\left(1+\frac{[I]}{K'_i}\right)\right]$$

$$\text{If } v_0 = k_2[ES] \text{ and } v_{\max} = k_2[E]_T \text{ then,}$$

$$v_0 = \frac{v_{\max}[S]}{\left(1+\frac{[I]}{K_i}\right)K_M + \left(1+\frac{[I]}{K'_i}\right)[S]}$$

For the Lineweaver-Burke reverse plots, the mixed or non-competitive inhibition reciprocal ecuation is:

$$\frac{1}{v_0} = \left[\left(1+\frac{[I]}{K_i}\right)\frac{K_M}{v_{\max}}\right]\frac{1}{[S]} + \left(1+\frac{[I]}{K'_i}\right)\frac{1}{v_{\max}}$$

## Kinetic Screening Graphics

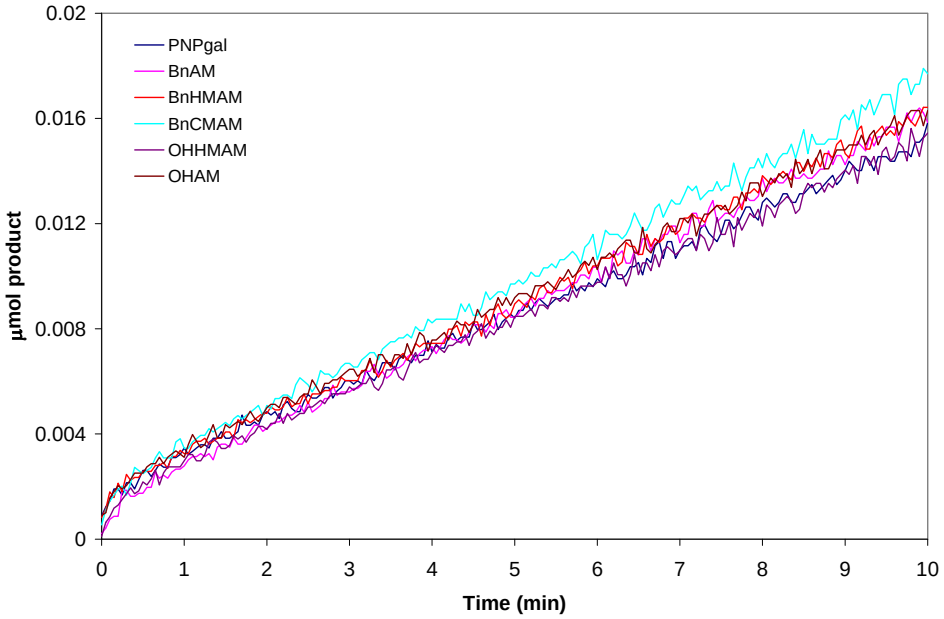


Figure B-1. Kinetic assay of α-gal at pH 7.5

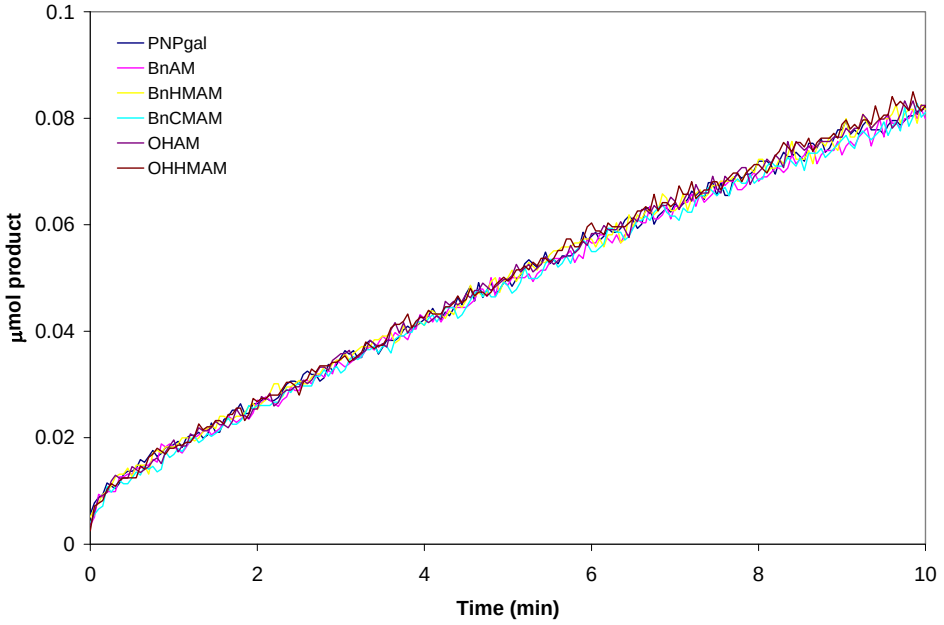


Figure B-2. Kinetic assay for α-gal at pH 6

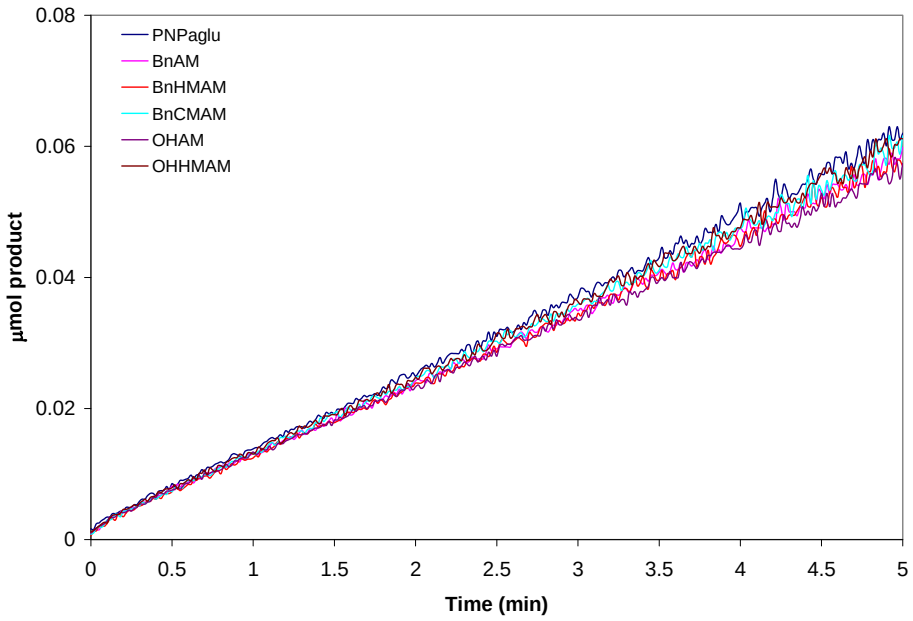


Figure B-3. Kinetic assay for α-glu at pH 7.5

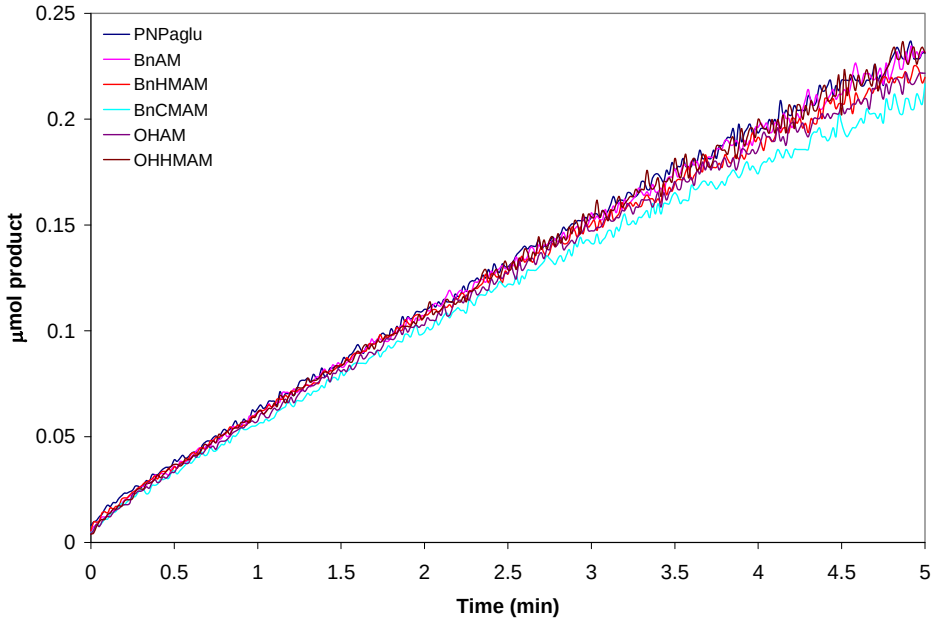


Figure B-4. Kinetic assay for α-glu at pH 6

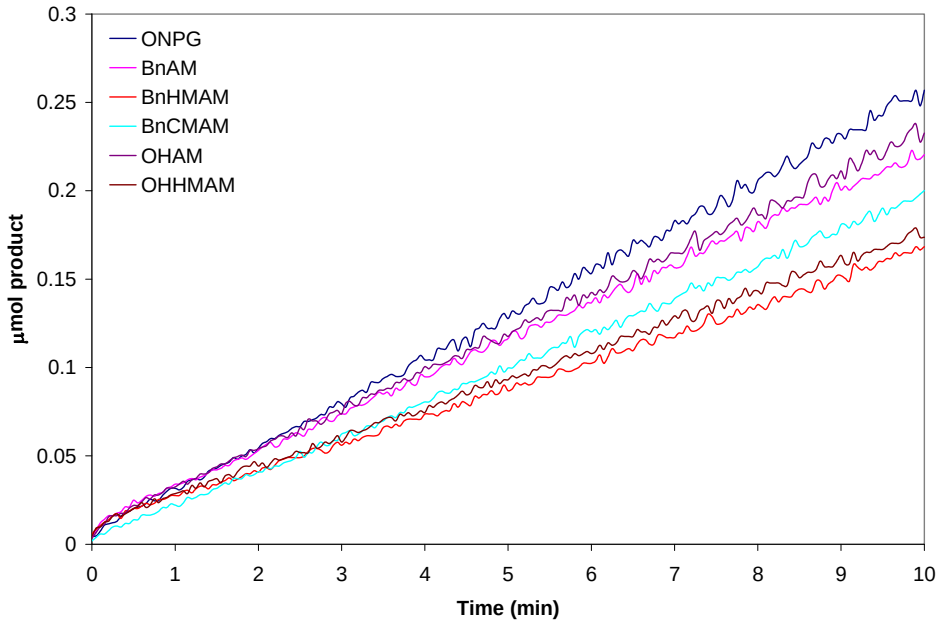


Figure B-5. Kinetic assay for β-galAsp at pH 7.5

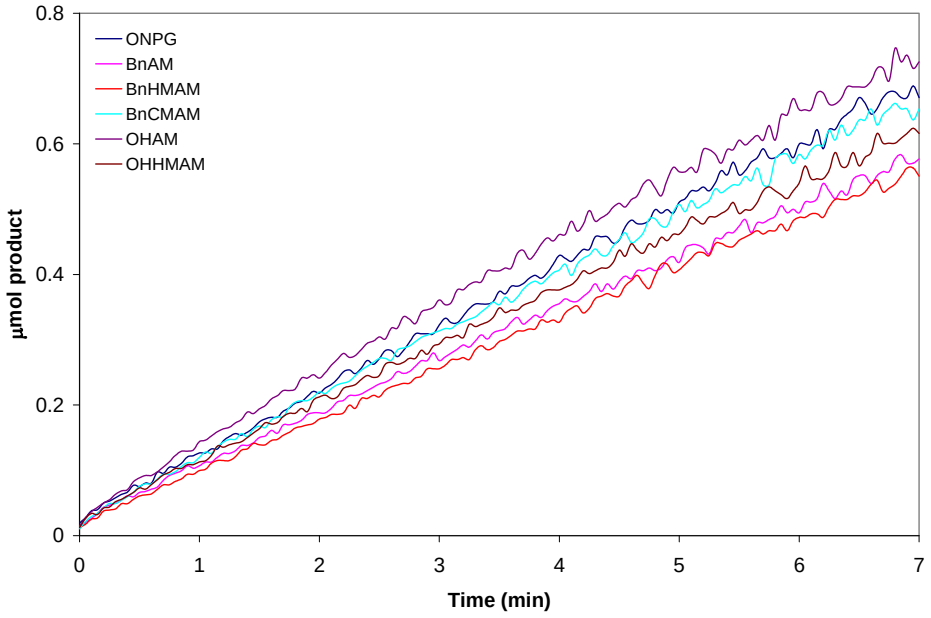


Figure B-6. Kinetic assay for β-galAsp at pH 6

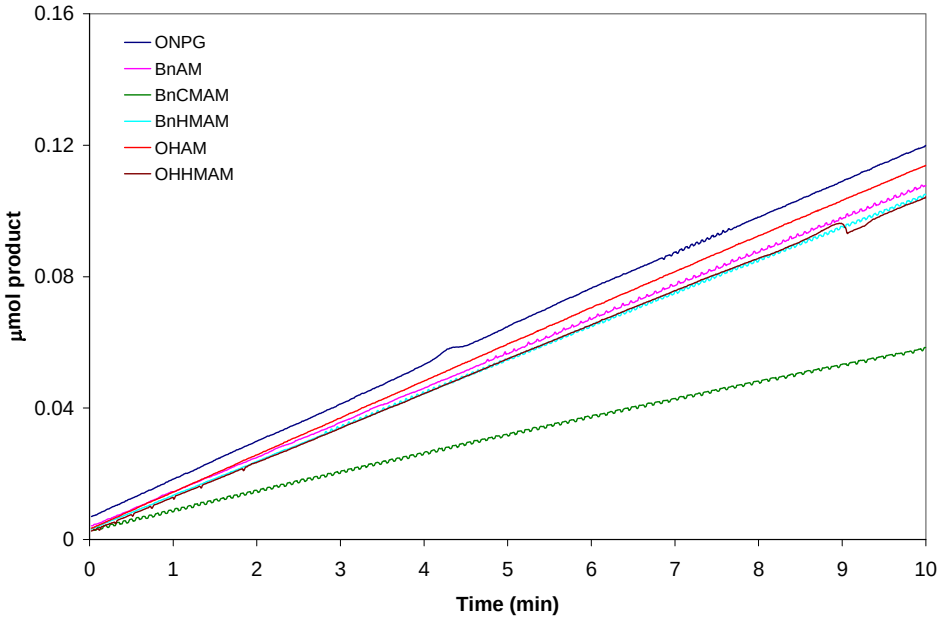


Figure B-7. Kinetic Assay of β-galEcoli at pH 7.5

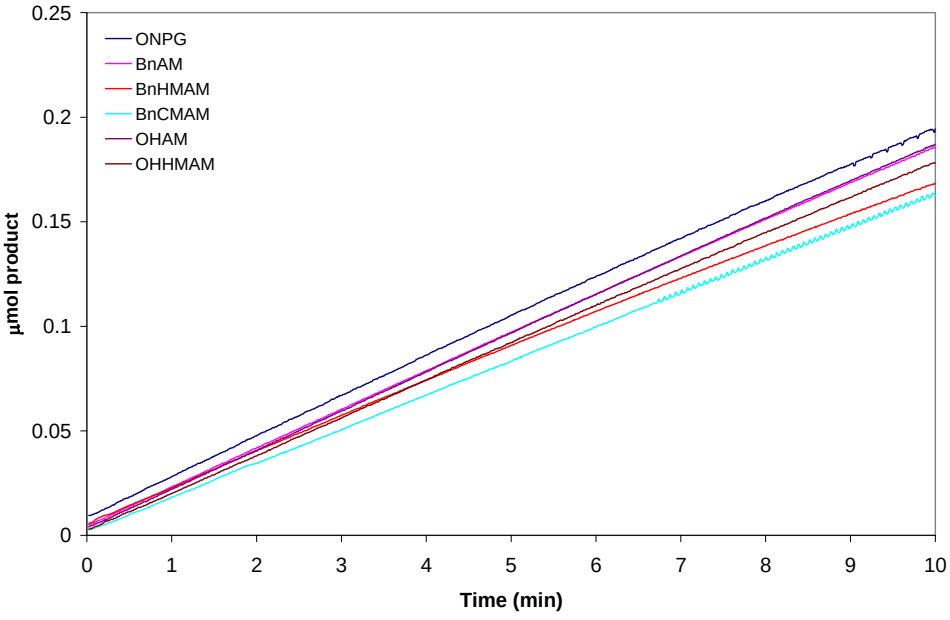


Figure B-8. Kinetic assay for β-galEcoli at pH 6

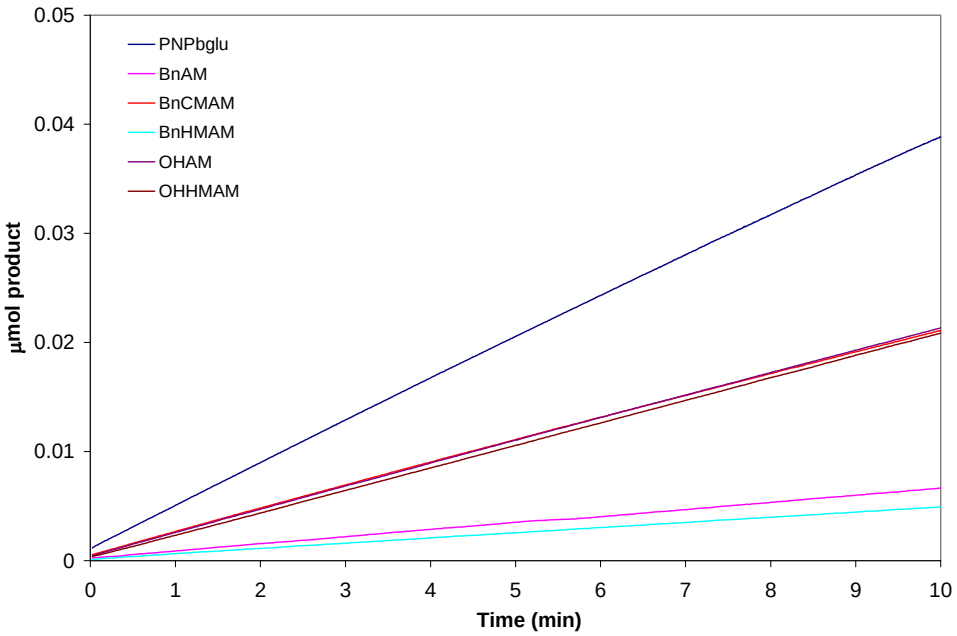


Figure B-9. Kinetic assay for β-glu at pH 7.5

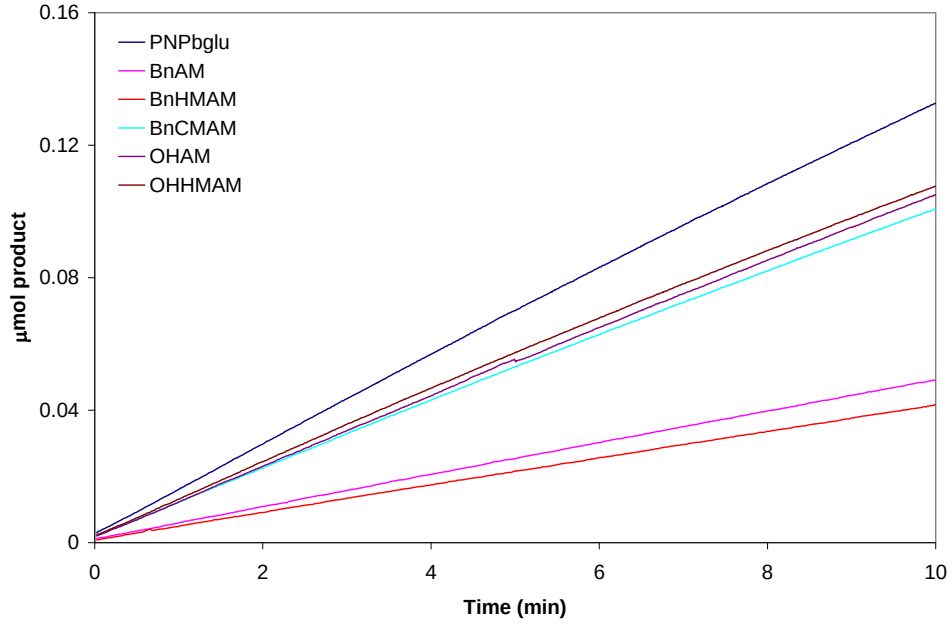


Figure B-10. Kinetic assay for β-glu at pH 6

**Lineweaver-Burke Reverse Plots**

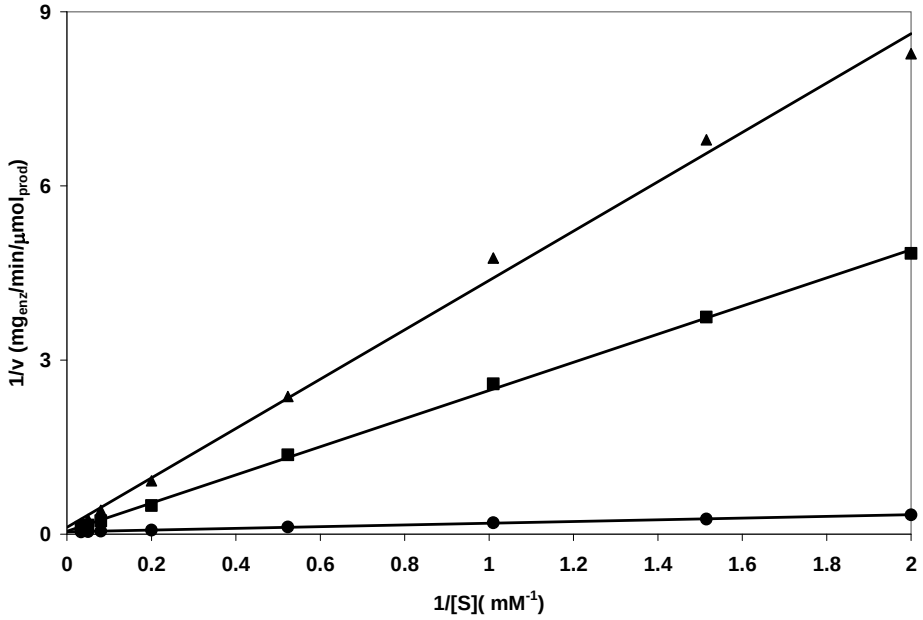


Figure B-11. Lineweaver-Burke plot of β-glu with BnHMAM. The concentrations of TS analogs were ▲, 4 mM; ■, 2 mM; ●, 0 mM.

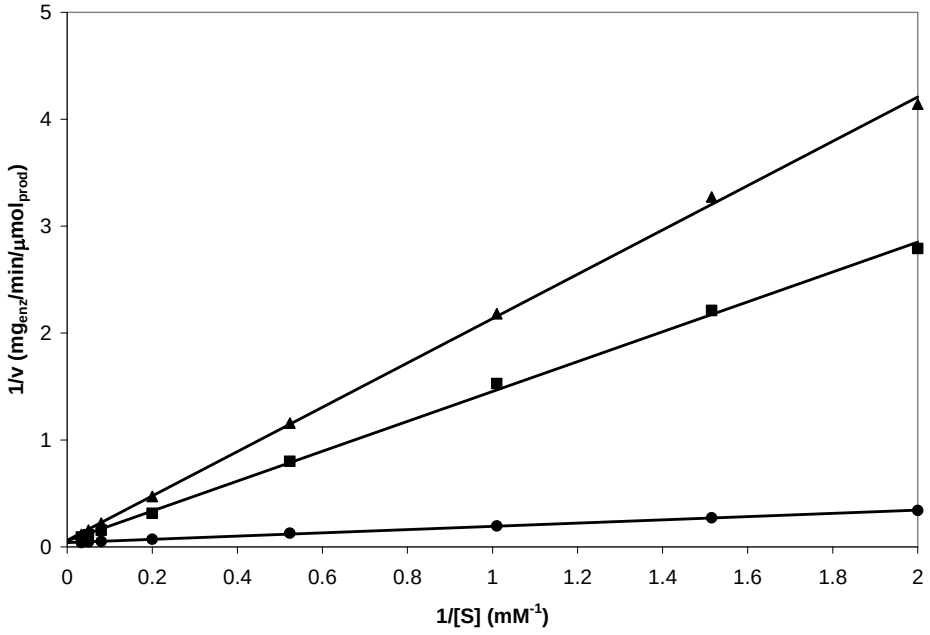


Figure B-12. Lineweaver-Burke plot of β-glu with BnAM. The concentrations of TS analogs were ▲, 4 mM; ■, 2 mM; ●, 0 mM.

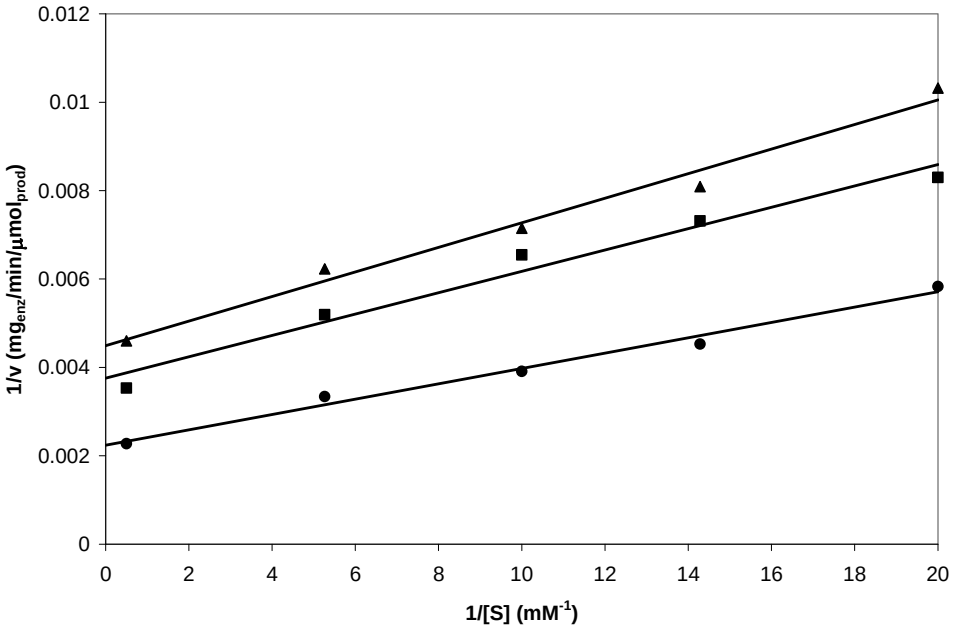


Figure B-13. Linweaver-Burke plot of β-galEcoli with BnCMAM. The concentrations of TS analogs were ▲, 0.6 mM; ■, 0.3 mM; ●, 0 mM.

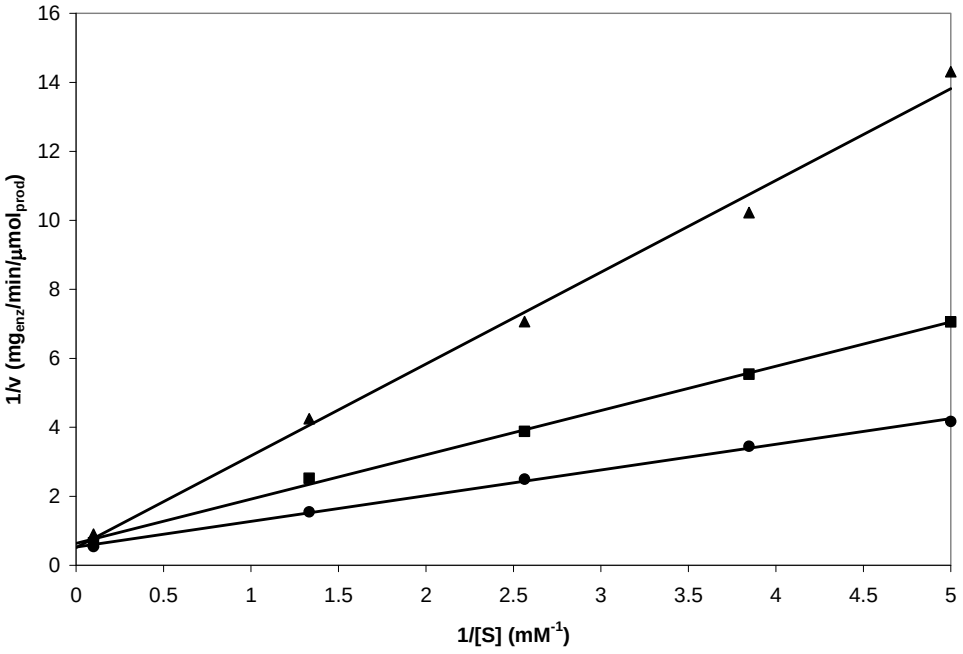


Figure B-14. Linweaver-Burke plot of β-galAsp with BnHMAM. The concentrations of TS analogs were ▲, 3 mM; ■, 1 mM; ●, 0 mM.

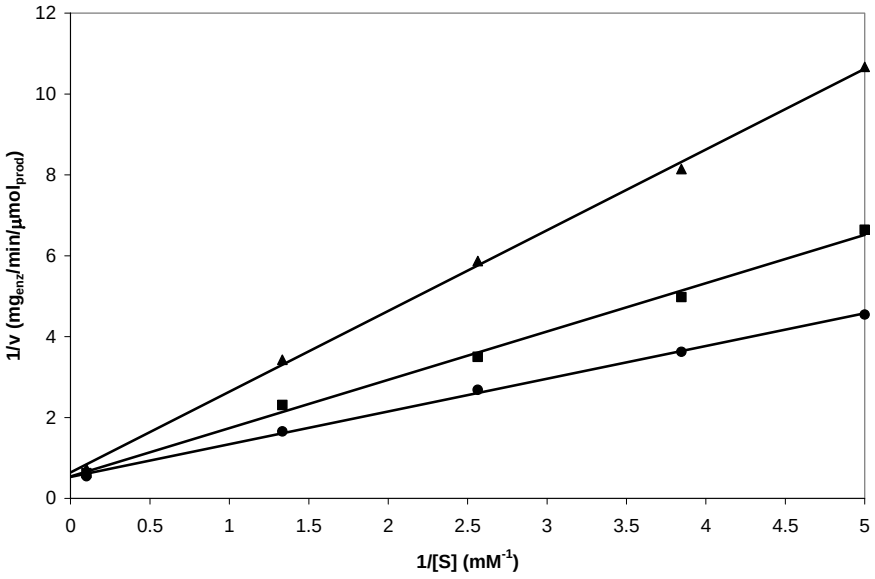


Figure B-15. Linweaver-Burke plot of β-galAsp with OHHMAM. The concentrations of TS analogs were ▲, 3 mM; ■, 1 mM; ●, 0 mM.

**Michaelis-Menten Curves**

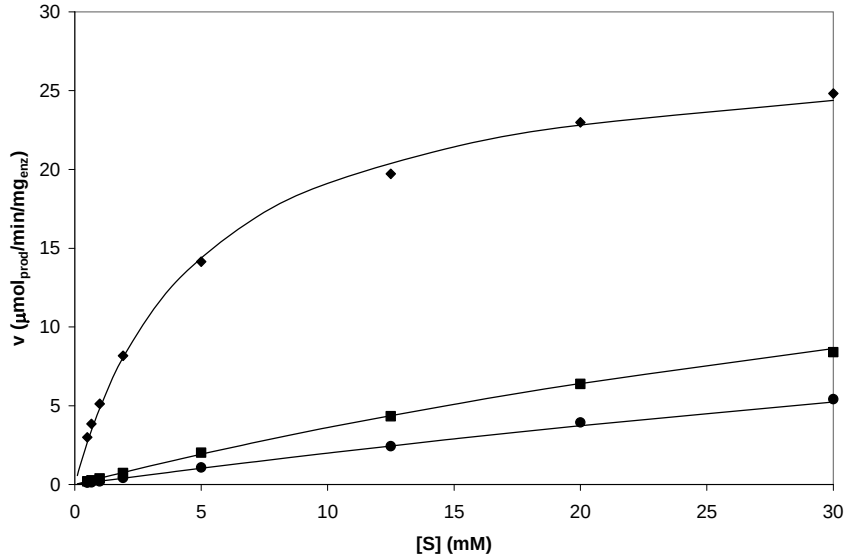


Figure B-16. Michaelis-Menten curves of β-glu with BnHMAM. The concentrations of TS analogs were ▲, 4 mM; ■, 2 mM; ●, 0 mM.

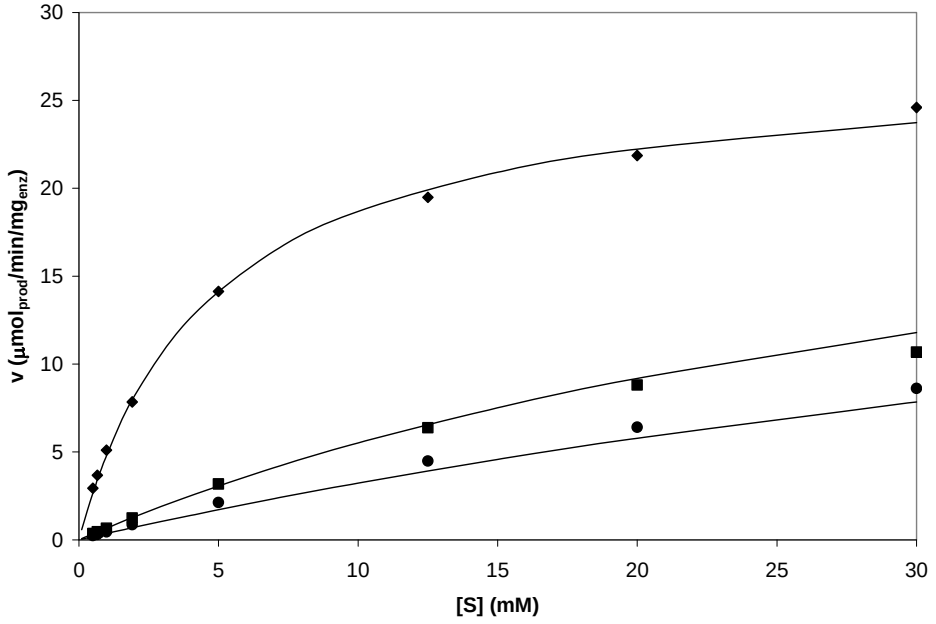


Figure B-17. Michaelis-Menten curves of β-glu with BnAM. The concentrations of TS analogs were ▲, 4 mM; ■, 2 mM; ●, 0 mM.

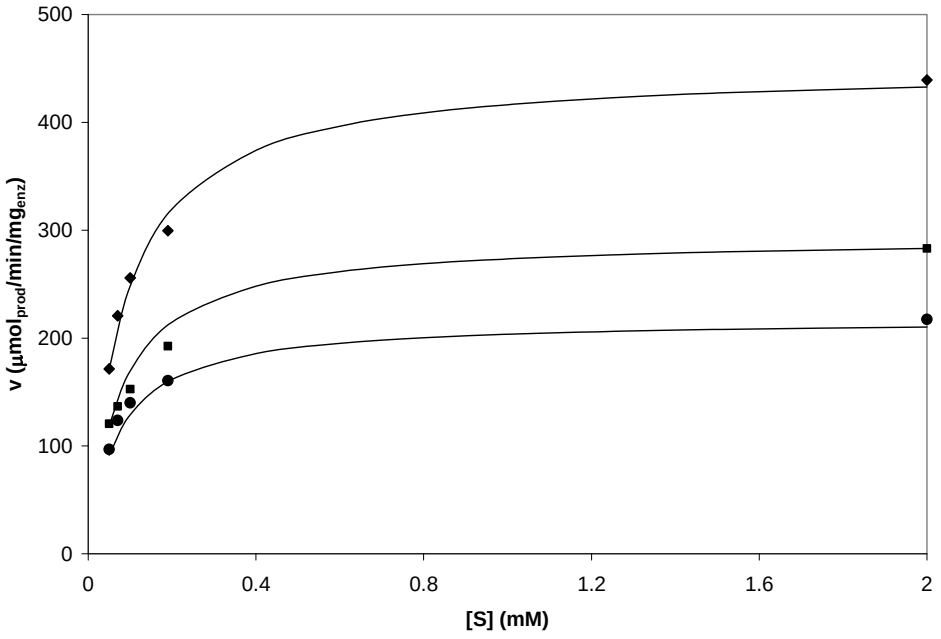


Figure B-18. Michaelis-Menten curves of β-galEcoli with BnCMAM. The concentrations of TS analogs were ▲, 0.6 mM; ■, 0.3 mM; ●, 0 mM.

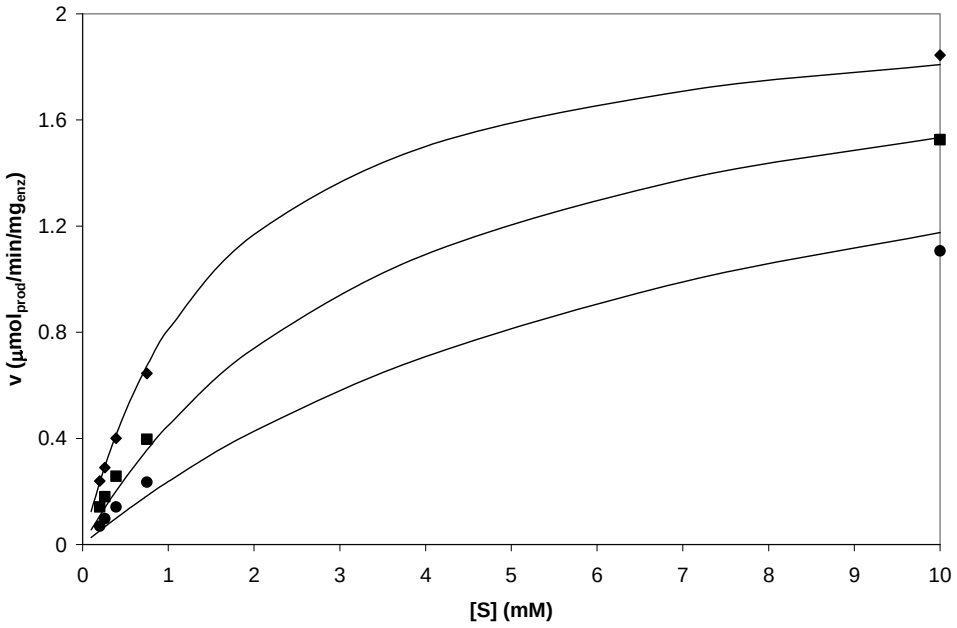


Figure B-19. Michaelis-Menten curves of β-galAsp with BnHMAM. The concentrations of TS analogs were ▲, 3 mM; ■, 1 mM; ●, 0 mM.

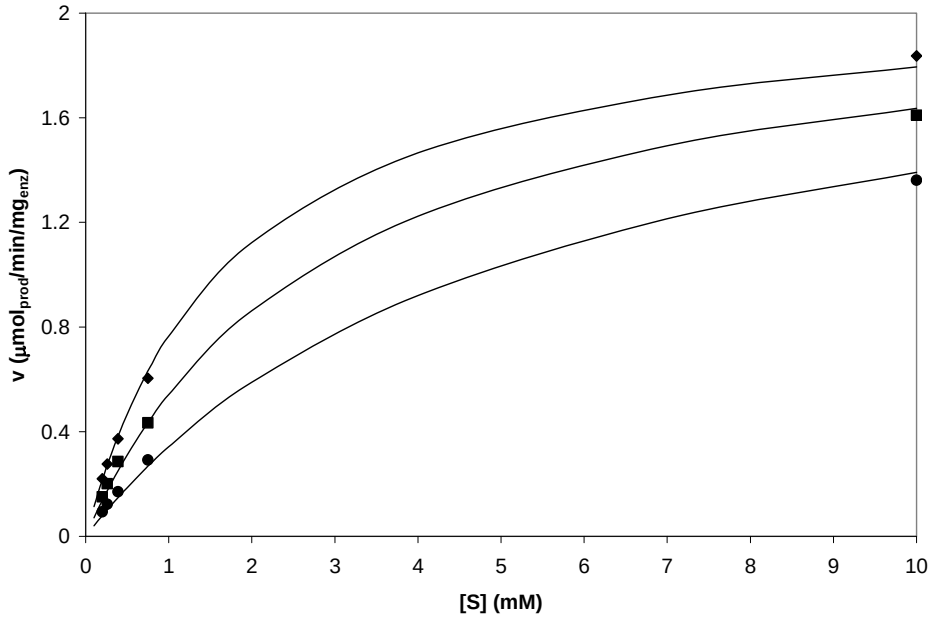


Figure B-20. Michaelis-Menten curves of β-galAsp with OHHMAM. The concentrations of TS analogs were ▲, 3 mM; ■, 1 mM; ●, 0 mM.

**Ki Determination with Lineweaver-Burke Plots Information**

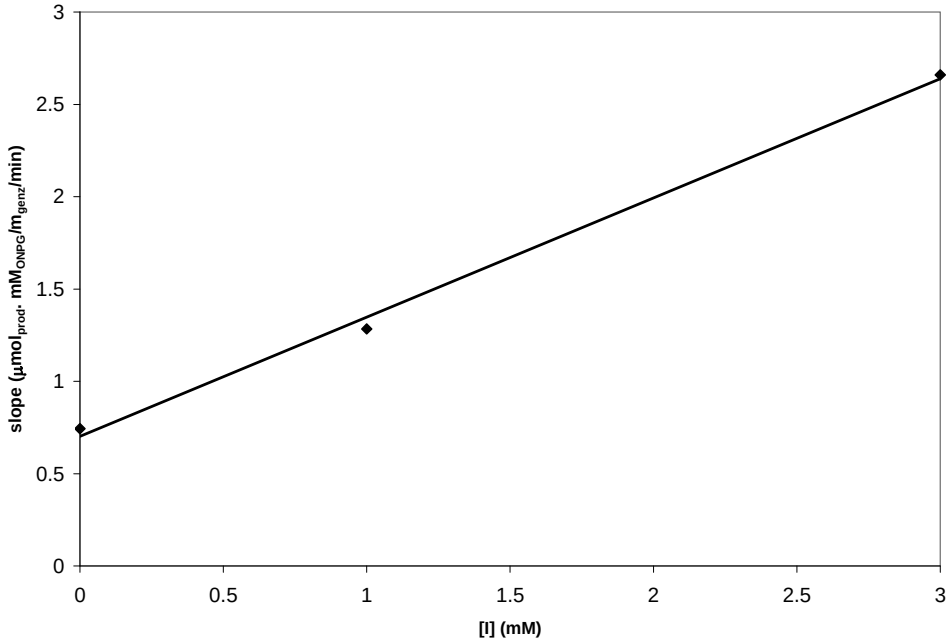


Figure B-21. Ki determination of β-galAsp with BnHMAM

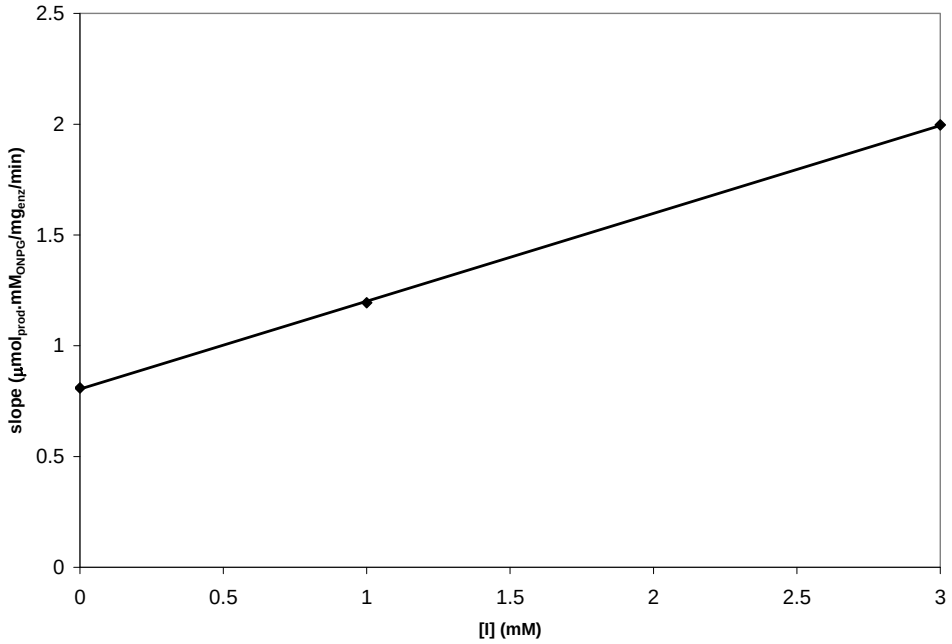


Figure B-22. Ki determination of β-galAsp with OHHMAM

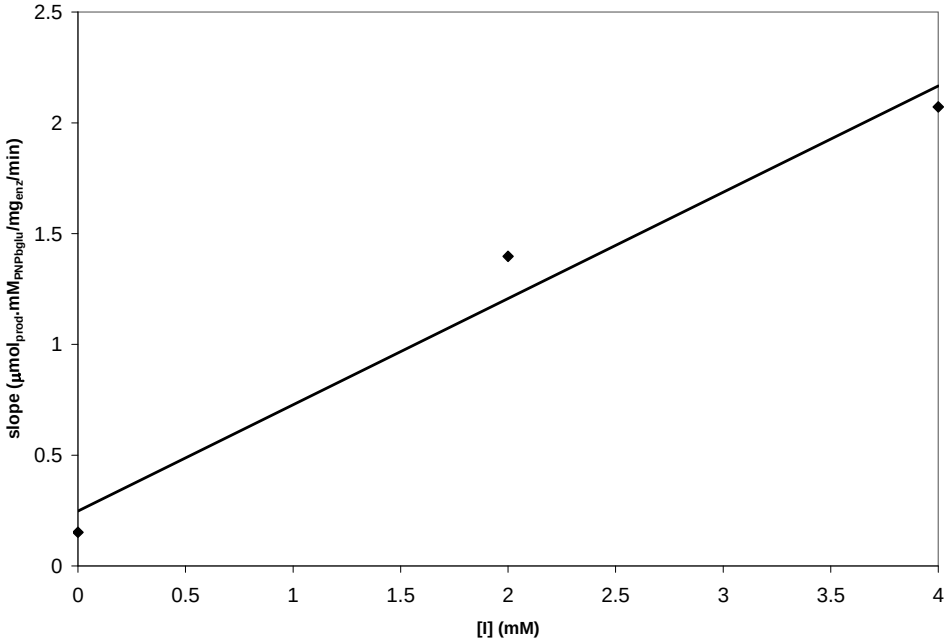


Figure B-23. Ki determination of β-glu with BnAM

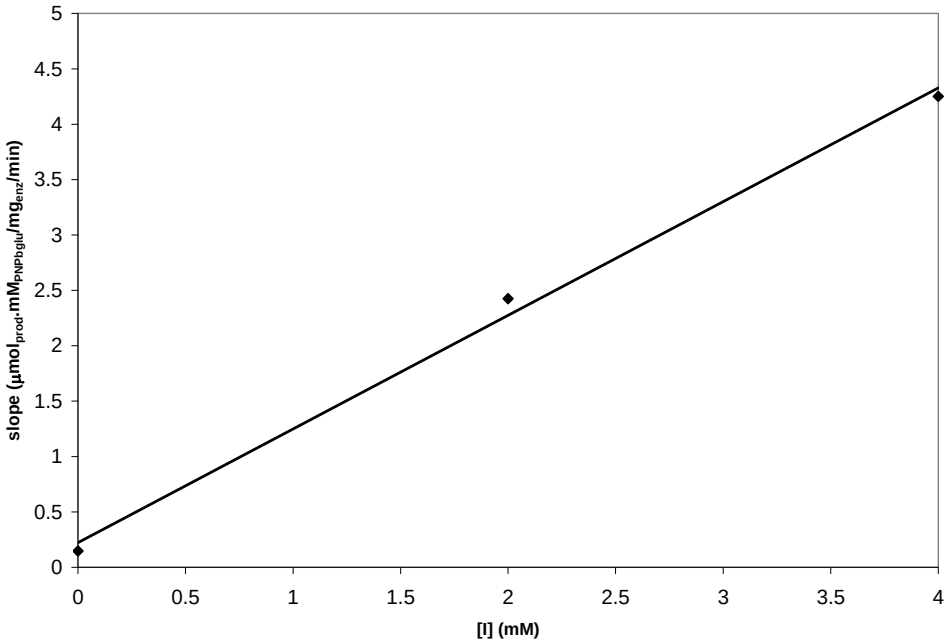


Figure B-24. Ki determination of β-glu with BnHMAM

LIST OF REFERENCES


(1) Wolfenden, R.; Lu, X. D.; Young, G. *J. Am. Chem. Soc.* **1998**, *120*, 6814-6815.

(2) Varki, A. *Glycobiology* **1993**, *3*, 97-130.

(3) Ly, H. D.; Withers, S. G. *Annu. Rev. Biochem.* **1999**, *68*, 487-522.

(4) Sinnott, M. L. *Chem. Rev.* **1990**, *90*, 1171-1202.

(5) Kornfeld, S. *J. Clin. Invest.* **1986**, *77*, 1-6.

(6) Voet, D.; Voet, J. G. *Biochemistry*; Wiley: New York, 1990.

(7) Kornfeld, R.; Kornfeld, S. *Annu. Rev. Biochem.* **1985**, *54*, 631-664.

(8) Stryer, L. *Biochemistry*; 4th ed.; W.H. Freeman: New York, 1995.

(9) Winchester, B.; Fleet, G. W. J. *Glycobiology* **1992**, *2*, 199-210.

(10) McCarter, J. D.; Withers, S. G. *Curr. Opin. Struct. Biol.* **1994**, *4*, 885-892.

(11) Rye, C. S.; Withers, S. G. *Curr. Opin. Chem. Biol.* **2000**, *4*, 573-580.

(12) Vasella, A.; Davies, G. J.; Bohm, M. *Curr. Opin. Chem. Biol.* **2002**, *6*, 619-629.

(13) Withers, S. G. *Carbohydr. Polym.* **2001**, *44*, 325-337.

(14) Zechel, D. L.; Withers, S. G. *Acc. Chem. Res.* **2000**, *33*, 11-18.

(15) Horenstein, N. A. In *Adv. Phys. Org. Chem.* **2006**, *41*, 275-314.

(16) Bruner, M.; Horenstein, B. A. *Biochemistry* **1998**, *37*, 289-297.

(17) Horenstein, B. A. *J. Am. Chem. Soc.* **1997**, *119*, 1101-1107.

(18) Kempton, J. B.; Withers, S. G. *Biochemistry* **1992**, *31*, 9961-9969.

(19) Henrissat, B. *Biochem. J.* **1991**, *280*, 309-316.

(20) Davies, G. J.; Gloster, T. M.; Henrissat, B. *Curr. Opin. Struct. Biol.* **2005**, *15*, 637-645.

(21) Henrissat, B.; Bairoch, A. *Biochem. J.* **1993**, *293*, 781-788.

(22) Henrissat, B.; Callebaut, I.; Fabrega, S.; Lehn, P.; Mornon, J. P.; Davies, G. *Proc. Natl. Acad. Sci. U. S. A.* **1995**, *92*, 7090-7094.

(23) Davies, G.; Henrissat, B. *Structure* **1995**, *3*, 853-859.

(24) Jacobson, R. H.; Zhang, X. J.; Dubose, R. F.; Matthews, B. W. *Nature* **1994**, *369*, 761-766.

(25) Herrchen, M.; Legler, G. *Eur. J. Biochem.* **1984**, *138*, 527-531.

(26) Gebler, J. C.; Aebersold, R.; Withers, S. G. *J. Biol. Chem.* **1992**, *267*, 11126-11130.

(27) Wakarchuk, W. W.; Campbell, R. L.; Sung, W. L.; Davoodi, J.; Yaguchi, M. *Protein Sci.* **1994**, *3*, 467-475.

(28) Kuroki, R.; Weaver, L. H.; Matthews, B. W. *Science* **1993**, *262*, 2030-2033.

(29) Elbein, A. D. *Annu. Rev. Biochem.* **1987**, *56*, 497-534.

(30) Fleet, G. W. J.; Karpas, A.; Dwek, R. A.; Fellows, L. E.; Tyms, A. S.; Petursson, S.; Namgoong, S. K.; Ramsden, N. G.; Smith, P. W.; Son, J. C.; Wilson, F.; Witty, D. R.; Jacob, G. S.; Rademacher, T. W. *FEBS Lett.* **1988**, *237*, 128-132.

(31) Schramm, V. L.; Horenstein, B. A.; Kline, P. C. *J. Biol. Chem.* **1994**, *269*, 18259-18262.

(32) Conchie, J.; Hay, A. J.; Strachan, I.; Levvy, G. A. *Biochem. J.* **1967**, *102*, 929-&.

(33) Reese, E. T.; Parrish, F. W.; Ettlinge.M *Carbohydr. Res.* **1971**, *18*, 381-&.

(34) Pan, Y. T.; Hori, H.; Saul, R.; Sanford, B. A.; Molyneux, R. J.; Elbein, A. D. *Biochemistry* **1983**, *22*, 3975-3984.

(35) Kayakiri, H.; Nakamura, K.; Takase, S.; Setoi, H.; Uchida, I.; Terano, H.; Hashimoto, M.; Tada, T.; Koda, S. *Chem. Pharm. Bull.* **1991**, *39*, 2807-2812.

(36) Kim, Y. J.; Takatsuki, A.; Kogoshi, N.; Kitahara, T. *Tetrahedron* **1999**, *55*, 8353-8364.

(37) Bleriot, Y.; Dintinger, T.; Genregrandpierre, A.; Padrines, M.; Tellier, C. *Bioorg. Med. Chem. Lett.* **1995**, *5*, 2655-2660.

(38) Pan, Y. T.; Kaushal, G. P.; Papandreou, G.; Ganem, B.; Elbein, A. D. *J. Biol. Chem.* **1992**, *267*, 8313-8318.

(39) Papandreou, G.; Tong, M. K.; Ganem, B. *J. Am. Chem. Soc.* **1993**, *115*, 11682-11690.

(40) Tong, M. K.; Papandreou, G.; Ganem, B. *J. Am. Chem. Soc.* **1990**, *112*, 6137-6139.

(41) Panday, N.; Canac, Y.; Vasella, A. *Helv. Chim. Acta* **2000**, *83*, 58-79.

(42) Field, R. A.; Haines, A. H.; Chrystal, E. J. T.; Luszniak, M. C. *Biochem. J.* **1991**, *274*, 885-889.

(43) Heightman, T. D.; Vasella, A. T. *Angew. Chem., Int. Ed. Engl.* **1999**, *38*, 750-770.

(44) Fleet, G. W. J.; Son, J. C.; Green, D. S.; Dibello, I. C.; Winchester, B. *Tetrahedron* **1988**, *44*, 2649-2655.

(45) Inouye, S.; Tsuruoka, T.; Ito, T.; Niida, T. *Tetrahedron* **1968**, *24*, 2125-&.

(46) Hardick, D. J.; Hutchinson, D. W.; Trew, S. J.; Wellington, E. M. H. *Tetrahedron* **1992**, *48*, 6285-6296.

(47) Chen, S. H.; Danishefsky, S. J. *Tetrahedron Lett.* **1990**, *31*, 2229-2232.

(48) Ganem, B. *Acc. Chem. Res.* **1996**, *29*, 340-347.

(49) Ganem, B.; Papandreou, G. *J. Am. Chem. Soc.* **1991**, *113*, 8984-8985.

(50) Li, Y. K.; Byers, L. D. *Biochim. Biophys. Acta* **1989**, *999*, 227-232.

(51) Campbell, J. A.; Davies, G. J.; Bulone, V.; Henrissat, B. *Biochem. J.* **1997**, *326*, 929-939.

(52) Palcic, M. M. *Methods Enzymol.* **1994**, *230*, 300-316.

(53) Paulson, J. C.; Colley, K. J. *J. Biol. Chem.* **1989**, *264*, 17615-17618.

(54) Bourne, Y.; Henrissat, B. *Curr. Opin. Struct. Biol.* **2001**, *11*, 593-600.

(55) Coutinho, P. M.; Deleury, E.; Davies, G. J.; Henrissat, B. *J. Mol. Biol.* **2003**, *328*, 307-317.

(56) Lairson, L. L.; Withers, S. G. *Chem. Commun.* **2004**, 2243-2248.

(57) Persson, K.; Ly, H. D.; Dieckelmann, M.; Wakarchuk, W. W.; Withers, S. G.; Strynadka, N. C. J. *Nat. Struct. Biol.* **2001**, *8*, 166-175.

(58) Dall'Olio, F.; Chiricolo, M. *Glycoconjugate J.* **2001**, *18*, 841-850.

(59) Kleineidam, R. G.; Schmelter, T.; Schwarz, R. T.; Schauer, R. *Glycoconjugate J.* **1997**, *14*, 57-66.

(60) Muller, B.; Schaub, C.; Schmidt, R. R. *Angew. Chem., Int. Ed. Engl.* **1998**, *37*, 2893-2897.

(61) Schauer, R. *Arch. Biochem. Biophys.* **2004**, *426*, 132-141.

(62) Wang, X. F.; Zhang, L. H.; Ye, X. S. *Med. Res. Rev.* **2003**, *23*, 32-47.

(63) Lehninger, A. L.; Nelson, D. L.; Cox, M. M. *Lehninger principles of biochemistry*; 4th ed.; W.H. Freeman: New York, 2005.

(64) HarduinLepers, A.; Recchi, M. A.; Delannoy, P. *Glycobiology* **1995**, *5*, 741-758.

(65) Bernacki, R. J.; Kim, U. *Science* **1977**, *195*, 577-580.

(66) Harvey, B. E.; Thomas, P. *Biochem. Biophys. Res. Commun.* **1993**, *190*, 571-575.

(67) Datta, A. K.; Sinha, A.; Paulson, J. C. *J. Biol. Chem.* **1998**, *273*, 9608-9614.

(68) Datta, A. K.; Paulson, J. C. *J. Biol. Chem.* **1995**, *270*, 1497-1500.

(69) Chiu, C. P. C.; Watts, A. G.; Lairson, L. L.; Gilbert, M.; Lim, D.; Wakarchuk, W. W.; Withers, S. G.; Strynadka, N. C. J. *Nat. Struct. Mol. Biol.* **2004**, *11*, 163-170.

(70) Bruner, M.; Horenstein, B. A. *Biochemistry* **2000**, *39*, 2261-2268.

(71) Klohs, W. D.; Bernacki, R. J.; Korytnyk, W. *Cancer Res.* **1979**, *39*, 1231-1238.

(72) Schaub, C.; Muller, B.; Schmidt, R. R. *Glycoconjugate J.* **1998**, *15*, 345-354.

(73) Schaub, C.; Muller, B.; Schmidt, R. R. *Eur. J. Org. Chem.* **2000**, 1745-1758.

(74) Schworer, R.; Schmidt, R. R. *J. Am. Chem. Soc.* **2002**, *124*, 1632-1637.

(75) Schroder, P. N.; Giannis, A. *Angew. Chem., Int. Ed. Engl.* **1999**, *38*, 1379-1380.

(76) Sun, H. B.; Yang, J. S.; Amaral, K. E.; Horenstein, B. A. *Tetrahedron Lett.* **2001**, *42*, 2451-2453.

(77) Young, J. E. P. Ph.D., University of Florida, 2005.

(78) Salaun, J. *Top. Curr. Chem.* **2000**, *207*, 1-67.

(79) Wong, H. N. C.; Hon, M. Y.; Tse, C. W.; Yip, Y. C.; Tanko, J.; Hudlicky, T. *Chem. Rev.* **1989**, *89*, 165-198.

(80) Rappoport, Z. *The Chemistry of the cyclopropyl group*; Wiley: Chichester, West Sussex; New York, 1995.

(81) Buchi, G.; Hofheinz, W.; Paukstel.Jv *J. Am. Chem. Soc.* **1969**, *91*, 6473-&.

(82) McCoy, L. L. *J. Am. Chem. Soc.* **1959**, *80*, 6568-6572.

(83) Baldwin, J. E.; Andrist, A. H.; Ford, P. W. *Chem. Ind.* **1971**, 930-&.

(84) Peterson, D. J.; Robbins, M. D. *Tetrahedron Lett.* **1972**, 2135-&.

(85) Barnier, J. P.; Champion, J.; Conia, J. M. *Org. Synth.* **1981**, *60*, 25-28.

(86) Hiyama, T.; Kanakura, A.; Morizawa, Y.; Nozaki, H. *Tetrahedron Lett.* **1982**, *23*, 1279-1280.

(87) Morgans, D. J.; Feigelson, G. B. *J. Am. Chem. Soc.* **1983**, *105*, 5477-5479.

(88) Zhang, R.; Mamai, A.; Madalengoitia, J. S. *J. Org. Chem.* **1999**, *64*, 547-555.

(89) Simmons, H. E.; Smith, R. D. *J. Am. Chem. Soc.* **1959**, *81*, 4256-4264.

(90) Gadwood, R. C.; Lett, R. M.; Wissinger, J. E. *J. Am. Chem. Soc.* **1986**, *108*, 6343-6350.

(91) Grieco, P. A.; Oguri, T.; Wang, C. L. J.; Williams, E. *J. Org. Chem.* **1977**, *42*, 4113-4118.

(92) Anciaux, A. J.; Hubert, A. J.; Noels, A. F.; Petiniot, N.; Teyssie, P. *J. Org. Chem.* **1980**, *45*, 695-702.

(93) Carey, F. A.; Sundberg, R. J. *Advanced organic chemistry*; 4th ed.; Kluwer Academic/Plenum: New York, 2000.

(94) Casey, C. P.; Polichnowski, S. W.; Shusterman, A. J.; Jones, C. R. *J. Am. Chem. Soc.* **1979**, *101*, 7282-7292.

(95) Doyle, M. P. *Chem. Rev.* **1986**, *86*, 919-939.

(96) Ghanem, A.; Lacrampe, F.; Schurig, V. *Helv. Chim. Acta* **2005**, *88*, 216-239.

(97) Doyle, M. P.; Austin, R. E.; Bailey, A. S.; Dwyer, M. P.; Dyatkin, A. B.; Kalinin, A. V.; Kwan, M. M. Y.; Liras, S.; Oalmann, C. J.; Pieters, R. J.; Protopopova, M. N.; Raab, C. E.; Roos, G. H. P.; Zhou, Q. L.; Martin, S. F. *J. Am. Chem. Soc.* **1995**, *117*, 5763-5775.

(98) Afeefy, H. Y.; Buckthal, D. J.; Hamilton, G. A. *Bioorg. Chem.* **1990**, *18*, 41-48.

(99) Blanchette, A.; Sauriollord, F.; Stjacques, M. *J. Am. Chem. Soc.* **1978**, *100*, 4055-4062.

(100) Gianni, M. H.; Adams, M.; Kuivila, H. G.; Wursthorn, K. *J. Org. Chem.* **1975**, *40*, 450-453.

(101) Schmidt, B.; Pohler, M.; Costisella, B. *Tetrahedron* **2002**, *58*, 7951-7958.

(102) Tian, Z.; Cui, H.; Wang, Y. *Synth. Commun.* **2002**, *32*, 3821-3829.

(103) Fritschi, H.; Leutenegger, U.; Pfaltz, A. *Helv. Chim. Acta* **1988**, *71*, 1553-1565.

(104) Carpino, L. A.; Han, G. Y. *J. Org. Chem.* **1972**, *37*, 3404-&.

(105) Gani, D.; Young, D. W. *J. Chem. Soc., Perkin Trans. 1* **1985**, 1355-1362.

(106) Collado, I.; Pedregal, C.; Bueno, A. B.; Marcos, A.; Gonzalez, R.; Blanco-Urgoiti, J.; Perez-Castells, J.; Schoepp, D. D.; Wright, R. A.; Johnson, B. G.; Kingston, A. E.; Moher, E. D.; Hoard, D. W.; Griffey, K. I.; Tizzano, J. P. *J. Med. Chem.* **2004**, *47*, 456-466.

(107) Ebinger, A.; Heinz, T.; Umbricht, G.; Pfaltz, A. *Tetrahedron* **1998**, *54*, 10469-10480.

(108) Scriven, E. F. V.; Turnbull, K. *Chem. Rev.* **1988**, *88*, 297-368.

(109) Carlsen, P. H. J.; Katsuki, T.; Martin, V. S.; Sharpless, K. B. *J. Org. Chem.* **1981**, *46*, 3936-3938.

(110) Garuti, L.; Roberti, M.; De Clercq, E. *Bioorg. Med. Chem. Lett.* **2002**, *12*, 2707-2710.

(111) Holan, G.; Samuel, E. L.; Ennis, B. C.; Hinde, R. W. *J. Chem. Soc. C* **1967**, 20-&.

(112) Smith, K. M.; Craig, G. W.; Eivazi, F.; Martynenko, Z. *Synthesis* **1980**, 493-494.

(113) Terzioglu, N.; van Rijn, R. M.; Bakker, R. A.; De Esch, I. J. P.; Leurs, R. *Bioorg. Med. Chem. Lett.* **2004**, *14*, 5251-5256.

(114) Tong, Y. C. *J. Heterocycl. Chem.* **1980**, *17*, 381-382.

(115) Crank, G.; Mursyidi, A. *Aust. J. Chem.* **1982**, *35*, 775-784.

(116) Faust, J. A.; Mori, A.; Sahyun, M. *J. Am. Chem. Soc.* **1959**, *81*, 2214-2219.

(117) Majchrzak, M. W.; Kotelko, A.; Guryn, R. *Synth. Commun.* **1981**, *11*, 493-495.

(118) Koskinen, A. M. P.; Munoz, L. *J. Org. Chem.* **1993**, *58*, 879-886.

(119) Baumgarten, H. E.; Smith, H. L.; Staklis, A. *J. Org. Chem.* **1975**, *40*, 3554-3561.

(120) Huang, H. C.; Seid, M.; Keillor, J. W. *J. Org. Chem.* **1997**, *62*, 7495-7496.

(121) Pellicciari, R.; Marinozzi, M.; Camaioni, E.; Nunez, M. D.; Costantino, G.; Gasparini, F.; Giorgi, G.; Macchiarulo, A.; Subramanian, N. *J. Org. Chem.* **2002**, *67*, 5497-5507.

(122) Plake, H. R.; Sundberg, T. B.; Woodward, A. R.; Martin, S. F. *Tetrahedron Lett.* **2003**, *44*, 1571-1574.

(123) Radlick, P.; Brown, L. R. *Synthesis* **1974**, 290-292.

(124) Zhao, D. B.; Wang, Z.; Ding, K. L. *Synlett* **2005**, 2067-2071.

(125) Reichelt, A.; Gaul, C.; Frey, R. R.; Kennedy, A.; Martin, S. F. *J. Org. Chem.* **2002**, *67*, 4062-4075.

(126) Figueira, M. J.; Caamano, O.; Fernandez, F.; Blanco, J. M. *Tetrahedron* **2002**, *58*, 7233-7240.

(127) Dalcanale, E.; Montanari, F. *J. Org. Chem.* **1986**, *51*, 567-569.

(128) Grof, C.; Riedl, Z.; Hajos, G.; Egyed, O.; Csampai, A.; Stanovnik, B. *Heterocycles* **2005**, *65*, 1889-1902.

(129) Stick, R. V.; Stubbs, K. A. *J. Carbohydr. Chem.* **2005**, *24*, 529-547.

(130) Berkessel, A.; Glaubitz, K.; Lex, J. *Eur. J. Org. Chem.* **2002**, 2948-2952.

(131) Loudon, G. M.; Radhakrishna, A. S.; Almond, M. R.; Blodgett, J. K.; Boutin, R. H. *J. Org. Chem.* **1984**, *49*, 4272-4276.

(132) Zhang, L. H.; Kauffman, G. S.; Pesti, J. A.; Yin, J. G. *J. Org. Chem.* **1997**, *62*, 6918-6920.

(133) Reese, C. B. *Tetrahedron* **2002**, *58*, 8893-8920.

(134) Beaucage, S. L.; Caruthers, M. H. *Tetrahedron Lett.* **1981**, *22*, 1859-1862.

(135) Reese, C. B.; Zhang, P. Z. *J. Chem. Soc., Perkin Trans. 1* **1993**, 2291-2301.

(136) Pitsch, S.; Weiss, P. A.; Jenny, L.; Stutz, A.; Wu, X. L. *Helv. Chim. Acta* **2001**, *84*, 3773-3795.

(137) Chappell, M. D.; Halcomb, R. L. *Tetrahedron* **1997**, *53*, 11109-11120.

(138) Chattopadhyaya, J. B.; Reese, C. B. *Nucleic Acids Res.* **1980**, *8*, 2039-2053.

(139) Puech, F.; Gosselin, G.; Balzarini, J.; Declercq, E.; Imbach, J. L. *J. Med. Chem.* **1988**, *31*, 1897-1907.

(140) Gilham, P. T.; Khorana, H. G. *J. Am. Chem. Soc.* **1958**, *80*, 6212-6222.

(141) Khorana, H. G.; Razzell, W. E.; Gilham, P. T.; Tener, G. M.; Pol, E. H. *J. Am. Chem. Soc.* **1957**, *79*, 1002-1003.

(142) Zhou, G. C.; Parikh, S. L.; Tyler, P. C.; Evans, G. B.; Furneaux, R. H.; Zubkova, O. V.; Benjes, P. A.; Schramm, V. L. *J. Am. Chem. Soc.* **2004**, *126*, 5690-5698.

(143) Gao, F.; Yan, X. X.; Shakya, T.; Baettig, O. M.; Ait-Mohand-Brunet, S.; Berghuis, A. M.; Wright, G. D.; Auclair, K. *J. Med. Chem.* **2006**, *49*, 5273-5281.

(144) Strauss, E.; Zhai, H.; Brand, L. A.; McLafferty, F. W.; Begley, T. P. *Biochemistry* **2004**, *43*, 15520-15533.

(145) Page, M. I.; Williams, A. *Enzyme mechanisms*; Royal Society of Chemistry: London, 1987.

(146) Chevrier, C.; Defoin, A.; Tarnus, C. *Bioorg. Med. Chem.* **2007**, *15*, 4125-4135.

(147) Tanaka, Y.; Kagamiishi, A.; Kiuchi, A.; Horiuchi, T. *Journal of Biochemistry* **1975**, *77*, 241-247.

(148) Sinnott, M. L.; Smith, P. J. *J. Chem. Soc., Chem. Commun.* **1976**, 223-224.

(149) Withers, S. G.; Rupitz, K.; Street, I. P. *J. Biol. Chem.* **1988**, *263*, 7929-7932.

(150) Lodish, H. F.; Darnell, J. E. *Molecular cell biology*; 3rd ed.; Scientific American Books: New York, 1995.

(151) Barrantes, F. J. *The nicotinic acetylcholine receptor : current views and future trends*; Springer: Berlin ; New York, 1998.

(152) Sargent, P. B. *Annu. Rev. Neurosci.* **1993**, *16*, 403-443.

(153) Toyoshima, C.; Unwin, N. *Nature* **1988**, *336*, 247-250.

(154) Changeux, J. P. *Trends Pharmacol. Sci.* **1990**, *11*, 485-492.

(155) Gotti, C.; Zoli, M.; Clementi, F. *Trends Pharmacol. Sci.* **2006**, *27*, 482-491.

(156) Corringer, P. J.; Le Novere, N.; Changeux, J. P. *Annu. Rev. Pharmacol. Toxicol.* **2000**, *40*, 431-458.

(157) Unwin, N. *Cell* **1993**, *72*, 31-41.

(158) Miyazawa, A.; Fujiyoshi, Y.; Unwin, N. *Nature* **2003**, *423*, 949-955.

(159) Filatov, G. N.; White, M. M. *Mol. Pharmacol.* **1995**, *48*, 379-384.

(160) Labarca, C.; Nowak, M. W.; Zhang, H. Y.; Tang, L. X.; Deshpande, P.; Lester, H. A. *Nature* **1995**, *376*, 514-516.

(161) Karlin, A. *Neuron* **2004**, *41*, 841-842.

(162) Oddo, S.; LaFerla, F. M. *J. Physiol. (Paris)* **2006**, *99*, 172-179.

(163) Meyer, E. M.; Kuryatov, A.; Gerzanich, V.; Lindstrom, J.; Papke, R. L. *J. Pharmacol. Exp. Ther.* **1998**, *287*, 918-925.

(164) Gerzanich, V.; Peng, X.; Wang, F.; Wells, G.; Anand, R.; Fletcher, S.; Lindstrom, J. *Mol. Pharmacol.* **1995**, *48*, 774-782.

(165) Sheridan, R. P.; Nilakantan, R.; Dixon, J. S.; Venkataraghavan, R. *J. Med. Chem.* **1986**, *29*, 899-906.

(166) Barlow, R. B.; Johnson, O. *Br. J. Pharmacol.* **1989**, *98*, 799-808.

(167) Glennon, R. A.; Dukat, M.; Liao, L. *Curr. Top. Med. Chem.* **2004**, *4*, 631-644.

(168) Beers, W. H.; Reich, E. *Nature* **1970**, *228*, 917-&.

(169) Papke, R. L.; Bencherif, M.; Lippiello, P. *Neurosci. Lett.* **1996**, *213*, 201-204.

(170) Kem, W. R. *Toxicon* **1971**, *9*, 23-&.

(171) Kem, W. R.; Mahnir, V. M.; Papke, R. L.; Lingle, C. J. *J. Pharmacol. Exp. Ther.* **1997**, *283*, 979-992.

(172) Defiebre, C. M.; Meyer, E. M.; Henry, J. C.; Muraskin, S. I.; Kem, W. R.; Papke, R. L. *Mol. Pharmacol.* **1995**, *47*, 164-171.

(173) Meyer, E. M.; Tay, E. T.; Papke, R. L.; Meyers, C.; Huang, G. L.; deFiebre, C. M. *Brain Res.* **1997**, *768*, 49-56.

(174) Papke, R. L.; Meyer, E. M.; Lavieri, S.; Bollampally, S. R.; Papke, T. A. S.; Horenstein, N. A.; Itoh, Y.; Papke, J. K. P. *Neuropharmacology* **2004**, *46*, 1023-1038.

(175) Stokes, C.; Papke, J. K. P.; Horenstein, N. A.; Kem, W. R.; McCormack, T. J.; Papke, R. L. *Mol. Pharmacol.* **2004**, *66*, 14-24.

(176) Papke, R. L.; Papke, J. K. P. *Br. J. Pharmacol.* **2002**, *137*, 49-61.

(177) Papke, R. L.; Schiff, H. C.; Jack, B. A.; Horenstein, N. A. *Neurosci. Lett.* **2005**, *378*, 140-144.

(178) Mullen, G.; Napier, J.; Balestra, M.; DeCory, T.; Hale, G.; Macor, J.; Mack, R.; Loch, J.; Wu, E.; Kover, A.; Verhoest, P.; Sampognaro, A.; Phillips, E.; Zhu, Y. Y.; Murray, R.; Griffith, R.; Blosser, J.; Gurley, D.; Machulskis, A.; Zongrone, J.; Rosen, A.; Gordon, J. *J. Med. Chem.* **2000**, *43*, 4045-4050.

(179) Marrero, M. B.; Papke, R. L.; Bhatti, B. S.; Shaw, S.; Bencherif, M. *J. Pharmacol. Exp. Ther.* **2004**, *309*, 16-27.

(180) Bodnar, A. L.; Cortes-Burgos, L. A.; Cook, K. K.; Dinh, D. M.; Groppi, V. E.; Hajos, M.; Higdon, N. R.; Hoffmann, W. E.; Hurst, R. S.; Myers, J. K.; Rogers, B. N.; Wall, T. M.; Wolfe, M. L.; Wong, E. *J. Med. Chem.* **2005**, *48*, 905-908.

(181) Morgan, T. K.; Lis, R.; Marisca, A. J.; Argentieri, T. M.; Sullivan, M. E.; Wong, S. S. *J. Med. Chem.* **1987**, *30*, 2259-2269.

(182) Ishihara, T.; Kakuta, H.; Moritani, H.; Ugawa, T.; Sakamoto, S.; Tsukamoto, S.; Yanagisawa, I. *Bioorg. Med. Chem.* **2003**, *11*, 2403-2414.

(183) Chen, F. C. M.; Benoiton, N. L. *Can. J. Chem.* **1976**, *54*, 3310-3311.

(184) Leonik, F. M.; Papke, R. L.; Horenstein, N. A. *Bioorg. Med. Chem. Lett.* **2007**, *17*, 1520-1522.

(185) Stotter, P. L.; Friedman, M. D.; Dorsey, G. O.; Shiely, R. W.; Williams, R. F.; Minter, D. E. *Heterocycles* **1987**, *25*, 251-258.

(186) Varnes, J. G.; Gardner, D. S.; Santella, J. B.; Duncia, J. V.; Estrella, M.; Watson, P. S.; Clark, C. M.; Ko, S. S.; Welch, P.; Covington, M.; Stowell, N.; Wadman, E.; Davies, P.; Solomon, K.; Newton, R. C.; Trainor, G. L.; Decicco, C. P.; Wacker, D. A. *Bioorg. Med. Chem. Lett.* **2004**, *14*, 1645-1649.

(187) Wadsworth, W.; Emmons, W. D. *J. Am. Chem. Soc.* **1961**, *83*, 1733-&.

(188) Hiebert, C. K.; Silverman, R. B. *J. Med. Chem.* **1988**, *31*, 1566-1570.

(189) Jung, M. E.; Lyster, M. A. *J. Org. Chem.* **1977**, *42*, 3761-3764.

(190) Murias, M.; Handler, N.; Erker, T.; Pleban, K.; Ecker, G.; Saiko, P.; Szekeres, T.; Jager, W. *Bioorg. Med. Chem.* **2004**, *12*, 5571-5578.

(191) Palmer, B. D.; Smaill, J. B.; Rewcastle, G. W.; Dobrusin, E. M.; Kraker, A.; Moore, C. W.; Steinkampf, R. W.; Denny, W. A. *Bioorg. Med. Chem. Lett.* **2005**, *15*, 1931-1935.

(192) Vonangerer, E.; Strohmeier, J. *J. Med. Chem.* **1987**, *30*, 131-136.

(193) Schmid, C. R.; Beck, C. A.; Cronin, J. S.; Staszak, M. A. *Org. Process Res. Dev.* **2004**, *8*, 670-673.

(194) Thorberg, S. O.; Johansson, L.; Gawell, L.; Sahlberg, C. *J. Labelled Compd. Radiopharm.* **1986**, *23*, 927-934.

(195) Barros, M. T.; Maycock, C. D.; Ventura, M. R. *J. Chem. Soc., Perkin Trans. 1* **2001**, 166-173.

(196) Johnson, C. R.; Adams, J. P.; Braun, M. P.; Senanayake, C. B. W.; Wovkulich, P. M.; Uskokovic, M. R. *Tetrahedron Lett.* **1992**, *33*, 917-918.

(197) William, A. D.; Kobayashi, Y. *J. Org. Chem.* **2002**, *67*, 8771-8782.

(198) Suzuki, A. *Proc. Jpn. Acad., Ser. B* **2004**, *80*, 359-371.

(199) Alo, B. I.; Kandil, A.; Patil, P. A.; Sharp, M. J.; Siddiqui, M. A.; Snieckus, V.; Josephy, P. D. *J. Org. Chem.* **1991**, *56*, 3763-3768.

(200) Felpin, F. X. *J. Org. Chem.* **2005**, *70*, 8575-8578.

(201) Fan, R. H.; Hou, X. L.; Dai, L. X. *J. Org. Chem.* **2004**, *69*, 689-694.

(202) Kim, H. S.; Barak, D.; Harden, T. K.; Boyer, J. L.; Jacobson, K. A. *J. Med. Chem.* **2001**, *44*, 3092-3108.

# BIOGRAPHICAL SKETCH

Fedra Marina Leonik, daughter of Jorge P. Leonik and Susana E. Sarabia, was born in Buenos Aires, Argentina, on May 20, 1978. She graduated with a Bachelor of Science degree in chemistry from the School of Science (Facultad de Ciencias Exactas y Naturales), University of Buenos Aires (UBA), Argentina, where she studied the variation in digestibility and dispersibility of milk proteins during storage, under the supervision of Dr. Maria Susana Vigo. She moved to Gainesville, Florida, on August 2002 to pursue her PhD in chemistry at the University of Florida. In May 2003, she married Daniel G. Kuroda in Buenos Aires, Argentina. She received her PhD in chemistry in August, 2008, under the guidance of Dr. Nicole A. Horenstein. After completion of her studies, she and her husband will carry on their carreers in Pennsylvania.